NASA

ORBIT TRANSFER VEHICLE
ENGINE STUDY, PHASE A - EXTENSION

(Volume II-A: Study Results)

(NASA-CR-161515) ORBIT TRANSFER VEHICLE ENGINE STUDY, PHASE A EXTENSION. VOLUME 2A: STUDY RESULTS Final Report (Rocketdyne) 213 p HC A10/MF A01 CSCL 21H

N80-28428

Unclas
G3/20 28175

ROCKETDYNE
A DIVISION OF ROCKWELL INTERNATIONAL

prepared for

NATIONAL AERONAUTICS AND SPACE ADMINISTRATION
George C. Marshall Space Flight Center
Huntsville, Alabama 35812

Rockwell International
Rocketdyne Division
6633 Canoga Avenue
Canoga Park, California 91304

RI/RD80-155-2

ORBIT TRANSFER VEHICLE ENGINE STUDY, PHASE A - EXTENSION

(Volume II - A: Study Results)

CONTRACT NO. NAS8-32996

30 JUNE 1980

PREPARED FOR:

NATIONAL AERONAUTICS AND SPACE ADMINISTRATION
MARSHALL SPACE FLIGHT CENTER, ALABAMA 35812

PREPARED BY

ADVANCED PROGRAMS
CANOGA PARK, CALIFORNIA

APPROVED BY

H. G. DIEM
PROGRAM MANAGER

ROCKETDYNE DIVISION, ROCKWELL INTERNATIONAL CORPORATION
6633 CANOGA AVENUE, CANOGA PARK, CALIFORNIA 91304

FOREWORD

This report presents the results of studies conducted during the Extension Period of the Orbital Transfer Vehicle Engine Study, Phase A - Contract. Engine trade studies and system analyses leading to a baseline engine selection for the Advanced Expander Cycle Engine Point Design Study were conducted by Rocketdyne, a Division of Rockwell International, under contract NAS8-32996--administered by Marshall Space Flight Center of the National Aeronautics and Space Administration (NASA). The NASA Contracting Officer's Representative and Alternate Contracting Officer's Representative were Mr. Dale Blount and Mr. James F. Thompson, respectively. Mr. H. G. Diem was the Rocketdyne Program Manager. The technical effort was conducted under the direction of Mr. A. J. Sobin, Study Manager.

The Final Report is submitted in three parts:

- Vol. I , Executive Summary
- Vol. II-A, Study Results
- Vol. II-B, Programmatics and Cost

CONTENTS

CONTENTS

FIGURES

FIGURES

FIGURES

TABLES

TABLES

ACKNOWLEDGEMENTS

Important contributions were made by the following personnel:

Engine Performance and Mission Analysis	-	A. Martinez, J. Glass, D. Nguyen
Heat Transfer	-	J. Shoji, W. Wagner, C. Laren, J. Lee
Engine System Design	-	H. Marker, A. Feight, R. Wahl
Weight Analysis	-	D. Carson
Control Systems Analysis	-	L. Sack, M. Taniguchi, G. Tellier, E. Lum
Turbomachinery	-	A. Csomor, R. Sutton
Reliability and Safety	-	C. Meisl, R. Cole, W. Haigler
Programmatics, Program, Risk, and Cost	-	C. Meisl

INTRODUCTION AND SUMMARY

The Orbital Transfer Vehicle (OTV) in which the oxygen/hydrogen OTV engine will be utilized is part of the planned space transportation system (STS). The OTV, carried into a low earth orbit by the Space Shuttle Orbiter, will extend the operating regime of the STS beyond the capability of the basic Space Shuttle, to include higher altitude orbits, geosynchronous orbits, and other space missions. For the past several years, NASA, the Department of Defense, and various vehicle and propulsion system contractors, including Rocketdyne, have been studying OTV related requirements, missions, vehicle configurations, and engine systems for this application. The goals of the vehicle and propulsion system studies have been the definition of and technology development for a high-performance, low-operating cost, reusable long life space system with the required operational versatility and payload retrieval capability. The basic OTV user requirements for the OTV propulsion system are shown in Fig. 1, together with an artist conception of the vehicle.

Two concepts have been defined by NASA as potential designs for the Orbital Transfer Vehicle: these are the all-propulsive orbit transfer vehicle (APOTV) and the aero-maneuvering orbit transfer vehicle (AMOTV). The baseline design of these preliminary studies had assumed an uprated shuttle orbiter with 100,000-pound payload capability to low earth orbit. As an interim vehicle, the current 65,000-pound payload capability shuttle orbiter would be used.

The baseline mission defined by NASA for the OTV Phase A Engine Studies was a four-man, 30-day sortie from low earth orbit to geosynchronous orbit and return to low earth orbit. A reusable oxygen-hydrogen upper stage with the high performance which these propellants offer is essential to achieving a defined round trip payload of 13,000 pounds.

The Phase A Extension OTV Engine Study performed by Rocketdyne has resulted in:

(1) Performance optimization of advanced expander cycle engines in the 10 to 20K pound thrust range,

(2) Selection of a recommended advanced expander engine configuration based on maximized performance and minimized mission risk, and definition of the components for this configuration,

HIGH THRUST OTV USER REQUIREMENTS

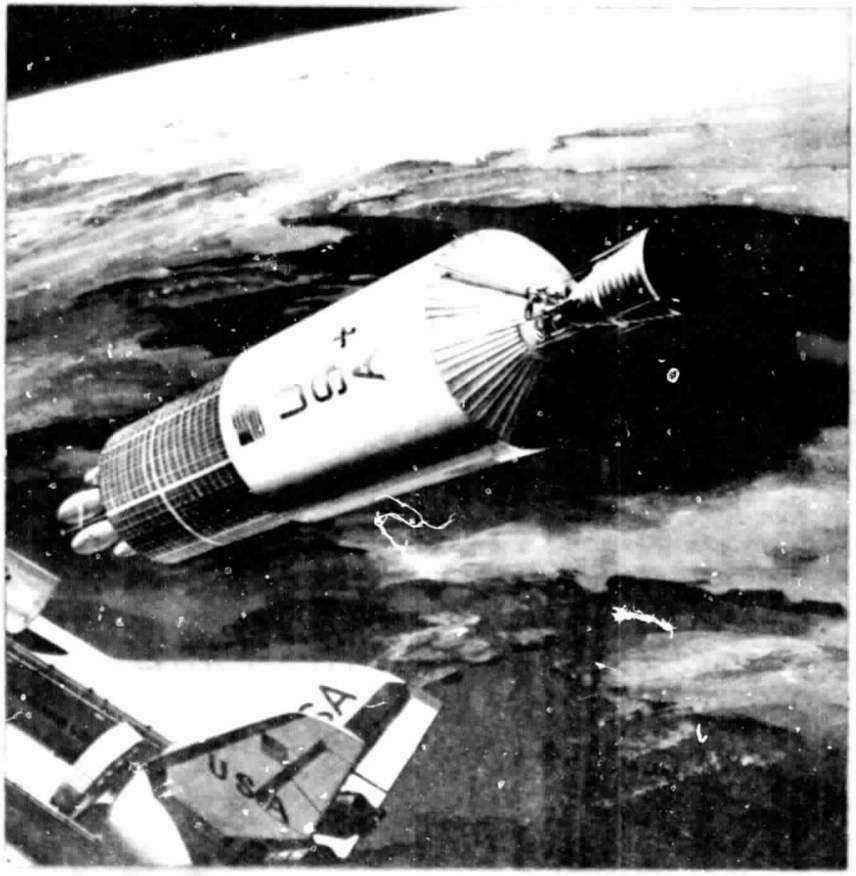

SC235-617A

- HIGH PERFORMANCE
- OPERATIONAL FLEXIBILITY
- MULTIPLE REUSE
- QUICK TURNAROUND
- MANRATED
- MINIMUM COST

Figure 1

(3) Characterization of the low thrust adaptation requirements and performance for the staged combustion engine,

(4) Generation of a suggested safety and reliability approach for OTV engines independent of engine cycle,

(5) Definition of program risk relationships between expander and staged combustion cycle engines, and

(6) Development of schedules and costs for the DDT&E, production, and operation phases of the 10K pound thrust expander engine program.

The Phase A Extension OTV Engine Study concluded that an advanced expander cycle engine is a viable contender for selection as the OTV main engine. This appraisal of the expander is based on performance optimization, on reliability and development risk assessment, and on a comparative cost evaluation. In addition, the gain in simplicity of the expander cycle engine configuration over the staged combustion engine configuration and the ability to directly apply to the expander the technology developed from the staged combustion engine programs make the advanced expander an attractive choice for OTV propulsion.

To accomplish the effort described in the Statement of Work (SOW), the following 5 technical study tasks were defined:

Task 8 Advanced Expander Cycle Engine Optimization

Task 9 Alternate Low Thrust Capability

Task 10 Safety, Reliability and Development Risk Comparison

Task 11 10K Expander Engine Programmatics

Task 12 Vehicle Systems Studies Support

This report is organized by study tasks and summarizes the results of these tasks. The work was performed during a 9-month period from July 1979 through May 1980.

TASK 8: ADVANCED EXPANDER CYCLE ENGINE OPTIMIZATION

The overall objective of Task 8 was to optimize the performance of expander cycle engines with vacuum thrusts of 10K, 15K, and 20K, and with a maximum retracted length of 60 inches and a mixture ratio of 6:1. The information generated forms the basis for a point design engine. The resulting engine configuration meets the engine requirements and life listed in Table 1. The variables and trades considered included but were not limited to those shown in Table 2. The requirements of Table 2 conform with the Phase A Extension SOW and were considered to be the detailed objectives of Task 8. All of the detailed objectives listed have been realized.

TABLE 2. CONTRACT DATA REQUIREMENTS AND DETAILED OBJECTIVES OF TASK 8

Trade Study Areas

8.1 Combustion chamber length and diameter

8.2 Cooling jacket pressure loss and heat pickup

8.3 Cycle variations such as turbine exhaust heat regeneration, series or parallel turbine flow path, and turbine gas reheat

8.4 Control requirements and methods considering minimum control/passive control and impact on weight, cost and reliability

8.5 Power balance at turbine bypass flows and pump discharge pressures reflecting statistical deviations from nominal operating efficiencies and weight/performance trades

8.6 Chilldown and/or start losses

TABLE 1

OTV ENGINE REQUIREMENTS
PHASE A EXTENSION

TECHNOLOGY LEVEL

- O_2/H_2 Bell Nozzle Engine
- 1980 State-of-the-art
- Man-rated System

CONFIGURATION

- Engine Length (IN)
  60/110 (Max/Min)
- Gimbal +15 / -6 } Degrees Pitch
  ±6 degrees yaw
- Boost pump inlet temperature/NPSH
  LO_2 = 162.7/2 (R/FT)
  LH_2 = 37.8/15

PERFORMANCE/OPERATING CHARACTERISTICS

- Mixture ratio = 6:1 to 7:1
- Thrust, TBD*
  10,000:15,000:20,000 lb
- Specific Impulse, TBD*
- Chamber pressure, TBD*
- Weight, TBD*
- Engine Power Cycle, TBD*

* TBD by effects on vehicle performance and weight (Reference NASA TMX - 73394)

OPERATIONAL

- Idle mode for low thrust maneuvers
- GO_2 and GH_2 tank pressurization
- Service free life,
  60 cycles or 2 hours
- Service life between overhauls, 300 cycles or 10 hours.

The engine configuration selection was based upon a payload performance optimization and upon an assessment of the mission risks associated with each of the engine and component concepts defined. Performance optimization consisted of quantitative evaluation of engine system parameters affecting chamber pressure, specific impulse, engine weight, and mission average specific impulse and their final influence on payload. Parameters considered in the performance optimization are presented in Table 3. Aspects considered in the risk assessment are indicated in Table 4.

TABLE 3. PARAMETERS CONSIDERED IN PAYLOAD PERFORMANCE OPTIMIZATION

Parameters Affecting P_c, Steady State I_s, and Engine Weight, W_{ENG}

- Turbine Arrangement
- Main Pump Drive and Speed
- Smooth Combustor Length
- Thrust Chamber Thermal Enhancement
- Expansion Area Ratio
- Turbines Bypass Flow Margin
- Pressure Drop Margin
- Maximum H_2 Bulk Temperature
- Turbine Gas Regeneration
- Turbine Gas Reheat
- Boost Pump Drive
  - Geared
  - Gas Driven
  - Hydraulic

Parameters Affecting Mission Average $\bar{I}_s$

- Boost Pump Drive
- Autogeneous Heat Exchanger Location
- Turbine Gas Regeneration Heat Exchanger Location
- Controller Type

TABLE 4. ASPECTS CONSIDERED IN RISK ASSESSMENT

State-of-the-Art
Soundness of Mechanical Design
Life
Man Rating (Complexity, Safety, Reliability)
Cost, Producibility
Maintainability
Handling
Off-Design Flexibility
Control Flexibility
Development Flexibility
Packaging Flexibility
Component Integration Flexibility

Section I presents the engine configuration selected based on performance maximization with particular attention to reduction of mission risks. Judicious selection of performance levels and component designs was made to provide ample mission risk margins. Section II presents the performance optimization results in more detail, and Section III extends the results of the 10K and 15K thrust level to the 20K thrust level.

SECTION I. SELECTED ENGINE CONFIGURATION, SUMMARY

The design characteristics of the baseline engine configuration selected from Task 8 studies are presented in Table 5. This selection resulted from specific impulse performance and weight optimization of the engine in the 10K-15K lbs range of thrust. Selection of component design and performance levels was made to provide design margins that will reduce engine development risks. Although, for the engine length selected, performance optimizes at an area ratio of 900:1, the recommended design utilizes a nozzle with expansion area ratio of 625:1. The lower value facilitates altitude testing in idle mode, reduces test and fabrication costs, and results in a lower engine weight.

TABLE 5. PERFORMANCE-OPTIMIZED ADVANCED EXPANDER CYCLE ENGINE BASELINE DESIGN CHARACTERISTICS

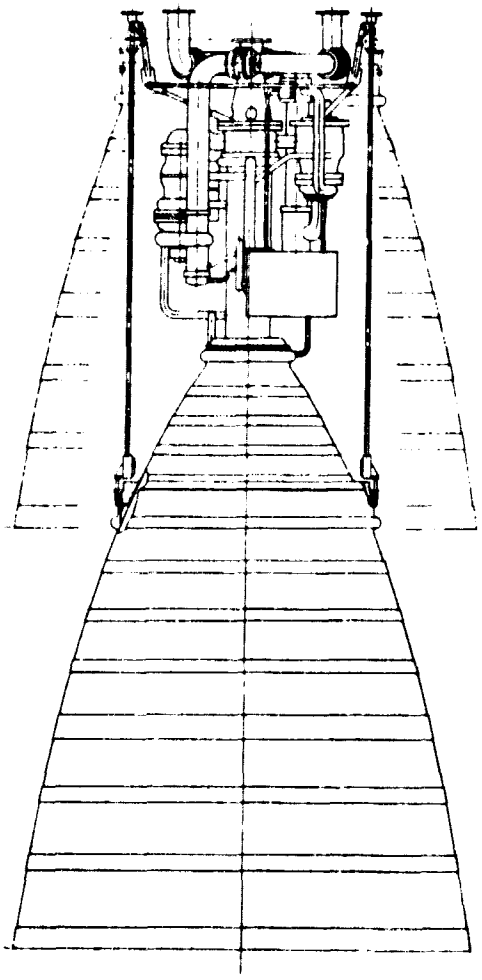

BASELINE DESIGN CHARACTERISTICS

• FULL THRUST (VAC), LB	15,000
• MIXTURE RATIO	6
• CHAMBER PRESSURE, PSIA	1610
• EXPANSION AREA RATIO	625
• SPECIFIC IMPULSE, SEC	482.5
• PUMP DISCHARGE PRESSURE, PSIA	
◦ OXYGEN	2682
◦ HYDROGEN	4621
• PUMP SPEEDS, RPM	
◦ OXYGEN	58,100
◦ HYDROGEN	107,140
• TURBINE INLET TEMP, R	965
• RETRACTED LENGTH, IN.	80
• EXTENDED LENGTH, IN.	117
• ENGINE DRY WEIGHT, LB	415
• TECHNOLOGY BASIS	1980

DESIGN FEATURES

- FULL-FLOW REGEN COOLING
- SERIES MAIN TURBINES
- GH_2-DRIVEN LOW PRESSURE PUMPS
- SMOOTH-WALL 20 IN. LONG COMBUSTION CHAMBER
- AUTOGENOUS TANK PRESSURIZATION

POWER CYCLE CONFIGURATION

Power Cycle parameter optimization was carried out in the range of thrusts 10K-20K lbs. For each thrust, the cycle parameter optimization resulted in higher chamber pressures than earlier studies had shown, which increased specific impulse and decreased engine weight. The trends of increasing gravity losses with decreasing thrust forced the optimum payload to occur in each optimization case at or near 15,000 lbs of thrust. Cycle optimization produced similar results at all of the thrusts investigated but was most pertinent at 15K lb thrust.

Four major areas of power cycle optimization were examined: main turbine arrangement, cycle energy source, high pressure pump design, and boost pump drive. Cycle configurations resulting from the first two areas were: parallel main turbines, series main turbines, turbine gas regeneration and turbine gas reheat. These cycles and combinations thereof are illustrated in Fig. 1a. They were evaluated with smooth-wall combustors and with thermally enhanced combustor configurations.

Main Turbine Arrangement

The selected chamber pressure of 1610 psia is consistent with 1980 technology and was obtained with optimized turbomachinery operating in a series main turbine arrangement (Fig. 2) for maximum utilization of available energy in the hydrogen coolant. A series turbine arrangement makes maximum use of the hydrogen flow available and, therefore, maximizes power in a flow limited power cycle like the topping expander cycle. Turbine design is sensitive to volumetric flowrate and the series design maximizes flow to both turbines. The series turbine arrangement also provides geometry conducive to higher values of turbine admission and improved turbine efficiencies. Parallel main turbines were evaluated and found to yield chamber pressures 255 psia lower than the series main turbine arrangement.

The selected engine main fuel turbine is a two-stage impulse turbine with 3.1 inch rotor diameter, which operates at a tip speed of 1600 ft/sec. All turbine blade stages are fully shrouded. Exit guide vanes are used to minimize discharge turbulence losses. Hydrogen turbine inlet gas temperatures of 955 R are

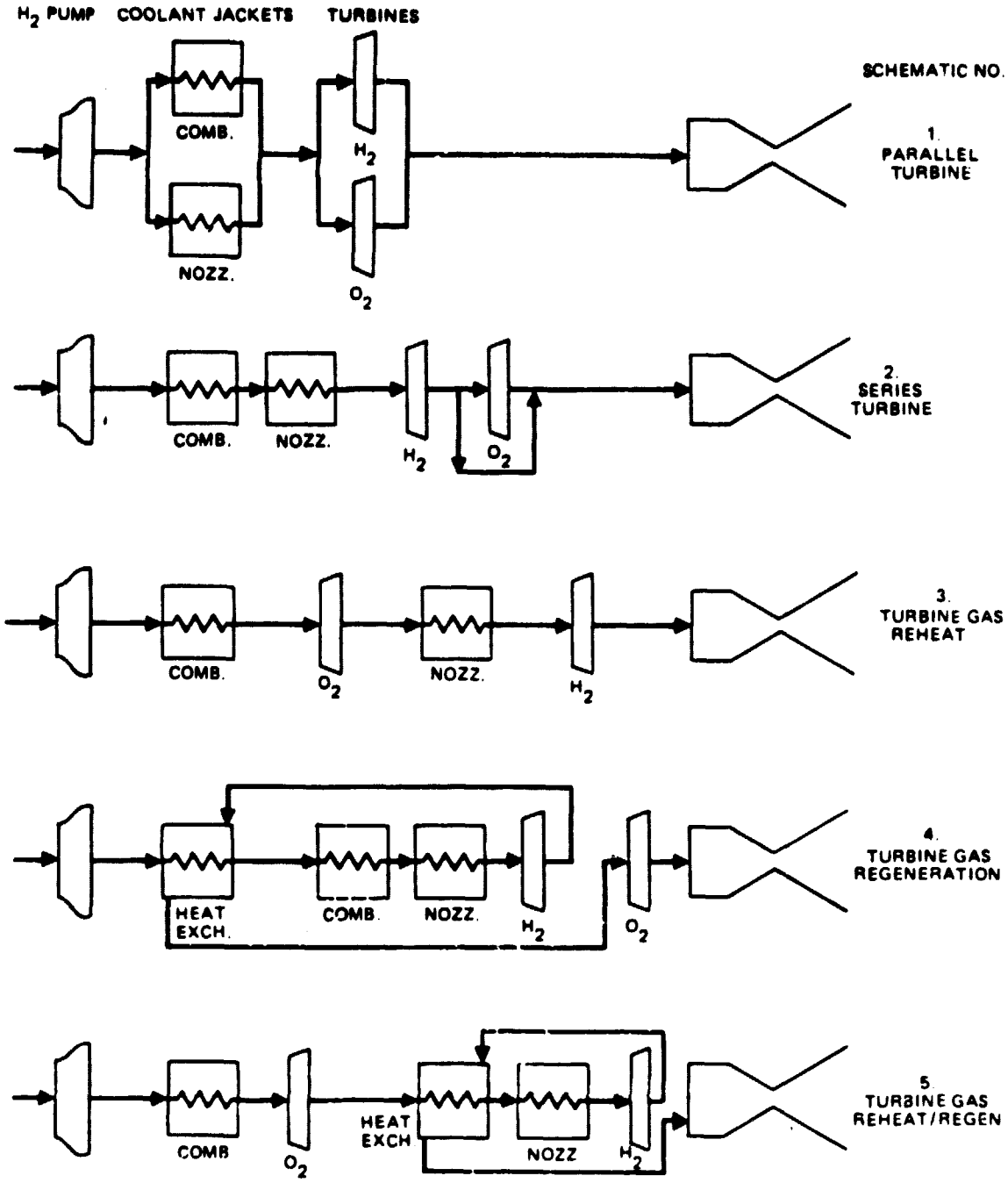

Figure 1a. Expander Engine Schematics

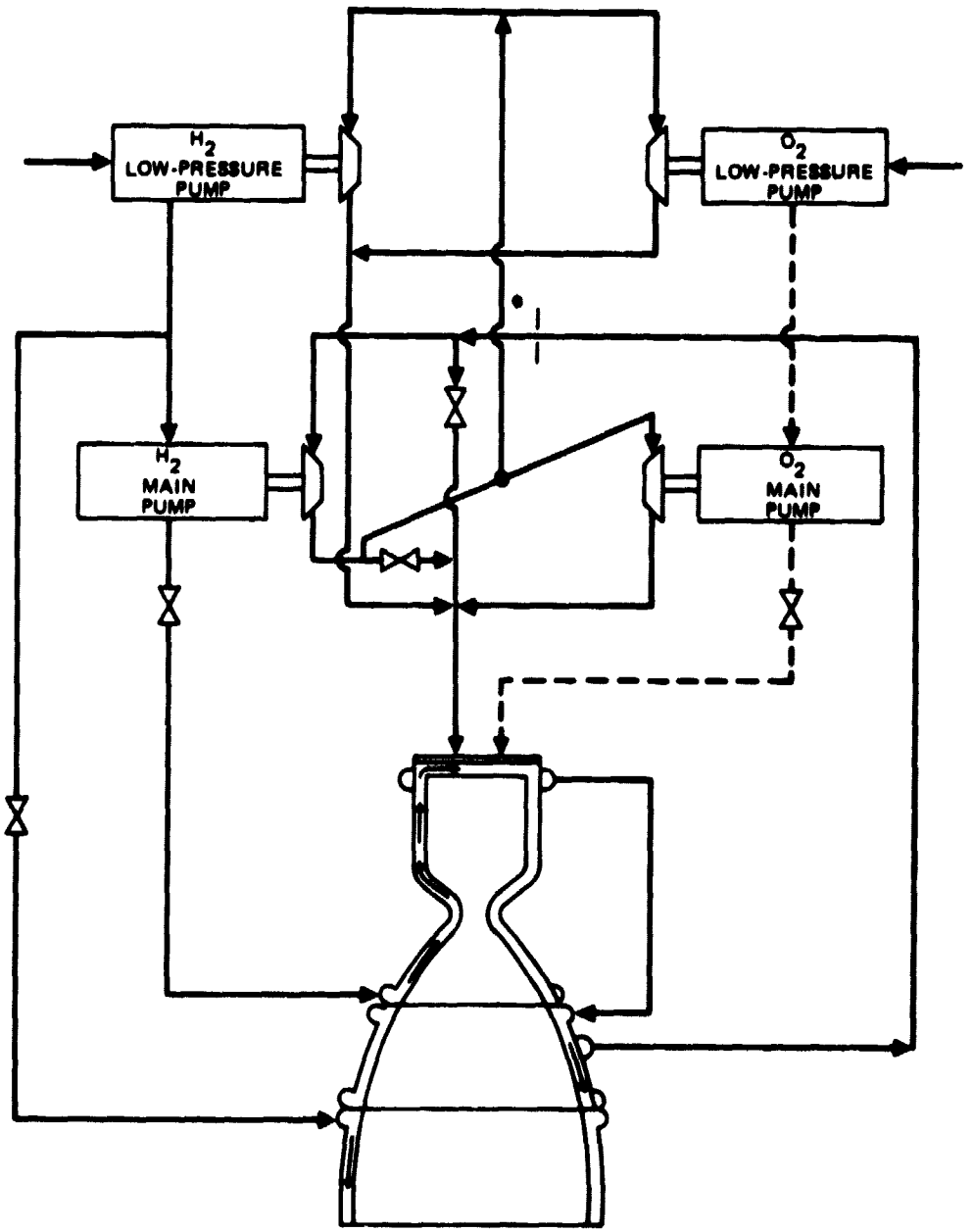

Figure 2. Advanced Expander Cycle Baseline Engine

obtained through a combination of up-pass combustor cooling and one and one-half down pass nozzle cooling with combustor and nozzle in series, utilizing full regenerative hydrogen flow. This scheme allows the highest turbine inlet temperature through high hydrogen bulk temperatures in the nozzle where heat fluxes are lowest; and lower bulk temperatures in the high heat flux combustor for increased life margin.

Cycle Energy Source

A smooth-wall combustor with a length of 20 inches from injector face to throat was selected as the main source of thermal energy input into the hydrogen coolant based on trade studies where turbine gas regeneration, turbine gas reheating, and combustion chamber thermal enhancement methods were evaluated as means of augmenting the turbine gas inlet temperature.

The turbine gas regeneration cycles (Fig. 1a) provided high turbine inlet temperatures with low combustor heat inputs and resulted for most combustor lengths, in higher chamber pressures than cycles that did not use regeneration, Fig. 3. However, the lower combustor heat inputs led to specific impulses only slightly higher than the basic unregenerated engine cycle due to lower hydrogen injection temperatures from the turbines to the main injector. A turbine gas regeneration cycle with the heat exchanger located between the combustor and nozzle coolant jackets provided the highest specific impulse increase (1.4 sec), yet penalized the engine system with a heavy heat exchanger, and required a high heat exchanger thermal effectiveness of 90 percent. As thermal effectiveness is synonymous with heat exchanger surface area, large heat exchangers are required for what appears to be not very significant gains in specific impulse. Further optimization of the heat exchanger design is required before this cycle can become competitive.

Thrust chamber thermal enhancement provided significant increases in both chamber pressure and specific impulse over the smooth-wall combustor (Fig. 3). The performance increases (ΔI_s = 5 sec) are significant but do not warrant the selection of this concept as the baseline mainly because of the development status of this configuration. The thermally enhanced thrust chamber has not been hot-fire

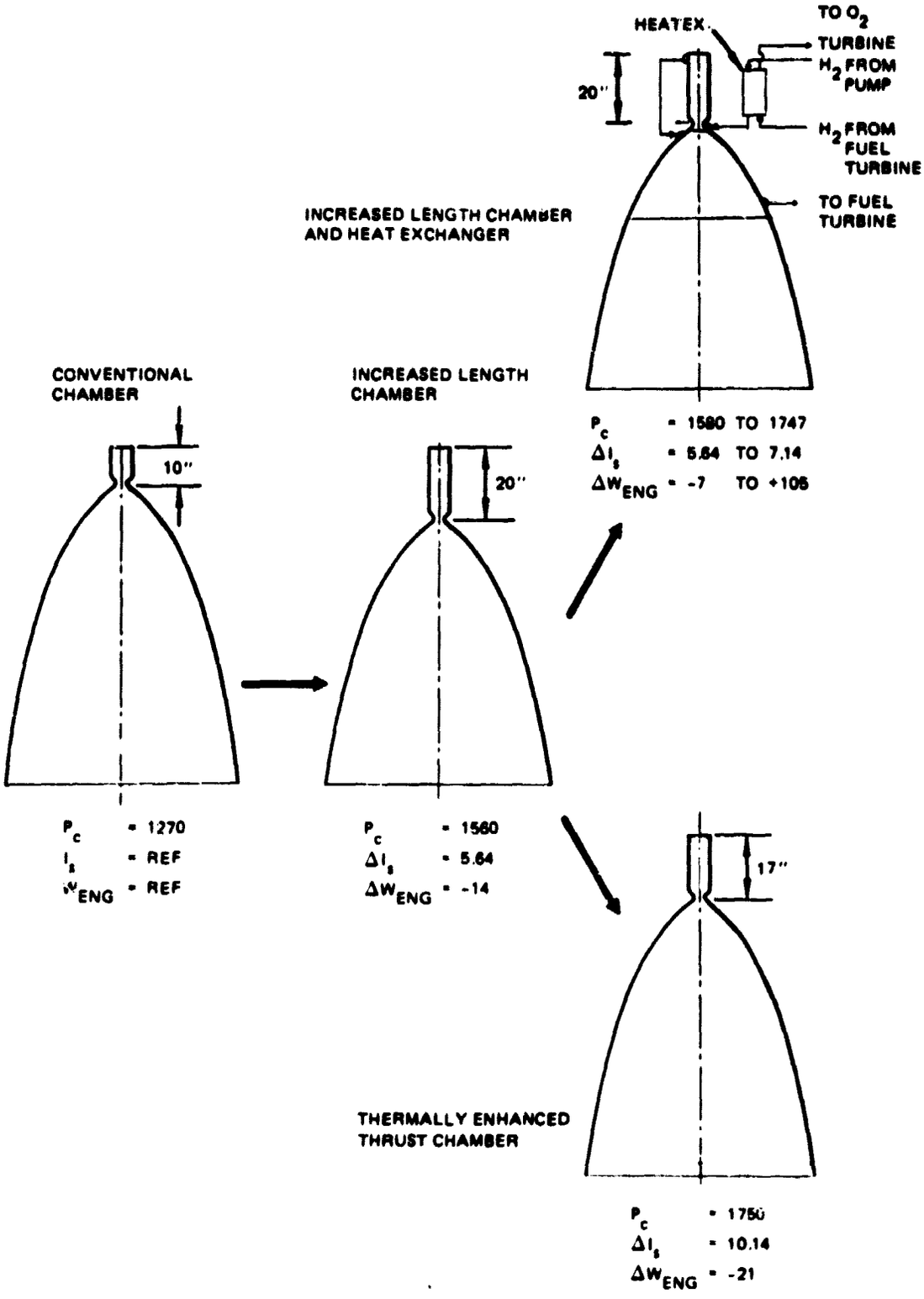

Figure 3. Heat Transfer Enhancement Concepts and Regeneration Comparison

tested and, therefore, must be treated as advanced state of the art. The thermal enhancement combustor chamber, however, was retained as an alternate (or backup) concept to provide an added margin for the 20 inch combustor heat loads since it could be incorporated in a later development configuration. The baseline engine will be designed with the capability of accepting thermal enhancement as an engine growth concept.

High Pressure Pump Designs

Within the bearing DN limits established by the 1980 technology groundrule and other groundrules for pump and turbine parameters, hydrogen pump speeds of 107,000 rpm are required to provide maximum efficiency of utilization of turbine derived power. The engine pump speeds and bearing DN are consistent with 20 mm diameter bearings which have received extensive testing in the Advanced Space Engine (ASE) fuel (MK48F) and oxidizer (MK48-0) pump technology development programs.

Because of the high torque required to drive both main pumps from a single turbine and the resultant impact on gear life, a single turbine with geared drives was ruled out for the high pressure turbomachinery. Similar life considerations were used to rule out dual turbines with synchronizing gears even though this scheme may be advantageous for ease of engine control during engine transient buildup and decay.

The fuel pump design is a three-stage centrifugal machine with inducer and axial inlet, similar to the successful design of the ASE. The fuel impellers are 3.5 inches in diameter with a tip speed and stage specific speed of 1630 ft/sec and 675 respectively. The oxidizer pump is a single stage centrifugal pump of 2.2 inches impeller diameter, 560 ft/sec tip speed and 1280 specific speed. Dimensions and speeds conform with 1980 state of the art groundrules listed in the main body of this report.

Boost Pump Drive

The impact of boost pump drive method upon overall engine performance is small

because of the low horsepower requirements for these pumps, therefore, other factors must provide the basis for selection of the boost pump drive method.

Gaseous hydrogen turbine drives were attractive for the low pressure hydrogen and oxygen pumps based upon trade studies considering performance, transient characteristics, flexibility of design, complexity, and packaging and testing flexibility. The boost turbines are placed in parallel arrangement with the main oxidizer turbine. Adequate flow and pressure ratio is obtained for these turbines at these locations. The gaseous hydrogen turbine drive approach provides for the possibility of some degree of control over the start transient. Operation is initiated early in the sequence of events and thus enhances system chilldown during tank head idle mode (THI). This turbine drive allows for maximum flexibility of packaging, provides flexibility in off-design operation, has good life capability, and provides flexibility during development testing since boost pump components can be tested separate from the main pumps.

Geared drives were studied on the basis of the maximum life demonstrated (5.56 hours) at a pitch line velocity of 16,000 fpm (Ref. 1). A pitch line velocity of 25,000 fpm would be required to maintain high main pump performance. This high pitch line velocity coupled with a 10 hour life requirement could result in a significant development problem.

Partial flow hydraulic drives, which utilize a portion of the main pump output flow for the turbine power are the second best choice for the oxidizer boost pump which provides high performance, flexibility in packaging and good life capability. However, the startup of the hydraulic turbines would lag the main pump startup and, therefore, would not provide any benefit during start chilldown. In addition, the reintroduction of two-phase flow from chilldown of the hydraulic turbine loop into the main pump inlet may inhibit pump operation during the start transient.

Another configuration studied was the full-flow hydraulic turbine where the hydraulic driven turbine is placed behind the main pump inducer and utilizes the full main pump flow. The advantages of the full-flow hydraulic boost pump

drive are integrated packaging, zero leakage and thus zero nonpropulsive propellant losses, and good life capability. However, low required NPSH for the boost pumps and limited turbine diameter (main pump inducer diameter) result in low available horsepower for boost pump drive. Coupling of boost pump and main pump heads results in reduced main pump speeds, efficiency and increased weight. In addition, the boost pumps do not start until the main pumps start rotation providing, therefore, no start chilldown benefit. The integrated arrangement also limits packaging and component development flexibilities.

Cooling Circuit

The cooling circuit selected is a full-flow regenerative scheme depicted in Fig. 4. All of the hydrogen flow, except for pump seal leakage and that used in supplemental cooling, is used in cooling the thrust chamber and nozzle in series arrangement. This hydrogen flow enters the combustor coolant jacket from the pump outlet at an expansion area ratio of 6:1 and cools the combustor by flowing in an up-pass manner. Entrance at this area ratio provides the lowest coolant temperatures at the most critical chamber cross section (0.5 in. upstream of throat) which governs chamber life. It also results in the lowest hydrogen bulk temperatures exiting the combustor coolant jacket and, therefore, enhances chamber life. The coolant flow is collected at the injector plane and routed to the nozzle coolant distributing manifold at an expansion area ratio of 6:1. From here it flows to the end of the nozzle (ϵ = 210) in a down-pass manner from where the coolant is returned in up-pass manner to exit the nozzle at an area ratio of 100. From here the heated hydrogen is directed to the fuel turbine. This circuit allows for the highest fuel turbine inlet temperatures since they are governed by the maximum allowable nozzle coolant bulk temperatures (1260 R) compatible with safe nozzle wall temperatures.

A one and one-half up-pass circuit starting part way down the nozzle and having as final point the injector plane was considered but not selected since the maximum hydrogen bulk temperature is controlled by the maximum allowable combustor wall temperature and results in the lowest fuel turbine inlet temperatures (1000 R).

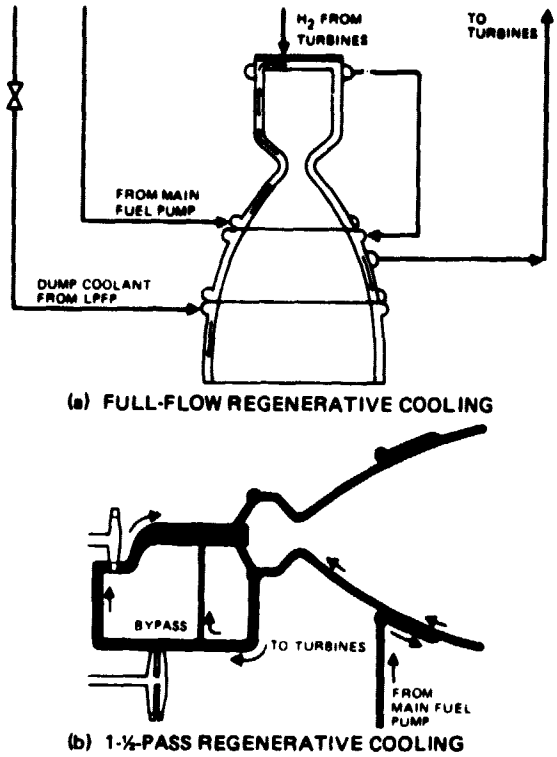

Figure 4. Cooling Circuits Schematics

COMBUSTOR AND NOZZLE DESIGN

Injector

Coaxial injection elements and a transpiration cooled rigimesh faceplate have been selected for the baseline engine design. This configuration offers proven performance, reliability, and complete fabrication experience for minimum iteration during design and development. The coaxial/rigimesh concept has been applied successfully, using liquid oxygen and gaseous hydrogen, to numerous Rocketdyne injector designs varying in chamber pressure from 700 psi to 4000 psi, with corresponding thrust levels from 3000 to 470,000 pounds of thrust. Because of the high level of experience with the selected injector system, a high level of confidence exists in the disciplines of combustor stability and performance prediction. Performance prediction is provided with the SDER computer program which correlates to existing designs within $\pm$ 2%. The confidence that stable combustion can be achieved is based on extensive coaxial injector element testing and studies performed to identify and improve stability characteristics.

The injector proposed has 108 concentric elements with oxidizer flowing through the center orifice and fuel in the outer tube. The outer element length will reflect stability considerations in its sizing. The faceplate is rigimesh to provide for transpiration cooling of the combustion chamber surface. A piston ring at the edges of the rigimesh plate allows for axial growth of the injector. Element distribution will provide uniform mass distribution over the entire injector face.

Combustion Chamber

The combustion chamber is configured with a smooth hot wall and a length of 20 inches. The hot wall is regeneratively cooled with hydrogen flowing in axial passages from the throat region toward the injector face. The coolant channel geometry favors a contraction ratio of 4 which allows doubling the number of passages from the throat to the combustion chamber. The chamber configuration represents 1980 technology. Existing chamber fabrication technology is directly applicable to this design; heat pickup correlation is traced to directly applicable ASE thrust chamber testing. Structurally, the mechanism responsible for low cycle fatigue in the channel geometry is understood, is directly applicable to the design, and finds basis in SSME, ASE, and 40K thrust chamber testing. Materials will consist of a NARLOY Z hotwall with conventional coolant channels milled into the outer diameter. The channels are closed out with an .011 copper electroplating and a .055 nickel-cobalt structural electroplate over the copper.

Combustion Chamber Alternate

A combustion chamber length of 20 in. is necessary for the specific impulse and combustion chamber pressure performance desired for the advanced expander engine. Larger chamber diameters increase surface area but simultaneously decrease heat transfer coefficient so that no significant gains are obtained in heat loads. One alternative to length is the thermally enhanced thrust chamber which provides approximately 28 percent heat load enhancement in a shorter 17 in. long chamber. However, because heat transfer verification and low cycle fatigue (LCF) impact cannot be assessed with the same level of confidence as for the smooth wall design, the thermally enhanced thrust chamber concept is proposed as a possible alternate for future engine growth.

Fixed Nozzle

Configuration trade study results for the fixed portion of the nozzle reveal a highly developed state of current technology in this area. The selected design configuration has a thorough development basis in performance, reliability, fabrication and maintainability. It consists of a NARLOY Z channel cooled configuration in the high heat flux region near the throat plane and a thin wall A286 brazed lightweight tube structure from an expansion ratio of 6 to 210. The coolant makes a full pass down and a half-pass up in this arrangement. The configuration provides a low wall temperature with a low nozzle pressure drop cooling requirement. The tubular section uses 320 A286 tubes through the ε = 100, 2 to 1, splice point and down to the extendible nozzle attach plane where the tubes are manifolded to an equal number of A286 tubes for the half-pass back up to the ε = 100 point.

EXTENDIBLE NOZZLE DESIGN

Dump-cooled Nozzle

Because cooled metallic nozzles are considered current state-of-the-art, a hydrogen dump-cooled nozzle was selected for the baseline engine configuration. The retractable nozzle extends from an area ratio of 210 to 625. The single downpass cooling circuit is formed by 1080 round tapered tubes, and made from nickel plated Inconel 625 material. The exiting coolant flow is manifolded to a plenum that feeds an annular expansion nozzle with area ratio of 30:1. The heated hydrogen (1720 F) at this area ratio provides a specific impulse of 507 sec; approxiamtely 5 percent higher than the thrust chamber specific impulse and sufficient to offset some of the losses incurred in non-propulsion leakage flows of the pumps and turbines. Cooling of this nozzle is feasible at all engine mixture ratios and only requires at off-design different coolant flow splits with other thrust chamber components than at on-design mixture ratio. No structural problems are expected with this type nozzle during start and shutdown transients, full thrust, or during normal handling. Its fabrication is more elaborate, weight and cost higher than concepts such as the radiation cooled

carbon-carbon nozzle but its technology is more readily available. Performances of dump cooled and radiation cooled nozzles are comparable with no significant changes expected from either nozzle type.

Radiation Cooled Nozzles

Refractory metallic and carbon-carbon radiation cooled nozzles were examined for application to the extendible nozzle. The Space Shuttle OMS 6,000 lb thrust engine uses a Columbium nozzle which has a disilicide coating to prevent oxidation. Exploratory development testing has been conducted by industry on a carbon-carbon nozzle for application to both solid and liquid propellants. Each of these concepts will be given further evaluation during the Advanced Expander Engine Point Design Study contract. Detailed comparisons will be made in the areas of life capability, fabrication, weight and cost. Upon the completion of these studies, the extendible nozzle configuration will be finalized.

A carbon-carbon nozzle concept was examined in extendible nozzle trade studies. This concept was found to be lighter in weight and simpler in construction than the dump-cooled nozzle concept. A nozzle wall with approximately 1/8 in. wall thickness was found sufficient to provide, with adequate external support (hat-band), the rigidity and strength required during mainstage operation. The nozzle can be radiation cooled at the nozzle area ratios used for the extendible nozzle and since carbon strength increases with temperature it can stand expected temperatures near 2200 F. Carbon heated to these temperatures in the presence of superheated steam, however, undergoes reaction and conversion into carbon monoxide, hydrogen and traces of methane (well known water-gas reaction) with erosion of the carbon surface. Metallic surface coatings and metallic species diffused in the carbon matrix are some of the protective means that have been proposed, but need experimental evaluation.

Start and shutdown transients and possible oxygen rich cutoffs are other conditions that may aggravate the erosion of the carbon and is considered to be an obstacle in meeting nozzle life requirements. An additional area of concern is the thermal shock experienced by the nozzle during start and shutdown.

Nozzle Area Ratio

The performance of the engine is presented in Fig. 5 as a function of expansion area ratio. These data can be used for selection of the final area ratio desired of the nozzle. It is seen that nozzle area ratio can be reduced from the peak value of 900 to a value of 625 while incurring a specific impulse loss of only 0.5 sec. Idle mode testing places an additional requirement on altitude simulation test facilities. The use of lower area ratios to reduce the possibility of flow separation and damage to the nozzle due to increased heat and pressure loads in separated flow is, therefore, advantageous.

POWER AND CONTROL MARGINS

Engine power margins required for engine-to-engine component efficiency variations and control margins are met by providing a 10 percent system pressure drop reserve in conjunction with a 10 percent turbine bypass flow reserve. These combined reserves provide for probable variations in turbomachinery efficiencies indicated in Table 6 which were obtained from SSME experience together with coolant jacket pressure drop and heat load uncertainties as established in ASE thrust chamber testing. In addition, these reserves provide for a 5 percent turbine bypass flow for thrust control and 3 percent margin on this latter requirement. This provides a total of 8 percent of turbine flowrate as a thrust control allowance. All these contingencies can be met (as shown in Table 6) with either 23% bypass flow or 19.8% pressure drop reserve. To balance out possible disadvantages inherent in either method a 10/10 percent split was selected. Larger turbine bypass flowrates tend to reduce turbomachinery component efficiencies and make design more difficult, while larger pressure drop reserves affect pump discharge pressures adversely. The margins are based on worse case engine to engine variations. The flow and pressure drop margin equivalences in Table 6 are based on influence coefficients for off-design engine operation obtained in computer model studies.

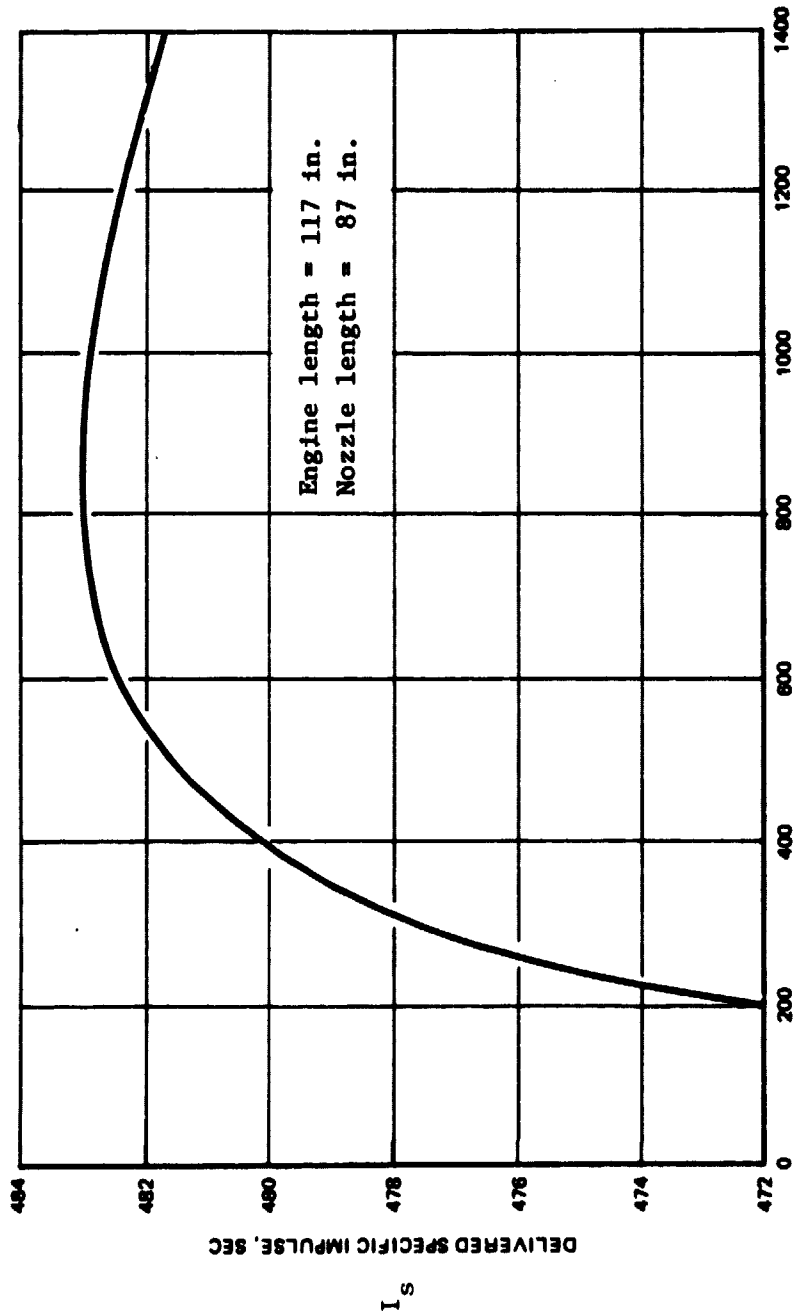

Figure 5. Baseline Expander Engine Performance

TABLE 6. BASELINE ENGINE POWER AND CONTROL FLOW MARGINS

	Engine-to-Engine Variation	Equivalent Turbine Bypass Flow Margin, %			Equivalent ΔP Margin % Upstream Turbine
Component Uncertainties:					
Fuel Pump Efficiency, Points	± 1.6	2.47	- or	-	2.12
Fuel Turbine Efficiency, Points	± 2.0	2.19	- or	-	1.88
Oxidizer Pump Efficiency, Points	± 0.8	0.18	- or	-	.15
Oxidizer Turbine Efficiency, Points	± 2.0	0.46	- or	-	.40
Coolant Jacket Pressure Drop, % Nominal	± 8.0	1.00	- or	-	.86
Coolant Jackets Heat Load, % Nominal	± 12.0	8.76	- or	-	7.53
Control Requirements for Mixture Ratio Excursions:					
Turbines Bypass Control Flow	-	5.00	- or	-	4.30
Control Flow Margin	-	3.00	- or	-	2.58
Total Margin Requirements (All Flow or All ΔP)		23.06	or		19.82
Margin Requirements (50-50 Split Between Flow and ΔP)		10	and		10

ENGINE CONTROL SYSTEM

To enable control of thrust and mixture ratio level during mainstage and start, Rocketdyne has defined a simple three-valve closed-loop control system. The control points selected have capability to fully control the engine thrust and mixture ratio over the full range of required engine operating conditions. The control modulates the areas of the oxidizer main valve, the turbine bypass

valve, and the oxidizer turbine bypass valve to achieve independently the proper balance of propellant flows for independent control of thrust and mixture ratio.

In mainstage, closed loop thrust and mixture ratio control are exercised as required by the system controller and vehicle commands. The three modulated valves depicted on schematic in Fig. 6 are used for control of thrust during start transients and mainstage, and for control of mixture ratio between 6:1 and 7:1. Thrust control is most sensitive to modulation of the turbine's bypass valve located in parallel arrangement with the two main turbines. Mixture ratio control is most sensitive to the main oxidizer valve situated in the liquid oxygen line downstream of the main oxidizer pump. An oxidizer turbine bypass valve increases the sensitivity of the thrust control valve during mixture ratio extremes. It performs its function by varying the flow-split between oxidizer and fuel turbines.

Closed Loop Control

The thrust and mixture ratio levels are variable upon vehicle command. The control is required to maintain engine thrust and mixture ratio, within anticipated values of $\pm$5 percent and $\pm$2 percent, respectively, of the commanded mainstage values. This type of precision is similar to Centaur upper stage engine thrust and mixture ratio precision requirements of $\pm$2 percent. These can be relaxed somewhat for the OTV, especially on the thrust requirement. Space Shuttle Main Engine (SSME) precision requirements are +6000 lb in thrust ($\pm$1.25%) and $\pm$2 percent in mixture ratio. A closed loop control is required for this type of precision.

As illustrated in Table 7 for a staged combustion cycle (SSME) wide variation in thrust and mixture ratio would be experienced if the engine used no controller with mechanical valve sequencing, or electrical sequencing with no valve positive control (open-loop control). Full range controls, or mainstage trim controls (closed-loop control techniques) provide the lowest thrust and mixture ratio variations. The same would be true for an expander cycle engine except variations will not be as pronounced in the case of the open-loop controls.

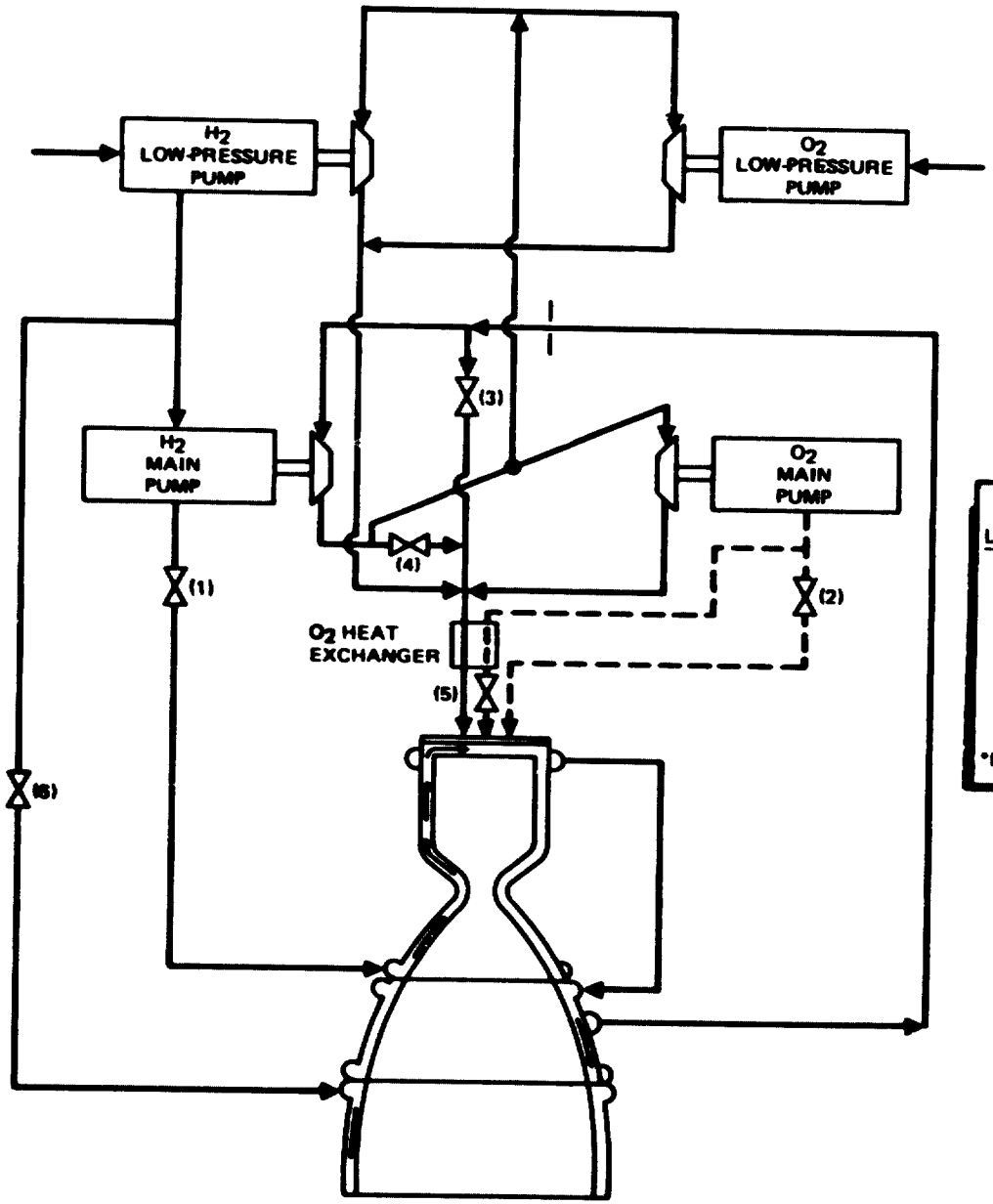

LEGEND:

(1) MFV	–	MAIN FUEL VALVE
*(2) MOV	–	MAIN OXIDIZER VALVE
*(3) TBV	–	TURBINE BYPASS VALVE
*(4) OTBV	–	OXIDIZER TURBINE BYPASS VALVE
(5) GOV	–	GASEOUS OXIDIZER VALVE
(6) DFV	–	DUMP FUEL VALVE

*MODULATED VALVES

Figure 6. Advanced Expander Engine-Control Schematic

TABLE 7. EXPANDER CYCLE ENGINE PERFORMANCE AND CONTROL TYPES

ENGINE CONTROL CONCEPT	IN-RUN & RUN-TO-RUN		IN-RUN	
	THRUST VARIATION	MR VARIATION	THRUST VARIATION	MR VARIATION
No Controller Mechanical Sequencing	20%	0.8 Units	7%	0.3 Units
Electrical Sequencing No Valve Positive Control	20%	0.8 Units	7%	0.3 Units
Mainstage Trim Controls	2%	0.1 Units	2%	0.1 Units
Full Range Controls	2%	0.1 Units	2%	0.1 Units

As shown by control system trade studies, open-loop control with limited authority trim adds a closed loop to a scheduled open loop control. This control achieves the precision of closed loop for steady-state performance via the trim loop (Table 7). It does not achieve the dynamic response precision of a closed-loop control system because the trim loop is ineffective for large transients. This type of control is thus not effective during start and shutdown.

A closed-loop control is necessary to meet the projected OTV requirements. It has the following advantages:

1. It allows replacement of components (other than the main combustion chamber and injector) without hot-refine of the engine.
2. It minimizes the need for calibrating control valves and actuators.
3. It maintains performance even with a change in operating characteristics of components, thus enhancing engine capability to exceed required life.

Engine Controller Functions

The closed-loop engine control system selected (Fig. 7) provides the elements of sensing and monitoring engine performance, the electronic controller (one of whose functions is to generate electronic commands to modulate and sequence the valves), the final control elements (valves) to execute those commands, the ignition system, and the electrical harness to interconnect the engine control system.

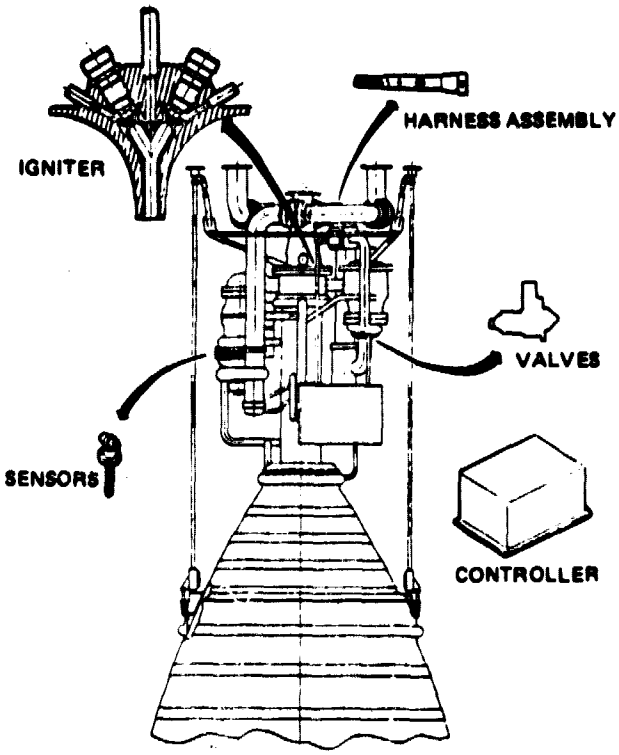

Figure 7. Engine Control System

The control of the engine and its operating modes during start, mainstage and shutdown account for approximately 11 percent of the functions required of the engine controller and control system. Other major function categories comprise the following percentages of the total function; Checkout and Status Monitoring 34%, Input/Output Data Processing 21%, and Protection of Engine and Man-Rated Capability 34%.

Checkout and status monitoring includes those functions starting during engine preparation for flight and continuing during engine operation. They ascertain the viability of each component to operate and to continue operating during the flight. The input/output data processing includes all those listed

functions for engine maintenance and performance evaluation, the processing of commands and monitoring of status, failures and initial conditions. The protection of engine and manrated capability group includes all the functions concerned with safe and reliable operation of the engine. It is believed that all of these functions must be present in the OTV engine control system to provide the reliability required of this reusable engine as used in the OTV manned missions. The man rating and safety requirements for the OTV cannot be met without the engine control, engine health monitoring and checkout provided by the controller.

ENGINE OPERATION

Engine starts to full thrust are effected from idle mode conditions. Idle mode occurs in two stages. The first, tank-head-idle, provides pump and system conditioning flows under existing tank vapor pressures. The second, pumped idle mode, provides autogeneous pressurization of the propellant tanks enabling the engine pumps to obtain required NPSH during mainstage operation.

Tank Head Idle

In tank-head idle the main propellant pumps are restrained from rotation while the low pressure pumps are allowed to operate and aid in the delivery of flow for thermal conditioning of the system. Initial trade studies indicate that it is desirable to have gas driven boost turbines which can start the boost pumps ahead of the main pumps to provide the latter with required NPSH and to aid in start conditioning.

Initial tradeoff also indicates that the heat exchanger required to vaporize the liquid oxygen prior to entry into the thrust chamber can be located in the turbine bypass circuit just upstream of the main injector (Fig. 6). The heat exchanger provides stability on the thrust chamber oxygen side during tank head idle. With turbine bypass valves closed in tank head idle, maximum hydrogen flow is routed through the heat exchanger and through the low pressure pump turbines. Further tradeoff in these areas will be performed in the Point-Design Expander Engine Study.

Pump-Fed Idle

Upon completion of pump chilldown and system conditioning, the engine enters the pump-fed idle stage to provide pressurization flow to the propellant tanks. This enables the engine to obtain pump NPSH required for transition to mainstage. To initiate this stage, all valves are opened at rates and to positions which provide for quick engine response and ensure stability of the pumps and coolant jackets during steady-state pump-fed idle conditions. Additional optimization of valve opening and sequencing will be performed using the transient analysis computer model being developed for the Point-Design Expander Engine Study. The main oxidizer valve opening will also receive optimization to provide mixture ratios compatible with system stability and high performance.

Pump-fed idle steady-state thrust is approximately 1800 pounds at a chamber pressure of approximately 200 psia. At this pressure, flow instability is not expected in the thrust chamber coolant jackets. Desired mixture ratios are maintained as high as cooling and power constraints allow (but not greater than 7:1) and will be established during Point-Design Studies. The engine will run in pump-fed idle mode until tank pressures providing NPSH of 2 and 15 are available for the oxidizer and fuel pumps respectively, at which time the engine can receive the mainstage thrust command.

Mainstage start is initiated through pre-established ramping of the turbine bypass and main oxidizer valves. Ramp rates are determined to prevent excessive miture ratio and thrust overshoots in the thrust chamber. Optimization of valve opening rates will be performed in the Point-Design Study with the transient model to achieve thrust chamber pressure and temperature environments compatible with engine prescribed cycle life. Engine shutdown transient requirements and valve operation will also be examined to obtain satisfactory results for maintaining engine life.

ENGINE BALANCE AND PERFORMANCE

A detailed power and flow balance point at design mixture ratio of 6:1 and at off-design mixture ratio of 7:1 is presented in Table 8 for the selected concept. System operating pressures at design mixture ratio are indicated in pressure-budget schematic in Fig. 8.
Important features of the balance include:

- 10 percent fuel flow and 10 percent pressure drop reserves
- Full-flow regenerative cooling of both combustor and nozzle
- Dump-flow cooling of retractable nozzle
- Series main turbine arrangement
- Three-stage fuel pump and single-stage oxidizer pump
- Hydrogen gas driven low-pressure pumps

This design is the result of optimization to maximize engine specific impulse with resulting design values for chamber pressure, nozzle area ratio, and nozzle percent length for an engine retracted length of 60 in. The engine dimensions are depicted in Fig. 9. Delivered engine performance at on- and off-design mixture ratio according to JANNAF performance loss breakdown procedures is detailed in Fig. 10. The performance in Fig. 10 has as starting point, the theoretical one-dimensional equilibrium performance of the propellants reacted at the conditions existing in the tanks. To this base performance, the effects of the propellant heating, pressurization, combustion, friction, divergence, and leakage losses are superimposed. Combustion, kinetic and nozzle divergence losses amount to 7.6 seconds and are broken down as shown in Fig. 10a. These losses have been verified through correlation with measured AST performance. The effects of regenerative heating of the propellants and reduction of entropy during the expansion process in the nozzle appears in the net regenerative heat gain and boundary layer loss terms. These are the two larger contributions to the performance. The difference between these two terms (1.77 seconds) reflects the interaction between regenerative heating and friction drag. Pump leakage losses and the improved specific impulse effect of heating and dumping hydrogen in the dump coolant nozzle are included in the dump and leakage loss of 1.14 second. The delivered engine specific impulse is 482.5 sec.

TABLE 8. ENGINE DESIGN POINT BALANCE

Design Variables	MR = 6 Values	MR = 7 Values
General		
Thrust, lbf	15,000	15,000
Chamber Pressure, psia	1610	1568
Mixture Ratio, Engine	6:1	7.0:1
Mixture Ratio, Thrust Chamber	6.45:1	7.58:1
Specific Impulse (Engine), seconds	482.5	474.3
Specific Impulse (Thrust Chamber), seconds	483.4	475.0
Engine Fuel Flowrate, lb/sec	4.44	3.95
Thrust Chamber Fuel Flowrate, lb/sec	4.12	3.64
Engine Oxidizer Flowrate, lb/sec	26.62	27.67
Thrust Chamber Oxidizer Flowrate, lb/sec	26.58	27.63
Dump Coolant Fuel Flowrate, lb/sec	0.2c	0.28
Turbomachinery		
Low-Pressure Oxidizer Pump Speed, rpm	6889	6921
Low-Pressure Oxidizer Pump Efficiency	0.71	0.70
Low-Pressure Oxidizer Pump Horsepower	9.76	10.03
Low-Pressure Oxidizer Pump Inlet Pressure	16.33	16.33
Low-Pressure Oxidizer Pump Outlet Pressure	86.33	86.33
Low-Pressure Oxidizer Pump Diameter, inches	3.18	3.18
Low-Pressure Fuel Pump Speed, rpm	28,546	26,367
Low-Pressure Fuel Pump Efficiency	0.71	0.71
Low-Pressure Fuel Pump Horsepower	20.45	15.92
Low-Pressure Fuel Pump Inlet Pressure, psia	18.82	18.82
Low-Pressure Fuel Pump Outlet Pressure, psia	73.82	67.0
Low-Pressure Fuel Pump Diameter, inches	2.73	2.73

TABLE 8. ENGINE DESIGN POINT BALANCE

Design Variables	MR = 6 Value	MR = 7 Value
General Turbomachinery		
High-Pressure Oxidizer Pump Speed, rpm	58,111	58,360
High-Pressure Oxidizer Pump Efficiency	0.723	0.722
High-Pressure Oxidizer Pump Horsepower	351.	363
High-Pressure Oxidizer Pump Outlet Pressure, psia	2662	2638
High-Pressure Oxidizer Pump Diameter, inches	2.2	2.2
High-Pressure Fuel Pump Speed, rpm	107,141	98,937
High-Pressure Fuel Pump Efficiency	0.58	0.57
High-Pressure Fuel Pump Horsepower	1749	1349
High-Pressure Fuel Pump Outlet Pressure, psia	4542	3920
High-Pressure Fuel Pump Diameter, inches	3.50	3.50
High-Pressure Oxidizer Turbine Diameter, inches	4.70	4.70
High-Pressure Oxidizer Turbine Flowrate, lb/sec	2.92	2.92
High-Pressure Oxidizer Turbine Admission, %	20	20
High-Pressure Oxidizer Turbine Tip Speed, ft/sec	1333	1339
High-Pressure Oxidizer Turbine Velocity Ratio	0.48	0.55
High-Pressure Oxidizer Turbine Efficiency	0.68	0.67
High-Pressure Oxidizer Turbine Pressure Ratio (total-to-total)	1.16	1.16
High-Pressure Fuel Turbine Diameter, inches	3.10	3.10
High-Pressure Fuel Turbine Flowrate, lb/sec	3.70	3.26
High-Pressure Fuel Turbine Admission, %	37	37
High-Pressure Fuel Turbine Tip Speed, ft/sec	1600	1478
High-Pressure Fuel Turbine Velocity Ratio	0.44	0.40
High-Pressure Fuel Turbine Efficiency	0.70	0.69
High-Pressure Fuel Turbine Pressure Ratio (total-to-total)	1.64	1.52
Cooling Jacket		
Combustor Coolant Flowrate, lb/sec	4.12	3.64
Combustor Coolant Pressure Drop, psid	411	323
Combustor Heat Input, Btu/sec	10,813	10,134
Combustor Exit Temperature, R	807	842
Nozzle Coolant Flowrate, lb/sec	4.12	3.64
Nozzle Coolant Pressure Drop, psid	7.0	5.0
Nozzle Heat Input, Btu/sec	2027	1893
Nozzle Exit Temperature, R	955	990

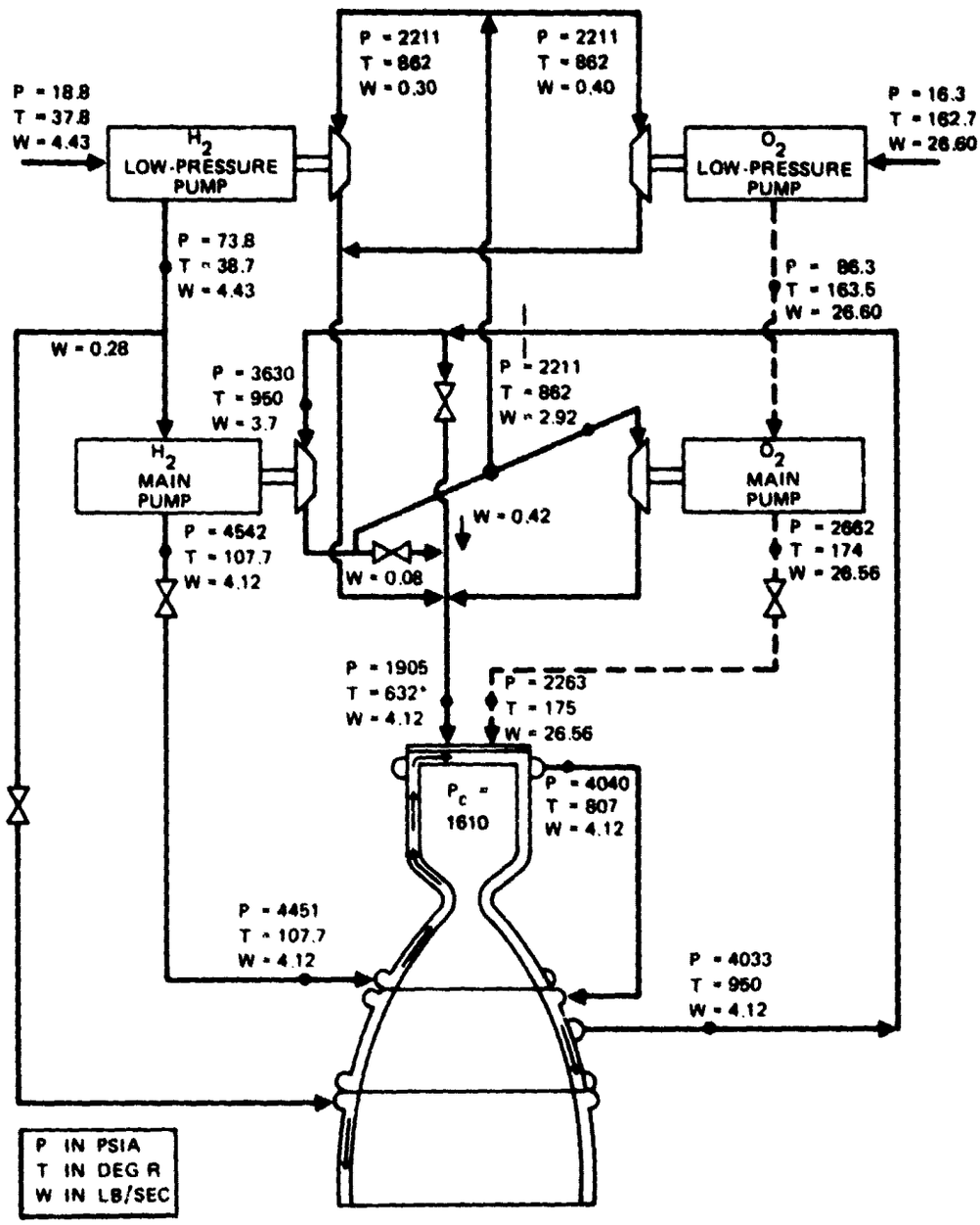

Figure 8. Baseline Engine Pressure, Temperature, and Flowrate Budget

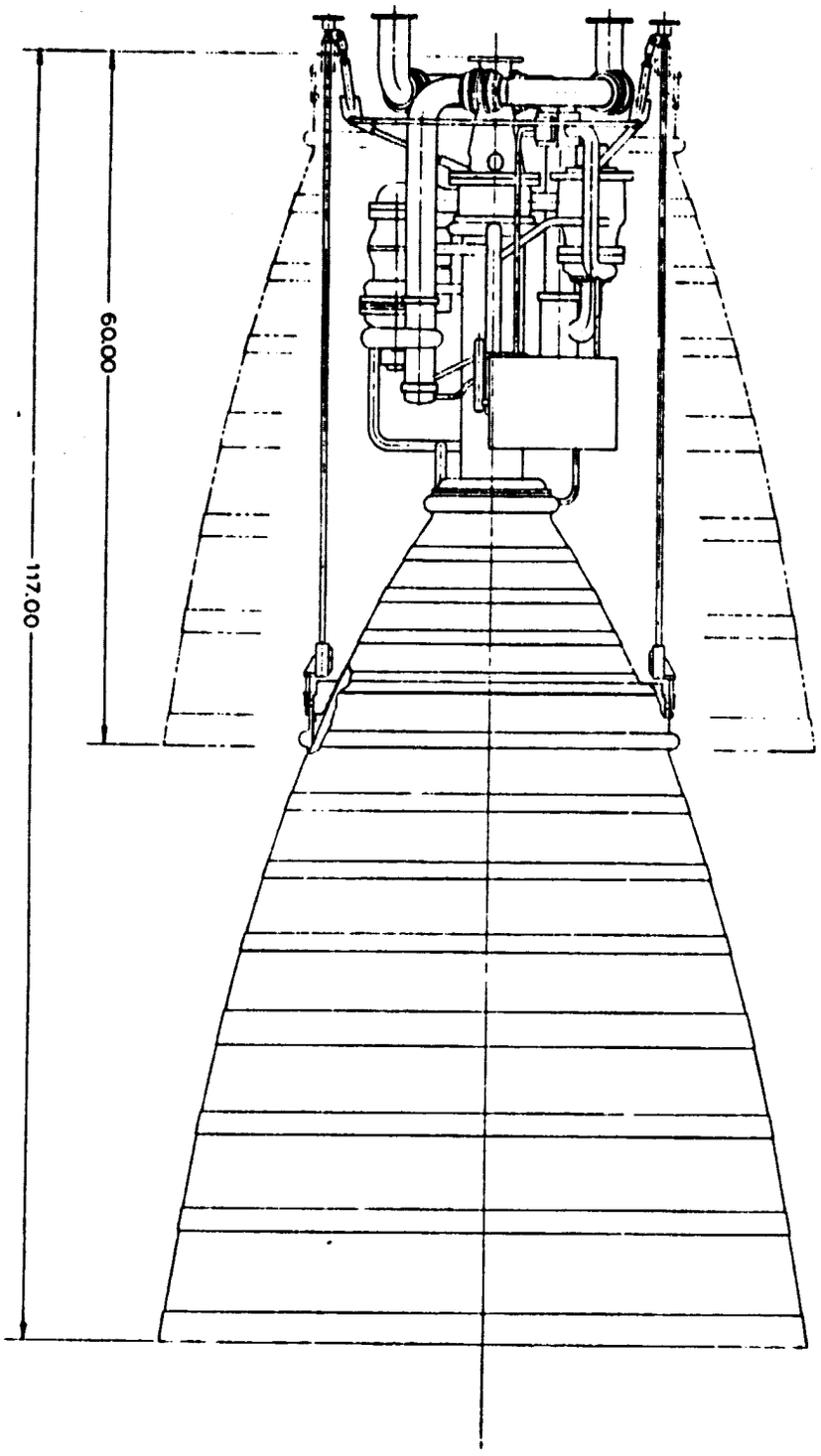

Figure 9. Engine Geometry

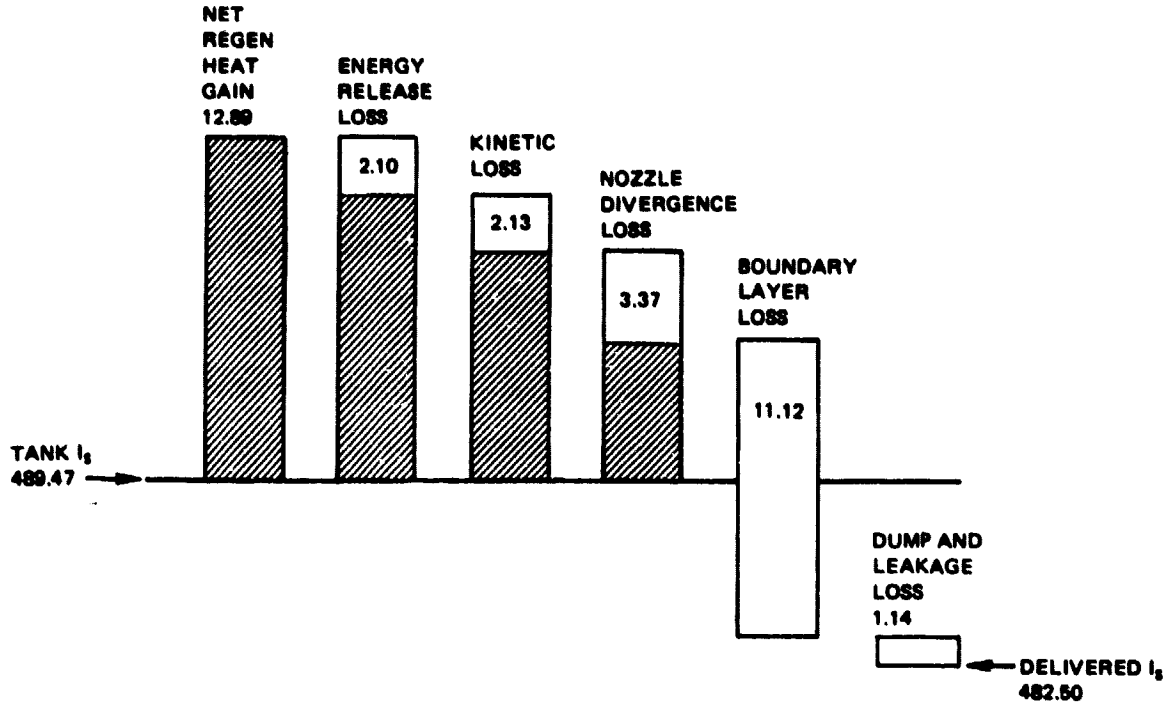

a. MR = 6:1

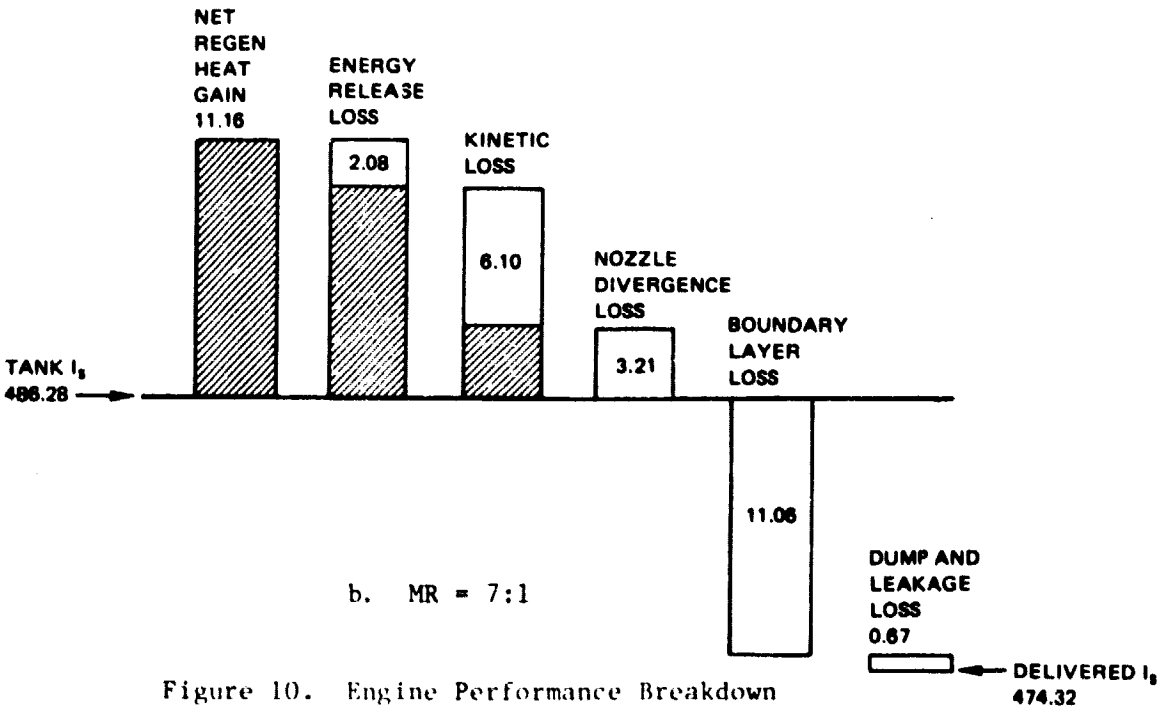

b. MR = 7:1

Figure 10. Engine Performance Breakdown

Off-Design Engine Performance

Off-design engine performance is indicated in Fig. 10b. The engine operates at the same thrust at off-design mixture ratio of 7:1 as it does at design mixture ratio of 6:1. Constant thrust is accomplished with the thrust and mixture ratio control valves. The engine delivers 474.3 seconds of specific impulse. The major difference between the on-design and off-design performance is in the kinetic loss which is approximately 3 times higher at off-design, because of the higher thrust chamber mixture ratio: 6.45 for design, 7.58 for off-design.

SECTION II - DETAILED DISCUSSION OF TASK 8 STUDY RESULTS

In Task 8, engine performance optimizations were conducted to select the engine configuration recommended for the Advanced Point Design Engine Study. These optimizations were performed in the range of thrusts of 10K - 20K lbs. Parameters considered in the performance optimization are shown in Table 3. Engine configurations and component concepts were chosen on the basis of performance maximization with particular attention to reduction of overall mission risks. Trade studies were conducted to evaluate associated risks through assessment of aspects indicated in Table 4. These studies were used to guide the selection of the engine configuration.

POWER CYCLE CONFIGURATION

Four major areas of power cycle configuration optimization were examined: main turbine arrangement, cycle energy source, high pressure pump design, and boost pump drive. Cycle configurations resulting from the first two areas were parallel main turbines, series main turbines, turbine gas regeneration, and turbine gas reheat. These cycles and combinations thereof are illustrated in Fig. 11. These cycle configurations were evaluated in conjunction with smooth-wall combustors and with thermally-enhanced combustors. In each case, combustor length was allowed to vary between the limits of 10-26 inches. The lower limit represents the length of a conventional combustion-performance optimized combustor. The upper limit was set by the smooth-wall chamber bulk temperature limit (1000 R) determining wall material temperature limits desired for required combustor life.

Main Turbine Arrangement

The main turbine arrangements of series and parallel were evaluated with the first two cycle configurations indicated in Fig. 11. All the combustors used in this evaluation used thermal enhancement. The cycle optimizer code was allowed to optimize engine specific impulse under the following constraints;

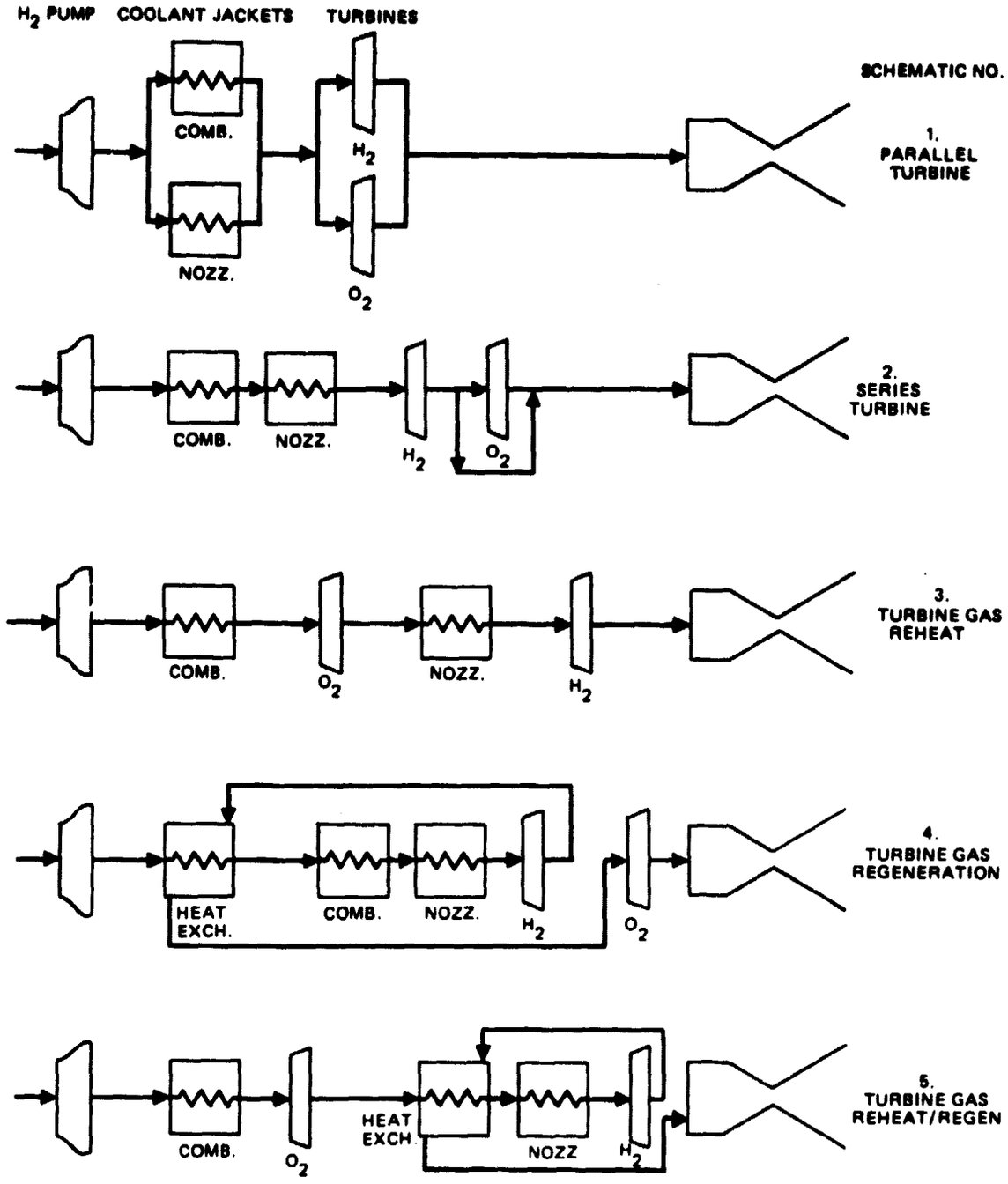

Figure 11. Expander Engine Schematics

bearing DN, turbine and pump geometry relating to 1980 state-of-the-art; combustor length limits of 10 to 20 inches; coolant jacket bulk temperature limits of 1000 R and 1260 R, respectively, for combustor and nozzle; and certain flow and pressure drop margins to be discussed in another section. The optimizer was allowed to vary nozzle expansion area ratio, pump speed, chamber pressure, pressure ratio and combustor length to arrive at an optimum delivered specific impulse and a corresponding chamber pressure. Results for the series versus parallel turbine case, for a thrust level of 15,000 lb, can be seen in Fig. 11a by comparing the first two cycle configurations shown. The series turbine arrangement attains approximately 230 psi higher in chamber pressure than the parallel turbine arrangement. The reason for this is that more flow is available to each turbine in the series configuration than in the parallel arrangement. The higher flowrate allows higher turbine power. It allows also higher volume flow in the turbines and, therefore, improved turbine efficiencies and higher turbine arc of admission. The higher chamber pressure in the series turbine arranged engine results in higher nozzle expansion area ratio and thus approximately 2 seconds higher specific impulse.

Turbine Gas Reheat and Regeneration

The same procedure and constraints used in the main turbine arrangement studies were used to evaluate the turbine gas reheat and turbine gas regeneration concepts. The turbine gas regenerator was placed either upstream of the combustor coolant jacket or between the combustor and nozzle coolant jackets as illustrated in Fig. 11.4 and 11.5. The evaluation of the gas reheat and regeneration cycles was carried out with two groups of cases. In one group the combustor length was not allowed to optimize and was instead given discrete values and a maximum permissible length of 20 inches. Thus the maximum coolant bulk temperatures were not attained in all cases. Both the smooth wall combustor and the thermally enhanced combustor were evaluated.

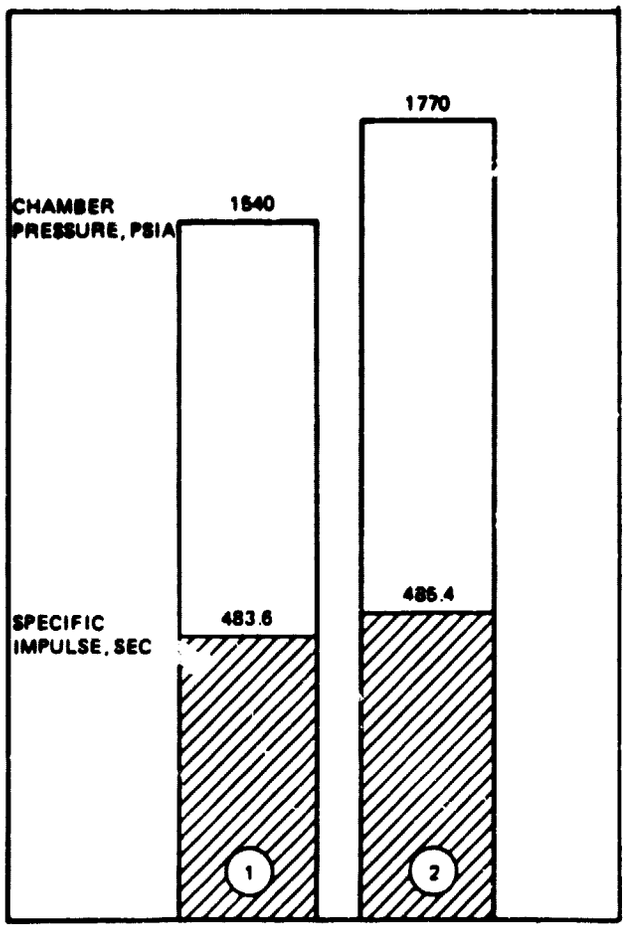

Figure 11a. Chamber Pressure and Specific Impulse for Parallel and Series Turbine Cycles

Smooth Wall Combustor. The nozzle outlet temperature (turbine inlet temperature) for these cycles is shown in Fig. 12 as a function of combustor length. It is seen that a smooth wall combustor achieves a maximum turbine inlet temperature of 877 R at a length of 20 inches. In a regenerative cycle configuration (with heat exchanger) the smooth wall combustor achieves 928 R turbine inlet temperature at the full 20-inch combustor length. The heat loads for these cases are shown in Fig. 13. As length increases, the smooth wall combustor heat loads and nozzle outlet temperatures increase linearly with length.

A heat exchanger cycle increases hydrogen bulk temperature by storing heat from the turbine exhaust and pumping it into the cold hydrogen entering the combustor coolant jacket. With low heat loads from the coolant jackets, the regenerative cycle achieves higher nozzle outlet temperatures than the unregenerated configuration. The heat exchanger cycle increases the nozzle outlet temperature more at the short lengths than at the longer lengths. If the combustor length of the smooth wall chamber were allowed to extend beyond 20 inches, there would be a length where the combustor jacket bulk temperature would be at its 1000 R limit (Fig. 14). At this length, a heat exchanger is obviously not required to obtain the required heat load and bulk temperature limit, so that the curves with and without a heat exchanger will coincide. Extrapolation of the data in Fig. 14 indicates this will happen at a smooth wall combustor length of 26 inches. The heat exchanger in the regenerative cycle thus becomes of diminishing significance as the combustor length increases. The combustor length cannot be increased indefinitely without incurring higher specific impulse losses due to lower nozzle percent length, lower nozzle heat loads because of diminishing surface area, and loss of power-packaging volume as the extendable nozzle split plane moves closer to the combustor throat. A combustor length of 20 inches was therefore chosen as upper limit.

The corresponding chamber pressure curves are shown in Fig. 15. Since chamber pressure is a direct function of nozzle exit temperature, it is seen that it increases with the smooth wall chamber length. It is also seen that a regenerative cycle increases chamber pressure more at the shorter chamber lengths. As chamber length approaches 20 inches, the heat exchanger provides chamber pressure gains of less significance (22 psia at 20 inches length). The heat loads at this length (Fig. 13) are lower for the cycle with a regenerative heat

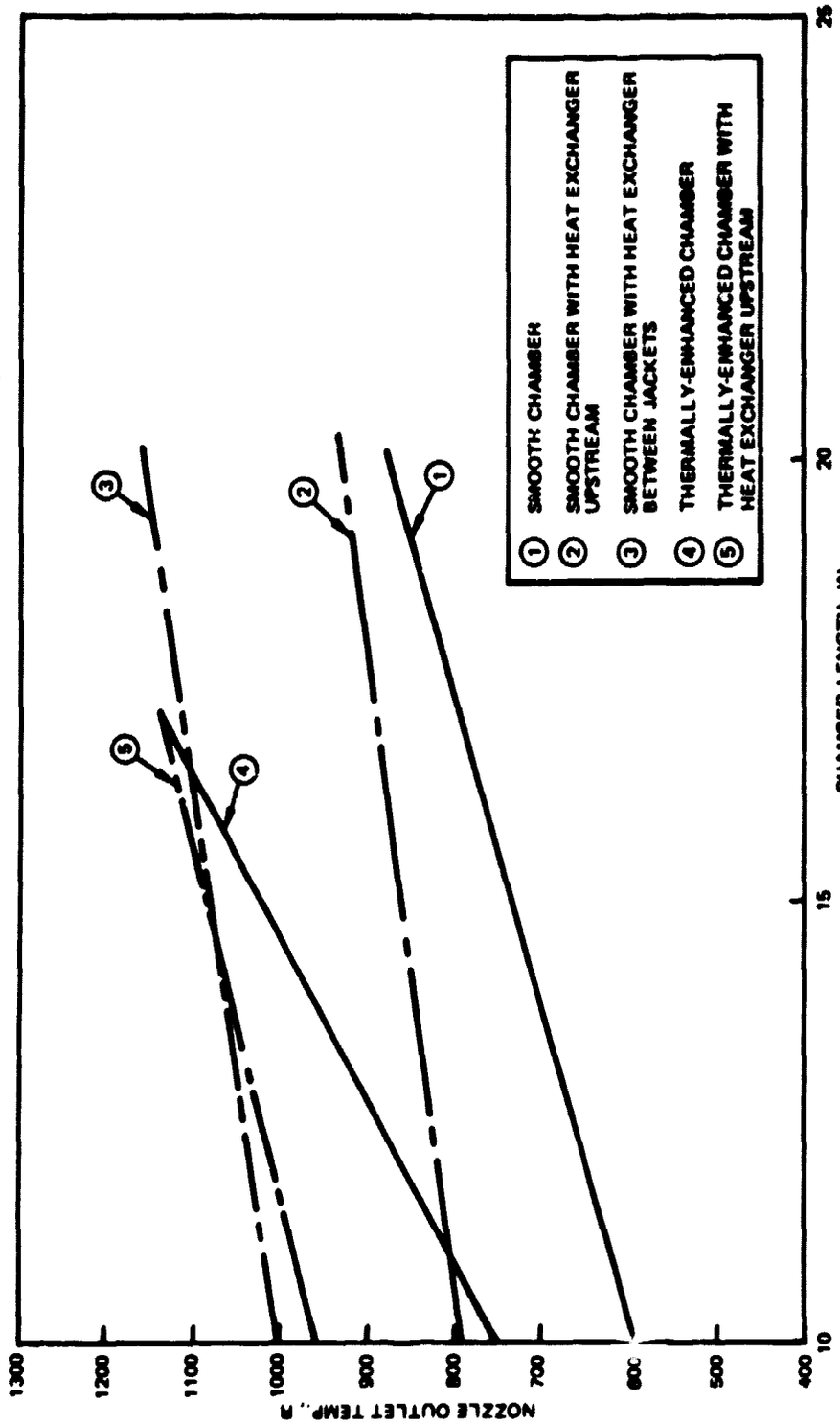

Figure 12. Nozzle Outlet Temperature vs Chamber Length

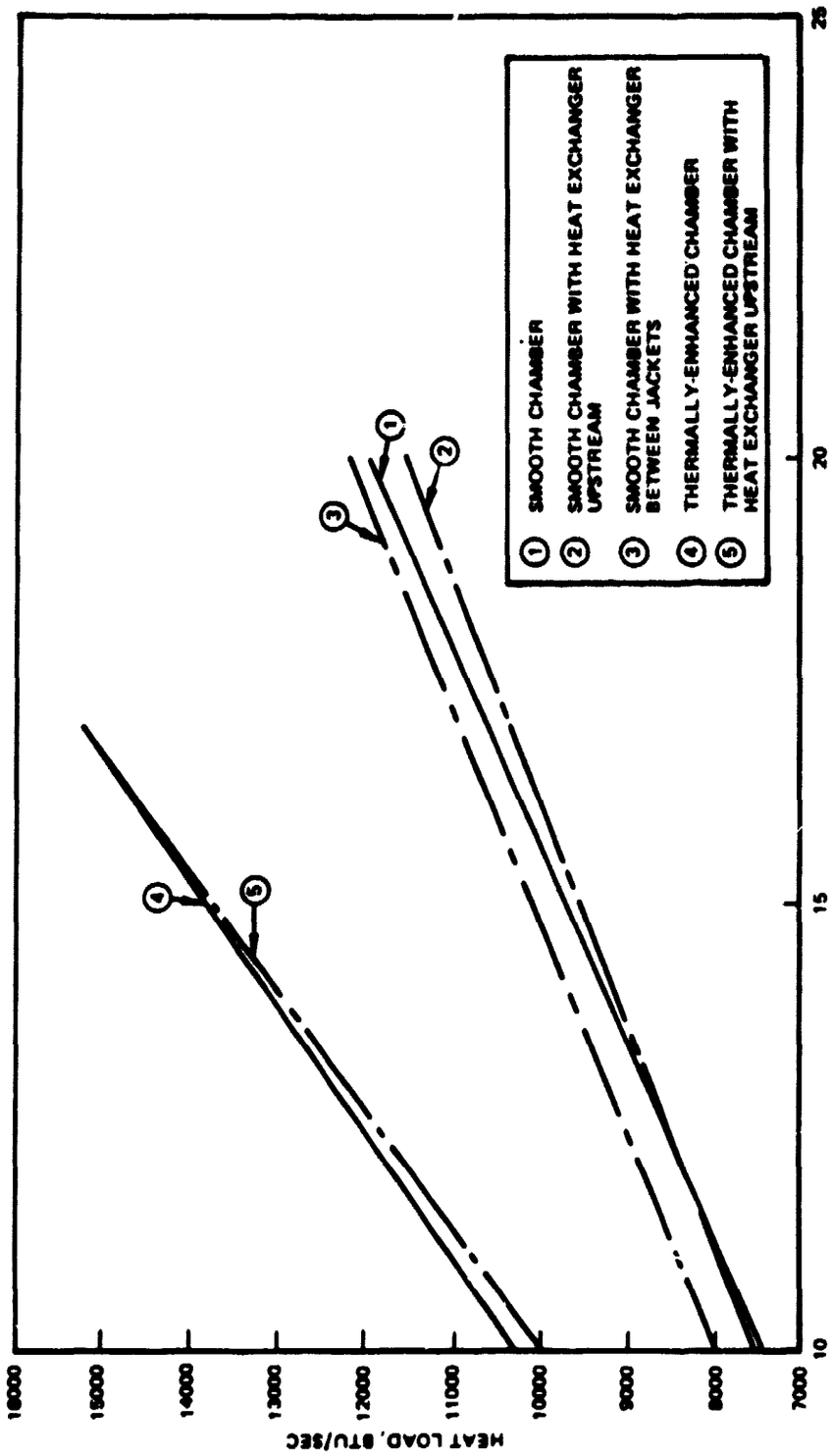

Figure 13. • Heat Load vs Chamber Length

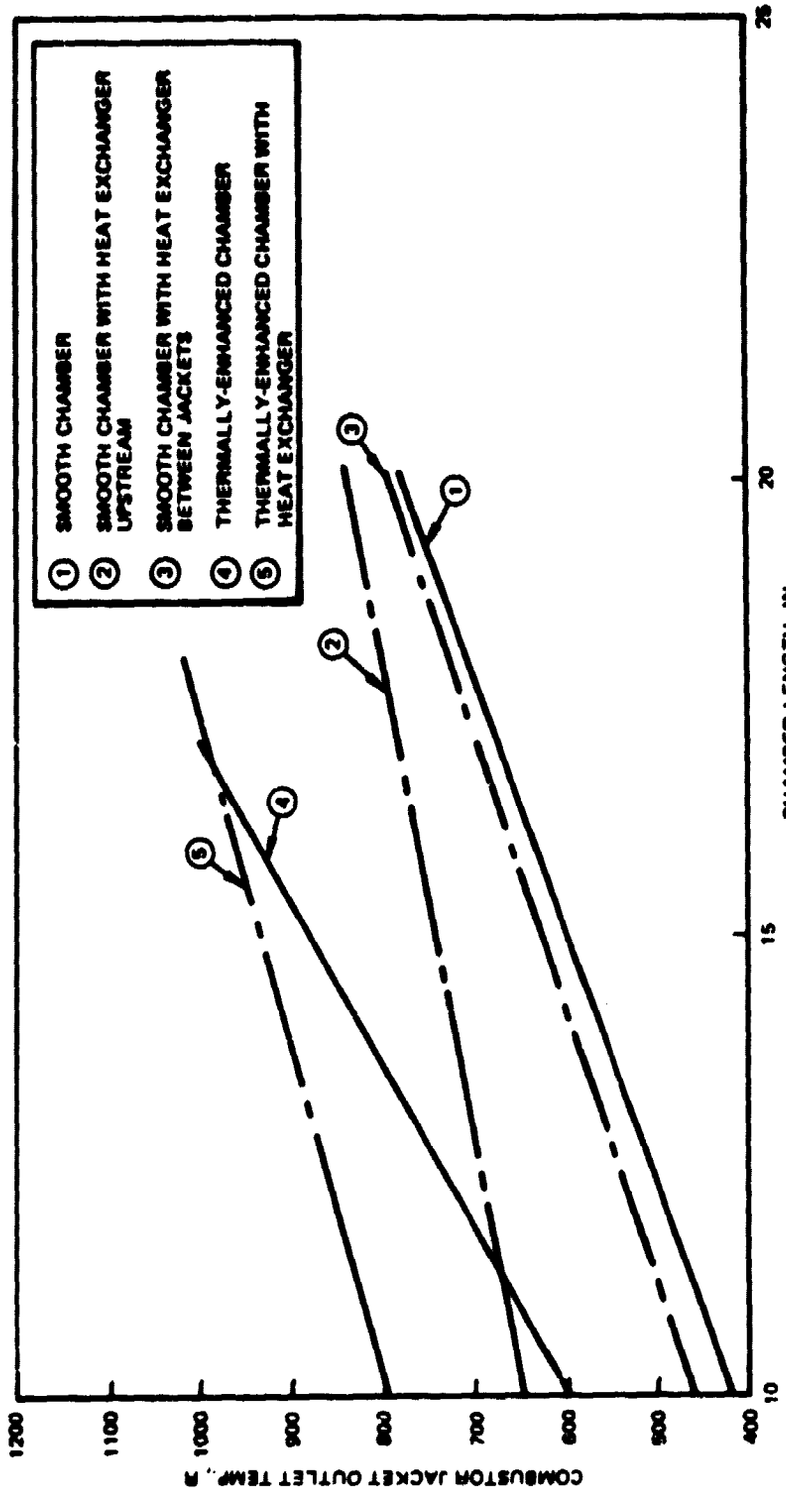

Figure 14. Combustor Jacket Outlet Temperature vs Chamber Length

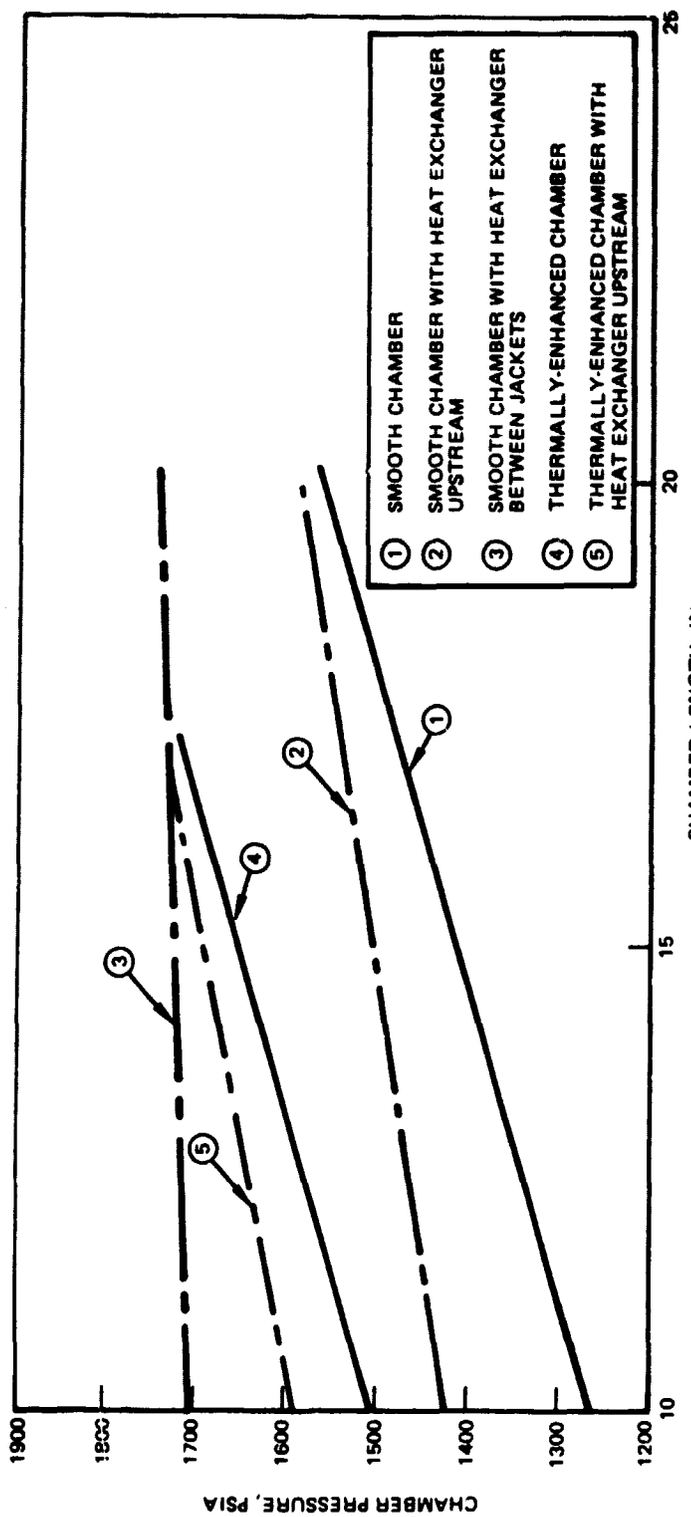

Figure 15. Chamber Pressure Variation with Chamber Length

exchanger than for the cycle without. The reason for this is that the heat exchanger raises the combustor inlet temperature which in turn lowers the combustor heat pickup capability. This is important because specific impulse (unlike chamber pressure) is sensitive to the main injector hydrogen inlet temperature which is lower in the case of the regenerative cycle at a chamber length of 20 inches (Fig. 16). Thus a turbine gas regenerative cycle achieves specific impulse performance equal to that of the non-regenerative smooth wall chamber configuration at a chamber length of approximately 18.5 inches, and at 20 inches its I_s performance is below that of the unregenerated smooth wall combustor (Fig. 17).

For the short length combustors (near 10 inches in length) the limit on the amount of turbine gas regeneration possible is determined by the oxidizer turbine located downstream of the heat exchanger, in the case where the heat exchanger is placed upstream of the combustor coolant jacket. At the short combustor length combustor heat is limited; too large a heat exchanger reduces the inlet temperature of the oxidizer turbine to a level where the cycle power balance is no longer possible. Therefore, the oxidizer turbine limits the size of the heat exchanger by placing a limit on the fuel turbine inlet temperature which, in turn, limits the chamber pressure attainable.

The performance of the smooth wall combustor with regenerative heat exchanger between combustor and nozzle jackets is shown in Fig. 17. The cycle configuration schematic is shown in Fig. 11. Since the bulk temperature limit is that of the nozzle (1260 R), the achievable turbine inlet temperatures are higher with this regenerative heat exchanger cycle. The chamber pressures and hydrogen inlet temperatures at the injector are also higher than with the unregenerated smooth-wall chamber, and thus the engine delivered I_s is higher by approximately 1.4 seconds.

The location of the oxidizer turbine in this case is downstream of the combustor and outside of the fuel turbine gas regeneration loop. Ample energy is available to the oxidizer turbine and it does not become cycle power limiting as in the case where the heat exchanger was placed upstream of combustor coolant jacket.

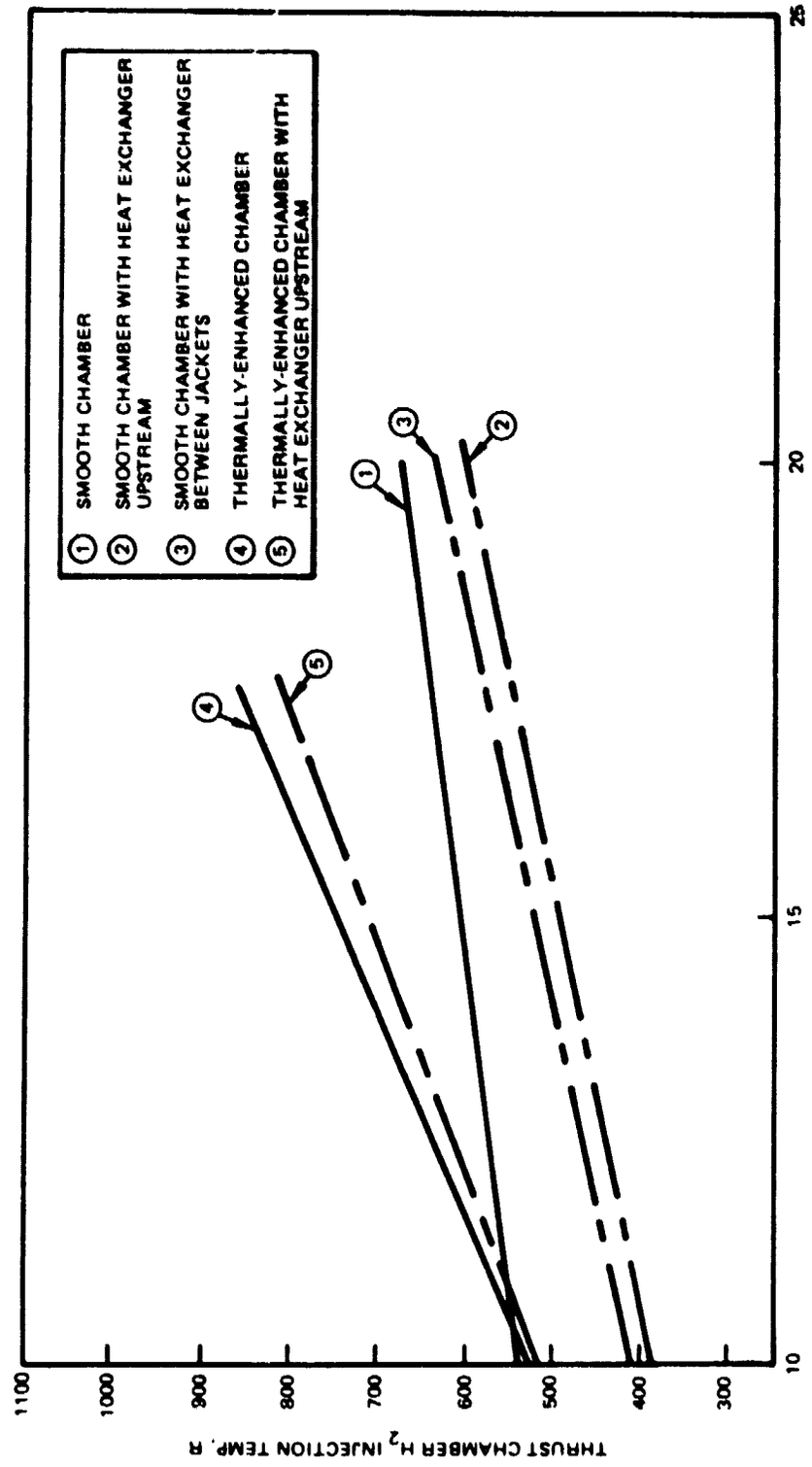

Figure 16. H_2 Injection Temperature vs Chamber Length

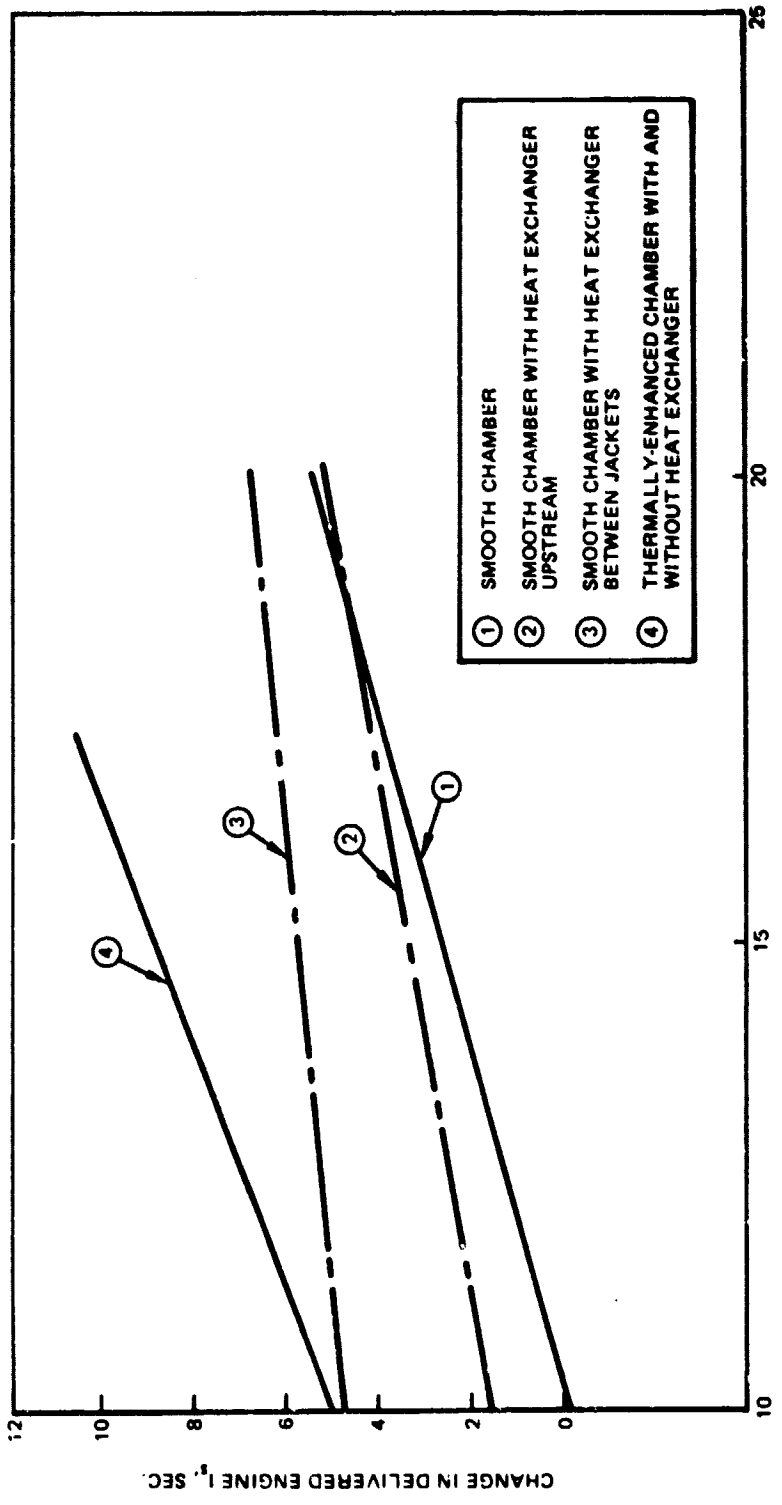

Figure 17. Performance Variation with Chamber Length

The weight of the heat exchanger required between coolant jackets is, however, high because of the low densities of the hydrogen at the combustor outlet bulk temperature. A regenerative heat exchanger weight of 120 lbs. was calculated. The weights of the heat exchangers when placed upstream of the combustor jacket were one order of magnitude less.

Expansion Area Ratio Effects. As chamber length is increased in the smooth wall combustor from 10 to 20 inches, nozzle expansion area ratio is affected by the increasing chamber pressure and the decreasing nozzle length. For the smooth wall chamber without a regenerative heat exchanger, the increase in nozzle area ratio caused by the chamber pressure increase more than compensates for the reduction in area caused by the combustor length increase and corresponding reduction of nozzle length. Therefore, at the 20 inch combustor length a gain in area ratio (Fig. 18) has been obtained and also a gain in hydrogen injector inlet temperature with a resultant gain of 5.6 seconds (Fig. 17) in specific impulse.

When a regenerative heat exchanger is used upstream of the combustor jacket, the gain in nozzle area ratio with chamber pressure (as combustor length is increased from 10 to 20 inches) is not sufficient to cancel the loss in nozzle area ratio caused by the 10 inch reduction in nozzle length. The nozzle at the 20-inch combustor length, has a lower area ratio and a lower hydrogen injection temperature and, therefore, a lower specific impulse, Fig. 17. With a heat exchanger placed between the coolant jackets the nozzle area ratio at the 20 inch combustor length point is also lower than for the 10 inch combustor length case but the hydrogen injector inlet temperature is higher and thus a gain of 1.4 sec. of specific impulse is obtained.

Thermally-Enhanced Combustor. The thermally-enhanced chamber reaches the combustor jacket bulk temperature limit of 1000 F at a length of 17.1 inches (Fig. 14). At this length, it also achieves its highest heat load, highest nozzle hydrogen outlet temperature, highest chamber pressure, and highest I_s. The I_s is 10.5 sec. higher than the conventional 10 inch length smooth wall chamber configuration.

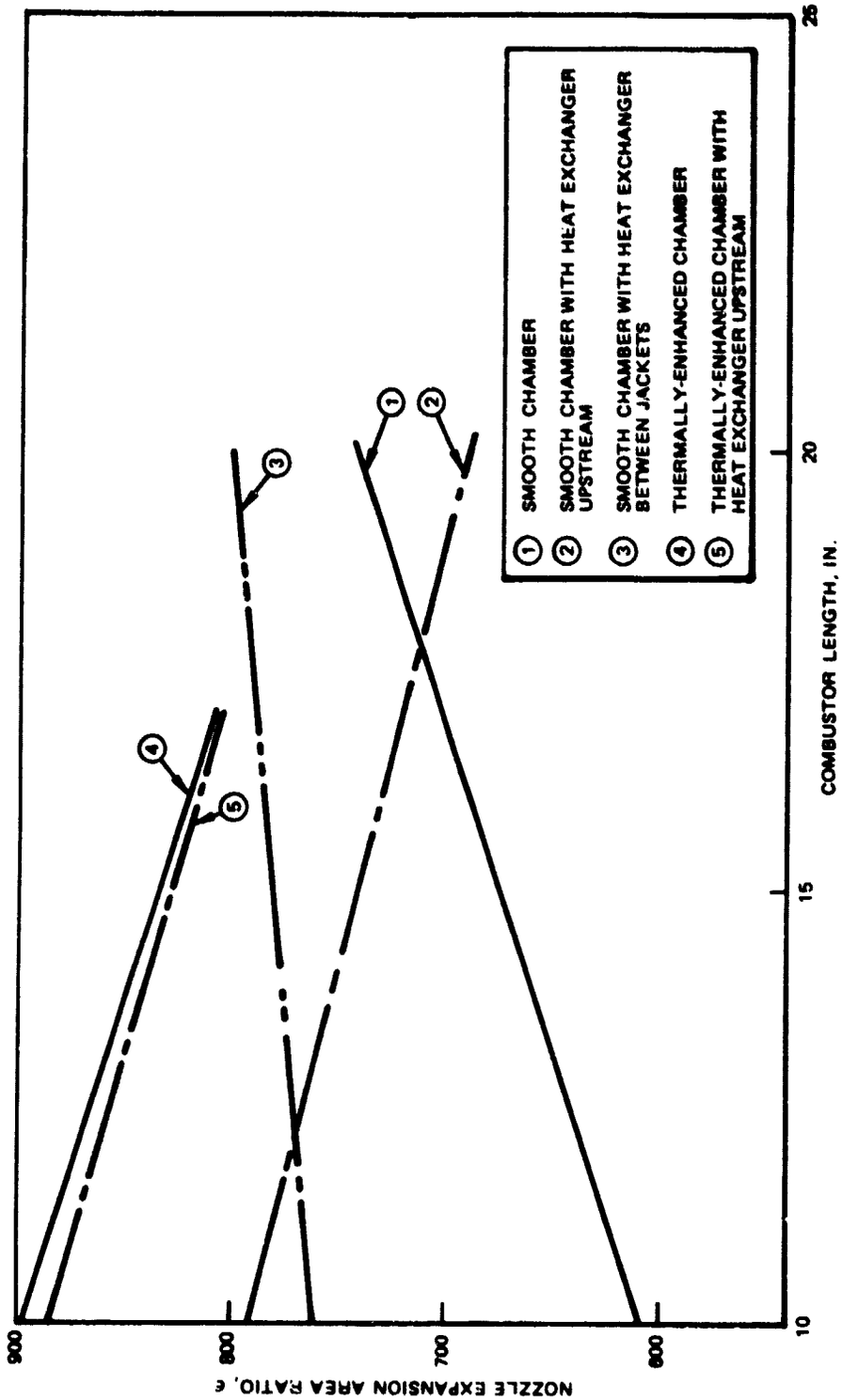

Figure 18. Nozzle Expansion Area Variation with Chamber Length

Between the combustor lengths of 10 and 17 inches, the thermally-enhanced chamber configuration loses more nozzle area ratio from the increase in chamber length, than it gains from the increase in chamber pressure (Fig. 18). The gain obtained in delivered engine specific impulse in the combustor length range 10-17 inches is mostly the result of the increase in fuel injection temperature (Fig. 16).

When the enhanced chamber engine configuration is provided with a heat exchanger upstream of the combustor coolant jacket, the nozzle outlet temperature is increased considerably for the short, 10 inch long combustor. This causes a moderate increase in chamber pressure, but at the same time a reduction in combustor jacket heat load, because the fuel inlet temperature increase reduces the heat load pickup capability of the combustor jacket. The overall result is a cancellation of the higher P_c benefits by the lower fuel injection temperature. As a result equal specific impulse values are delivered by the regenerated and the unregenerated thermally enhanced chamber configuration at a chamber length of 10 inches. As chamber length is increased in the regenerated thermally enhanced chamber case, the nozzle outlet temperature gains with combustor length diminish until at a combustor length of 17 inch no gains are obtained. The combustor jacket bulk temperature limit has been reached at this combustor length and the system does not require a heat exchanger for optimization. The optimizer turns the heat exchanger off at the 17 inch combustor length. Chamber pressure gains occurring as a result of the higher nozzle outlet temperatures as combustor length increases from 10 to 17 inches would increase area ratio, but the nozzle length reduction from increasing the combustor length in effect causes an overall reduction of area ratio. The combined result is no increase in specific impulse from the addition of a heat exchanger to the thermally enhanced chamber configuration in the combustor chamber length range of 10-17 inches.

Full-Optimization, Turbine Gas Reheat and Regeneration

The second group of cases to evaluate the turbine gas reheat and regeneration cycles utilized a full-optimization procedure using a thermally enhanced chamber where chamber length optimized within the maximum limit of 20 inches. The turbine gas regenerator in these cases was placed upstream of the combustor coolant jacket, Fig. 11. Results are shown in Fig. 19 for configurations No. 3, 4, and 5. It is seen that the turbine gas reheat cycle (3) attains approximately the same chamber pressure and specific impulse as the turbine gas regeneration cycle (4). The optimization of each of these two cycles results in very high and nearly identical nozzle expansion area ratio, and nozzle length, and therefore, similar specific impulse. The chamber pressure is determined by the maximum combustor coolant jacket hydrogen bulk temperature limit of 1000 R. Since both configurations have thermally enhanced combustors and combustor length is allowed to increase in both, the bulk temperature limits of 1000 R are reached in both configurations, resulting in equal chamber pressures. With nearly equal combustor lengths in each configuration, equal specific impulse is obtained with equal total length restraints (112 inches extended).

With the regenerator placed between the combustor and nozzle coolant jackets (cycle No. 5), the chamber pressure attained is 1774 psia, 38 psia higher than cycle No. 4. Regeneration is performed in the case of cycle No. 5 with the nozzle coolant jacket (Fig. 11) and since this component has higher bulk temperature limits, the turbine inlet temperature attained is 1225 R, 100 degrees higher than in cycle No. 4. The higher chamber pressure results in higher expansion area ratio but only a slightly higher specific impulse (.1 sec). The latter is the result of the nearly flat trend of specific impulse with area ratio at these high chamber pressures, and the fact that specific impulse at a given area ratio does not increase significantly with chamber pressure.

From the above examples, it follows that the maximum hydrogen bulk temperature prior to entry into the turbine determines the chamber pressure for a turbine flow limited cycle like the expander topping cycle. The bulk temperature limit is set by the wall temperature limit of the component just upstream of the turbine and is reflected in the hydrogen bulk temperature limits of 1000 R and 1260 R, respectively, for the combustor and nozzle coolant jackets. As long as sufficient thermal enhancement is provided in the combustor to achieve the imposed bulk temperature limit, any of the cycles defined will reach a maximum specific impulse nearly equal in every case. The thermally enhanced chamber is thus capable of delivering a specific impulse of 485.5 sec at a thrust of 15K lb.

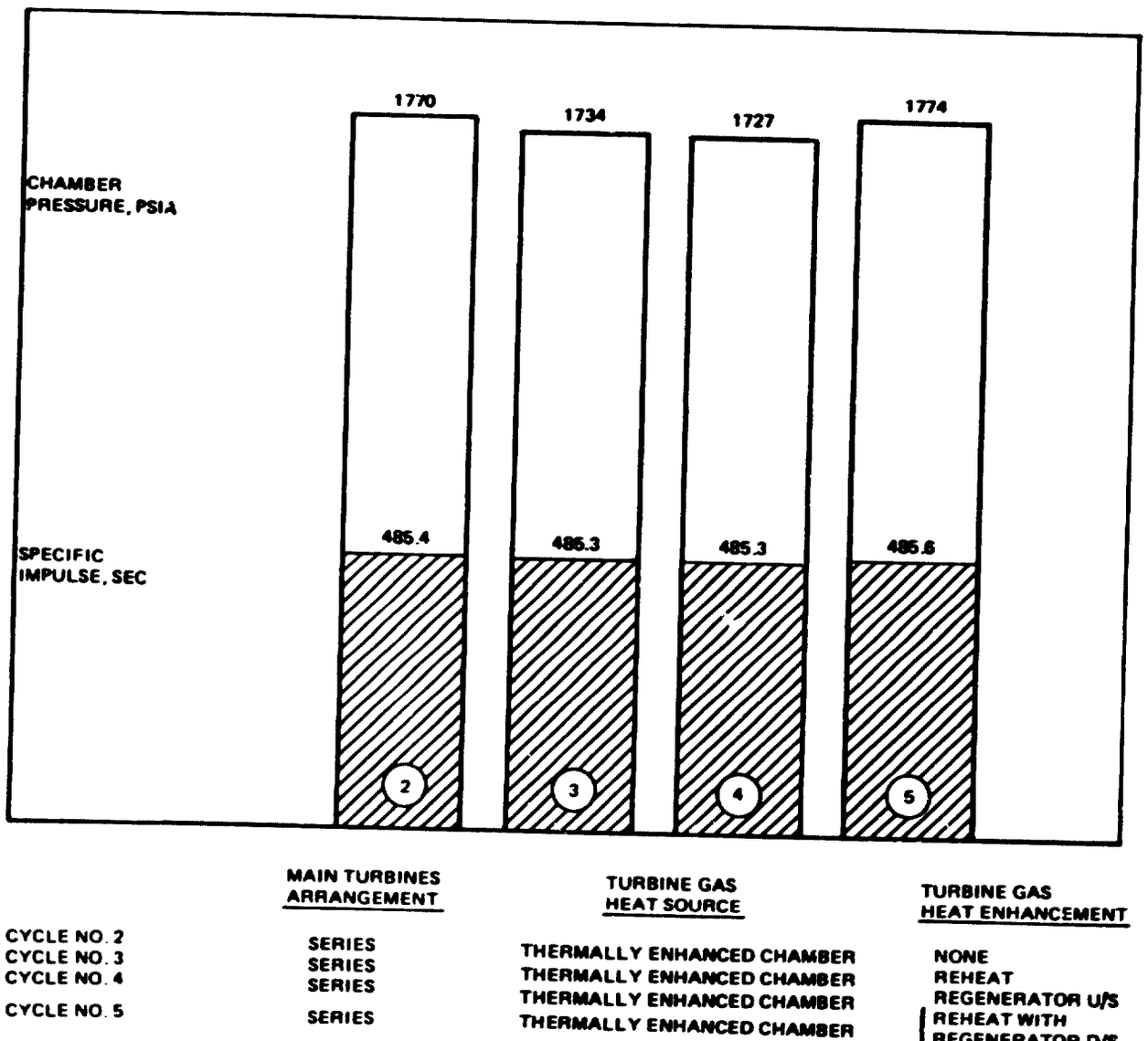

Figure 19. Main Turbine Arrangement and Turbine Gas Reheat and Regeneration @ 15,000 Lb. Thrust

SUMMARY - 15,000-LB THRUST RESULTS

A summary of important performance parameters of the optimization study is presented in Table 9 for the 15,000-lb-thrust level engine using a smooth-wall chamber with and without turbine-gas regenerator. The data are tabulated in the order of ascending specific impulse performance. It is seen that within the total engine length used in the optimization studies of 112 in., the maximum performance of 482.8 sec of I_s is obtained without a turbine gas regenerator at a combustor length of 26 inches, with a chamber pressure of 1663 psia, a nozzle expansion area ratio of 643 and a nozzle percent length of 66.2 percent of ideal. Optimization of nozzle length remains another possible option. Preliminary design studies indicate that gimbal plane-to-injector distances can be optimized as well as nozzle retracting mechanism length and location, all of which will provide efficient utilization of maximum available length. An increase of 10 inches in nozzle length is within the range of possible design improvements to be explored in the Advanced Expander Point Design Engine Study. The resulting improved engine length of 117 inches can provide higher specific impulse (483 sec) with a shorter combustor and nozzle area ratio of 900. Idle mode testing considerations would favor lower expansion area ratios to preclude the possibility of flow separation in the nozzle. Since the nozzle area ratio can be varied about the optimum without a large reduction in specific impulse, a loss of 0.5 sec in specific impulse can be incurred to provide an expansion area ratio reduction to 625 and an improvement in nozzle percent length. Both of these changes provide for ease during idle mode testing by increasing the nozzle exit discharge pressure and the flow inclination at the nozzle discharge plane. This last configuration is recommended for the Point-Design Study. No heat exchanger for turbine gas regeneration is required.

A summary of the thermally-enhanced chamber optimization results is shown in Table 10. It is seen that within the 112-inch engine length restriction a specific impulse of 485.4 sec is predicted without turbine gas regeneration. Engine length optimization as in the case of the smooth wall chamber can add nozzle length (10 in.) and area ratio and the potential of 2.6 sec increase in I_s. For reasons explained in the next section, this was not selected as the primary concept for the Point-Design Study.

TABLE 9. PERFORMANCE TRADE STUDIES AT 15K LB THRUST, SMOOTH-WALL CHAMBER

Turbine Gas Regeneration	Regenerator Location	Chamber Length, in.	Chamber Pressure, psia	Nozzle Area Ratio	Engine Length	Nozzle % Length	Specific Impulse, sec.	Bulk Temperature, R Comb.	Nozzle	Effective H_2-Injection Temp., R
No	-	10	1270	609	112	71.9	474.8	411	589	542.2
Yes	Upstream Comb. Jacket	10	1422	792	112	67.2	476.5	645	797	396.7
Yes	Between Jackets	10	1702	761	112	75.2	478.8	459	1004	419.1
No	-	20	1558	742	112	64.5	480.4	774	976.5	627.2
Yes	Upstream Comb. Jacket	20	1580	688	112	67.5	480.2	829	928	604.5
Yes	Between Jackets	20	1747	799	112	65.8	481.8	793	1160	641.2
No	-	26	1663	643	112	66.2	482.8	1000	1066	776.2
No	-	20	1610	900	117	67.1	483	817	955	682.2
No	-	20	1610	6.5	117	81.1	482.5	798	932	675.2

TABLE 10. PERFORMANCE TRADE STUDIES AT 15K LB THRUST, THERMALLY ENHANCED CHAMBER

Turbine Gas Regeneration	Regenerator Location	Chamber Length, in.	Chamber Pressure, psia	Nozzle Area Ratio	Engine Length	Nozzle % Length	Specific Impulse, sec	Bulk Temperature, R Comb.	Nozzle	Effective H_2-Injection Temp., R
No	-	10	1506	897	112	65	479.8	588	755	537.9
Yes	Upstream Comb. Jacket	10	1591	885	112	67.2	480.1	797	961	522.5
None Req'd.	-	17	1750	807	112	68.1	485.4	1000	1128	816.6

TECHNOLOGY LEVEL

A pictorial representation of the engines considered in the optimization studies is presented in Fig. 20 grouped according to technology level requirements. Specific impulse and engine weight (the parameters which influence payload directly) are shown as well as chamber pressure and area ratio (which affect engine development testing). In the group of engines constituting state-of-the-art technology it is seen that a gain of approximately 8 sec has been achieved above that of the engine with conventional combustor length; within a reasonable nozzle expansion area ratio (625). No technology advances are required to obtain the quoted performance. Chamber pressure (power) margins are provided for contingencies arising from engine-to-engine component performance variations, heat transfer, and system pressure drop. These will be discussed in a subsequent section.

Larger gains in performance can be obtained if technology advances are considered in the areas of improved heat exchangers for turbine gas regeneration and in heat transfer enhancement in the chamber. A moderate gain of 1.4 sec is indicated for the turbine gas regenerative cycle over the performance of the state-of-the-art concepts. Technology advances are required to reduce the size and weight of the heat exchanger so as to maximize the conversion of this performance advantage into payload advantages. With the present calculated heat exchanger weight, a loss in payload (22 lb) results. Exchange factors of 70 lb of payload per sec of I_s and 1 lb of payload per 1 lb of engine weight have been used from Phase A OTV Engine Study results.

A more significant gain in performance of 5 sec and a reduction in engine weight are obtained with the thermally enhanced chamber configuration over the state-of-the-art chambers for a corresponding gain in payload of 357 lbs. This concept, however, requires test verification before it can be implemented, therefore, it is included in the category requiring technology advances beyond the current 1980 level. Because of its potential, this concept is considered an alternate for future growth capability of the selected smooth-wall chamber concept.

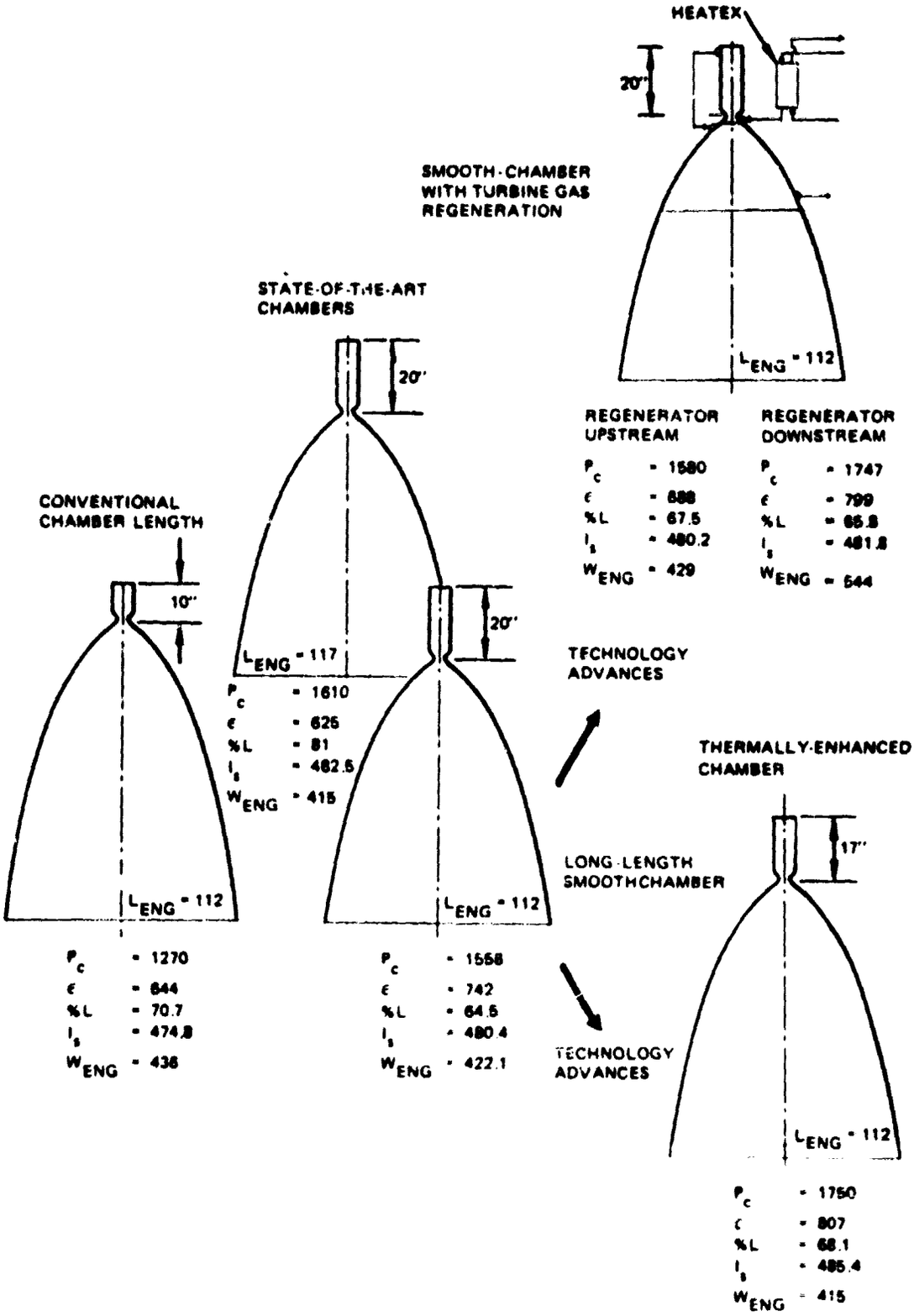

Figure 20. Performance Optimization Studies at 15K Lb

BOOST PUMP DRIVE

A performance trade study was conducted to evaluate the effect of boost pump drive method upon the optimum 15K expander cycle operating point.

One basic schematic was selected for study. Variations in boost drive method were applied to this schematic. The schematic selected was a series main turbine configuration with full-flow regen cooling and no heat exchanger. Fig. 21 shows the basic schematic. This figure is applicable to gear-driven or hydraulically driven boost pumps, because no gas path is shown for the low pressure turbine drive. A typical variant of this configuration is illustrated in Fig. 22, showing gas-driven boost turbines.

Placement of gas-driven boost turbines in this cycle is an important issue. The full-flow regen cooling scheme makes driving the boost turbines from the nozzle coolant jacket less attractive than in the case of split-flow cooling because there is no convenient way of partitioning the hydrogen flow between the boost turbine(s) and main flow. In addition, placing the boost turbine upstream of the main turbine is made difficult due to the lack of sufficient pressure drop to provide adequate boost turbine pressure ratio.

Running the boost turbine(s) downstream of the main fuel turbine and in parallel with the oxidizer turbine solves these problems, and appears attractive because the excess flow available to the oxidizer turbine is utilized. This arrangement was selected for study of the gas-driven boost turbine option.

The five alternate drive methods considered were:

1. Both low pressure turbines gas driven in parallel with the main oxidizer turbine.
2. Low pressure fuel turbine gas driven in parallel with main oxidizer turbine, low pressure oxidizer pump gear driven from high pressure oxidizer pump shaft.

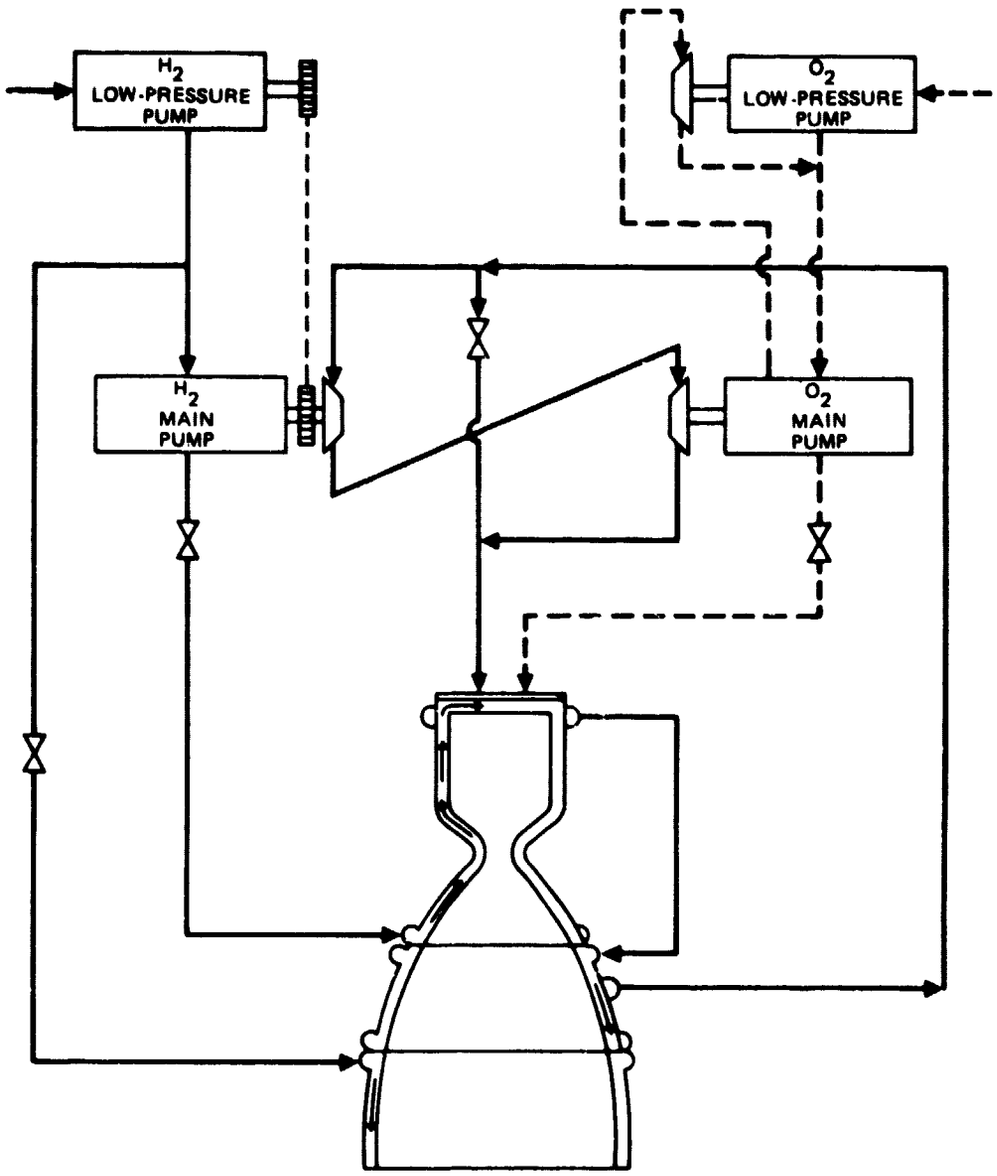

Figure 21. Cycle Schematic, Showing Hydraulic and Gear Boost Pump Drive

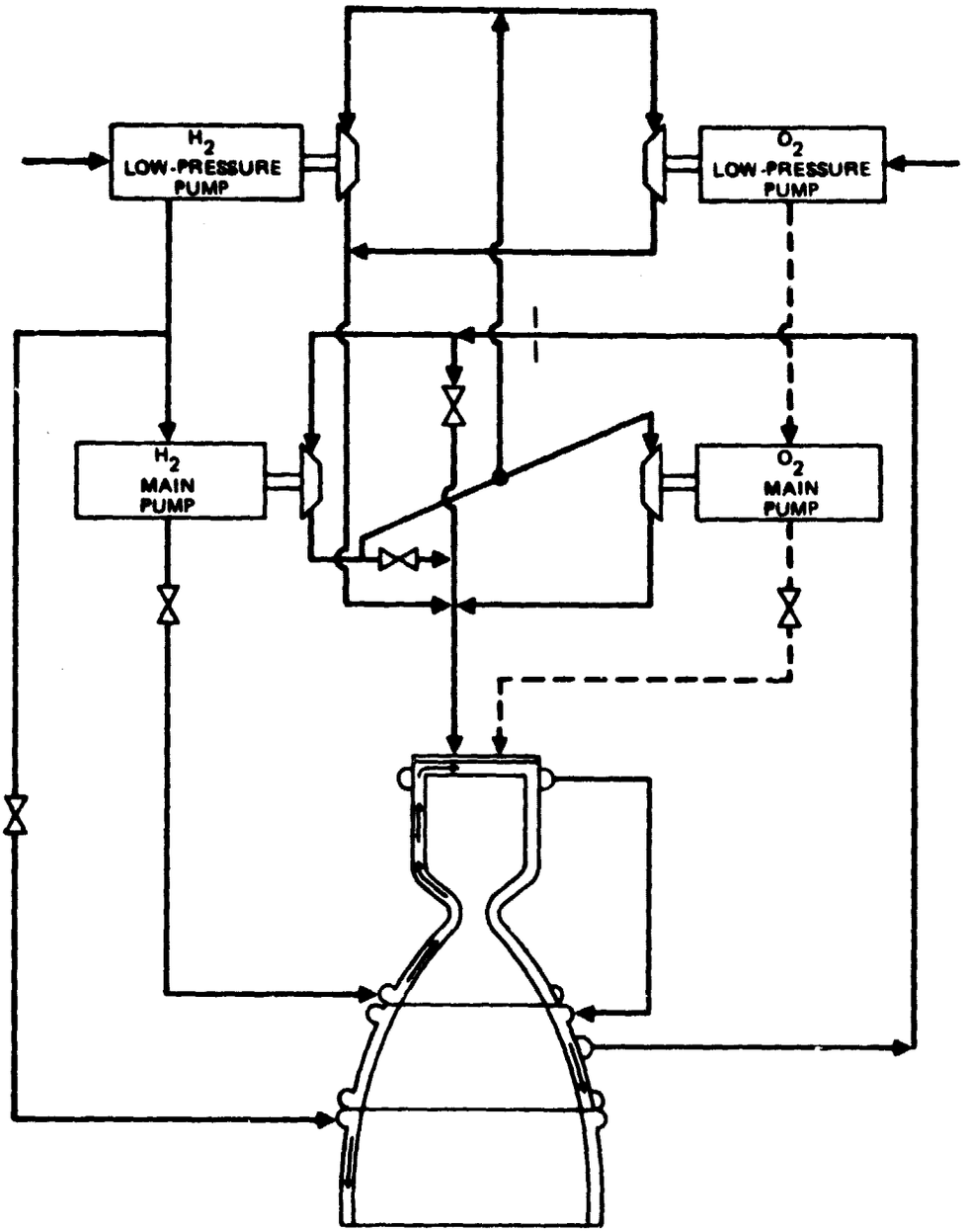

Figure 22. Gas Driven Boost Turbines

3. Low pressure fuel turbine gas driven in parallel with main oxidizer turbine, low pressure oxidizer turbine hydraulically driven

4. Both low pressure pumps gear driven from their respective main pumps

5. Low pressure turbines gas driven in parallel, and in series with main turbines which are also in parallel

The results of specific impulse optimization balance runs conducted for each of these options are summarized in Table 11.

It is apparent that the options (2), (3), and (4) are essentially equivalent in performance. Option (1) is somewhat lower in performance. Option (5) offers the poorest performance, due to pressure-ratio limits imposed by the series-parallel arrangement. Fig. 23 illustrates this arrangement. The pressure ratio of the main turbines are limited in this scheme by the flow requirement of the boost turbines, which are driven by the nozzle coolant gas. As main turbine pressure ratio is increased in response to higher P_c levels, the back pressure on the boost turbines is increased. This reduces the boost turbine pressure ratio, and increases their flow requirement. The system can respond by readjusting the coolant flow split to provide higher nozzle coolant flowrate. Nozzle flowrate is itself limited, however, by the cooling requirements of the combustor. Because of the split-flow cooling scheme, the two jackets compete for coolant flow. When the combustor coolant reaches its bulk temperature limit, no more flow can be diverted into the nozzle. The series-parallel arrangement thus limits chamber pressure to a value lower than that implied by the available power. This fact is illustrated by comparing the present case (gas-driven boost turbines, series-parallel, P_c = 1420) with case (1) Fig. 12 using gear-driven boost pumps. The latter case achieves a chamber pressure of 1540 psi, and a specific impulse of 483.6, approximately three seconds above that of the series-parallel case. However, the differences among all options examined are small in absolute terms.

TABLE 11
BOOST PUMP DRIVE METHODOLOGY STUDY

F = 15K

Case No.	Configuration Description	P_c	I_s	ϵ	P_{DF}	% L
1	LPFT Gas Driven LPOT Gas Driven	1742	485.8	757	4524	71.6
2	LPFT Gas Driven, LPOP Geared	1786	485.9	793	4897	70.6
3	LPFT Gas Driven LPOT Hydraulic	1795	486.0	842	4680	68.6
4	Geared/Geared	1717	485.6	751	4499	71.2
5	Boost Turbines in Parallel, in Series With Parallel-Arranged Main Turbines	1420	480.5	678	3722	71.5

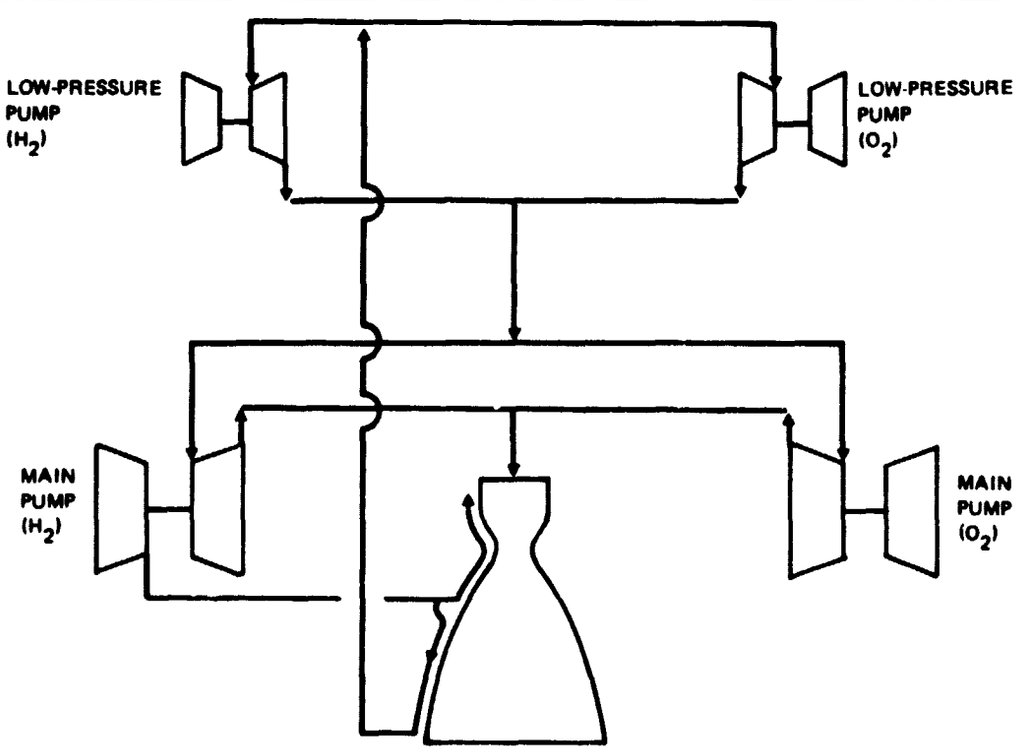

Figure 23. Series-Parallel Turbine Arrangement

POWER AND CONTROL MARGINS

Engine power margins required for engine-to-engine component efficiency variations and control margins are met by providing a 10 percent system pressure drop reserve in conjunction with a 10 percent turbine bypass flow reserve. These combined reserves provide for probable engine-to-engine variations in turbomachinery efficiencies and coolant jacket pressure drop and heat load uncertainties. These reserves were established from a study which determined what deviations are to be expected during the expander OTV engine testing in turbomachinery efficiencies, thrust chamber heat load, and coolant jacket pressure drop; and what sensitivities in chamber pressure are to be expected in the selected cycle configuration from variations in the turbine bypass flow and the pressure drop reserves.

Power Cycle Parameter Sensitivities

In order to assess the sensitivity of the expander cycle to variations in predicted efficiencies, heat load, pressure drop and turbine bypass flow, an analytical model was developed. The approach used was to write an expression for the system power balance as a function of the major system variables:

$$F = F\ (P_c,\ \eta_{t_{H_2}},\ \eta_{t_{O_2}},\ \eta_{P_{H_2}},\ \eta_{P_{O_2}},\ Q_C + Q_N,\ \Delta P_j,\ \bar{W}_m) \tag{1}$$

with F defined by:

$$F = \frac{HP_{turb}}{\dot{W}_{H_2}} - \frac{HP_{pump}}{\dot{W}_{H_2}} \tag{2}$$

Relation (2) results from the condition that the enthalpy increase in the pumps match the enthalpy drop in the turbines.

Differentiation of relation (1) yields:

$$dP_c = -\sum_{1}^{i}\left(\frac{\partial F}{\partial \eta_i}\Big/\frac{\partial F}{\partial P_c}\right) d\eta_i - \left(\frac{\partial F}{\partial Q}\Big/\frac{\partial F}{\partial P_c}\right) dQ$$

$$- \left(\frac{\partial F}{\partial \Delta P_j}\Big/\frac{\partial F}{\partial P_c}\right) d\Delta P_j - \left(\frac{\partial F}{\partial \bar{W}_m}\Big/\frac{\partial F}{\partial P_c}\right) d\bar{W}_m \qquad (3)$$

where

η_i represents the $i^{\underline{th}}$ turbine or pump efficiency

Q represents total available heat input in BTU/Sec

ΔP_j represents jacket pressure drop in psi

$\bar{W}_m$ represents margin flowrate, expressed as a fraction of total hydrogen flow

In order to obtain numerical estimates for each of the terms in relation (3), relation (2) was expanded as follows for a typical expander cycle where the main turbines are arranged in series. The horsepower of the boost pumps is ignored for simplicity, with only slight effect in accuracy due to the low level of boost pump power.

$$HP_p = \frac{.2618\ \Delta P_{H_2}\ \dot{W}_{H_2\ pump}}{\eta_{P_{H_2}}\rho_{H_2}} + \frac{.2618\ \Delta P_{O_2}\dot{W}_{O_2\ pump}}{\eta_{P_{O_2}}\rho_{O_2}}$$

ΔP_{O_2} and ΔP_{H_2} are further expanded in terms of P_c, turbine pressure ratio, and system pressure drops. The resulting expression for pump power, after algebraic manipulation and division by $\dot{W}_{H_2}$, is:

$$\frac{Hp_p}{\dot{W}_{H_2}} = \left[\frac{1}{K_3 \eta_{PH_2} \rho_{O_2}}\right] \left[P_{D_{H_2}} + \Delta P_{FV} - P_{in_{H_2}}\right] (1 - W_D) \quad (4)$$

$$+ M_R \left[\frac{K_2 P_c - P_{in_{O_2}} + \Delta P_{O_V}}{K_3 \eta_{PO_2} \rho_{O_2}}\right]$$

where

P_D is pump discharge pressure, psia

P_{in} is pump inlet pressure, psia

W_D is the fraction of hydrogen used as dump coolant

ΔP_{F_V} is main fuel valve pressure drop, psia

ΔP_{O_V} is main oxidizer valve pressure drop, psia

M_R is mixture ratio $(\dot{W}_{O_2}/\dot{W}_{H_2})$

K_1 = main fuel injector pressure drop multiplier

K_2 = main oxidizer injector pressure drop multiplier

K_3 = 1/.2618

A similar expansion of turbine power results in:

$$\frac{HP_{turb}}{\dot{W}_{H_2}} = \eta_{ft} (1 - W_D)(1 - W_m) C_{P_{H_2}} T_{in_{H_2}} K_5 f(Pr_{H_2}, \gamma) \quad (5)$$

$$+ \eta_{OT} [(1 - W_D)(1 - W_m)(1 - W_B)] C_{P_{O_2}} T_{in_{O_2}} K_5 f(Pr_{O_2}, \gamma)$$

with

$$f(Pr, \gamma) = \left[1 - \left(\frac{1}{Pr}\right)^{\frac{\gamma-1}{\gamma}}\right]$$

W_B = fraction of hydrogen bypassed around main oxidizer turbine

T_{in} = turbine inlet temp, R

C_p = hydrogen specific heat, $\frac{BTU}{lb\ R}$

$K_5 = \frac{778}{550}$, conversion from $\frac{BTU}{Sec}$ to HP

These relations (4 and 5) were incorporated into a short computer model written in the PROSE language. PROSE (Problem Solution Engineering System) is a high-level language which incorporates calculus concepts at the command level. It is thus possible to evaluate the partial derivative of, say, X with respect to Y by the PROSE statement

P = . PARTIAL (X,Y)

without becoming involved in the numerical details fo the differentiation.

The resulting model was exercised at a number of different thrust and chamber pressure levels. Table 12 summarizes the critical expander power cycle parameter sensitivities obtained with the model at two different thrust levels.

Engine-to-Engine Variations

Probable engine-to-engine variations in component parameters which affect the chamber pressure significantly are shown in Table 13. The turbomachinery efficiency variations were obtained from SSME experience and constitute the deviations used in determining maximum and minimum delivered performance. Coolant jacket pressure drop and coolant jacket heat load deviations were taken

TABLE 12
EXPANDER POWER CYCLE PARAMETER SENSITIVITIES

Partial	Units	Thrust = 10K	Thrust = 15K
$\frac{\partial F}{\partial P_c}$	$\left(\frac{lb}{psi}\right)$	+.50426	+.50420
$\frac{\partial F}{\partial \eta_{ft}}$	$\left(\frac{lb}{\%Points/100}\right)$	-693.84	-682.78
$\frac{\partial F}{\partial \eta_{ot}}$	$\left(\frac{lb}{\%Points/100}\right)$	-137.66	-144.92
$\frac{\partial F}{\partial \eta_{fp}}$	$\left(\frac{lb}{\%Points/100}\right)$	-998.93	-962.89
$\frac{\partial F}{\partial \eta_{op}}$	$\left(\frac{lb}{\%Points/100}\right)$	-128.91	-143.83
$\frac{\partial F}{\partial Q}$	$\left(\frac{lb}{Btu/sec}\right)$	-.0474	-.03275
$\frac{\partial F}{\partial \Delta P_j}$	$\left(\frac{lb}{psi}\right)$	+.1931	+.1774
$\frac{\partial F}{\partial W}$	$\left(\frac{lb}{lb/sec}\right)$	+619.51	+623.72

TABLE 13
COMPONENT UNCERTAINTIES AFFECTING CHAMBER PRESSURE

	Engine-to-Engine Variations
Fuel Pump Efficiency	±1.6
Fuel Turbine Efficiency, Points	±2.0
Oxidizer Pump Efficiency, Points	±0.8
Oxidizer Turbine Efficiency, Points	±2.0
Coolant Jacket Pressure Drop, % Nominal	±8.0
Coolant Jackets Heat Load, % Nominal	±12.0

from ASE experience. They represent the deviation between values calculated during the thrust chamber design effort and values measured during the experimental thrust chamber program.

Turbine Flow and Pressure Drop Reserves

The power cycle parameter sensitivities (exchange factors) and the probable engine-to-engine variations in these parameters (from the previous sections) were used to determine the turbine flow and system pressure drop reserves required of the expander cycle engine. As shown in Table 14 the contingencies required from Table 13 variations are met by providing a 10 percent system pressure drop reserve in addition to a 10 percent turbine bypass flow reserve. In addition, these reserves provide for a 5 percent turbine bypass flow for control during mixture ratio excursions, and 3 percent margin on this latter requirement. This provides a total of 8 percent of turbine flowrate as a control allowance. All these contingencies can be met (as shown in Table 14) with either 23 percent bypass flow or 19.8 percent pressure drop reserve. To balance out possible disadvantages inherent in either method a 10/10 percent split was selected. Larger turbine bypass flowrates tend to reduce turbomachinery component efficiencies and makes design more difficult, while larger pressure drop reserves affect discharge pressures adversely. The margins are based on worse-case engine to engine variations.

TABLE 14
BASELINE ENGINE POWER AND CONTROL FLOW MARGINS

	Engine-to-Engine Variation	Equivalent Turbine Bypass Flow Margin, %		Equivalent ΔP Margin % U/S Turbine
Component Uncertainties:				
Fuel Pump Efficiency, Points	±1.6	2.47	or	2.12
Fuel Turbine Efficiency Points	±2.0	2.19	or	1.88
Oxidizer Pump Efficiency Points	±0.8	0.18	or	.15
Oxidizer Turbine Efficiency	±2.0	0.46	or	.40
Coolant Jacket Pressure Drop, % Nominal	±8.0	1.00	or	.86
Coolant Jackets Heat Load, % Nominal	±12.0	8.76	or	7.53
Control Requirements:				
Turbines Bypass Control Flow	-	5.00	or	4.30
Control Flow Margin	-	3.00	or	2.58
Total Margin Requirements (All Flow or All ΔP)		23.06	or	19.82
Margin Requirements (50-50 Split Between Flow and ΔP)		10	and	10

The sensitivity coefficients (Table 12) used to obtain the flow and pressure drop margins in Table 14, agreed closely with results obtained with the cycle optimizer program. Several balances were conducted with this latter program to assess the effect of a resistance margin and a turbine bypass flow margin upon chamber pressure, at 15K lb thrust. Results are indicated in Fig. 24 for the turbine flow margin and in Fig. 25 for the system pressure drop margin. Reduction of the flow margin from its nominal value of 10 percent to zero results in an increase of 120 psia in chamber pressure. Reduction of the pressure drop reserve from its nominal value of 10 percent increases chamber pressure 138 psia. Thus, for the baseline configuration these changes would result in a chamber pressure of 1868 psia. The slopes of the lines in Figs. 24 and 25 are the flow and pressure drop sensitivity coefficients in Table 12.

FIGURE 24

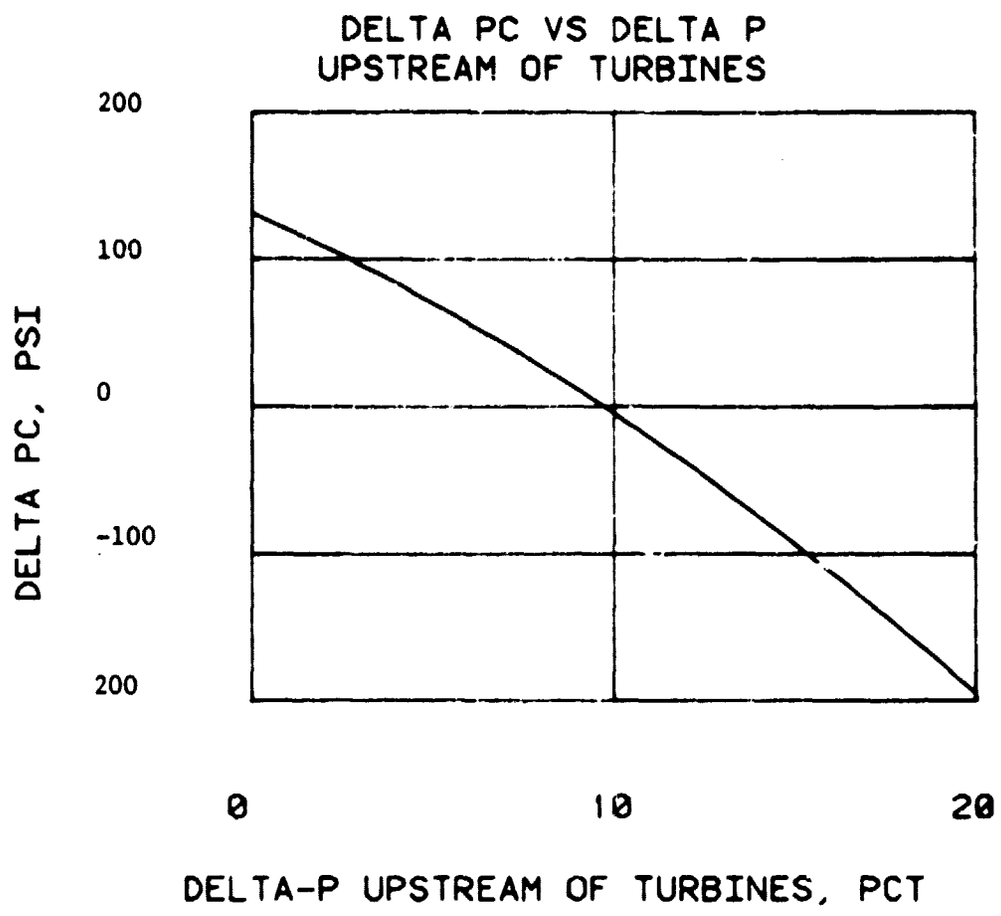
DELTA PC VS DELTA P
UPSTREAM OF TURBINES
200
100
0
-100
200
DELTA PC, PSI
0
10
20
DELTA-P UPSTREAM OF TURBINES, PCT

FIGURE 25

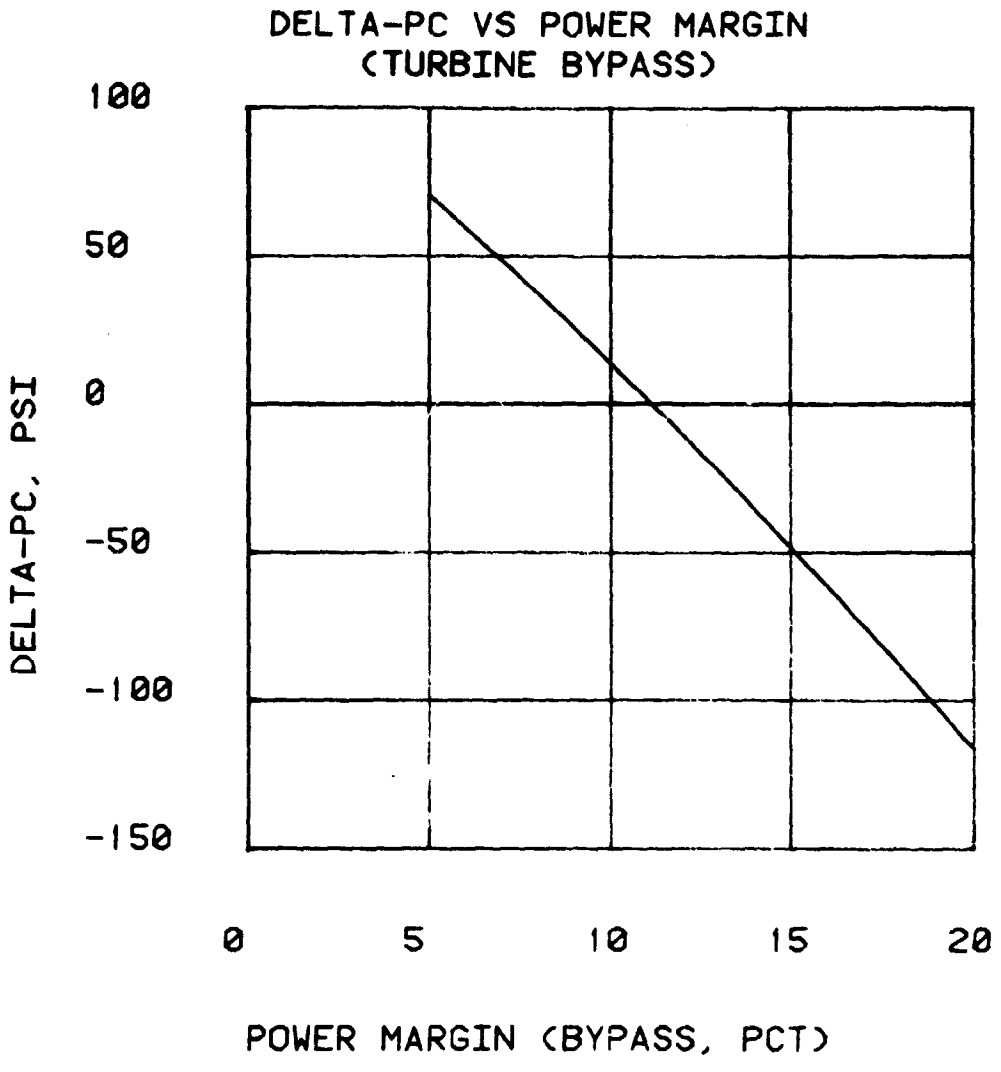
DELTA-PC VS POWER MARGIN
(TURBINE BYPASS)
100
50
0
-50
-100
-150
DELTA-PC, PSI
0
5
10
15
20
POWER MARGIN (BYPASS, PCT)

CYCLE OPTIMIZATION STUDIES AT 10K THRUST

The thrust levels which were studied in greatest detail were 10K and 15K. Effort was concentrated upon these two thrust levels because:

a) Vehicle trade studies indicated that a thrust level of approximately 15K is favored for best payload performance.

b) 10K remains a viable alternate thrust level with potential for multiple-engine installation.

Trends identified at a given thrust level are expected to be reflected in a consistent manner at any thrust level within the range of interest.

Cycle configuration trade studies at the 10K thrust level focused on comparison of a cycle which includes a regen heat exchanger (No. 4 in Fig. 11) with one which relies on thrust chamber thermal enhancement but without a regen heat exchanger (No. 2 in Fig. 11). Other cycle configurations were studied at the 15K thrust level.

CYCLE PERFORMANCE RANKING

The configurations affording the best performance in terms of delivered specific impulse or chamber pressure were selected and ranked according to P_c and I_s. The result of this ranking was presented in the previous section for the 15K thrust level and in Table 15 for the 10K thrust level.

System configuration variables which influence attainable performance most significantly include:

a) . Thrust chamber length

b) . Thrust chamber thermal enhancement factor (E.F.)

TABLE 15
PERFORMANCE TRADE STUDIES

F = 10K

Combustor Configuration	Chamber Length In.	Chamber Pressure psia	Area Ratio	Nozzle Percent Length	Specific Impulse Seconds	Bulk Temperature, R		H_2 Heat of Formation KCAL/MOLE
						Combustor	Nozzle	
Thermally Enhanced, Reheat	15.0*	1629	1095	70.6	486.9	987	1166	1.31
Thermally Enhanced, Heatex Between Jackets	16.6*	1652	1014	72.6	486.7	1000	1244	1.26
Ther. Enh., Regen Heatex	14.5*	1633	1060	72.4	486.7	981	1173	1.24
Smooth, Regen Heatex	18.76*	1533	956	70.0	482.9	821	972	0.65
Ther. Enh., Regen Heatex	10.0	1570	1142	71.9	482.5	789	1015	0.31
Smooth, No Heatex	20.0	1360	829	69.9	482.0	905	1032	0.78
Smooth, Regen Heatex	10.0	1527	1084	72.8	479.5	850	1062	-0.29

*Combustor Length Optimized

c) . Regen heat exchanger

d) . Turbine arrangement

e) . Coolant bulk temperature limit

Thrust chamber length was optimized in the range $10" \leq L \leq 20"$. For smooth-wall chambers, the optimum chamber length is less than 20 in. (the maximum length allowed). The system is driven to long chamber length due to the beneficial influence of the added heat transfer area. When thermally enhanced chanbers are considered, the optimum length is shorter, because the combustor bulk temperature limit can be achieved with less length. Inclusion of a regen heat exchanger shortens the chamber slightly, because of the higher coolant inlet temperature.

Placement of the regen heat exchanger is important due to its effect upon the level of cooling obtainable. Location of the heat exchanger upstream of both jackets results in the combustor bulk temperature limit being encountered for some level of heat exchanger heat transfer. Combustor bulk temperature is always reached before that of the nozzle. This limits the final nozzle exit temperature and hence the turbine inlet temperature. Location of the heat exchanger between the coolant jackets is better, because it allows the combustor jacket (upstream) to be fed with cold hydrogen, thus maximizing the heat absorbed by the coolant before the bulk temperature limit is reached.

GENERAL APPROACH

This subtask had the goal of determining the optimum cycle configuration on the basis of performance, i.e., the arrangement of pumps, turbines, and regen heat exchangers which yield maximum levels of specific impulse or chamber pressure.

The primary analytical tool used in this task is Rocketdyne's Variable Schematic Design Model. This is a non-linear optimizing computer code capable of modeling arbitrary networks of components. Expander cycle designs were

defined and modeled with this code with the object of maximizing P_c and/or I_s, subject to various groundrules and design constraints.

The outputs of these computer runs consist of detailed power balance descriptions, including pump and turbine operating point, thrust chamber performance and cooling, heat exchanger design (if present), and a detailed summary of hydrogen thermodynamic properties at each engine station.

ENGINE CYCLE CONFIGURATION OPTIONS

Several alternate expander cycle schematic configurations were selected for detailed trade studies during Task 8. These options are illustrated in Fig. 26. The alternate schematics include the following flow circuits:

1. A parallel-turbine cycle with split-flow cooling circuit. This cycle closely resembles the flow circuit of the ASE except for the lack of a preburner.
2. A series-turbine case utilizing a full-flow regen coolant circuit. This circuit resembles that of the RL-10 engine.
3. A conventional reheat cycle, with the oxidizer turbine between the combustor and nozzle cooling jackets and the fuel turbine downstream of the nozzle jacket to take advantage of the maximum hydrogen temperature.
4. A regenerative cycle using a heat exchanger to preheat the jacket coolant using heat extracted from the fuel turbine exhaust.
5. A combination of configurations 3 and 4, designated "Reheat/Regen." The regeneration loop is moved downstream of the combustor jacket and oxidizer turbine, and includes only the fuel turbine and nozzle jacket. The regen loop is thus in a "reheat" configuration with respect to the combustor and oxidizer turbine.

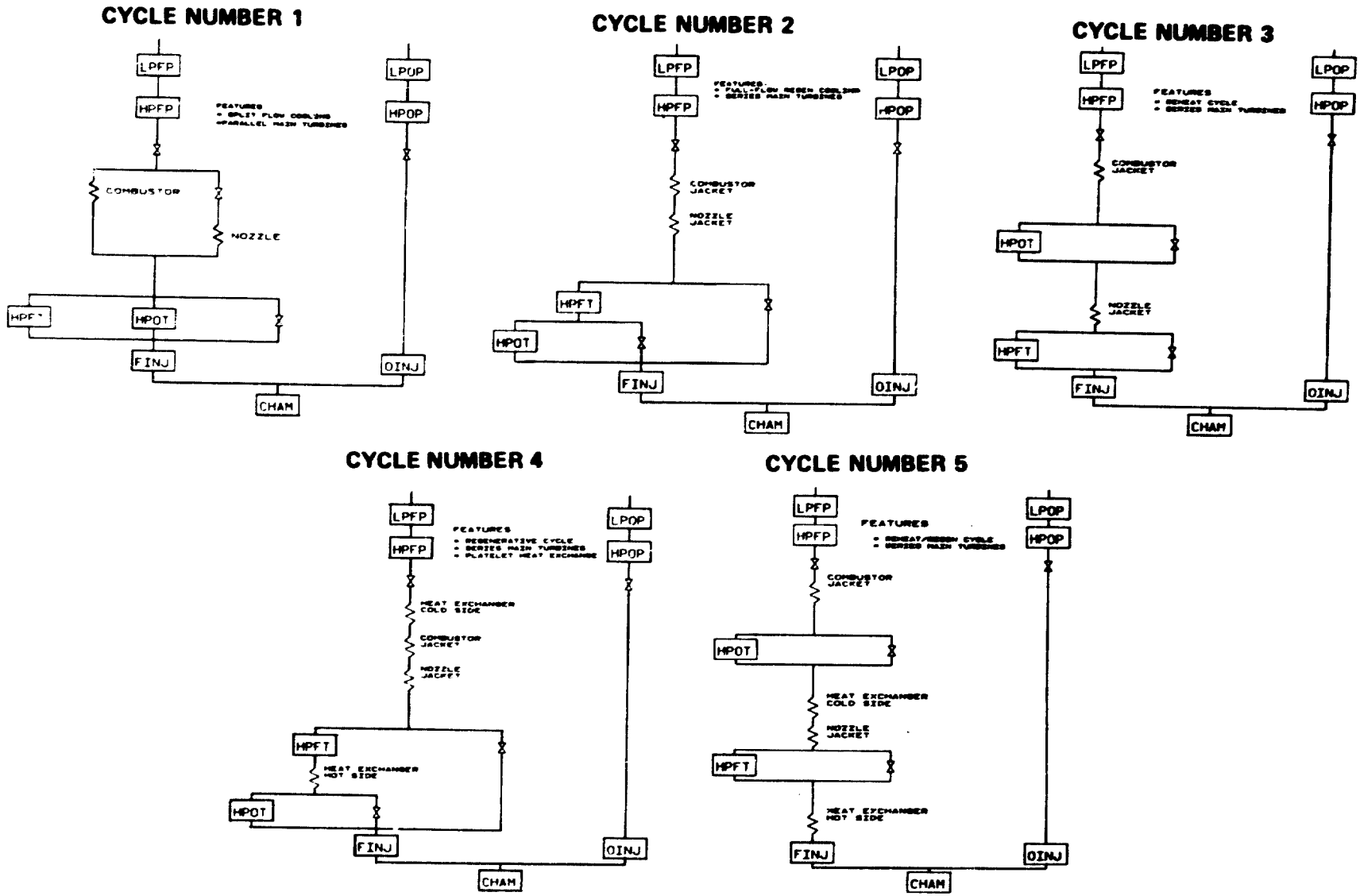

Figure 26. Cycle Configurations Studied

Many more configuration options are possible, including several combinations of features present in the circuits described above. Detailed analysis of all possible configurations would involve extremely high costs and would therefore obviously be out of the scope of the present effort. In order to reduce the analysis task to manageable proportions, it is necessary to select a subset of the possible configurations which are felt to be of interest due to performance potential or other attractive features. Careful selection of circuits for study will insure that the most important characteristics of the possible configurations are revealed.

STUDY GROUNDRULES

Groundrules under which the Task 8 analytical effort has been conducted are summarized in Table 16. These groundrules are for the most part identical with those established for the Phase A study. However, a number of improvements have been made to certain of the Phase A groundrules in the present study. Differences between Task 8 groundrules and the initial Phase A groundrules include:

a) Revised bulk temperature limits for both combustor and nozzle coolant.

b) Increased number of fuel pump stages from 2 to 3.

c) Chamber length is now varied to determine the optimum length in terms of I_s and P_c. Previously chamber length was set by combustion efficiency requirements.

d) Contraction ratio is now varied to determine the optimum ϵ_c in terms of I_s and P_c. Previously, contraction ratio was set by combustion efficiency requirements.

e) Thermally enhanced chamber designs are considered. Only smooth chamber designs were considered during Phase A.

f) Series turbine cases are included. Phase A considered only parallel turbine cases.

TABLE 16
DESIGN OPTIONS AND LIMITS

TURBINE TYPE	(Units)	Oxidizer One Row	Fuel Two Stage Impulse
Minimum Admission	(None)	.10	.10
Minimum Pressure Ratio	(None)	1.16	1.20
Minimum Hub/Tip Ratio	(None)	.60	.60
Minimum Blade Height	(Inches)	.30	.30
Minimum Pitch Diameter	(Inches)	2.50	2.50
Maximum Admission	(None)	1.00	1.00
Maximum Pressure Ratio	(None)	1.25	3.50
Maximum Hub/Tip Ratio	(None)	.90	.90
Maximum Tip Speed	(Ft/Sec)	1600.00	1600.00
Maximum AN^2	$((RPM-In)^2$	$4.00x10^{10}$	$4.00x10^{10}$
Maximum Bearing DN	(MM*RPM)	1.50_x10^6	$1.90x10^6$
MAIN PUMPS			
Inducer		Yes	Yes
Boost Pump Used		Yes	Yes
Number of Centrifugal Stages		1.	3.
Minimum Speed	(RPM)	30000.00	30000.00
Minimum Impeller Tip Diameter	(Inches)	1.00	1.00
Minimum Impeller Stage Specific Speed	(RPM*GPM**.5/Ft**.75)	400.00	400.00
Minimum Impeller Tip Width	(Inches)	.03	.03
Minimum Inducer Diameter	(Inches)	.75	.75
Maximum Speed	(RPM)	70000.00	150000.00
Maximum Impeller Tip Diameter	(Inches)	No Limit	No Limit
Maximum Impeller Stage Specific Speed	(RPM*GPM**.5/Ft**.75)	2000.00	2000.00
Maximum Impeller Tip Speed	(Ft/Sec)	1870.00	1870.00
Maximum Inducer Tip Speed	(Ft/Sec)	1870.00	1870.00
Maximum Inlet/Outlet Diameter Ratio	(None)	.80	.80

TABLE 16 (CONT.)

TURBINE TYPE	(Units)	Oxidizer One Row	Fuel Two Stage Impulse
Minimum Diameter	(Inches)	.75	.75
Maximum Diameter	(Inches)	No Limit	No Limit
Maximum Bulk Temperature	(Deg-R)	1000.00	1260.00
Reference Delta-P	(PSID)	165.20	6.20
Reference Heat Load	(BTU/Sec)	5045.80	2176.50
Reference Density	(LBM/ft**3)	2.770	.733
Reference Chamber Pressure	(PSIA)	1300.00	1300.00
Reference Chamber Temperature	(Deg-R)	6495.00	6495.00
Reference Characteristic Velocity	(Ft/Sec)	7560.00	7560.00
Reference Thrust	(LBF)	10000.00	10000.00
Reference Wall Temperature	(Deg-R)	1100.00	1100.00
Reference Inlet Temperature	(Deg-R)	70.00	571.00
Reference Enhancement Factor	(None)	2.05	
Reference Contraction Ratio	(None)	5.00	
Reference Chamber Length	(Inches)	10.00	
Reference Area Ratio (Regen)	(None)		330.00
Reference Area Ratio (Attach)	(None)		14.00
Reference Nozzle Length (Regen)	(Inches)		35.17

g) Initial Phase A studies did not consider cycles including regeneratively heat exchangers, as does the present effort.

h) Full-flow regen cooling circuits are included. Previous studies considered split-flow only.

SUMMARY OF RESULTS

Table 15 displays the results of full cycle optimization for the cycles considered at the 10K thrust level. Conclusions suggested by the optimizations conducted include the following:

1. Cycles with regen heat exchangers (4 and 5) do not perform as well in terms of maximum I_{sp} as do those without heat exchangers. This is because the heat exchanger does not increase the fuel enthalpy at the thrust chamber inlet.

2. Optimum area ratio in terms of specific impulse is approximately 900 to 1000 for the 10K cases. Higher area ratios improve the nozzle heat load, resulting in larger area ratio values when maximizing P_c. These higher area ratios cause increased losses and therefore do not contribute to higher specific impulse.

3. I_{sp} maxima in the range of 486 to 487 seconds are achievable at 10K thrust.

4. The poorest-performing cycle is Cycle No. 1, which has parallel main turbines and split-flow cooling. P_c of this cycle is reduced by the parallel arrangement, which causes:

    a) Reduced flow available to the main fuel turbine

    b) Reduced main oxidizer turbine U/C_o, which results in poorer turbine efficiency

    However, Cycle 1 has the lowest fuel pump discharge pressure levels, on account of the somewhat lower P_c combined with significantly lower turbine (overall) pressure ratio (when compared to series-turbine cases).

5. The best cycles in terms of I_{sp} are those using thermally enhanced chambers. However, performance differences among all cycles are rather small in magnitude, especially when cases with optimized combustor length are compared.

SENSITIVITY STUDIES OF SELECTED ENGINE CONFIGURATIONS

Parametric studies of the sensitivity of two representative expander cycle configurations are discussed in the following section. The cycles examined were the series-turbine expander cycle without turbine gas regeneration (schematic No. 2), and a similar cycle with turbine gas regeneration. Both cycles were analyzed with thrust-chamber thermal enhancement and without.

Cycle sensitivity to changes in chamber length, degree of thermal enhancement, heat exchanger effectiveness, and power margin were considered, as well as the influence of pump speed and number of pump stages.

Schematic No. 2 (Series Turbines)

Schematic No. 2 is a simple expander cycle system incorporating series main turbines. In this cycle, turbine inlet temperature increases are achieved primarily through: (1) increase in chamber surface area by lengthening the thrust chamber, (2) increase in chamber surface area by increasing contraction ratio, and (3) thrust chamber thermal enhancement to increase total heat transfer load.

All of these approaches were examined during study of several alternate cycles. A few general observations can be made concerning the three options:

1. Lengthening the thrust chamber can greatly improve the energy available to the turbines, but in a fixed total engine length will

force shortening the nozzle. This may result in a performance penalty as the nozzle percent length is forced off optimum.

2. Contraction ratio has a weaker effect upon total heat available than chamber length, in part because surface area is proportional to $\sqrt{\epsilon_c}$, but is directly proportional to L_c. Increases in contraction ratio reduce the hot-gas heat transfer coefficient, which further reduces the effectiveness of contraction ratio in increasing heat load.

3. Thermal enhancement chambers show promise for enhancing total heat load without forcing shorter nozzles, but technology issues remain to be resolved.

Maximum chamber pressure for the 10K thrust level is plotted as a function of thrust chamber thermal enhancement factor (E.F.) in Fig. 27.

Fig. 27 was prepared using a maximum fuel pump speed of 100,000 rpm and a maximum combustor coolant bulk temperature of 1000R. The figure illustrates the significant benefit obtainable from chamber thermal enhancement, which is due to increased turbine inlet temperatures. Fig. 28, a companion plot to Fig. 27, shows how delivered specific impulse at fixed area ratio is improved by thermal enhancement. The I_{sp} improvement results primarily from the higher hydrogen enthalpy level caused by higher heat loads resulting from thermal enhancement.

The total heat input available from the combustor is shown in Fig. 29 as a function of enhancement factor. A 27% increase in heat load is obtained when EF is doubled.

The thermal enhancement factor achievable is limited by life requirements to approximately 2.75. Higher factors result in excessive wall temperatures and thus in reduced life cycle.

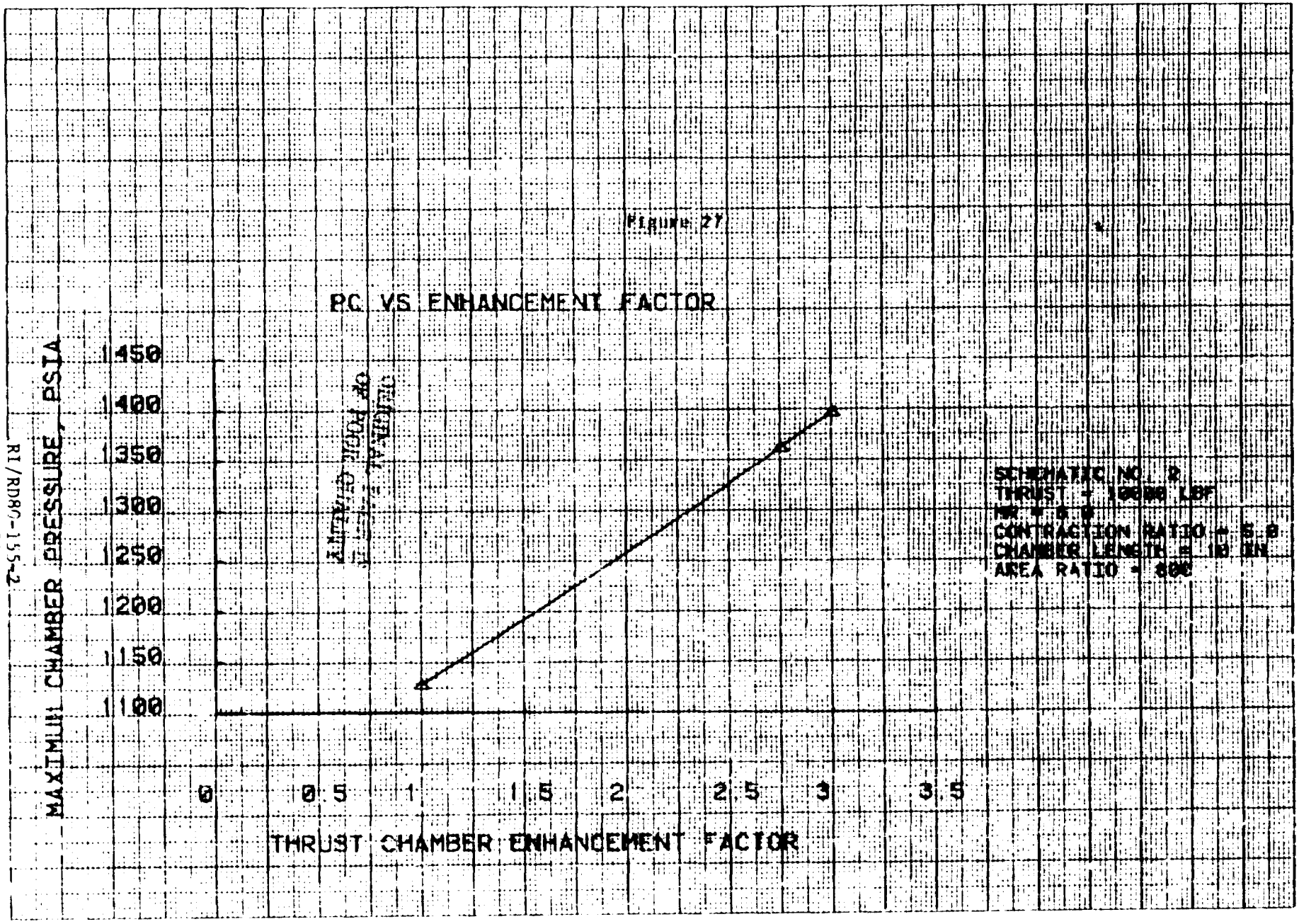
Figure 27
PC VS ENHANCEMENT FACTOR
MAXIMUM CHAMBER PRESSURE, PSIA
1450
1400
1350
1300
1250
1200
1150
1100
0
0.5
1
1.5
2
2.5
3
3.5
THRUST CHAMBER ENHANCEMENT FACTOR
VERTICAL LINES OF POOR QUALITY
SCHEMATIC NO. 2
THRUST = 16000 LBF
MR = 5.0
CONTRACTION RATIO = 5.0
CHAMBER LENGTH = 10 IN
AREA RATIO = 80%

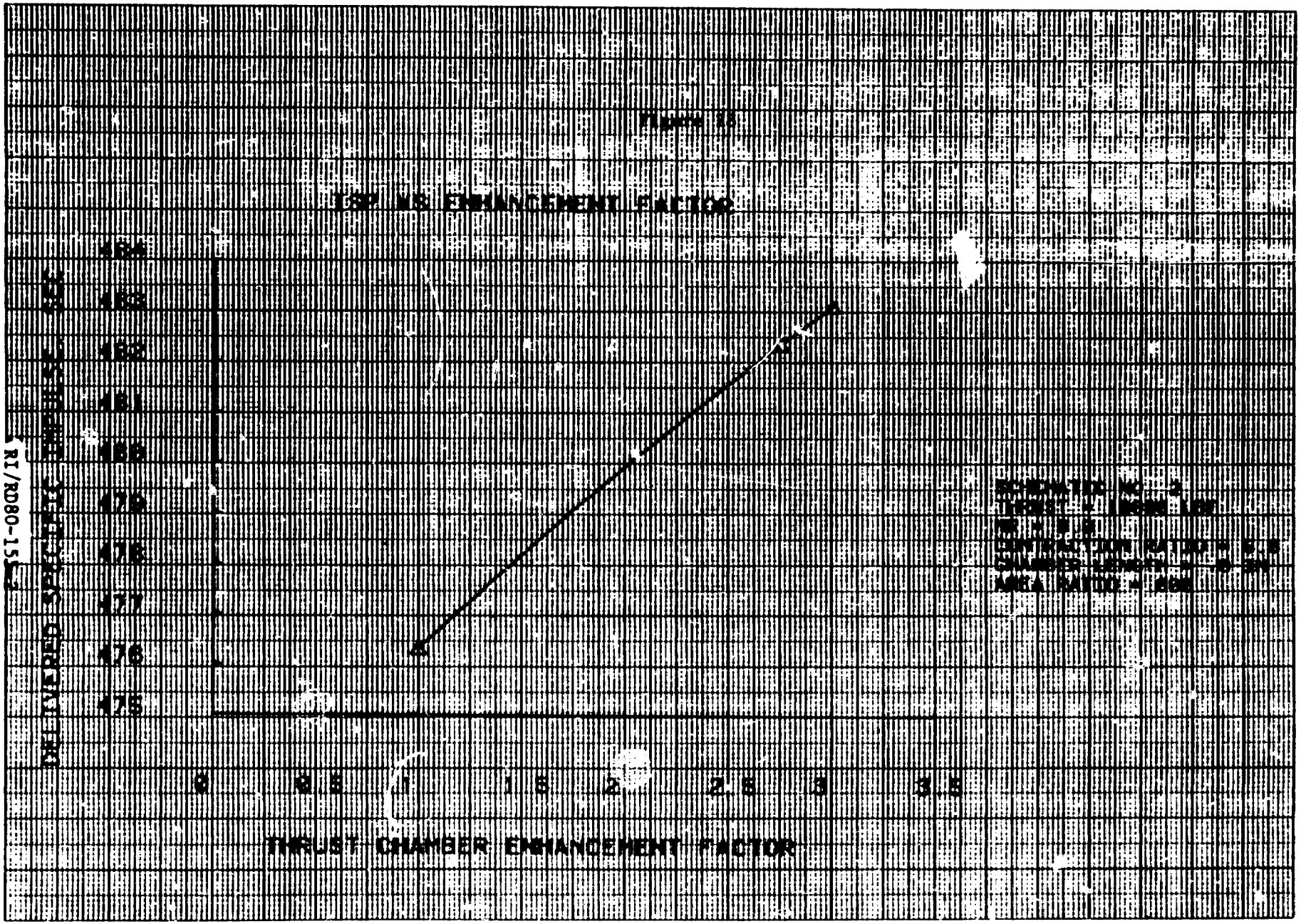
Figure 15
ISP VS ENHANCEMENT FACTOR
484
482
480
478
476
474
472
470
468
466
464
462
460
458
456
454
452
450
448
446
444
442
440
438
436
434
432
430
428
426
424
422
420
418
416
414
412
410
408
406
404
402
400
398
396
394
392
390
388
386
384
382
380
378
376
374
372
370
368
366
364
362
360
358
356
354
352
350
348
346
344
342
340
338
336
334
332
330
328
326
324
322
320
318
316
314
312
310
308
306
304
302
300
298
296
294
292
290
288
286
284
282
280
278
276
274
272
270
268
266
264
262
260
258
256
254
252
250
248
246
244
242
240
238
236
234
232
230
228
226
224
222
220
218
216
214
212
210
208
206
204
202
200
198
196
194
192
190
188
186
184
182
180
178
176
174
172
170
168
166
164
162
160
158
156
154
152
150
148
146
144
142
140
138
136
134
132
130
128
126
124
122
120
118
116
114
112
110
108
106
104
102
100
98
96
94
92
90
88
86
84
82
80
78
76
74
72
70
68
66
64
62
60
58
56
54
52
50
48
46
44
42
40
38
36
34
32
30
28
26
24
22
20
18
16
14
12
10
8
6
4
2
0
ISP (LBF-SEC/LBM)
0
.5
1
1.5
2
2.5
3
3.5
THRUST CHAMBER ENHANCEMENT FACTOR
SCIENTIFIC NO. 3
AREA RATIO = 208

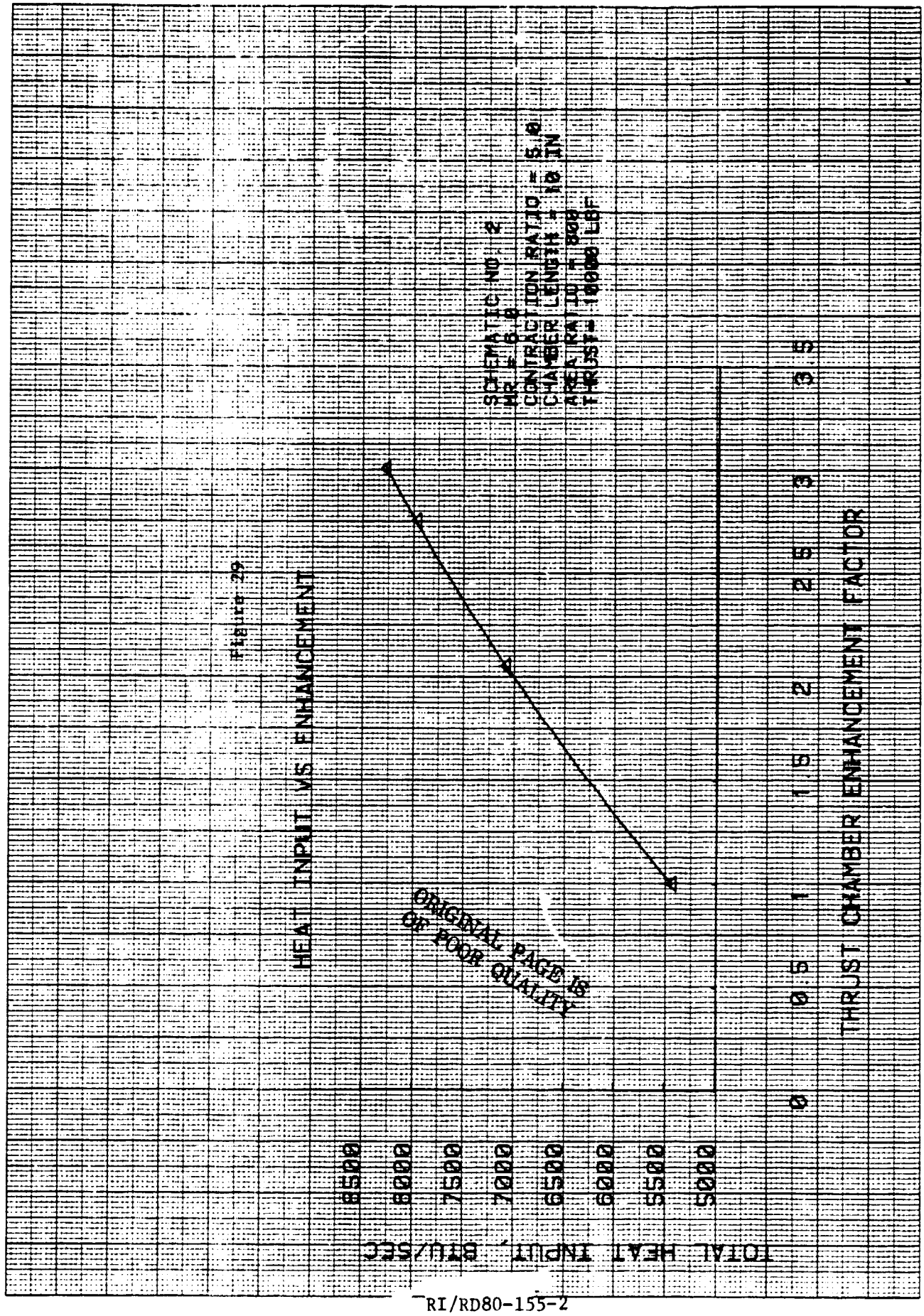

Figure 29

C-2

The curve shown in Fig. 30 reflects maximum chamber pressure as a function of thrust. This curve, like Fig. 27, is for a 10-inch chamber length, and with a fuel pump speed limit of 100,000 rpm. Increases in chamber length, pump speed, etc., will allow higher chamber pressures than shown. This plot was developed with data from schematic No. 2, a cycle with no regeneration. Alterations in cycle, i.e., addition of a reg heat exchanger or rerouting of the flow circuit can be expected to result in a different characteristic of P_c vs thrust. Figure 31 presents delivered specific impulse vs thrust for this cycle at a fixed area ratio of 800.

The influence of fuel pump speed upon maximum achievable chamber pressure is shown in Fig. 32. This curve reflects maximum P_c for a 3-stage fuel pump. Changes in the number of pump stages will affect maximum P_c. At approximately 126,000 rpm, the bearing DN limit of 1.9×10^6 is encountered. This limit prevents further increases in fuel pump speed. The DN limit will be reached at different speeds for thrust levels different from 10,000 lb, because pump bearing diameter is a function of pump torque, itself dependent on thrust and P_c. For example, at 15K thrust, the DN limit is reached at approximately 100,000 rpm in typical cycle configurations studied.

Chamber pressure is much less sensitive to oxidizer pump speed. This arises from two facts. The first is the smaller power absorbed by the oxidizer pump, which reduces the effect of the oxidizer pump and turbine upon the system power and flow balance. More important is the fact that, when the main turbines are arranged in series, there is usually a larger flow requirement in the fuel turbine than in the oxidizer turbine, which results in a significant portion of available hydrogen being bypassed around the oxidizer turbine. As long as some hydrogen is being bypassed, the oxidizer pump and turbine efficiency changes cannot affect chamber pressure. Instead, variations in efficiency merely cause the amount of bypass required to change. The hydrogen bypass is required both for off-design control and because a minimum pressure ratio in the oxidizer turbine is imposed. Setting a minimum pressure ratio (due to stability and fabricability considerations) prevents the oxidizer turbine from using all of the available hydrogen by operating at a lower pressure ratio.

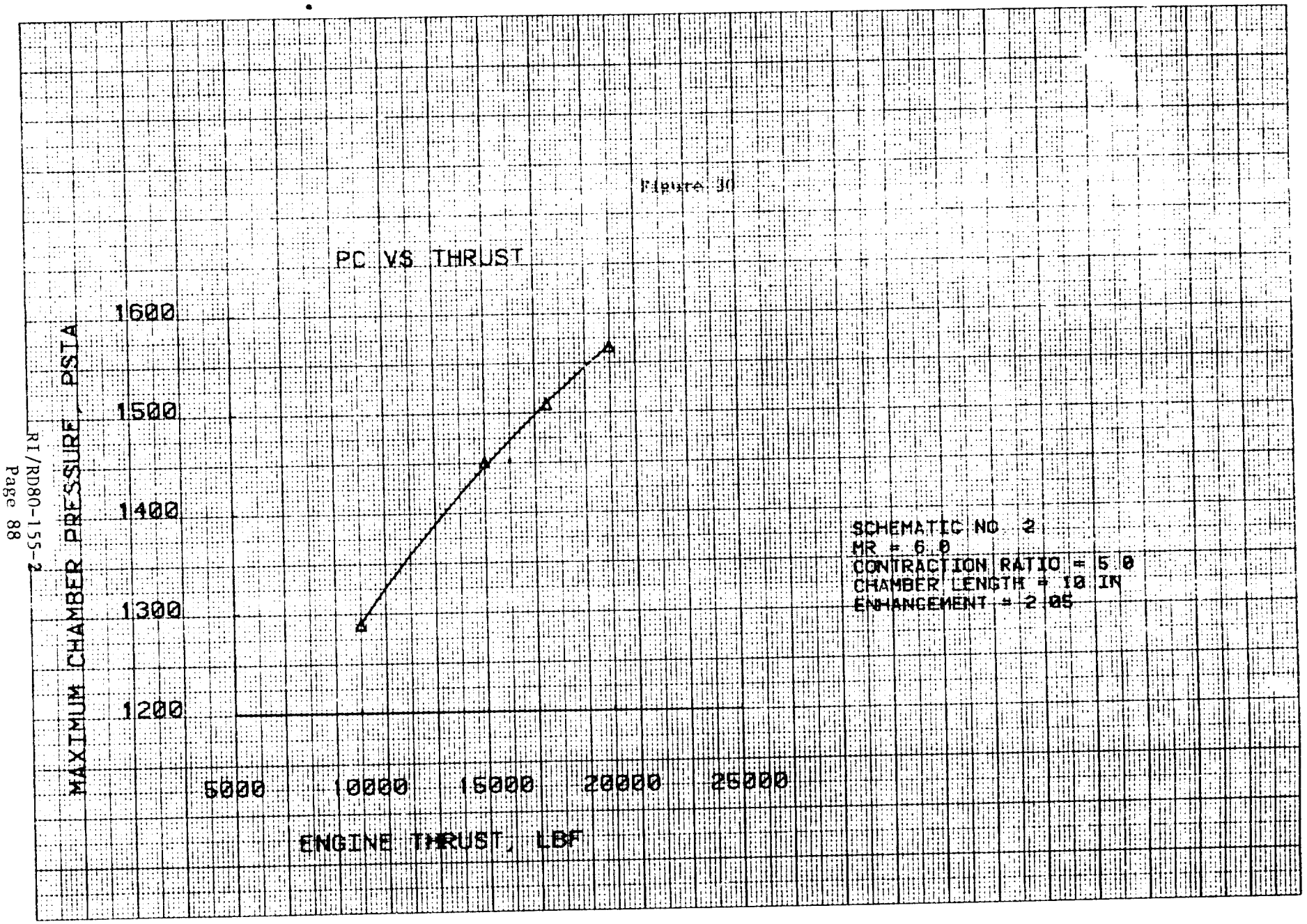
PC VS THRUST
MAXIMUM CHAMBER PRESSURE, PSIA
1600
1500
1400
1300
1200
5000
10000
15000
20000
25000
ENGINE THRUST, LBF
SCHEMATIC NO 2
MR = 6.0
CONTRACTION RATIO = 5.0
CHAMBER LENGTH = 10 IN
ENHANCEMENT = 2.05

Figure 30

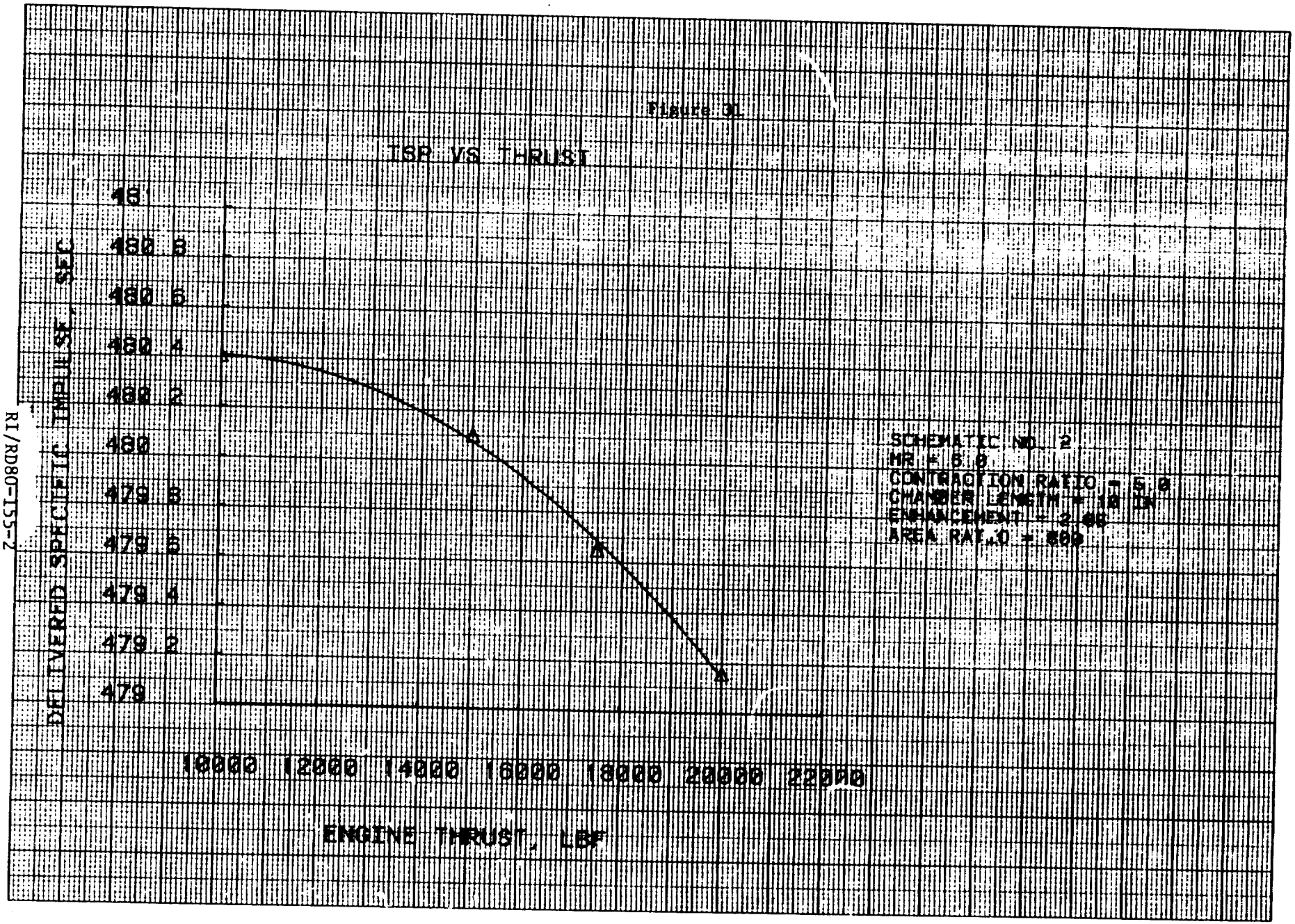
Figure 3L
ISP VS THRUST
DELIVERED SPECIFIC IMPULSE, SEC
481
480.8
480.6
480.4
480.2
480
479.8
479.6
479.4
479.2
479
10000 12000 14000 16000 18000 20000 22950
ENGINE THRUST, LBF
SCHEMATIC NO. 2
MR = 5.0
CONTRACTION RATIO = 5.0
CHAMBER LENGTH = 10 IN
ENHANCEMENT = 2.00
AREA RATIO = 600

Figure 32

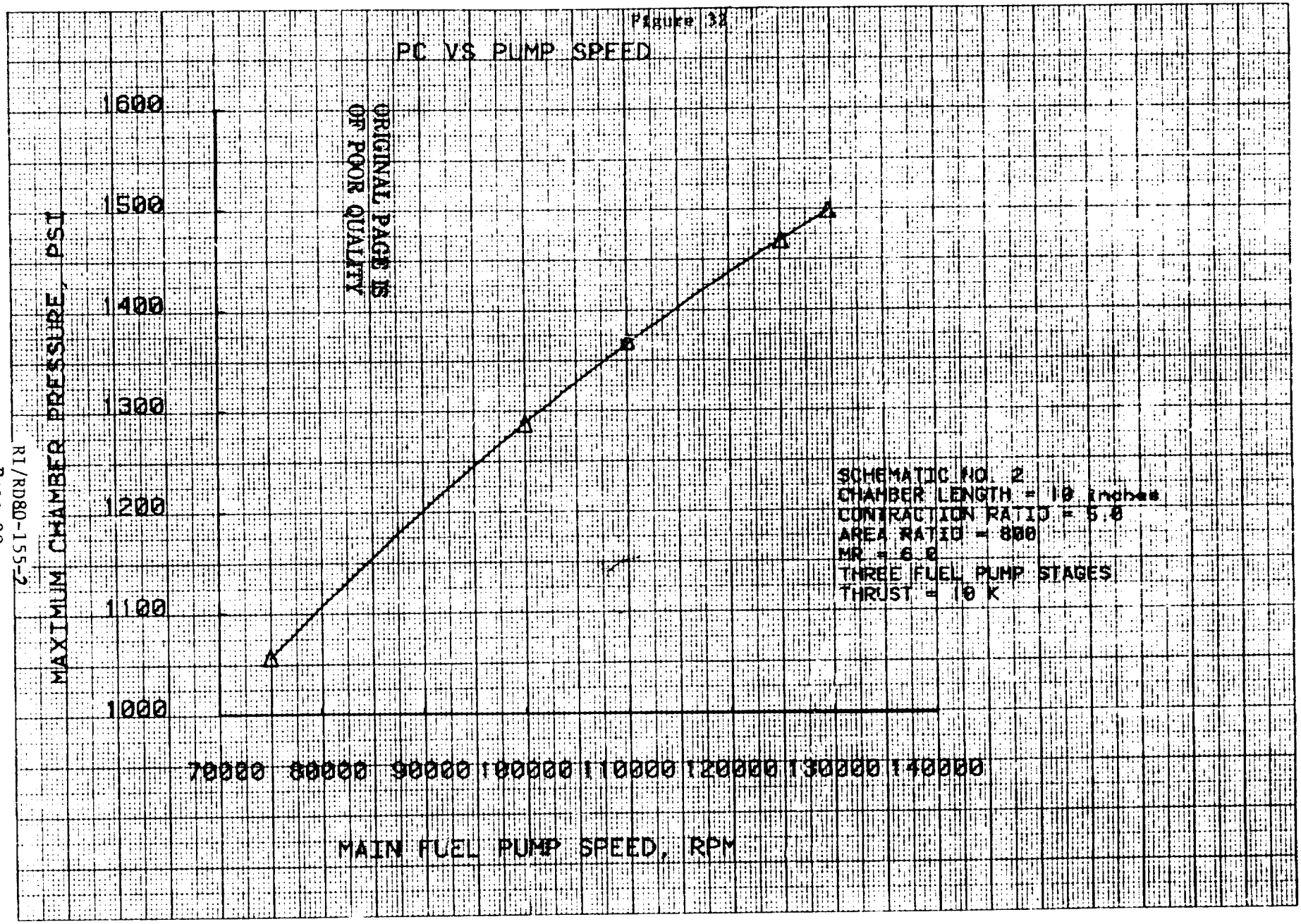
PC VS PUMP SPEED
ORIGINAL PAGE IS
OF POOR QUALITY
MAXIMUM CHAMBER PRESSURE, PSI
1600
1500
1400
1300
1200
1100
1000
70000
80000
90000
100000
110000
120000
130000
140000
MAIN FUEL PUMP SPEED, RPM
SCHEMATIC NO. 2
CHAMBER LENGTH = 10 inches
CONTRACTION RATIO = 5.0
AREA RATIO = 800
MR = 6.0
THREE FUEL PUMP STAGES
THRUST = 10 K

Fig. 33 shows the effect of increasing or decreasing the number of stages in the main fuel pump upon chamber pressure. The plot is shown as a set of discrete points, reflecting the fact that only integral values of stage number are possible. Increases in number of pump stages result in higher stage specific speeds and thus higher efficiencies. The improvement in stage efficiency yields higher chamber pressure potential, but at the price of increased complexity and cost.

The influence of pump staging on engine specific impulse is illustrated in Fig. 34. The data shown are for a fixed area ratio of 800:1. Delivered specific impulse is sensitive to pump staging becasue cycle chamber pressure increases with increasing stage count. This leads to reduced throat area for a given thrust level, and thus to increased nozzle percent length. The resulting expansion efficiency improvements cause the specific impulse to increase. This effect is distinct from and greater in magnitude than the small increase in theoretical specific impulse caused by the higher chamber pressure. It is noteworthy that if area ratio were varied to determine the optimum area ratio, still greater specific impulse improvement would be obtained. This is because higher chamber pressures permit increases in area ratio for a given nozzle percent length. The higher area ratio values give greater theoretical specific impulse, with little loss in expansion efficiency.

The effect of design-point power margin on maximum chamber pressure was examined. The power margin is expressed as the fraction of available hydrogen which is bypassed around the main turbines on design. This margin is needed for off-design control and for contingencies such as component variation from predicted performance. Fig. 35 illustrates the effect of varying the design level of the bypass margin from 5 to 20 percent of the total available hydrogen. Power margin can also be developed by placing a resistance such as an orifice or valve in the flow path. Using turbine bypass for margin amounts to imposing a limit upon the horsepower developed by the turbines, while use of a resistance is equivalent to "spilling" some energy which would otherwise be available to the pumps. Both methods reduce design-point P_C. A combination of these methods may also be used. The use of the turbine bypass has the advantage of ease of

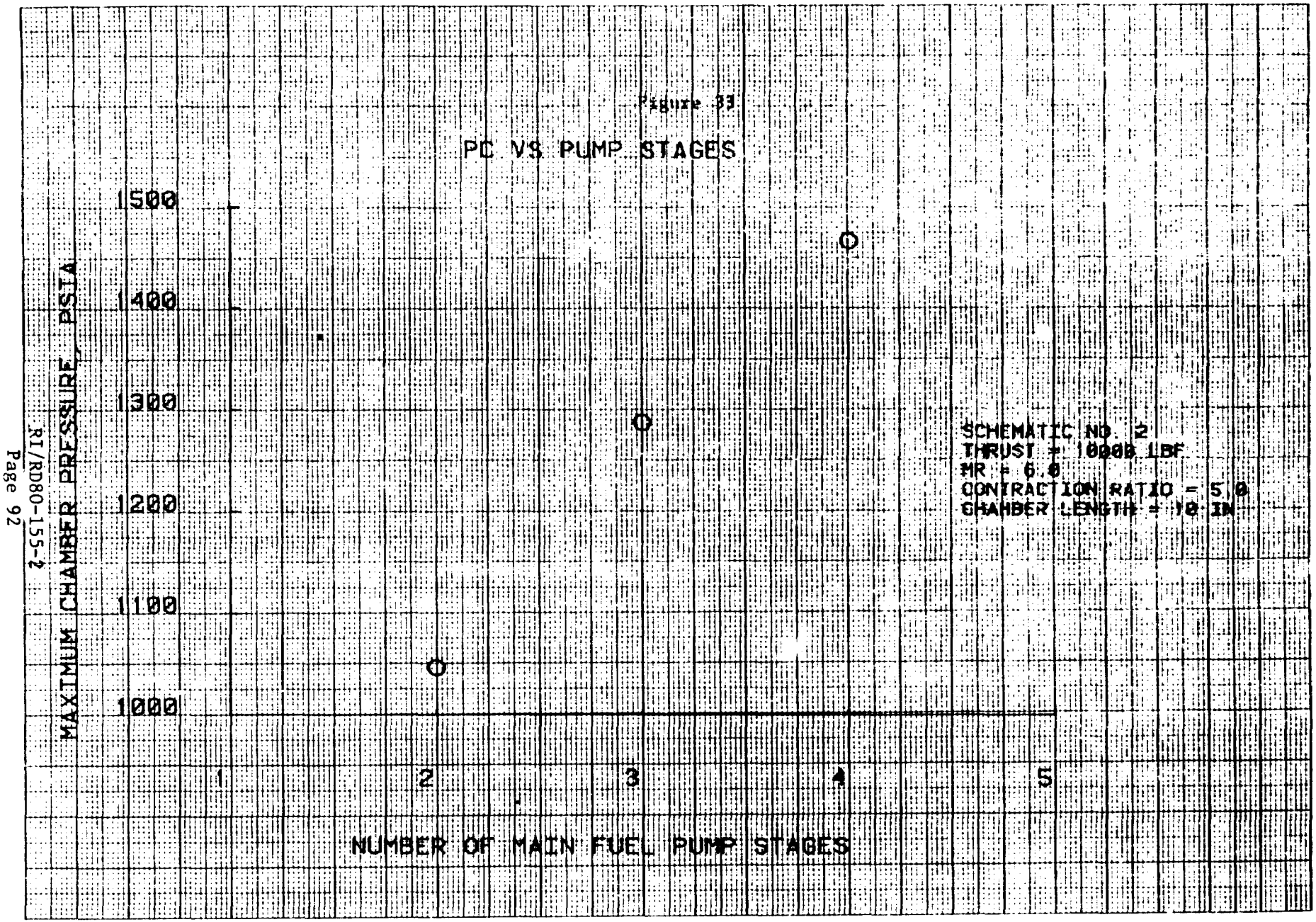
PC VS PUMP STAGES
MAXIMUM CHAMBER PRESSURE, PSIA
1500
1400
1300
1200
1100
1000
1
2
3
4
5
NUMBER OF MAIN FUEL PUMP STAGES
SCHEMATIC NO. 2
THRUST = 10000 LBF
MR = 6.0
CONTRACTION RATIO = 5.0
CHAMBER LENGTH = 10 IN

Figure 33

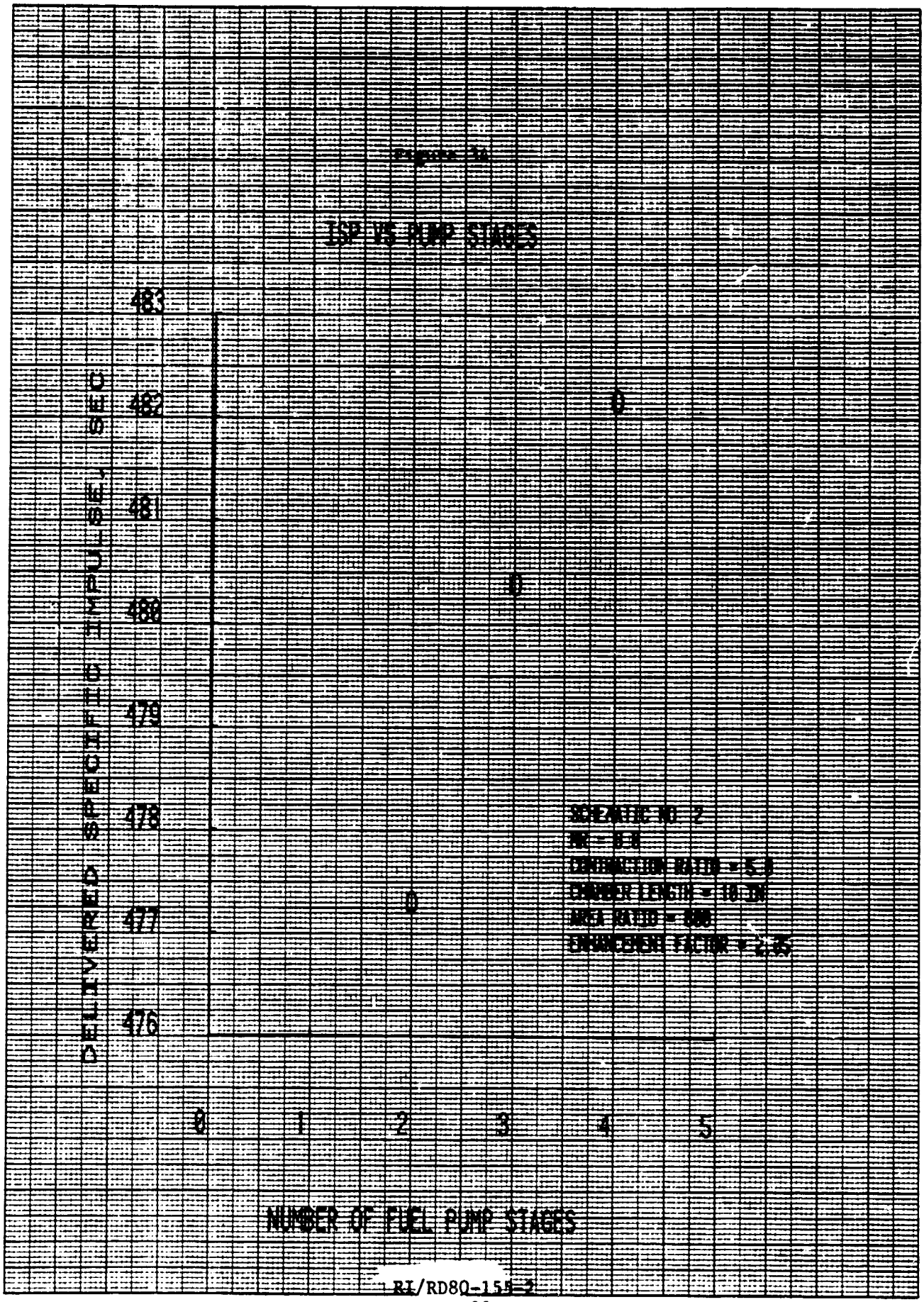

46 1513

K·E 10 X 10 TO THE CENTIMETER 18 X 25 CM
KEUFFEL & ESSER CO. MADE IN U.S.A.

FIGURE 35

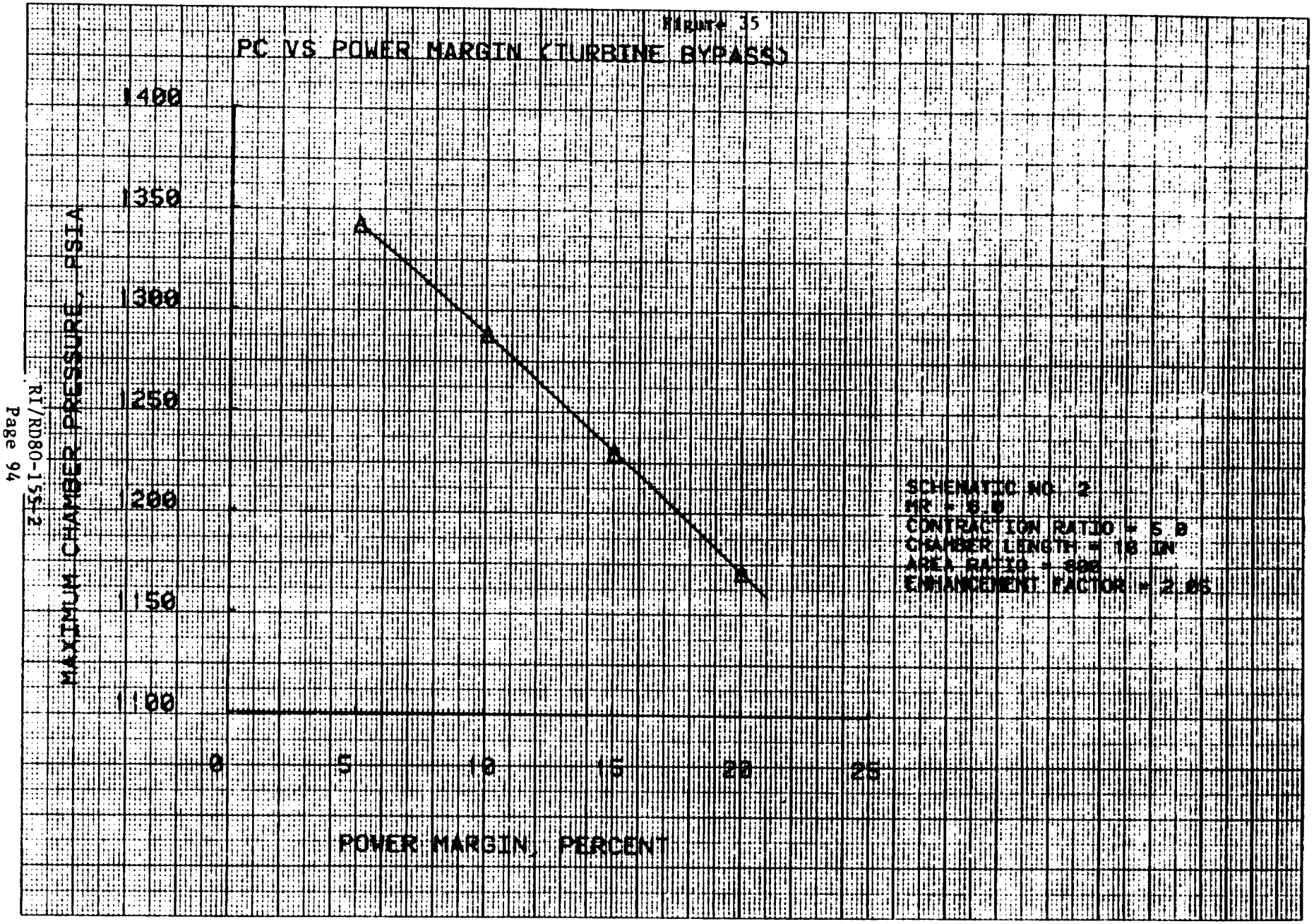
PC VS POWER MARGIN (TURBINE BYPASS)
MAXIMUM CHAMBER PRESSURE, PSIA
1400
1350
1300
1250
1200
1150
1100
0
5
10
15
20
25
POWER MARGIN, PERCENT
SCHEMATIC NO. 2
MR = 5.0
CONTRACTION RATIO = 5.0
CHAMBER LENGTH = 10 IN
AREA RATIO = 600
ENHANCEMENT FACTOR = 2.06

control, but reduces the volume flowrate through the turbines, forcing smaller admission fractions.

Figure 36 illustrates the sensitivity of specific impulse to power margin for a fixed area ratio.

Delivered specific impulse varies with design point engine mixture ratio as shown in Fig. 37. Once again, the data shown is for an 800:1 area ratio. A similar trend would be observed for optimum area ratios. The loss in I_{SP} is principally due to higher kinetic losses as mixture ratio is increased. The theoretical impulse also decreases from a mixture ratio of 6 to 7, but only about two seconds of the overall specific impulse reduction is due to changes in the theoretical I_{SP}.

Schematic No. 4 (Regen Cycle)

In schematic No. 4, a regenerative thermodynamic cycle is achieved by inclusion of a heat exchanger which acts as an accumulator of heat energy. This circuit results in higher fuel turbine inlet temperatures for a given level of total jacket heat load than does the more conventional design represented by schematic No. 2. Higher turbine temperatures imply that higher chamber pressures can be achieved with lower total heat loads in the cooling jackets. The oxidizer turbine operates at reduced inlet temperatures due to the cooling occurring in the heat exchanger. This benefits the power cycle in two ways:

1. Reduced oxidizer turbine inlet temperature results in improved velocity ratio (U/C_o), which leads to higher efficiency
2. Reduced oxidizer turbine outlet temperature, indicating that higher overall cycle thermal efficiency has been achieved.

Figure 36

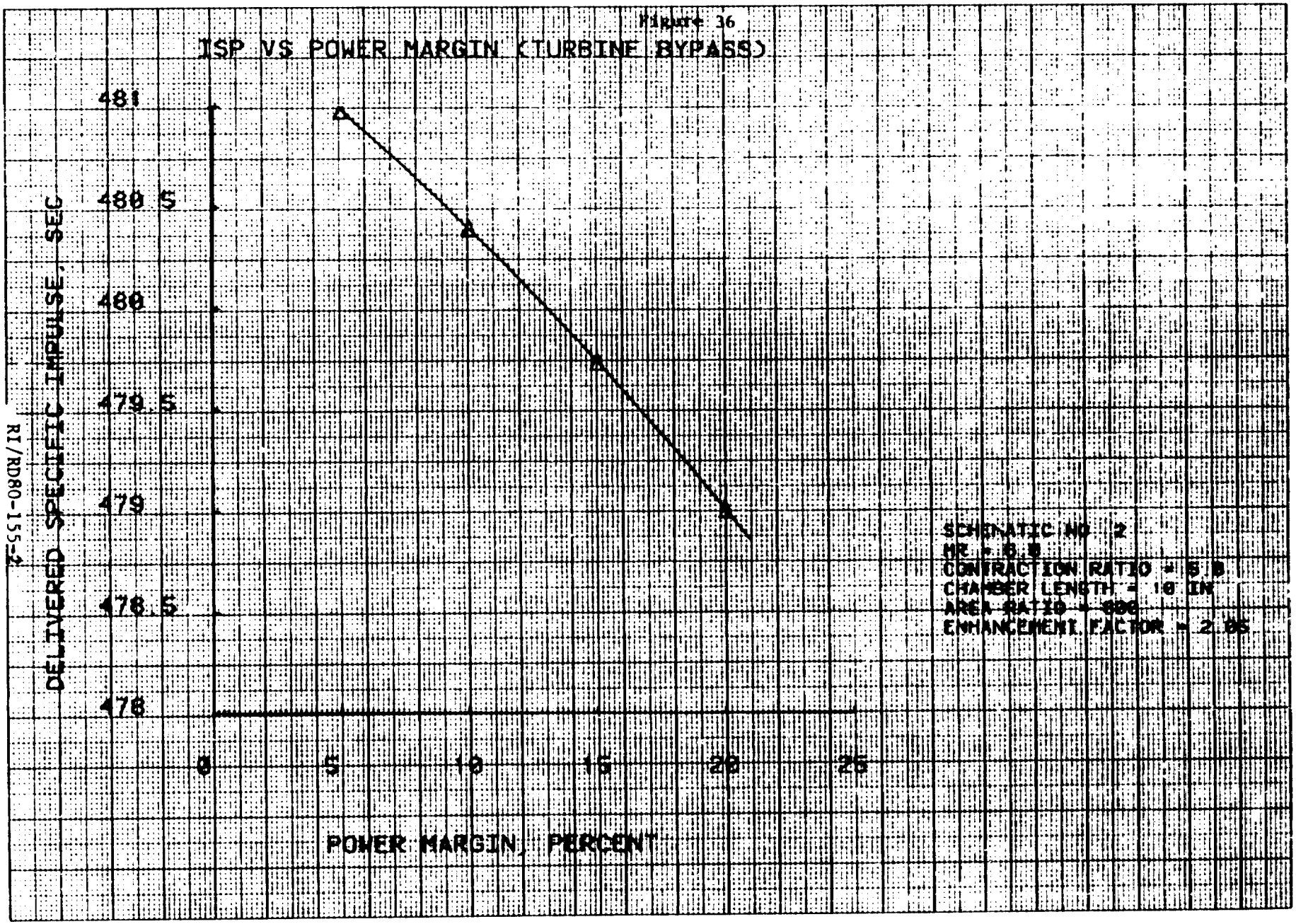
ISP VS POWER MARGIN (TURBINE BYPASS)
481
480.5
480
479.5
479
478.5
478
DELIVERED SPECIFIC IMPULSE, SEC
0
5
10
15
20
25
POWER MARGIN, PERCENT
SCHEMATIC NO 2
MR = 6.0
CONTRACTION RATIO = 5.0
CHAMBER LENGTH = 10 IN
AREA RATIO = 400
ENHANCEMENT FACTOR = 2.05

Figure 37

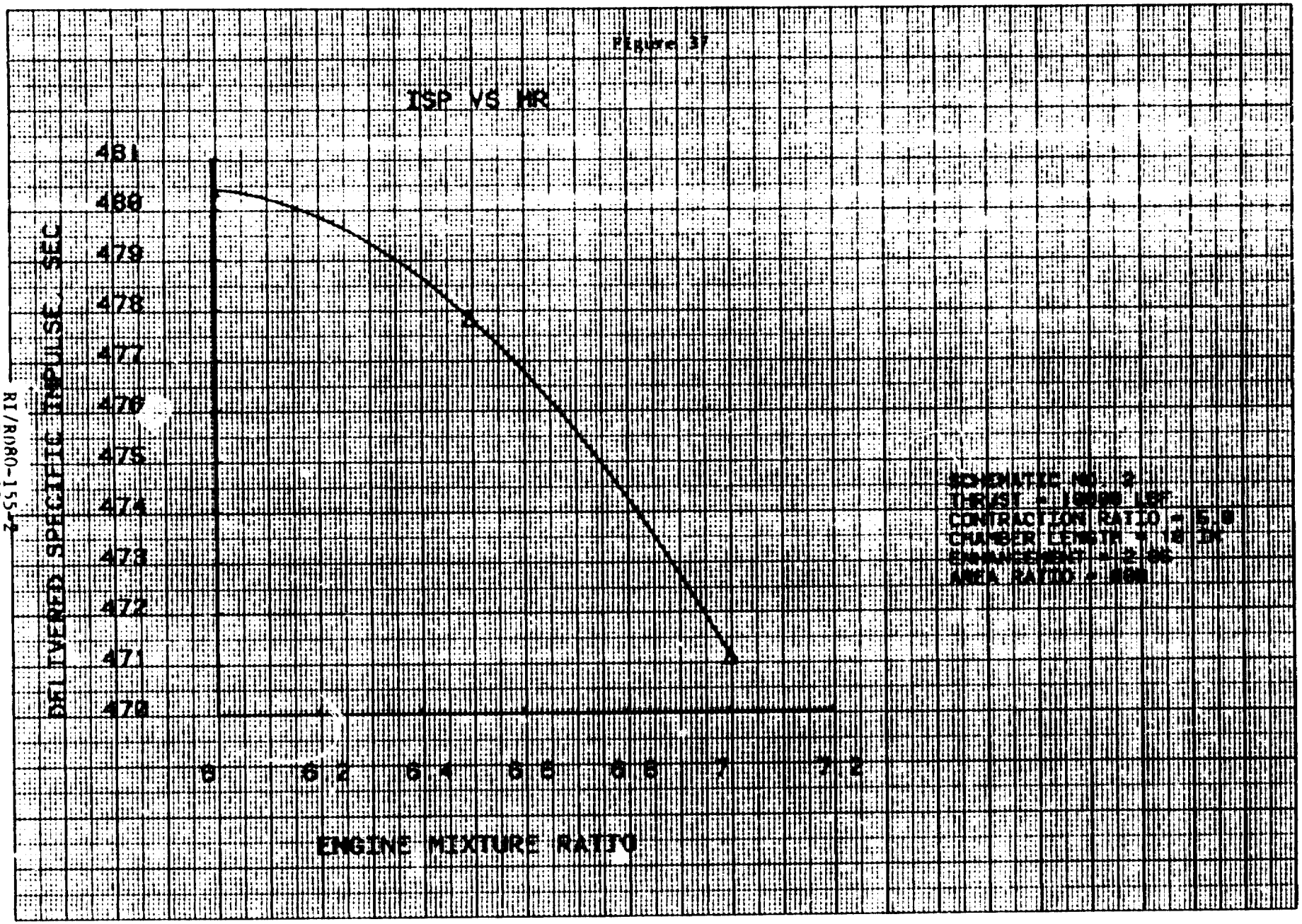
ISP VS MR
DELIVERED SPECIFIC IMPULSE, SEC
481
480
479
478
477
476
475
474
473
472
471
470
6
6.2
6.4
6.6
6.8
7
7.2
ENGINE MIXTURE RATIO
SCHEMATIC NO. 2
THRUST - 15000 LBF
CONTRACTION RATIO = 5.0
CHAMBER LENGTH = 10 IN
CONVERGENT = 2 DE
AREA RATIO = 800

Regen Heat Exchanger

The heat exchanger configuration incorporated into the balance model was a lightweight, high-efficiency exchanger design.

A large number of steady-state computer model balance runs were made in order to study schematic No. 4 in detail. In most cases, the maximum fuel pump speed was limited to 100,000 rpm, and the chamber length held to 10 inches. Also, in most cases the objective was to maximize the chamber pressure at which the system would find a balance.

The dependence of the maximum achievable cycle chamber pressure upon the effectiveness of the heat exchanger was examined. Figure 38 and 39 present the results of this study. In Fig. 38, the parameter is combustor bulk temperature. The figure implies that, for a fixed value of combustor T_{bulk}, increasing heat exchanger effectiveness results in reduced chamber pressure. In other words, if a given T_{bulk} can be achieved, it is better to do it through schemes which do not rely heavily upon the heat exchanger.

Figure 39 is a cross-plot of the same data, with combustor enhancement factor as the parameter. This shows that, for a given level of combustor thermal enhancement, increases in heat exchanger effectiveness result in increased P_c. It is important to recognize that certain levels of chamber pressure can be achieved only through a combination of thermal enhancement and heat exchanger heat transfer.

P_c is plotted vs fuel turbine pressure ratio in Fig. 40 for various levels of combustor bulk temperature. Data for this plot consists of cases which incorporate heat exchangers only, because removal of the exchanger results in inconsistent trends with pressure ratio.

The discharge pressure of the high pressure fuel pump is shown as a function of achieved chamber pressure in Fig. 41. The data shown is for fixed chamber length and area ratio and includes both regenerative (Cycle 4) and non-regen (Cycle 2)

Figure 18

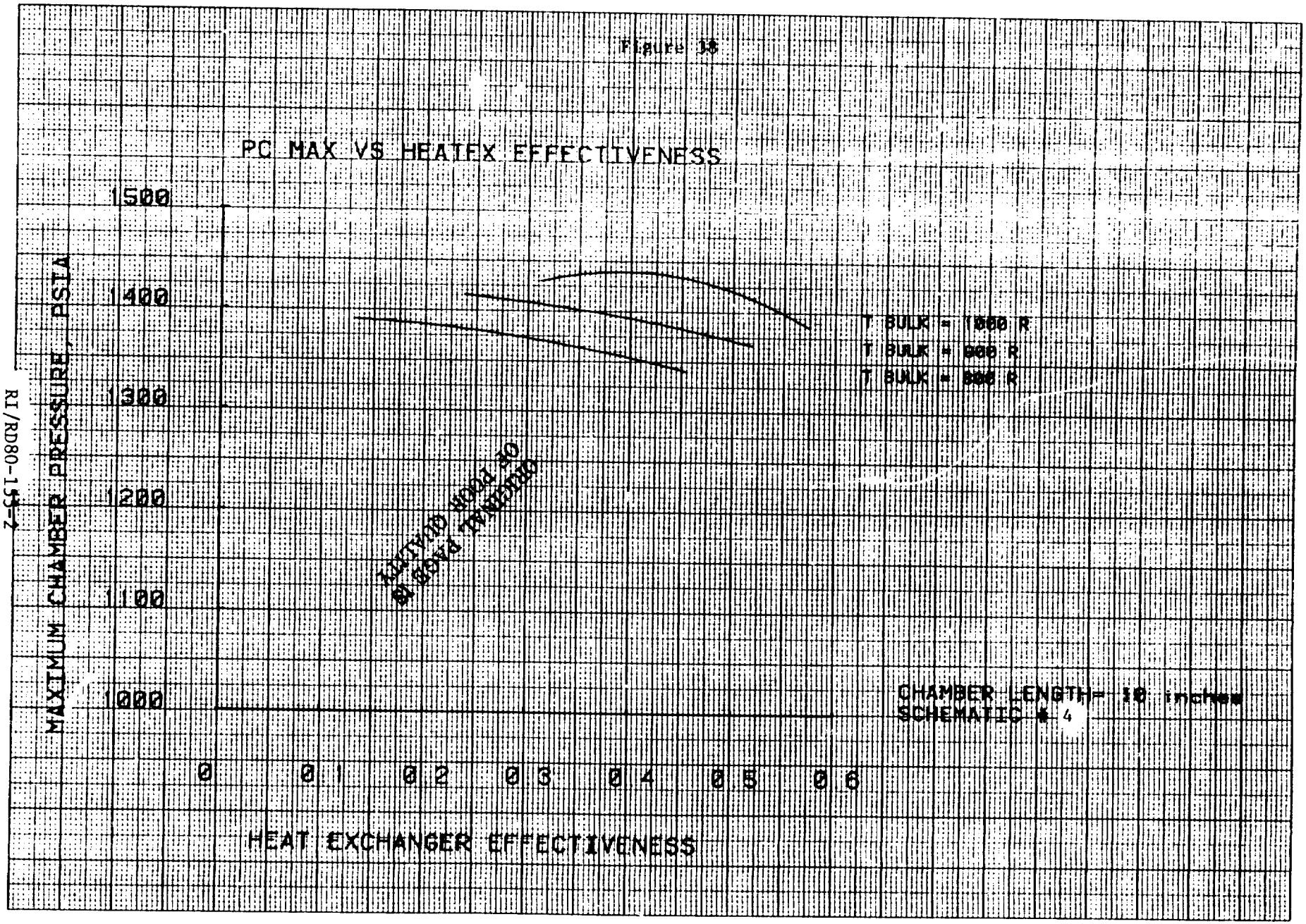

Figure 39

Maximum Chamber Pressure vs Heat Exchanger Effectiveness

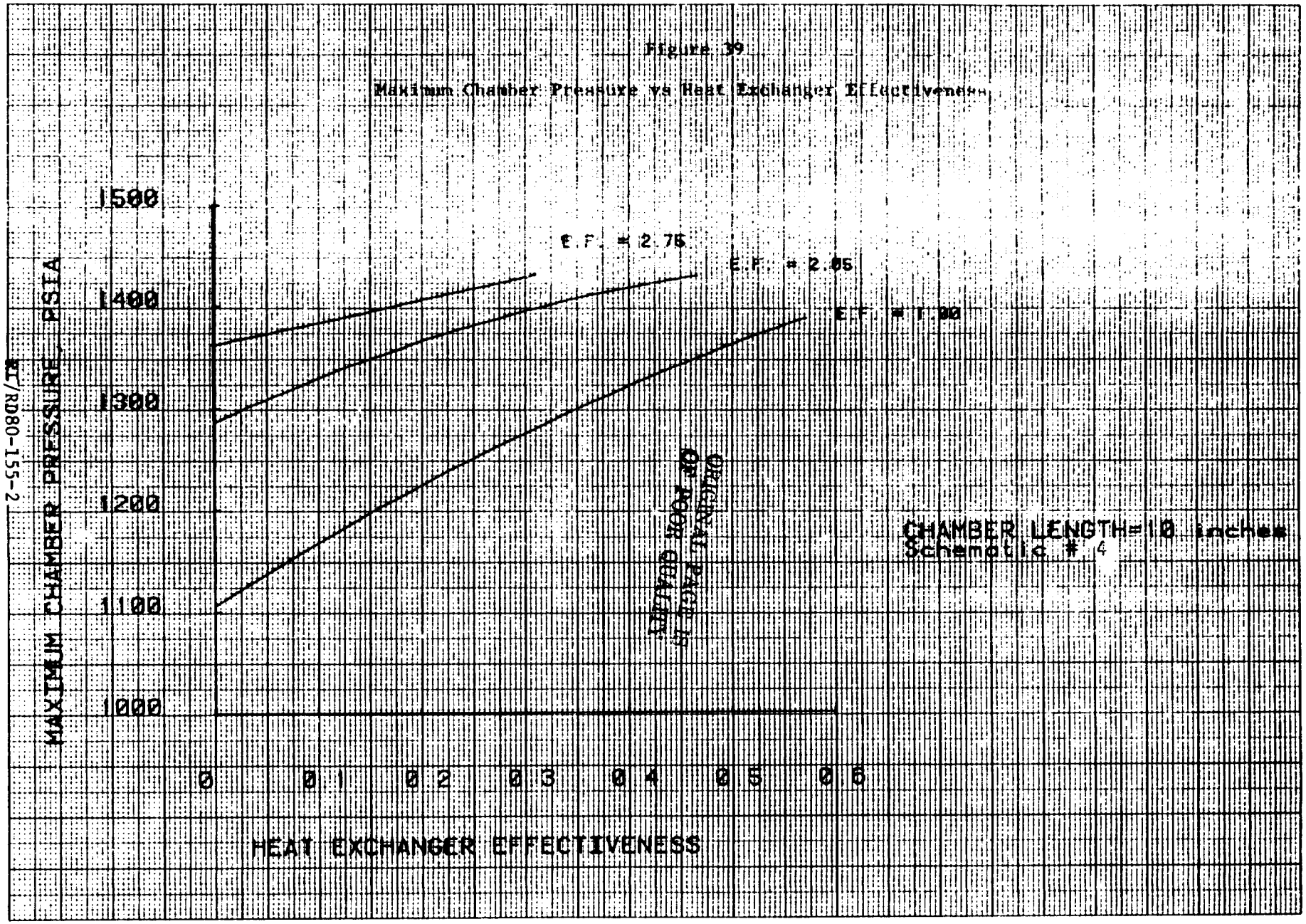

Figure 40

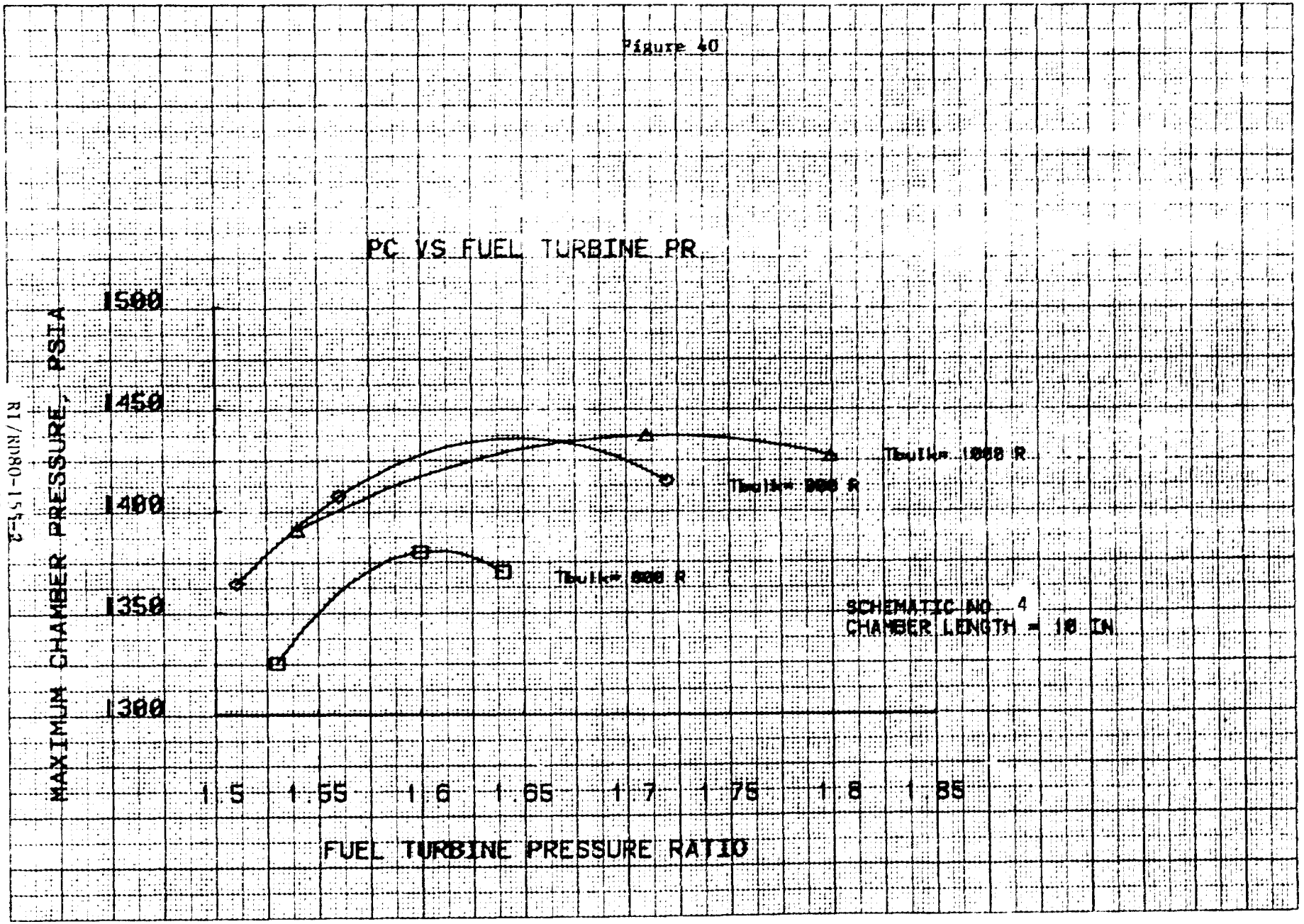
PC VS FUEL TURBINE PR
MAXIMUM CHAMBER PRESSURE, PSIA
1500
1450
1400
1350
1300
Tbulk= 1000 R
Tbulk= 900 R
Tbulk= 800 R
SCHEMATIC NO. 4
CHAMBER LENGTH = 10 IN.
1.5
1.55
1.6
1.65
1.7
1.75
1.8
1.85
FUEL TURBINE PRESSURE RATIO

Figure 41

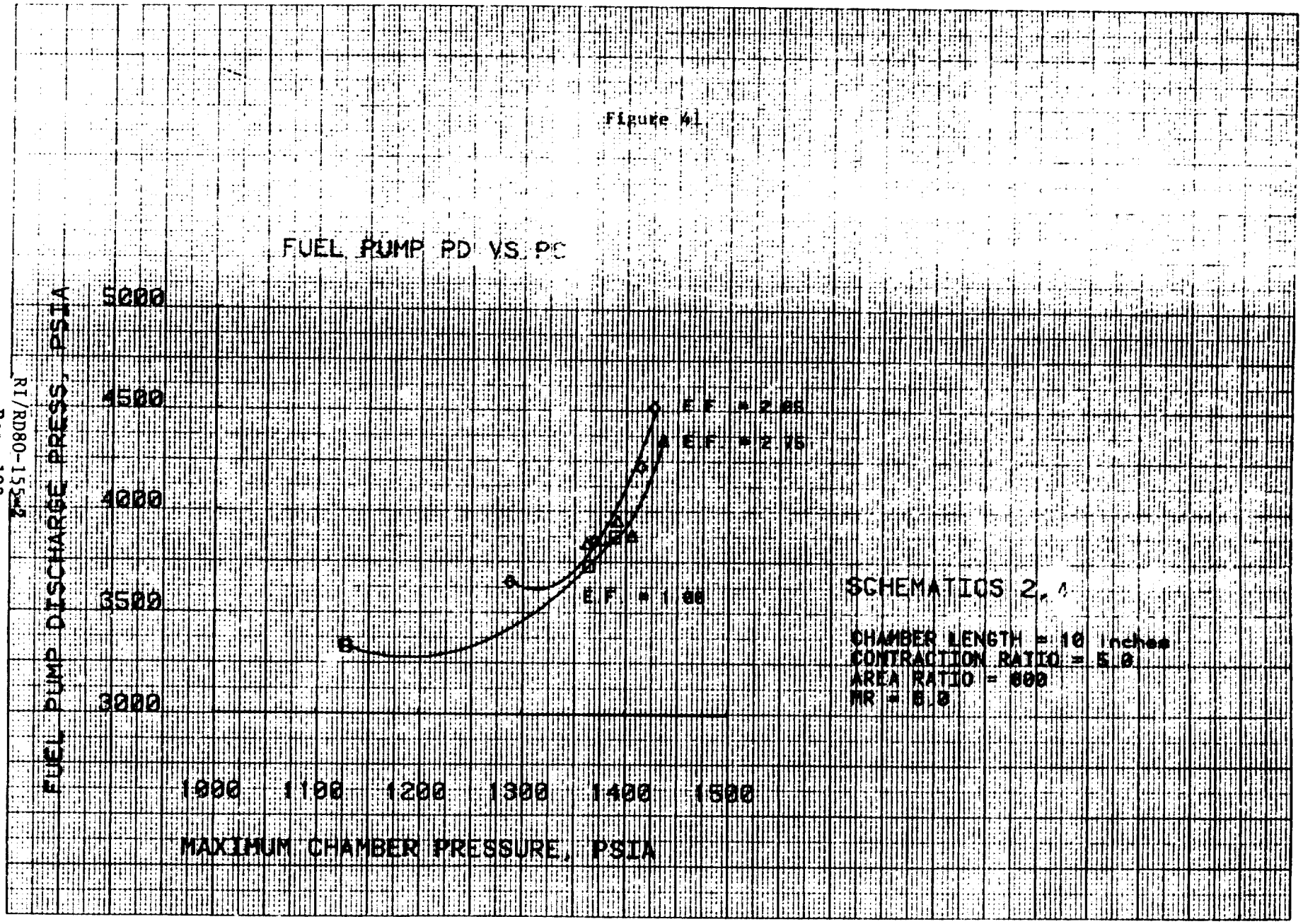
FUEL PUMP PD VS PC
FUEL PUMP DISCHARGE PRESS, PSIA
5000
4500
4000
3500
3000
1000
1100
1200
1300
1400
1500
MAXIMUM CHAMBER PRESSURE, PSIA
E F = 2.00
E F = 2.75
E F = 1.00
SCHEMATICS 2, 4
CHAMBER LENGTH = 10 inches
CONTRACTION RATIO = 5.0
AREA RATIO = 800
MR = 6.0

cases. Fuel pump P_D rises very rapidly above P_c = 1400 psia for the 10K thrust level, indicating that the ultimate power limit is being approached. Increasing fuel pump speed or number of stages would result in higher chamber pressures than shown.

Thrust chamber thermal enhancement influences fuel pump discharge as shown in Fig. 42. As thermal enhancement factor is increased, P_c increases due to higher turbine inlet temperatures (i.e., nozzle jacket outlet temperature), causing increased pump discharge pressures. At the same time, however, the increased jacket heat load causes reductions in heat exchanger heat load (at constant T_{bulk}). This results in lower heat exchanger pressure drop and increased jacket inlet density, both of which tend to reduce pump discharge pressure, as shown in Fig. 43. Thus, the curve of P_d vs E.F. passes through a maximum caused by these opposing influences.

Increases in jacket pressure drop (which consists essentially only of combustor jacket ΔP) result in higher fuel pump discharge pressures as illustrated in Fig. 44. Increases in jacket heat transfer enhancement are also displayed. Increasing E.F. allows higher chamber pressure and causes lower average coolant density, resulting in higher fuel pump P_D at larger values of E.F.

Figure 45 presents the effect of pressure ratio upon fuel pump discharge pressure. Curves are shown parametrically with bulk temperature. As seen above, increases in bulk temperature yield higher chamber pressures, causing discharge pressure to increase with T_{bulk} as well as with P_r.

Heat exchanger hot and cold side ΔP are plotted vs bulk temperature and enhancement factor in Fig. 46 and 47. Increasing bulk temperatures for a fixed-geometry combustor requires higher levels of heat exchanger heat load, greater exchanger length, and higher ΔP. Increasing enhancement factor for a given temperature reduces the requires heat exchanger load and thus reduces the pressure drop.

Figure 12

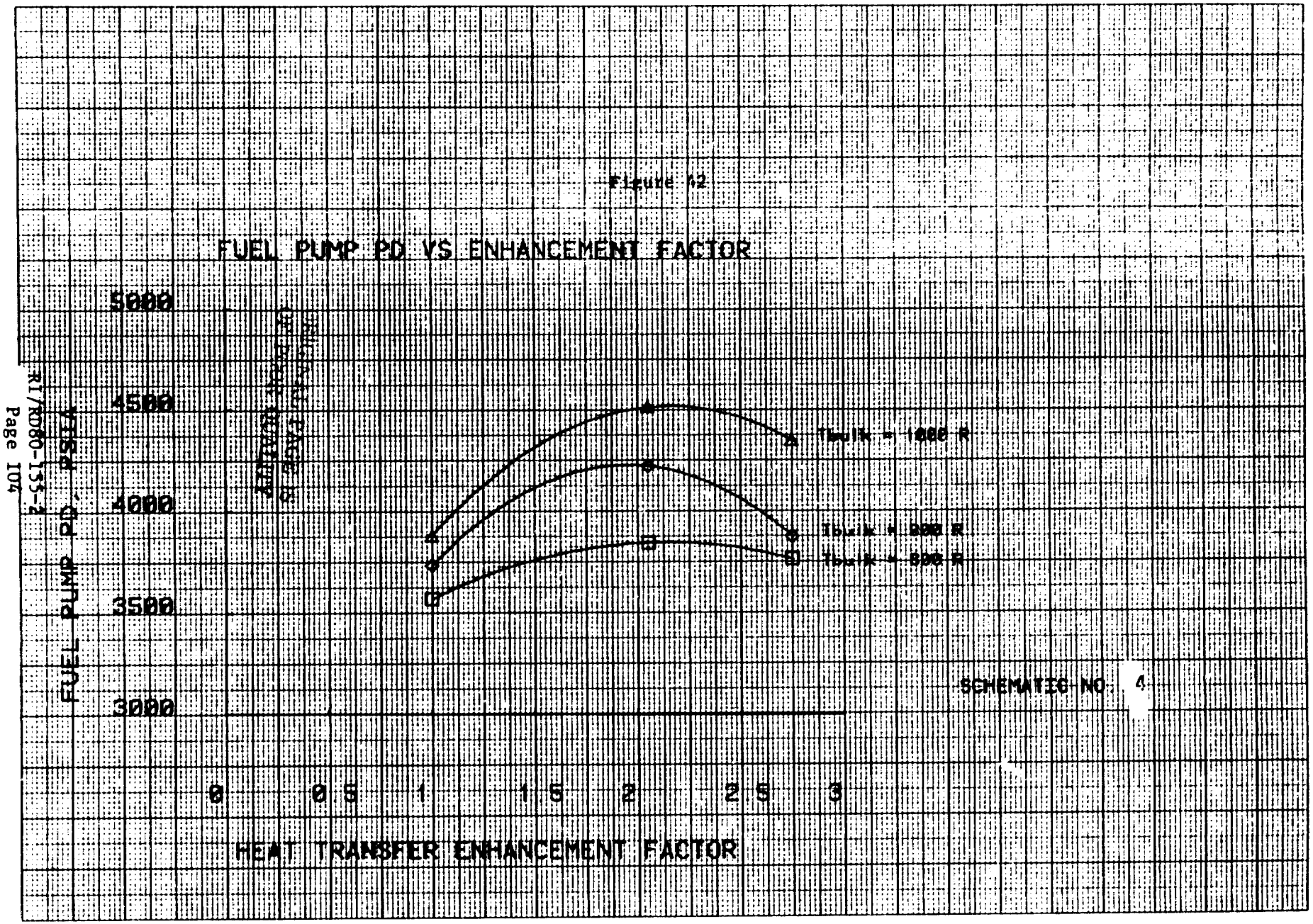
FUEL PUMP PD VS ENHANCEMENT FACTOR
FUEL PUMP PD, PSIA
5000
4500
4000
3500
3000
0
0.5
1
1.5
2
2.5
3
HEAT TRANSFER ENHANCEMENT FACTOR
Tbulk = 1000 R
Tbulk = 800 R
Tbulk = 600 R
SCHEMATIC NO. 4

Figure 43

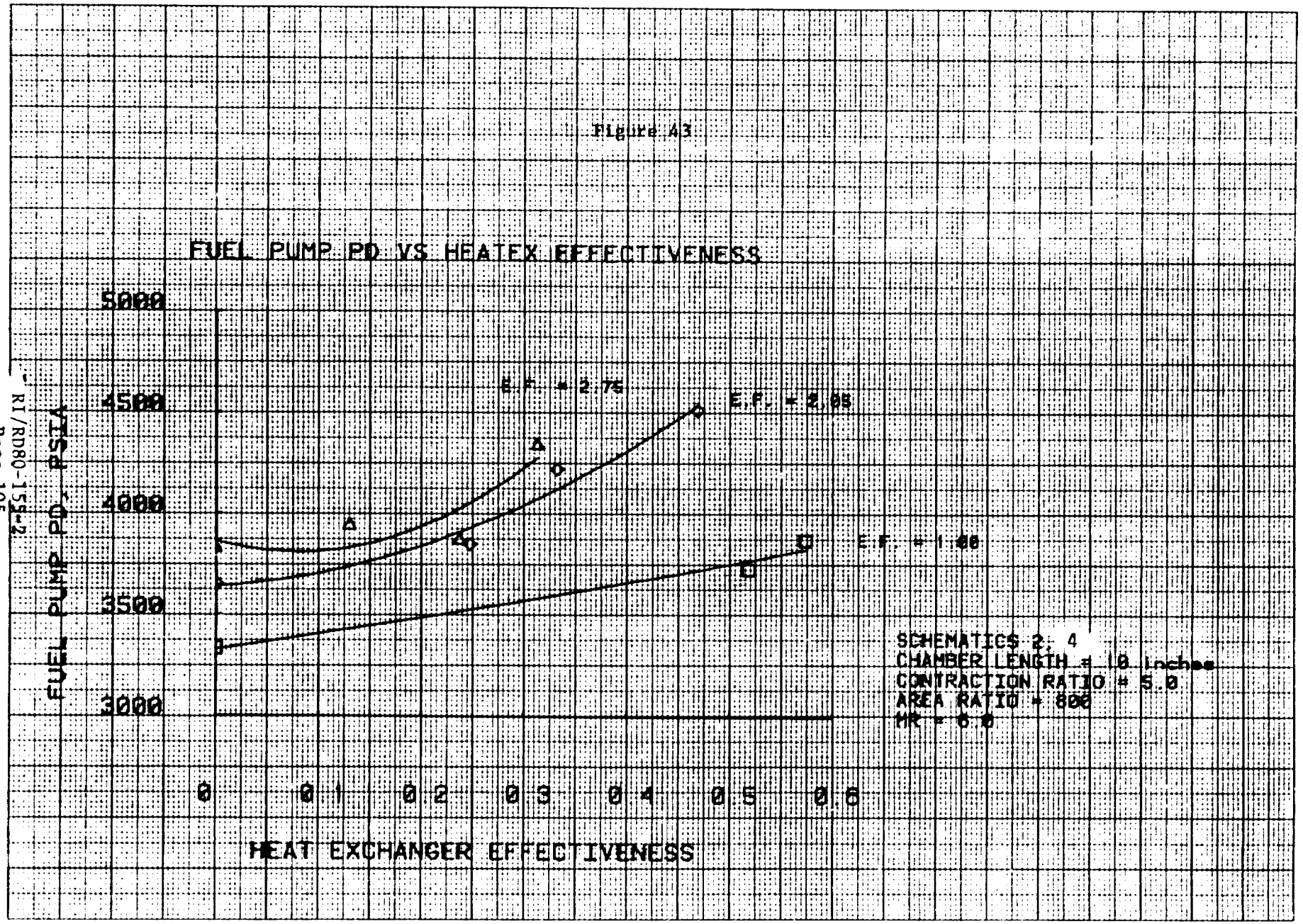
FUEL PUMP PD VS HEATEX EFFECTIVENESS
FUEL PUMP PD, PSIA
5000
4500
4000
3500
3000
E.F. = 2.75
E.F. = 2.05
E.F. = 1.00
SCHEMATICS 2, 4
CHAMBER LENGTH = 10 inches
CONTRACTION RATIO = 5.0
AREA RATIO = 800
MR = 6.0
0
0.1
0.2
0.3
0.4
0.5
0.6
HEAT EXCHANGER EFFECTIVENESS

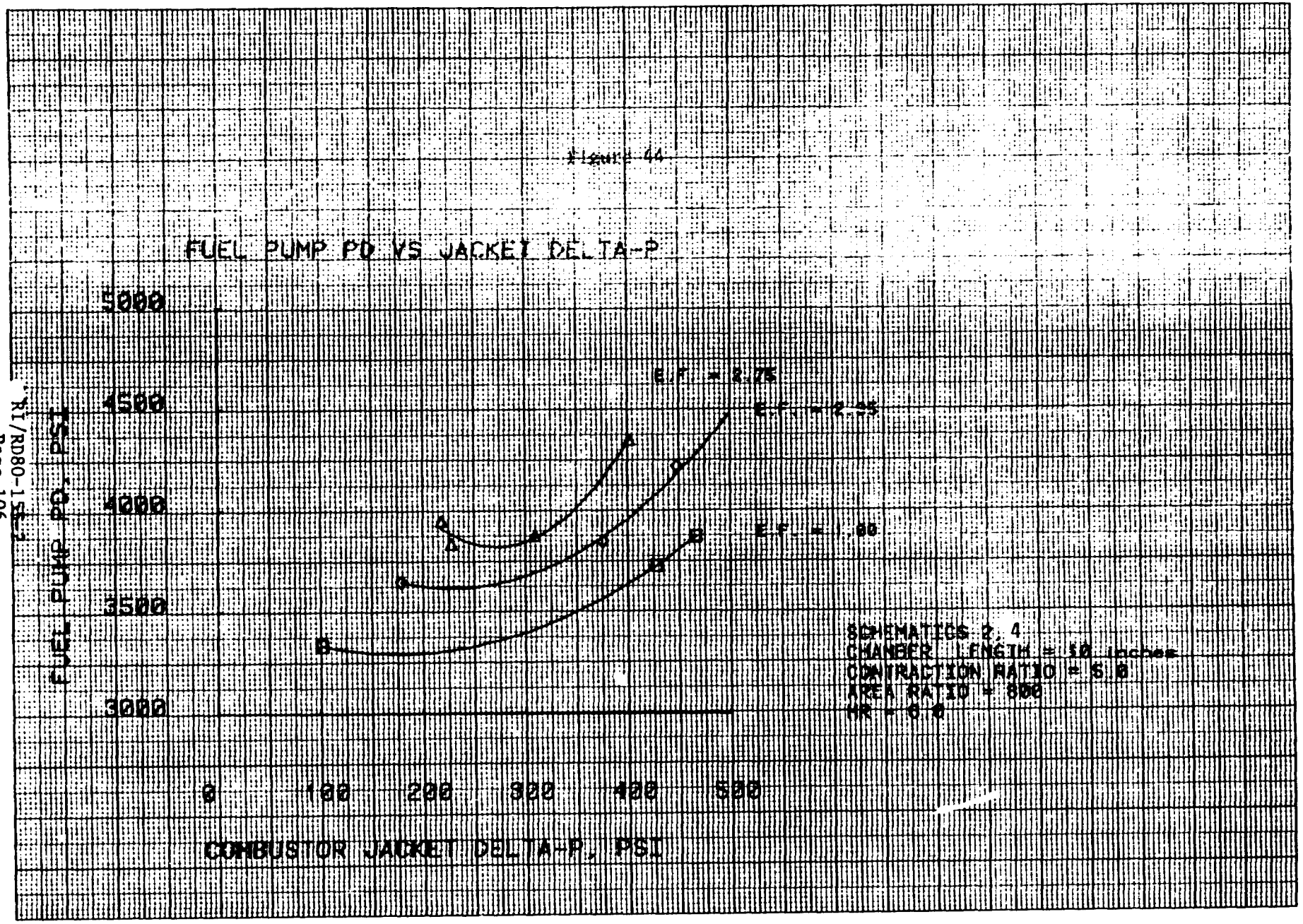
Figure 44
FUEL PUMP PD VS JACKET DELTA-P
5000
4500
4000
3500
3000
PSI
Fuel Pump Delta P
E.F. = 2.75
E.F. = 2.35
E.F. = 1.80
A
B
SCHEMATICS 2, 4
CHAMBER LENGTH = 10 inches
CONTRACTION RATIO = 5.0
AREA RATIO = 800
MR = 6.0
0
100
200
300
400
500
COMBUSTOR JACKET DELTA-P, PSI

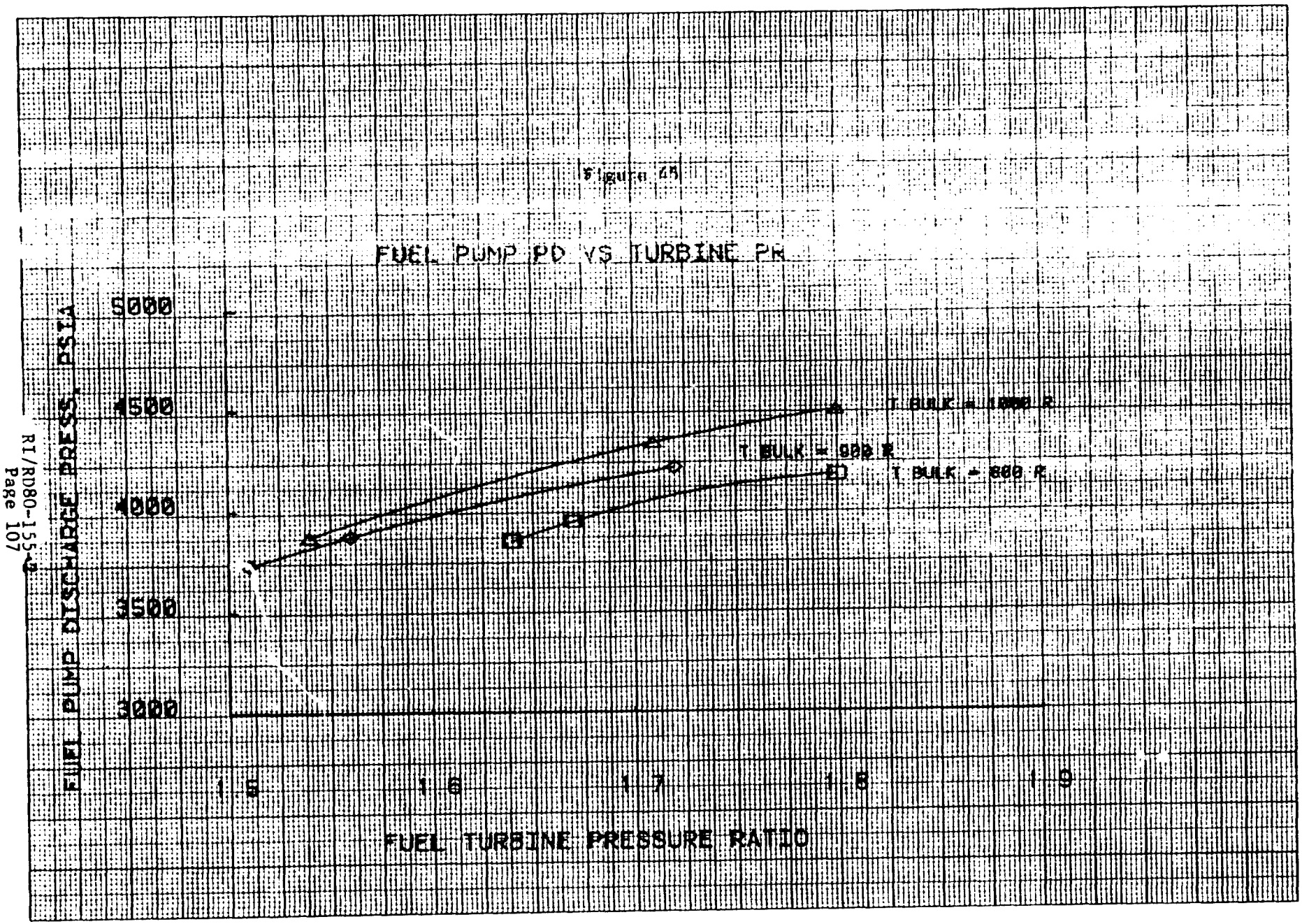
Figure 25
FUEL PUMP PD VS TURBINE PR
FUEL PUMP DISCHARGE PRESS - PSIA
5000
4500
4000
3500
3000
T BULK = 1000 R
T BULK = 900 R
T BULK = 800 R
1.5
1.6
1.7
1.8
1.9
FUEL TURBINE PRESSURE RATIO

Figure 46

Heat Exchanger Cold-Side ΔP vs Maximum Bulk Temperature

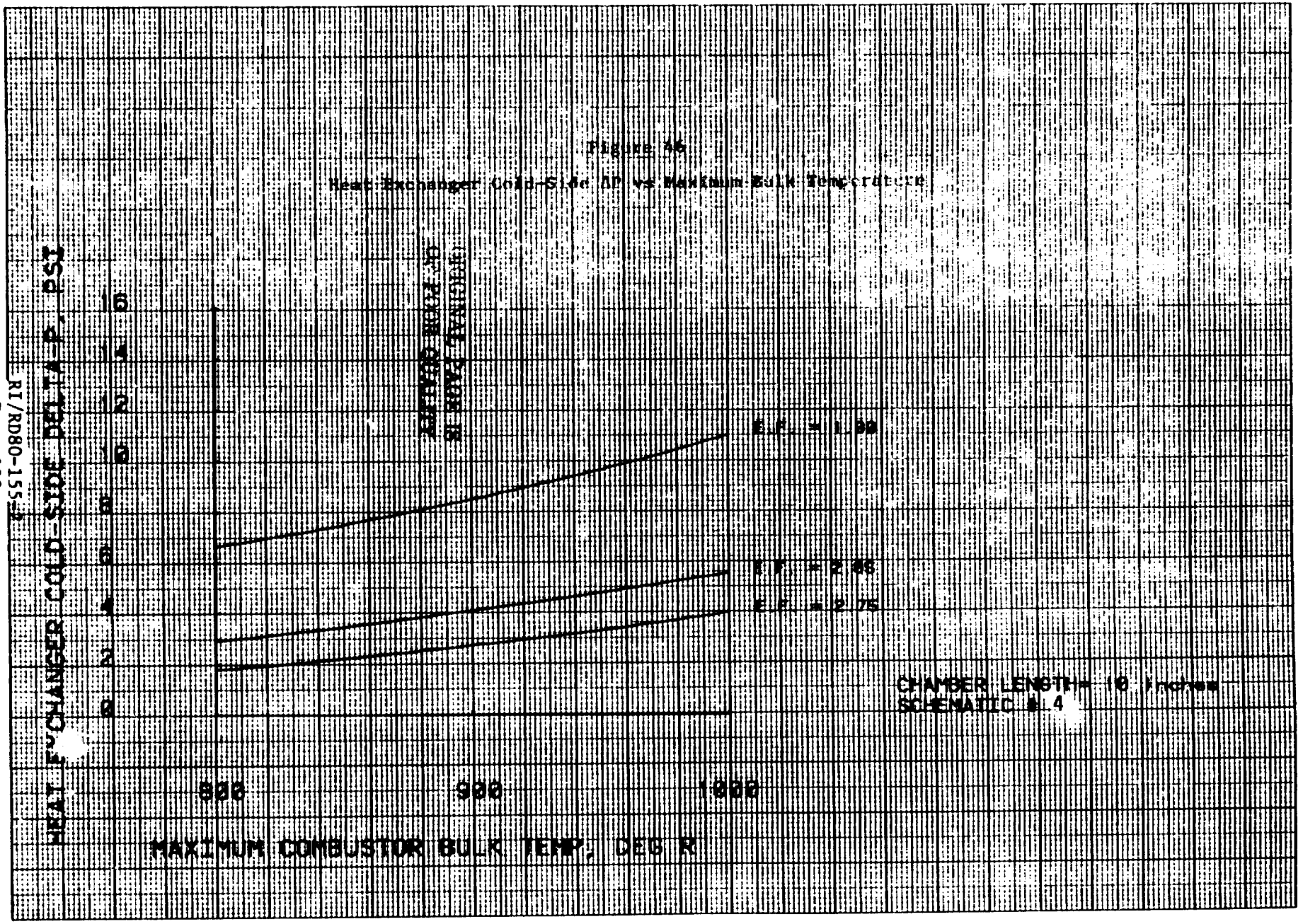

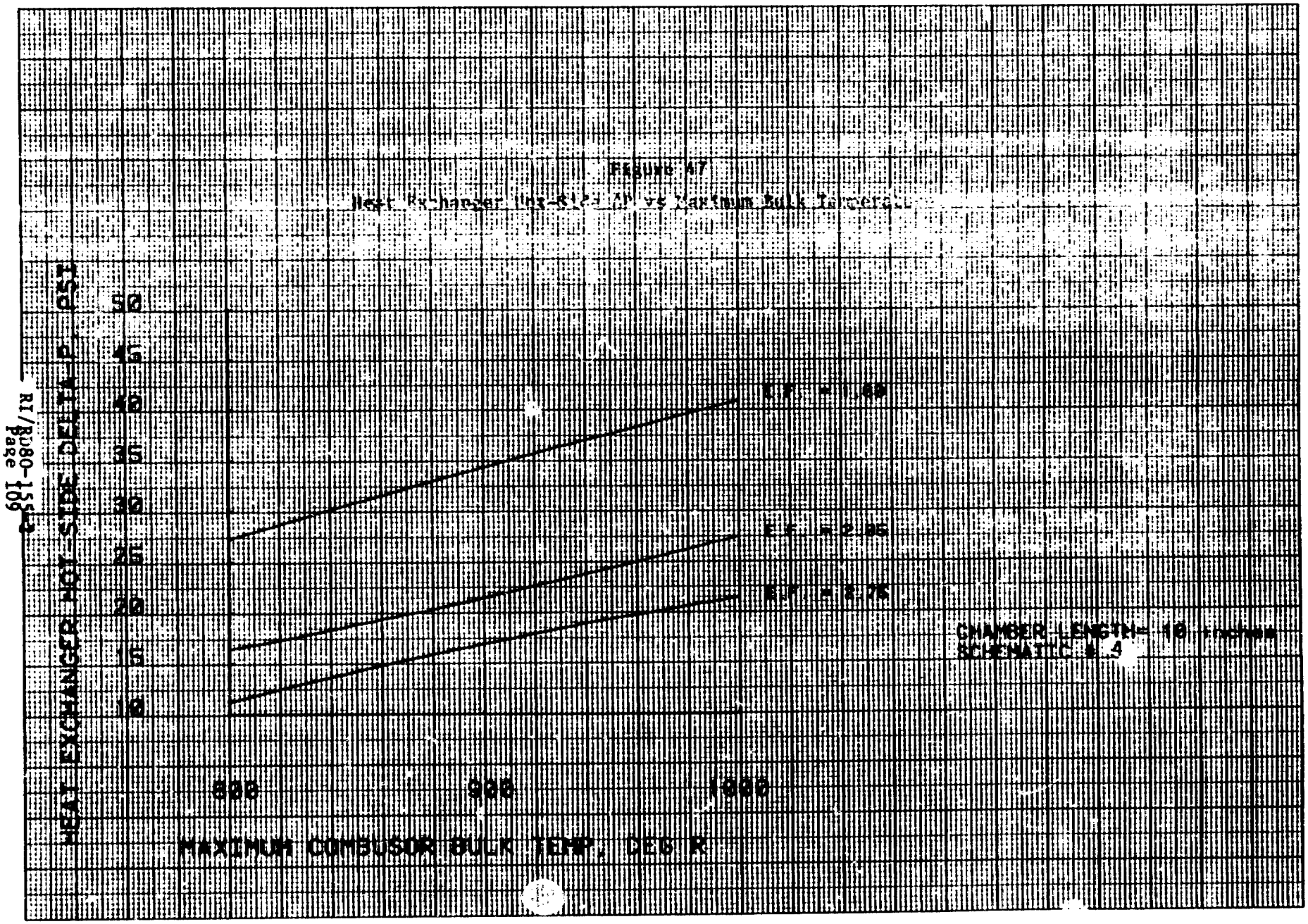

Figure A7
Heat Exchanger Hot-Side ΔP vs Maximum Bulk Temperature

SUMMARY - 10,000 POUND THRUST RESULTS

Cycle optimization studies conducted at the 10K thrust level lead to conclusions generally compatible with those conducted at the 15K thrust level and support the conclusion that the optimum cycle configuration is independent of thrust level. It has been seen that cycles incorporating a regen heat exchanger do not significantly improve engine specific impulse over those without a heat exchanger. Thrust chamber thermal enhancement offers significant performance improvement. Increases in chamber contraction ratio do not yield significant performance benefits.

Use of a series turbine arrangement, with the fuel turbine upstream of the oxidizer turbine, results in better performance than a parallel turbine setup. However, the low oxidizer turbine pressure ratio resulting from the series configuration must be examined to assess stability and fabricability. A series turbine arrangement also leads to higher fuel pump discharge pressures than a parallel arrangement.

SECTION III - 20K-POUND THRUST ENGINE OPTIMIZATION

This section extends the expander engine cycle performance optimization studies to the 20K-pound thrust level. Only those study results are discussed in this section which are affected by thrust level; all other results were considered in the previous two sections.

MAIN TURBINE ARRANGEMENT

The selected turbine arrangement at 20K thrust is the same as that for 10 and 15K: a series turbine arrangement was selected on the basis of highest performance potential.

CYCLE ENERGY SOURCE

A smooth-wall combustor is the principal source of energy input to the hydrogen working fluid. The higher thrust level of 20K permits longer chamber lengths to be used without encountering the hydrogen coolant bulk temperature limit of 1000R in the combustor. Thermally-enhanced chamber designs were only briefly considered at the 20K thrust level, because the earlier part of this task found that thermal enhancement did not meet the requirements for 1980 state-of-the art.

HIGH PRESSURE PUMP DESIGNS

Using the same pump design groundrules as in the earlier part of the study hydrogen pump speeds are reduced somewhat at 20K relative to 10K and 15K. This due to the larger bearing diameters required at this thrust level, which forces lower speed for a fixed bearing DN limit. Pump speeds are in the range of 95,000 to 102,000 rpm, depending on Pc and other drivers of pump discharge pressure.

A three stage fuel pump design is retained in the interest of simplicity, even though increased performance would result from additional stages. On the oxidizer side, a single-stage centrifugal pump is sufficient.

TURBINE GAS REHEAT AND REGENERATION

Turbine gas reheat and regeneration concepts were studied at the 20K thrust level for engines utilizing smooth-wall combustion chambers. Fig. 48 summarizes the results of full optimization runs for four configurations shown in Fig. 49. Both chamber pressure and delivered specific impulse (shaded) are shown. The configuration shown as "A" is the baseline design, which incorporates series turbines without reheat or regeneration. A maximum Pc of 1768 PSIA is achieved for a chamber length of 27.8 inches. Configuration "B" incorporates a regen heat exchanger upstream of the coolant jackets, and "C" is a reheat-type cycle in which the oxidizer turbine is supplied from the combustor jacket and the nozzle jacket is used to heat the hydrogen prior to admission to the fuel turbine. Configuration "D" is a combination of "B" and "C" which employs a regen heat exchanger upstream of the reheat (nozzle) jacket.

In each of configurations B, C, and D, full optimization of the system yields a system configuration in which the heat exchanger heat load is very low. That is, the cycle optimizes at an operating point for which the heat exchanger is not required due to the energy available from the lengthened combustor jacket. Other (non-optimum) points will result in incorporation of a regen heat exchanger for best I_S performance at shorter chamber lengths.

As seen previously for 10 and 15K, differences in performance among fully-optimized configurations are small, owing to common combustor coolant discharge temperature limits (1000R). This limits turbine inlet temperature (nozzle outlet temperature) leading to nearly equal chamber pressures and specific impulse values. Indeed, the difference in I_{SP} from the highest (Reheat-Regen) to the lowest (Reheat) is only 1.2 seconds. All configurations reach the combustor bulk temperature limit of 1000R at approximately 28 inches chamber length.

Configuration "D" has potential for somewhat higher nozzle exit temperatures by virtue of the heat exchanger which is placed upstream of the nozzle. However, chamber lengths greater than about 20 in. lead to a system temperature schedule which results in very small heat exchanger heat transfer rates. Thus, nozzle outlet temperatures for this configuration are limited to levels similar to those of other configurations (1040R). In this regard,

balances at 20K differ from those at 15K in which larger heat transfer rates were observed when the heat exchanger was placed between jackets. This is due in part to higher hydrogen flowrates at 20K, which result in a somewhat different temperature distribution around the system than was observed at 15K.

COMBUSTOR LENGTH EFFECTS

Sensitivity studies were conducted at the 20K thrust level to explore the influence of combustion chamber length and heat exchanger location upon system performance and operation.

Nozzle outlet temperature is shown in Fig. 50 as a function of chamber length. The smooth-wall combustor reaches a maximum turbine inlet temperature of 1041 R at a length of 27.8 inches. In the regenerative cycle, a similar (1038R) turbine temperature is reached at a length of 28.3 inches. A thermally-enhanced chamber design reaches 1095R with a length of 18.5 inches. None of the configurations approach the maximum allowed nozzle outlet temperature of 1250R.

The heat loads for these cases are shown in Fig. 51. All configurations show a linear relationship of total heat load to chamber length until the maximum length of approximately 28 inches (smooth) or 18.5 inches (enhanced) is reached.

As was seen at 15K, increases in chamber length tend to reduce heat exchanger effectiveness required to produce a given nozzle outlet temperature due to the higher temperature of the combustor outlet hydrogen. Heat exchanger utility is greatest for short chambers, where cold-side temperatures are lowest. Fig. 51 shows that the greatest difference (increase) in nozzle discharge temperature between configurations with regen heat exchangers and those without is seen at short chamber lengths. As combustor jacket bulk temperature increases toward its limit of 1000R, the heat exchanger heat load is gradually reduced until it reaches zero at about the same chamber length (28 in.) as that at which the combustor T bulk hits its limit when the heat exchanger is placed upstream of both jackets. When it is placed between the jackets, the heat exchanger heat load is reduced more quickly, reaching zero at around 19.5 inches (Fig. 52).

Heat exchanger heat load for a given chamber length depends in part upon the fraction of the total jacket heat load which is supplied in the nozzle. This fraction is in turn influenced by the attach area ratio; i.e., the area ratio marking the boundary between combustor and nozzle jackets. The present studies have employed an attach area ratio of 14:1, based principally on ease of fabrication. Future design iterations must address the optimization of this area ratio, both for the baseline configuration and for alternate configurations utilizing heat exchangers.

CYCLE OPTIMIZATION AT 20K THRUST

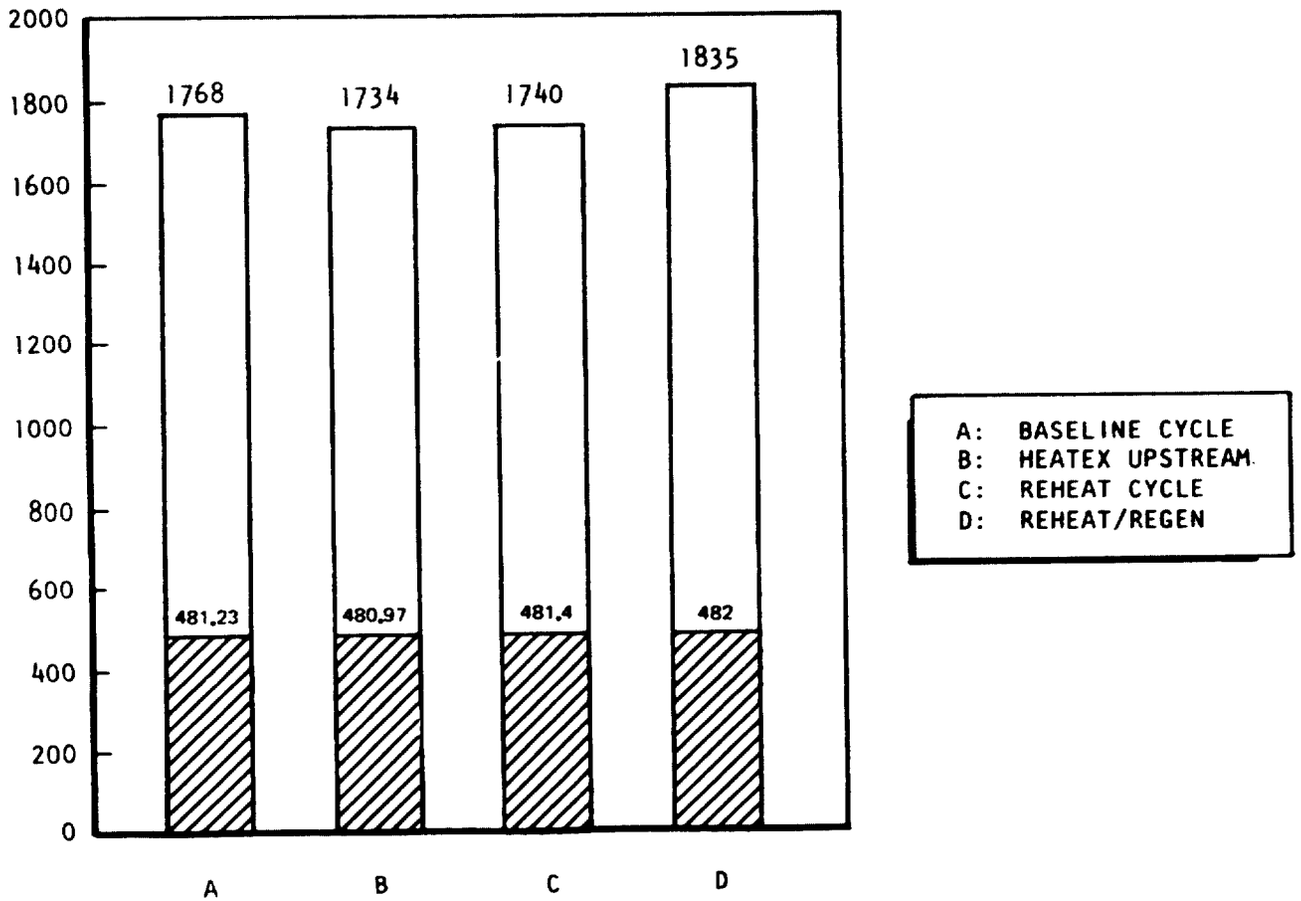

Figure 48

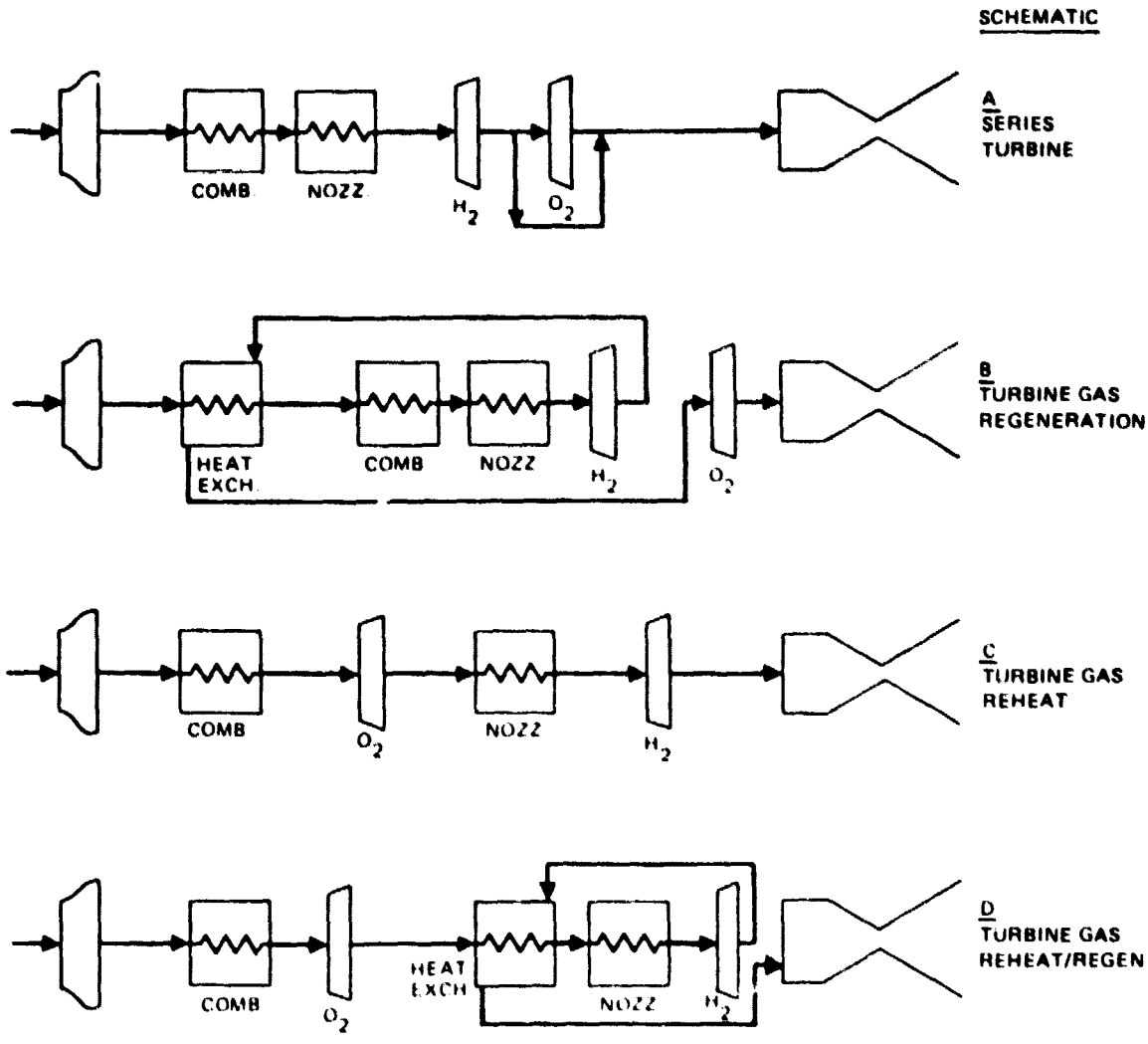

Figure 49. Schematics Studied at 20K Thrust

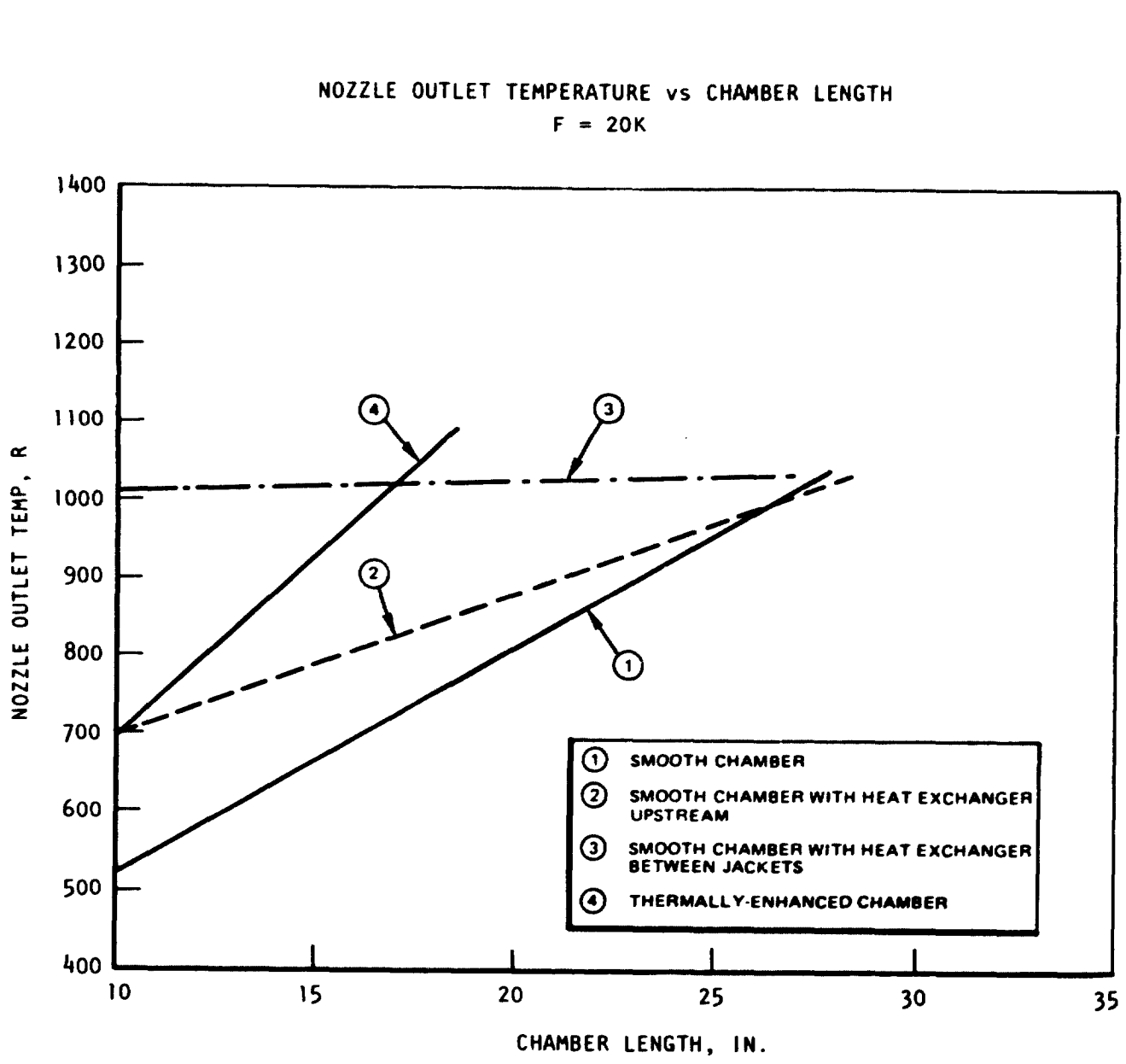

Figure 50
RI/RD80-155-2
Page 116

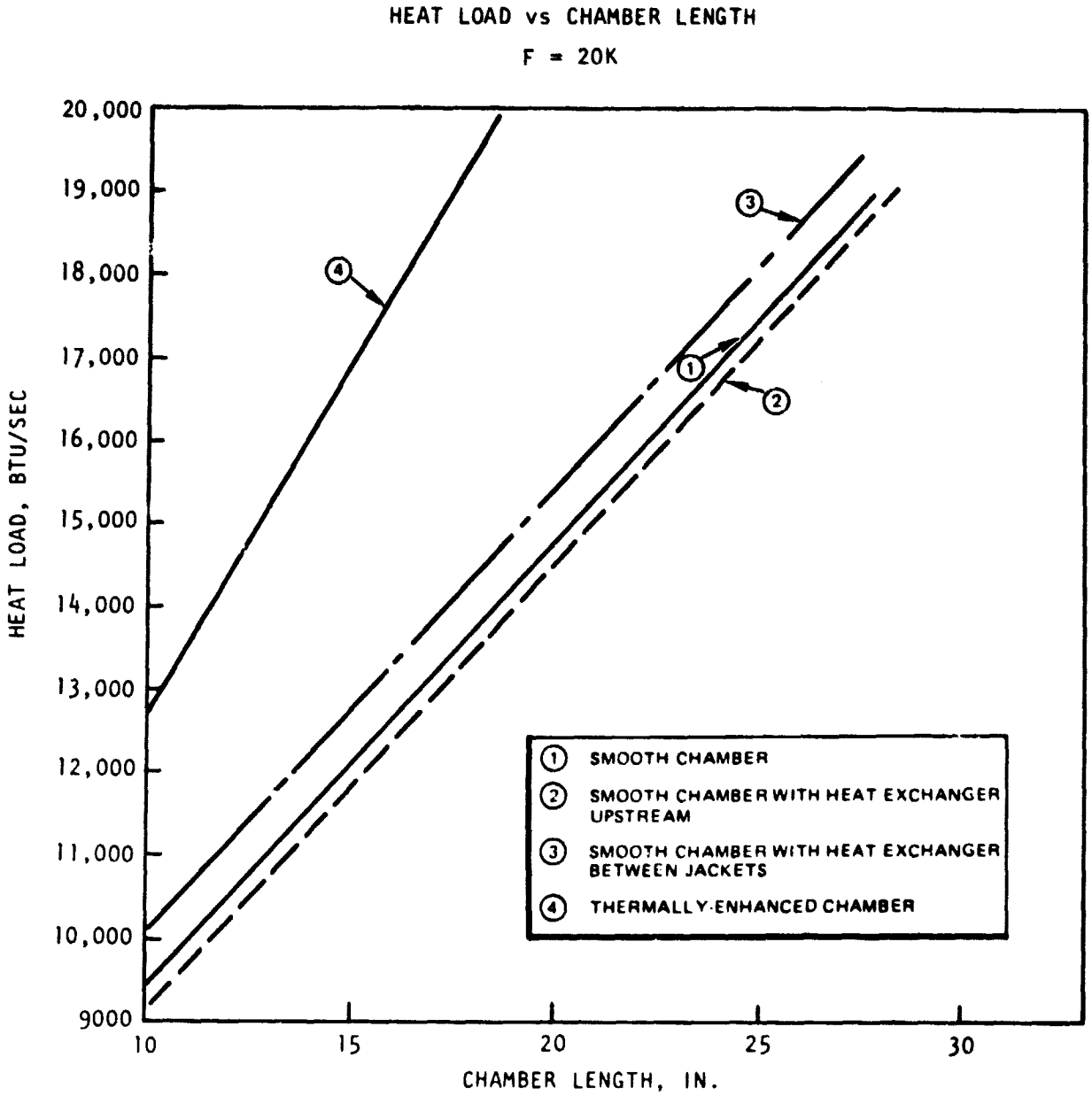
HEAT LOAD vs CHAMBER LENGTH
F = 20K
HEAT LOAD, BTU/SEC
20,000
19,000
18,000
17,000
16,000
15,000
14,000
13,000
12,000
11,000
10,000
9000
10
15
20
25
30
CHAMBER LENGTH, IN.
1 SMOOTH CHAMBER
2 SMOOTH CHAMBER WITH HEAT EXCHANGER UPSTREAM
3 SMOOTH CHAMBER WITH HEAT EXCHANGER BETWEEN JACKETS
4 THERMALLY-ENHANCED CHAMBER

Figure 51

HEAT EXCHANGER HEAT LOAD vs CHAMBER LENGTH
F = 20K

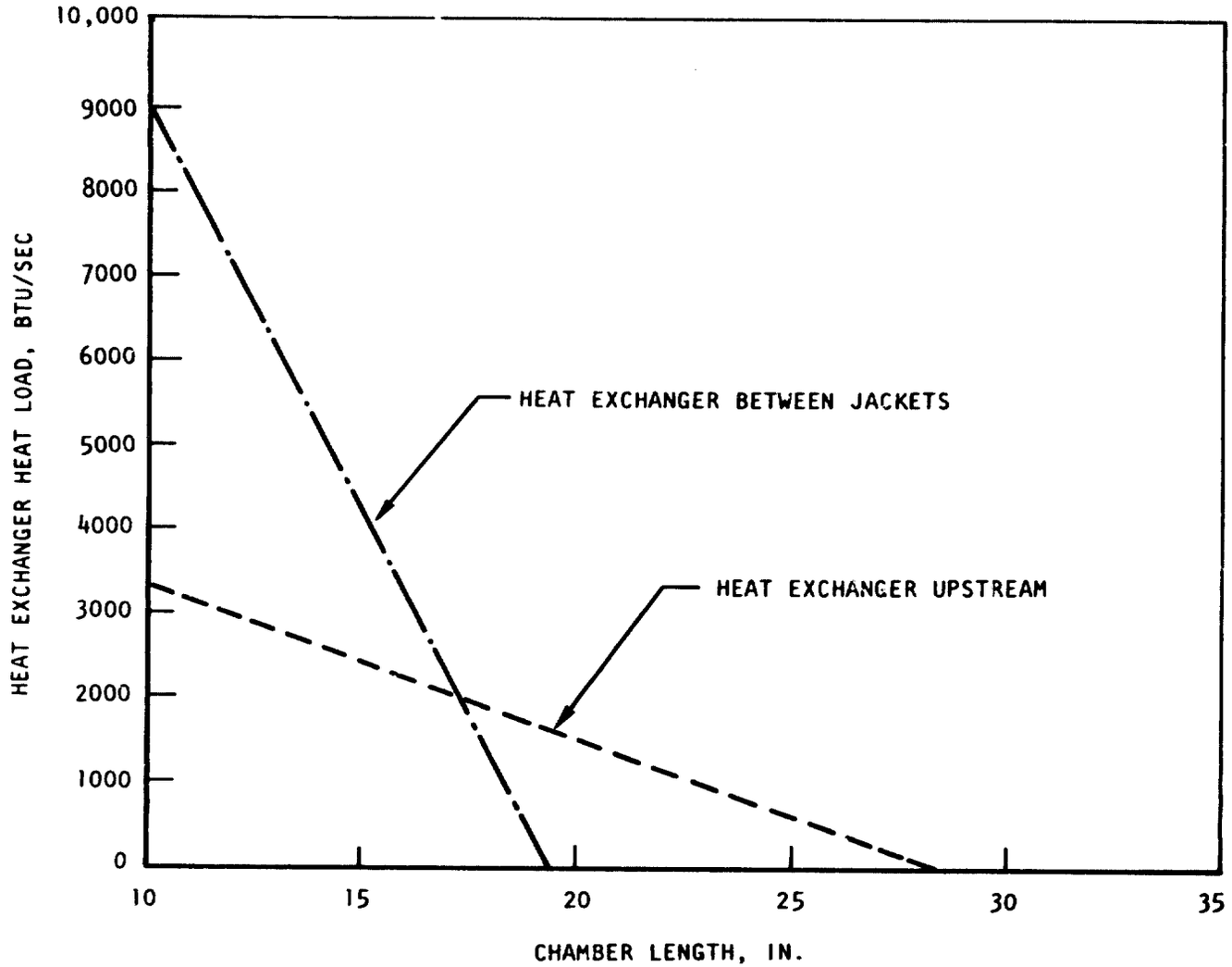

Figure 52

In Fig. 53, the outlet temperature of the combustor jacket is shown as a function of chamber length. The bulk temperature limit is reached at about 28 inches for smooth-walled combustors and at 18.5 inches for thermally-enhanced combusters. Note that the regen heat exchanger is capable of significant increases in combustor outlet temperature for short lengths, but the heat exchanger's effect vanishes as length is increased. As seen above and also at 15K, the heat exchanger is finally eliminated by the optimizer and the curves for the heat-exchanger equipped and the baseline configuration converge at a length sufficient to allow the combustor jacket alone to perform all of the allowed hydrogen heating.

Chamber pressure curves for the 20K level are displayed in Fig. 54. Chamber pressure trends are similar to those observed at 15K. Increases in chamber length yield turbine inlet temperature increases, causing Pc to rise with increasing length. Use of a regen heat exchanger provides significant Pc benefits only for short chambers, and actually results in lower Pc for longer chamber lengths. This is caused by the reduction in heat-transfer rate stemming from elevated jacket inlet temperatures and by heat exchanger delta-p. These effects oppose Pc increases and are cancelled at short length by the high turbine inlet temperatures made possible by the heat exchanger. At longer lengths the reduced heat exchanger heat load reduces benefits enough to allow the adverse effects of ΔP and inlet temperature to dominate.

When the heat exchanger is placed between the jackets (reheat/regen), it tends to hold turbine inlet temperature at a constant value, resulting in a flat Pc versus length line.

The reason for the essentially flat inlet temperature and Pc curves is that the optimized heat exchanger heat load is adjusted (higher for low combustor outlet temperature, lower for high combustor outlet temperature) so as to provide the maximum possible nozzle exit temperature regardless of the chamber length.

The influence of chamber length upon specific impulse for the 20K thrust level is shown in Fig. 55. Increases in length result in higher effective hydrogen injection temperatures (Fig.56) and thus in better specific impulse. At short chamber length, the regen heat exchanger improves Pc enough to allow significantly higher area ratio and thus higher I_{SP}. At longer lengths, the Pc benefit of the regen heat exchanger vanishes. Because the heat exchanger merely provides a means of storing or recirculating thermal energy, it cannot itself afford higher effective injection temperatures.

Placement of the heat exchanger between the jackets in the regen/reheat cycle avoids limits associated with the oxidizer turbine and combustor jacket and thus allows higher performance. However, limits associated with the requirement that heat exchanger delta-T remain positive are still present. This requirement of a positive temperature gradient within the heat exchanger places limitations on the possible temperature distribution within the system and ultimately limits either chamber length or total heat exchanger heat load.

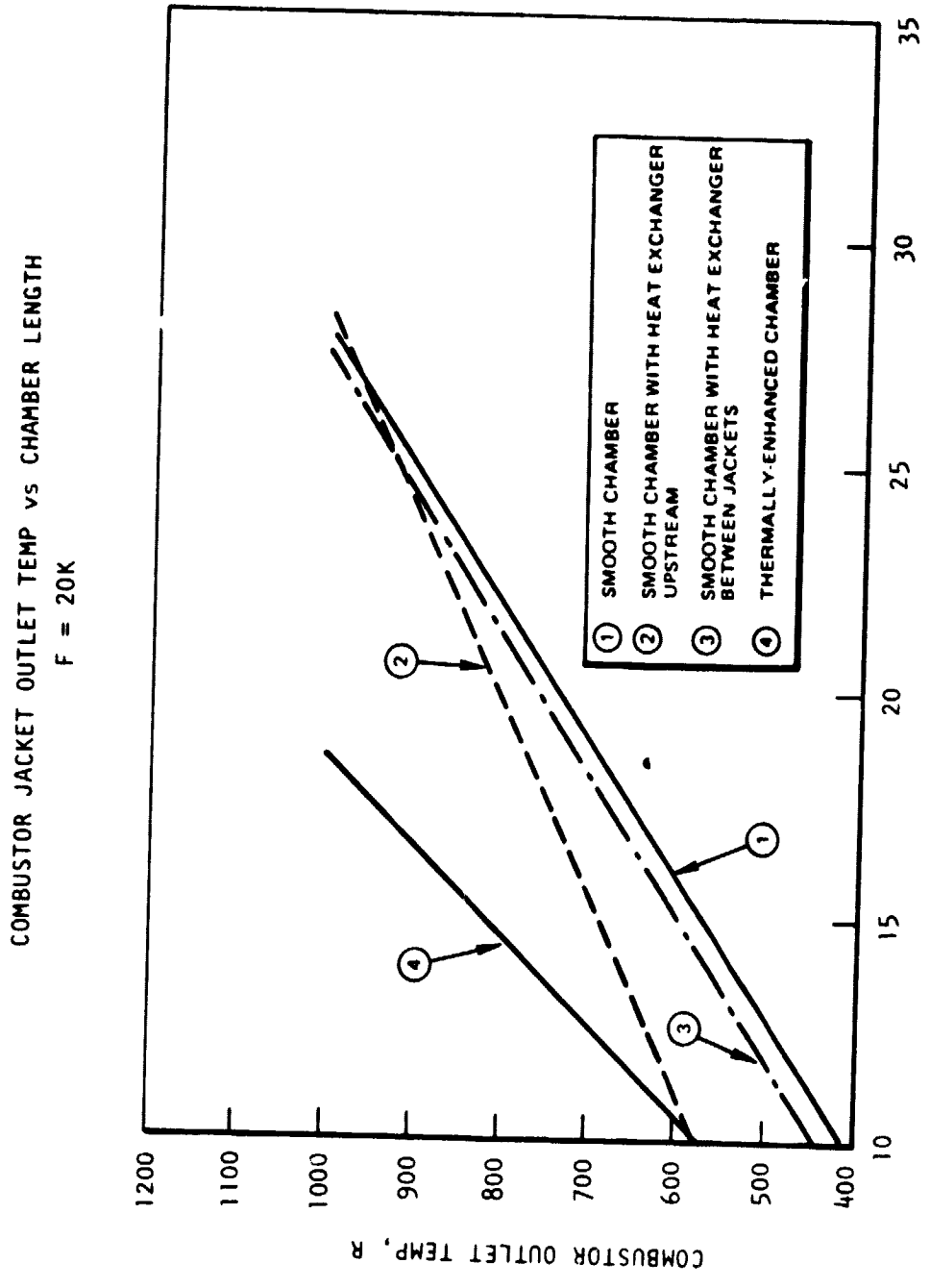
COMBUSTOR JACKET OUTLET TEMP vs CHAMBER LENGTH
F = 20K
COMBUSTOR OUTLET TEMP, R
1200
1100
1000
900
800
700
600
500
400
10
15
20
25
30
35
CHAMBER LENGTH, IN.
1 SMOOTH CHAMBER
2 SMOOTH CHAMBER WITH HEAT EXCHANGER UPSTREAM
3 SMOOTH CHAMBER WITH HEAT EXCHANGER BETWEEN JACKETS
4 THERMALLY-ENHANCED CHAMBER

Figure 53

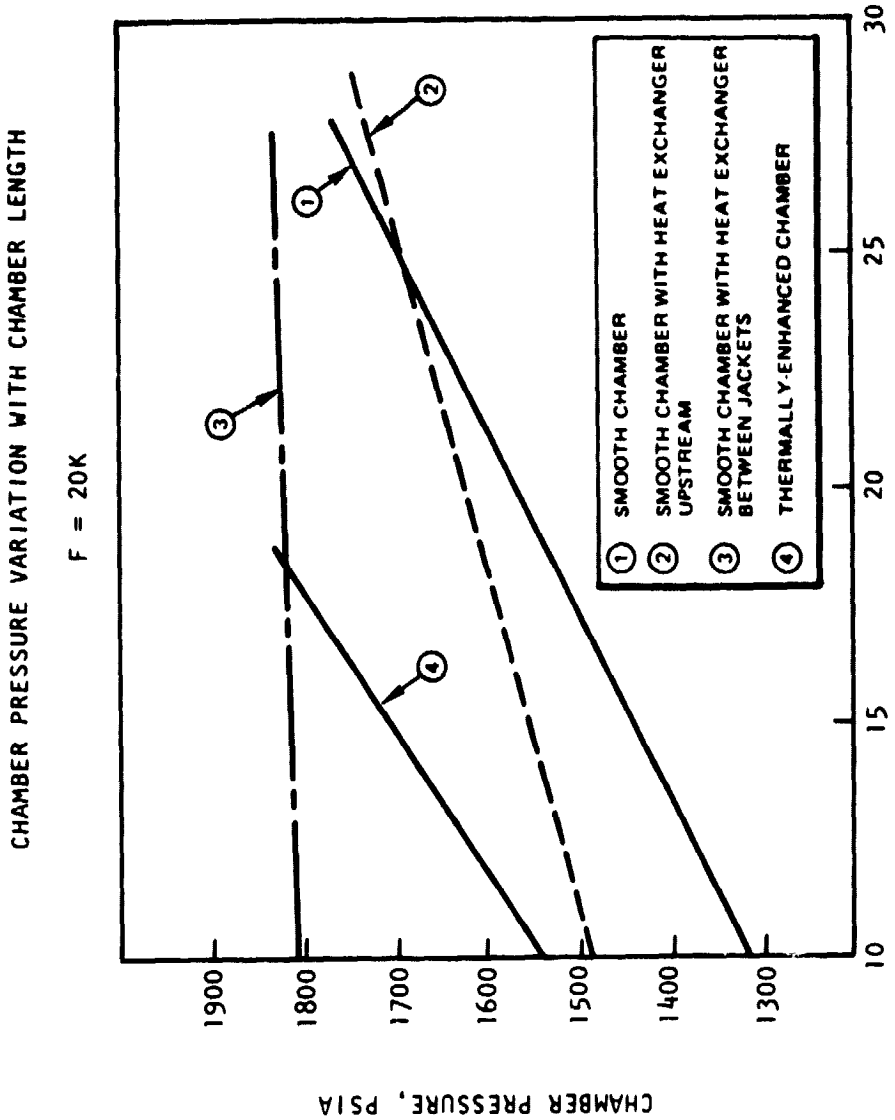
CHAMBER PRESSURE VARIATION WITH CHAMBER LENGTH
F = 20K
CHAMBER PRESSURE, PSIA
1900
1800
1700
1600
1500
1400
1300
10
15
20
25
30
CHAMBER LENGTH, IN.
① SMOOTH CHAMBER
② SMOOTH CHAMBER WITH HEAT EXCHANGER UPSTREAM
③ SMOOTH CHAMBER WITH HEAT EXCHANGER BETWEEN JACKETS
④ THERMALLY-ENHANCED CHAMBER

Figure 54

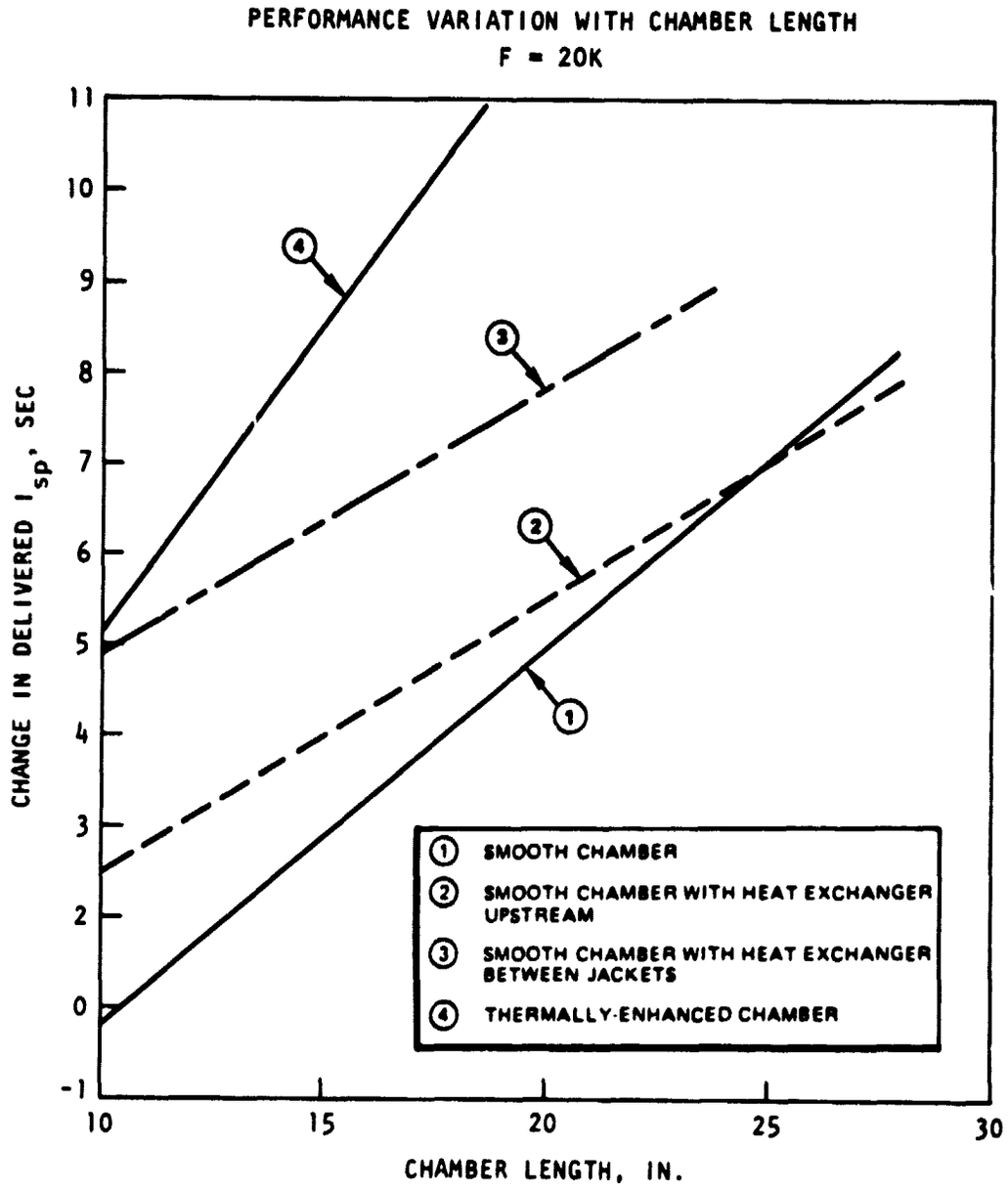
PERFORMANCE VARIATION WITH CHAMBER LENGTH
F = 20K
CHANGE IN DELIVERED I_{sp}, SEC
CHAMBER LENGTH, IN.
11
10
9
8
7
6
5
4
3
2
0
-1
10
15
20
25
30
4
3
2
1
1 SMOOTH CHAMBER
2 SMOOTH CHAMBER WITH HEAT EXCHANGER UPSTREAM
3 SMOOTH CHAMBER WITH HEAT EXCHANGER BETWEEN JACKETS
4 THERMALLY-ENHANCED CHAMBER

Figure 55

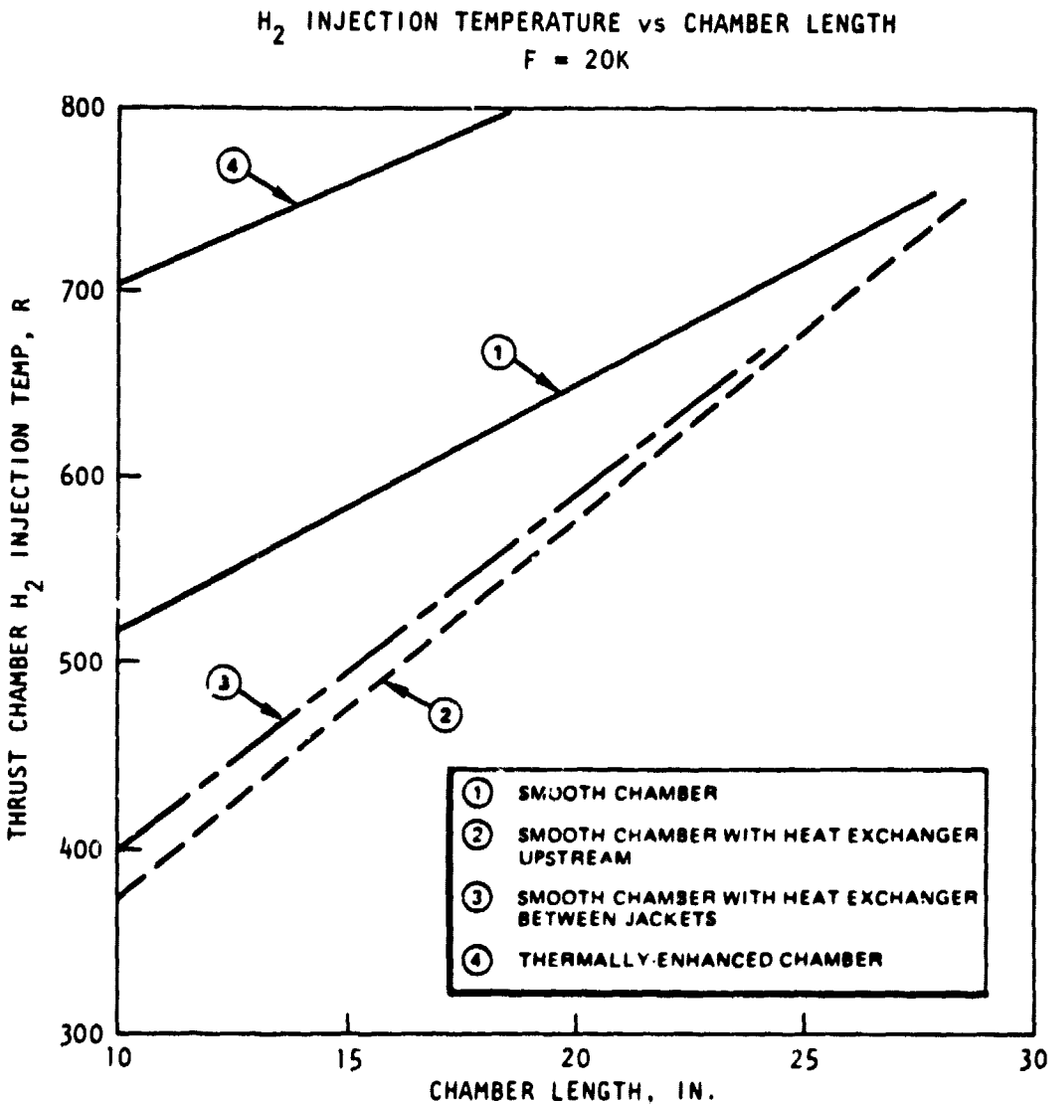
H_2 INJECTION TEMPERATURE vs CHAMBER LENGTH
F = 20K
THRUST CHAMBER H_2 INJECTION TEMP, R
800
700
600
500
400
300
10
15
20
25
30
CHAMBER LENGTH, IN.
1 SMOOTH CHAMBER
2 SMOOTH CHAMBER WITH HEAT EXCHANGER UPSTREAM
3 SMOOTH CHAMBER WITH HEAT EXCHANGER BETWEEN JACKETS
4 THERMALLY-ENHANCED CHAMBER

Figure 56

EXPANSION AREA RATIO EFFECTS

Fig. 57 shows that optimum nozzle area ratio tends to decrease as the chamber is lengthened at 20K thrust. In all configurations examined at 20K, the gain in optimum nozzle area ratio afforded by chamber pressure increases is insufficient to cancel the loss in optimum area ratio resulting from the shorter nozzle length. Use of a regenerative heat exchanger upstream of the combustor jacket does not alter this common trend of area ratio versus chamber length. In addition, the reduction in total heat transfer rate in the jacket caused by the heating of the hydrogen lowers both effective injection temperature and specific impulse below the levels associated with the baseline (non-regenerative) case. When the heat exchanger is placed between the cooling jackets (reheat/regen), the higher Pc levels allow higher optimum area ratios than for other configurations.

The overall trend of area ratio with increasing chamber length remains downward, although the total change in area ratio is rather small for this configuration.

NOZZLE EXPANSION AREA RATIO vs CHAMBER LENGTH
F = 20K

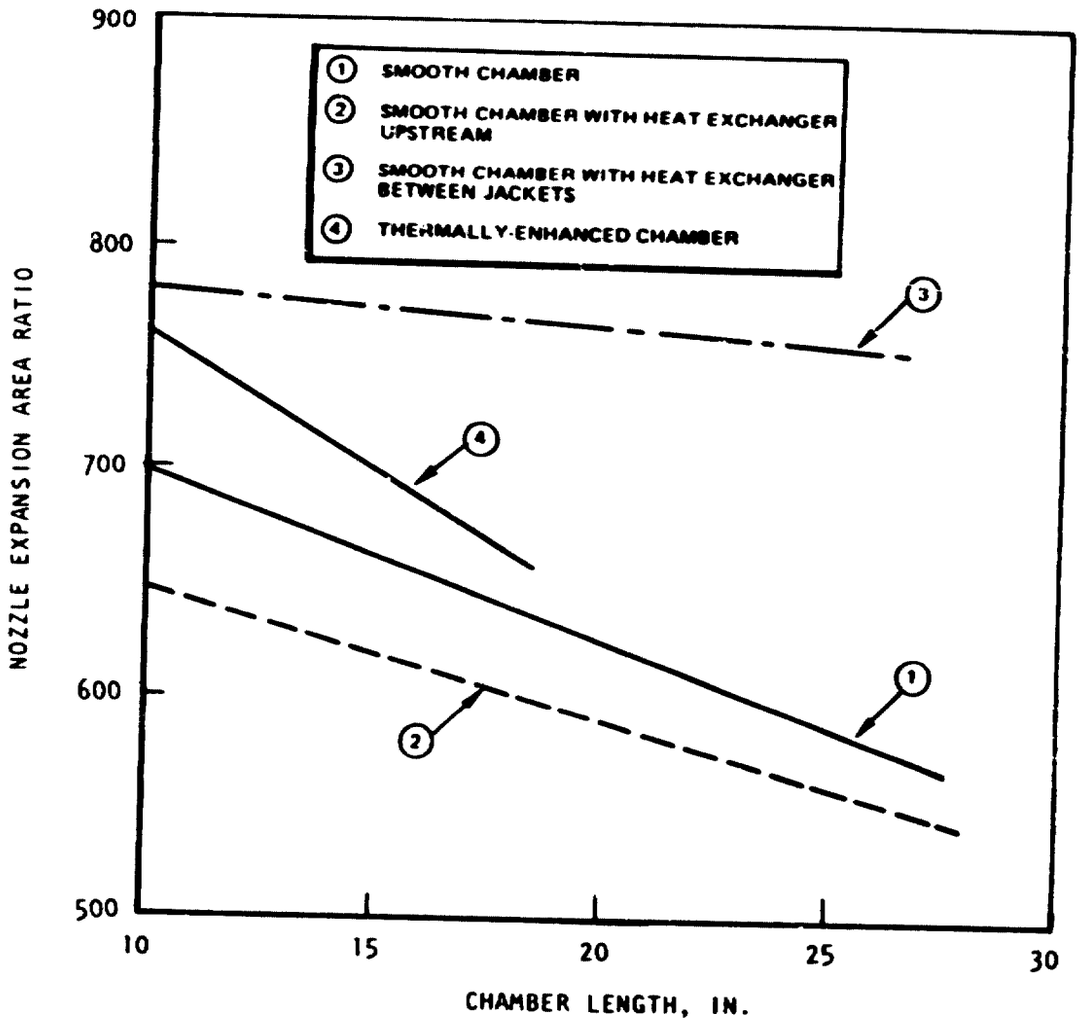

Figure 57

SUMMARY - 20,000 POUND THRUST RESULTS

A summary of important performance parameters of the optimization study is presented in Table17 for the 20,000 lb thrust expander engine. Data is presented for both smooth-wall and thermally-enhanced chambers, and for configurations with and without turbine-gas regeneration. The data is tabulated in order of ascending specific impulse performance. All of the data shown is for a fixed engine extended length of 112 inches, corresponding to a 60-inch retracted length.

The maximum performance (483.9 sec) for the cases considered is achieved by using the thermally-enhanced combustor at a combustor length of 18.5 inches. No regeneration is required for this configuration. Of the smooth-wall cases, the best performance is achieved by the reheat/regen configuration (heat exchanger between jackets) which reaches 482 seconds with a 24 inch chamber. Eliminating all reheat and regeneration, in combination with a four inch lengthening of the chamber, yields a specific impulse loss of 0.8 sec. The best performance obtainable from the baseline* configuration is therefore 481.2 seconds. It is apparent from the data presented in the table that there is a strong correlation between performance and effective hydrogen injection temperature, and a much weaker one between performance and chamber pressure.

Nozzle expansion area ratios for optimum performance at 20K thrust lie in the range of 500 to 800, depending on Pc and chamber length. These values are significantly lower than those seen at 10K and 15K, reflecting the reduced percent lengths (at fixed area ratio) resulting from the larger throat area of the 20K engines. Percent length reductions lead to increases in both kinetic and divergence losses, which drives the optimum area ratio lower in order to recover some of the lost percent length.

*See Table 17

Table 17

PERFORMANCE TRADE STUDIES AT 20K LB THRUST

Turbine Gas Regeneration	Regenerator Location	Chamber Length In	Chamber Pressure PSIA	Nozzle Area Ratio	Engine Length	Nozzle % Length	Specific Impulse Sec	Bulk Temp, R Comb	Bulk Temp, R Nozzle	Effective H_2-Injection Temp, R
No		18.51*	1821	656	112	65.6	483.9	1000	1095	794
Yes	Between Jackets	24.0	1835	758	112	65.1	482.0	1000	1042	675
No **		27.8	1768	565	112	61.5	481.2	996	1041	753
Yes	Upstream of Combustor	27.9	1734	541	112	62.1	480.9	1000	1040	751
No		20	1623	590	112	64.1	478.8	729	809	579
Yes	Between Jackets	13	1812	739	112	65.8	478.6	538	965	459
No		10*	1541	761	112	61.8	478.2	564	698	704
Yes	Between Jackets	10	1810	779	112	66.2	477.8	447	1021	398
Yes	Upstream of Combustor	10	1489	643	112	66.2	475.5	577	699	372
No		10	1316	700	112	59.6	473.8	412	529	519

* Indicates Thermally-Enhanced Combustor

** Selected Baseline Configuration at 20K Thrust

TASK 9: ALTERNATE LOW THRUST CAPABILITY

The feasibility and design impact on the OTV staged combustion cycle engine of adapting the engine to operate for extended periods in the 1-2K lb thrust range was investigated with the scope of the study as outlined in Table 18.

TABLE 18. ALTERNATE LOW THRUST CAPABILITY
SCOPE OF STUDY

- Expected changes in service life and reliability from the basic engine.
- Attainable specific impulse and mixture ratio at both thrust extremes.
- Estimate of RDT&E cost of additional hardware and operational cost for kitting.
- Impact on basic engine weight of providing the ability to be kitted for low-thrust and any additional weight of kit.
- Identification of new technology required to enable design and construction of an engine capable of efficient operation at two thrust extremes.

The OTV engine digital computer transient model was used to investigate engine operation at low thrust conditions. Pump operation and feed system stability were examined using the OTV engine start transient model. Heat exchanger flowrate requirements and thrust chamber coolant flowrate requirements were established analytically. LOX injector flowrate requirements for stability and thrust chamber combustion performance were assessed using ASE and J-2S test experience.

The objectives of the OTV computer model runs (Table 19) were to establish steady state chamber pressure and mixture ratio conditions, valve scheduling and valve positioning required for efficient combustion of propellants in the chamber and for stable system operation. The pumps were assumed to be

TABLE 19. SYSTEM OPERATION AND STABILITY, OBJECTIVES AND CONDITIONS - OTV START MODEL RUNS

OBJECTIVES

- Attainable steady-state chamber pressure
- Attainable steady-state mixture ratio
- Effect of main oxidizer valve (MOV) opening on mixture ratio
- Effect of pump H/Q map characteristics
- Effect of fuel pump recirculation
- Effect of turbine bypass for thrust control

OTV ENGINE START CONDITIONS

- Propellants in tanks at saturated conditions
- Pumps thermally conditioned to cryogenic temperature
- LOX heat exchanger flow and temperature modeled
- Injector/dome heat transfer not modeled

thermally conditioned to saturated propellant temperatures of 162.7R for the LOX and 37.8R for the hydrogen. Propellants were made available at tank pressure corresponding to NPSH values of 2 and 15 for the oxygen and hydrogen respectively at temperatures prescribed above. These conditions are all based on an assumed period of tank head idle mode operation prior to the low thrust operation.

The results of the study of extended low thrust operation of the OTV staged combustion engine indicate that long life, high performance operation of the engine in the low thrust mode (1-2K level) can be achieved with minimum modification (kitting) of the engine.

Modifications to the OTV 20K staged combustion engine which were considered were:

(1) Removal of the preburner injector, since in pump-fed idle the engine is run in an expander mode and does not require a preburner. Removal of the preburner injector increases the available turbine inlet pressure to the drive turbines. The preburner LOX line and valve can be removed in order to simplify the system.

(2) Modification of the main injector to increase the oxidizer side pressure drop so that potential feed system coupled instability is avoided. Two approaches are possible; one is to use a LOX post insert which incorporates an orifice to increase oxidizer side pressure drop, a second approach is to braze on new LOX posts which incorporate a smaller flow area.

(3) The use of fuel pump recirculation in order to avoid the positive slope region of the pump H-Q curve. This modification would add a line and valve from the pump discharge to the pump inlet in order to recirculate hydrogen and keep the pump at a higher flowrate. Computer model studies have indicated that this is an effective method to avoid pump instability problems when operating at low flow conditions. The computer modeling has included the effect of propellant heating which occurs when pump recirculation is used.

(4) Modifications to the hydrogen pump could be considered in order to have a pump H-Q curve without a positive slope region at low flow conditions. A modified fuel pump can be derived by a variety of changes, such as: (1) increased sweepback of the impeller blades to make the H-Q curve have more negative slope, (2) decrease the impeller O.D. to allow the pump speed to increase and operate at a more favorable Q/N, (3) decrease the tip

width of the impeller in order to modify the H-Q characteristic, and (4) redesign the first stage crossover diffuser to avoid stall at low flowrates.

Each of these modifications were considered and evaluated by means of the OTV staged combustion transient computer model.

The modifications which are recommended for kitting of the OTV staged combustion engine are: (1) removal of the preburner injector, (2) modification of the main injector to improve feed system stability, and (3) the use of fuel pump recirculation to avoid fuel pump operation in the positive slope region of the H-Q map. Modification to the fuel pump such as changes to the impellers would require more extensive fuel pump modification and development and could be considered as alternatives to the use of fuel pump recirculation.

Flow instabilities were not present in the oxidizer system during simulation of low thrust operation and based upon the computer simulation no changes to the oxidizer pump and feed system are recommended.

The attainable specific impulse at high and low thrust is shown in Table 20 for the OTV staged combustion engine which resulted from the OTV engine Phase A study (Contract NAS8-32996). This engine is a 20K thrust staged combustion system operating at 2000 psia chamber pressure in the high thrust mode with an expansion area ratio of 400:1. The specific impulse projected for low thrust operation includes the effects of increased reaction kinetic losses and the expected energy release efficiency at reduced flow conditions.

TABLE 20. ATTAINABLE THRUST AND MIXTURE RATIO AT BOTH THRUST EXTREMES

Engine System - 20K Vacuum Thrust Staged Combustion Cycle, Pc = 2000 psia, ϵ = 400 Mixture Ratio (O/F) = 6:1

	High Thrust Mode	Low Thrust Mode
Thrust, lbf	20,000	1,610*
Chamber pressure, psia	2,000	166
Mixture ratio, engine	6.0	6.0
Specific impulse, engine, sec	477.1	455.9
Engine fuel flowrate, lb/sec	5.99	.5022
Engine oxidizer flowrate, lb/sec	35.93	3.029
Main fuel pump speed, RPM	95,000	22,722
Main oxidizer pump speed, RPM	70,000	17,271
Main fuel pump discharge pressure, psia	4,563	268
Main oxidizer pump discharge pressure, psia	4,852	386
Main fuel pump recirculation flowrate, percent	0	64%

*Other points of operation below 1.6K are feasible.

The studies which have led to the definition of the low thrust OTV staged combustion cycle engine are discussed in more detail in the following sections.

LOW THRUST MODE COMPUTER MODEL

The OTV digital computer transient model was used to examine OTV engine thrust operation at the 1-2K thrust level. Low thrust operation of the staged combustion engine is accomplished in a pump-idle mode where the engine is operated as a pump-fed expander cycle system. The basic staged combustion engine is shown schematically in Fig. 58. This engine resulted from the OTV Phase A contract NAS 8-32996 studies and is dicusssed in detail in Rocketdyne report RI/RD 79-191-2 dated 9 July 1979. Modificiations to the OTV engine to make it suitable for extended operation at low thrust are shown schematically in Fig. 59. The preburner injector has been removed and fuel pump recirculation has been added.

Prior to pump-fed low thrust operation the engine is thermally conditioned by tank fed idle mode operation where the pumps are inoperative and the thrust chamber is operated under tank head pressures.

To initiate low thrust mode pump-fed operation from tank head idle the pump brakes are released. Initially sufficient energy to transition to pump feed idle is provided by the residual heat in the combustion chamber hardware. The hydrogen coolant is directed to the high pressure turbines since the preburner has been removed. The main oxidizer valve is opened to partially provide oxygen to the main chamber where it is combusted with the hydrogen exhausting from the main turbines. As the pumps increase speed chamber pressure increases to the nominal steady-state value. The computer model includes detailed component descriptions of the engine components. Propellant heating effects of fuel pump recirculation were incorporated into a later modification of the program In order to have realistic representations of the engine components

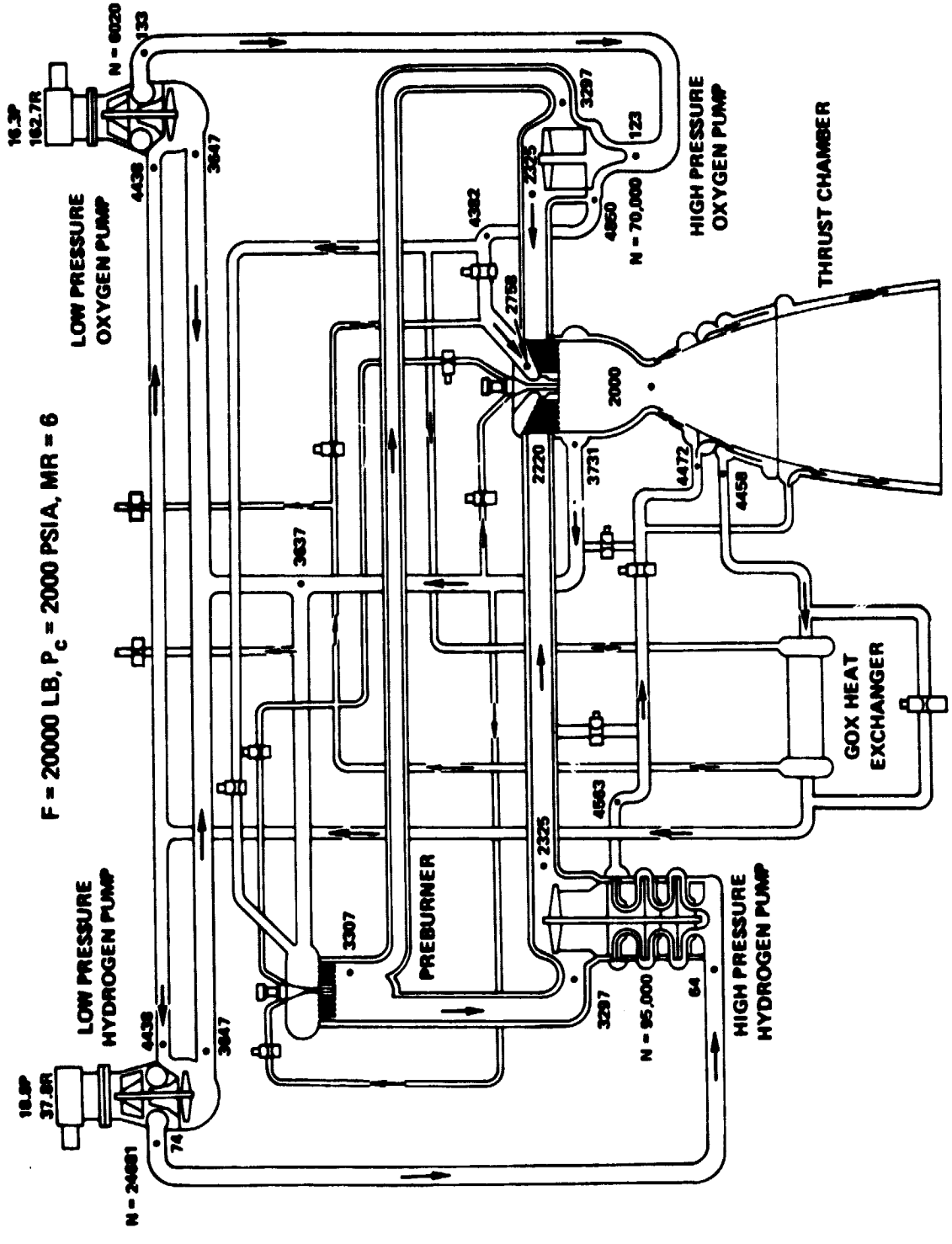

Figure 58. OTV ENGINE

STAGED COMBUSTION CYCLE SCHEMATIC

Rockwell International
Rocketdyne Division

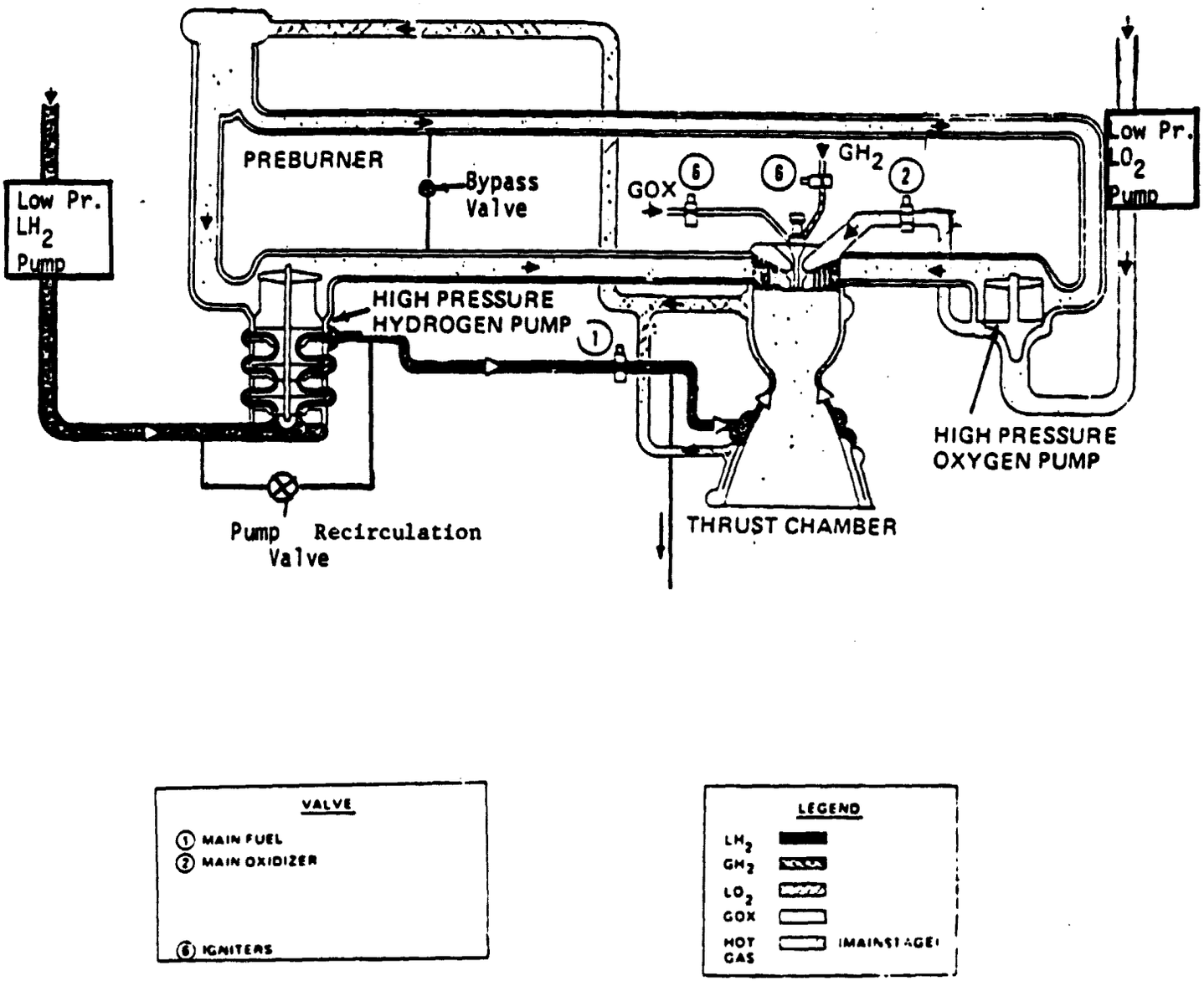

Figure 59. Modified OTV Staged Combustion Engine Schematic

the Rocketdyne Mark 48 fuel and oxidizer pumps and the thrust chamber which have been built and tested as part of the ASE technology program were used in the computer model representation. The use of the Mark 48 pump maps permtted a more detailed evaluation of the effects of fuel pump operation at low thrust conditions.

OTV ENGINE COMPUTER MODEL ANALYSES

The computer simulation effort was conducted in two phases or series of cases:

Phase I - The first case analyzed was the basic OTV engine in its unmodified form. Subsequent analyses in this phase included evaluation of elimination of the preburner injector, the effects of a fuel turbine bypass valve, and a change in the fuel pump to eliminate the positive slope portion of the pump H-Q curve.

Phase II - In Phase II the effects of fuel pump recirculation and fuel turbine bypass were evaluated. The effects of propellant heating upon main fuel pump performance were included in this analysis.

Phase I Results. The results for the Phase I analysis are shown in Fig. 60. and Table 21 for the following four cases:

Case 1 - Basic OTV engine unmodified - This engine reached a mixture ratio of approximately 2.60 before the fuel pump reached the positive slope portion of the H-Q curve where the computer model indicated a possible feed system instability. Prior experience has shown that operation of a liquid propellant on or near the positive slope portion of the H-Q curve can cause flow surges and stall. The actual occurrence of this condition would need to be verified during a demonstration test program.

Case 2 - The preburner injector was removed from the flow circuit the ΔP was reduced from the nominal case for ease of change in the computer mode). This permitted operation to a higher chamber pressure and a higher mixture ratio as shown in Fig. 60.

Case 3 - Case 3 of Fig. 60 illustrates use of the turbine bypass valve in conjunction with removal of the preburner injector. The turbine bypass valve is essentially a throttling method to reach lower thrust levels.

Case 4 - In this case the fuel pump was assumed to be modified to eliminate the positive flow region of the H-Q curve. With this modification operation up to a mixture of 7:1 was possible and details of steady state performance for six mixture ratios (from 2.1 to 6.9) are shown in Table 21. Figures 61 and 62 show main chamber, nozzle coolant, main chamber temperature, coolant temperature and chamber pressure for the cases given in Table 21. The fuel pump can be modified by increasing the sweepback of the impeller blades or by other changes such as decreasing the impeller O.D. to allow the pump to operate at a more favorable Q/N. Since the above changes to the fuel pump would require a major redesign, fuel pump recirculation was investigated in Phase II of this study

Phase II Results. In Phase II the effects of fuel pump recirculation and fuel turbine bypass were evaluated. Steady state performance over a range of mixture ratios is shown in Table 22. With the use of 45% fuel pump recirculation a chamber pressure of 153 psia is attainable at a mixture ratio of 6 (5.96 in Table 20). With the use of fuel pump recirculation there is an attendant increase in fuel temperature due to pump inefficiency and fuel density decreases. Fuel pump required power increases due to the lower density and as a result the

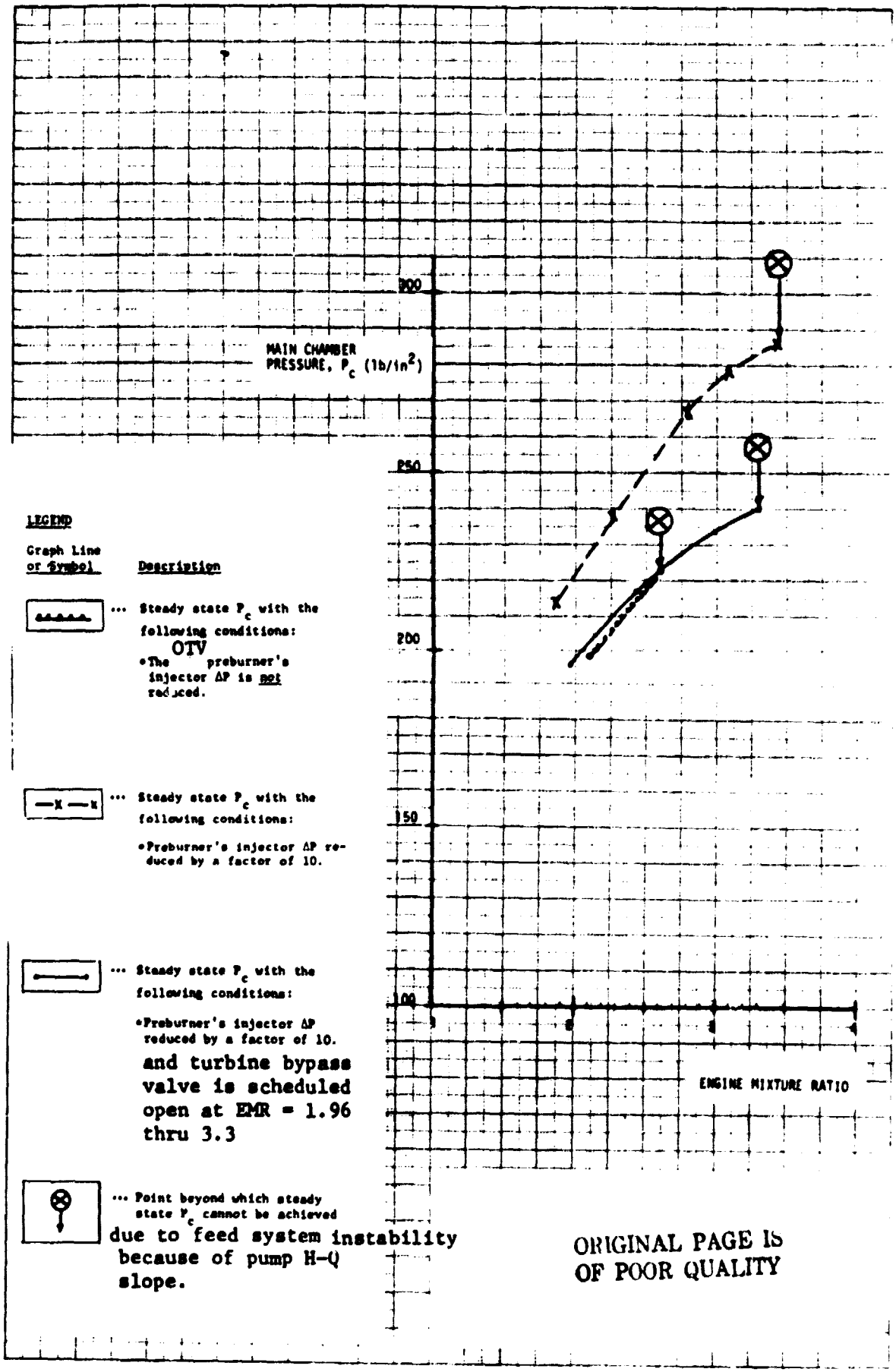

Figure 60. Phase I Results - Cases 1, 2, 3
RI/RD80-155-2, Page 138

Table 21. Steady State Performance With Modified Fuel Pump

	MR=2.16	MR=4.52	MR=5.47
THRUST, LBS.	1825	2385	2560
Main Chamber Pressure (lb/in^2)	191.9	256.1	266.8
SPECIFIC IMPULSE, SEC.	457	462	462.5
Pump			
Main Pump Speed (rpm)			
Fuel	26720.	26805.	26479.
Oxidizer	25941.	20381.	18794.
Boost Pump Speed (rpm)			
Fuel	15420.	14970.	14740.
Oxidizer	5320.	4113.	3776.
Main Pump Discharge Pressure (lb/in^2)			
Fuel	451.6	476.2	472.4
Oxidizer	799.4	521.9	450.3
Boost Pump Discharge Pressure (lb/in^2)			
Fuel	42.46	43.44	43.31
Oxidizer	95.79	80.00	76.06
Main Pump Flowrate (lb/sec)			
Fuel	1.266	.9348	.8555
Oxidizer	2.728	4.228	4.679
Preburner			
Gas Temperature (Deg-R)	255.9	486.7	555.9
Preburner Chamber Pressure (lb/in^2)	257.8	309.7	316.5
Turbine			
Main Turbine Flowrate (lb/sec)			
Fuel	.7859	.5721	.5222
Oxidizer	.3997	.2906	.2650
Boost Turbine Flowrate (lb/sec)			
Fuel	.09732	.06201	.05298
Oxidizer	.0811	.05168	.04415
Main Oxidizer Valve Position (%)	47.	57.	60.

TABLE 21, (CONCLUDED)

	MR=5.96	MR=6.52	MR=6.93
THRUST, LBS.	2600	2614	2680
Main Chamber Pressure (lb/in^2).....	266.5	261.9	264.4
SPECIFIC IMPULSE, SEC.	462.5	462.5	462.5
Pump			
Main Pump Speed (rpm)			
Fuel.....	26038.	25350.	25256.
Oxidizer.....	17903.	16972.	16437.
Boost Pump Speed (rpm)			
Fuel.....	14480.	14110.	14010.
Oxidizer.....	3586.	3371.	3265.
Main Pump Discharge Pressure (lb/in^2)			
Fuel.....	461.	441.9	440.3
Oxidizer.....	411.9	373.4	351.4
Boost Pump Discharge Pressure (lb/in^2)			
Fuel.....	42.95	42.36	42.26
Oxidizer.....	73.82	71.35	70.23
Main Pump Flowrate (lb/sec)			
Fuel.....	.8087	.7514	.7311
Oxidizer.....	4.821	4.901	5.063
Preburner			
Gas Temperature (Deg-R).....	582.6	607.7	631.2
Preburner Chamber Pressure.....	313.2	304.9	306.4
Turbine			
Main Turbine Flowrate (lb/sec)			
Fuel.....	.4930	.4576	.4447
Oxidizer.....	.2502	.2320	.2255
Boost Turbine Flowrate (lb/sec)			
Fuel.....	.04879	.04466	.04215
Oxidizer.....	.04066	.03722	.03512
Main Oxidizer Valve Position (%).....	62.	64.5	67.5

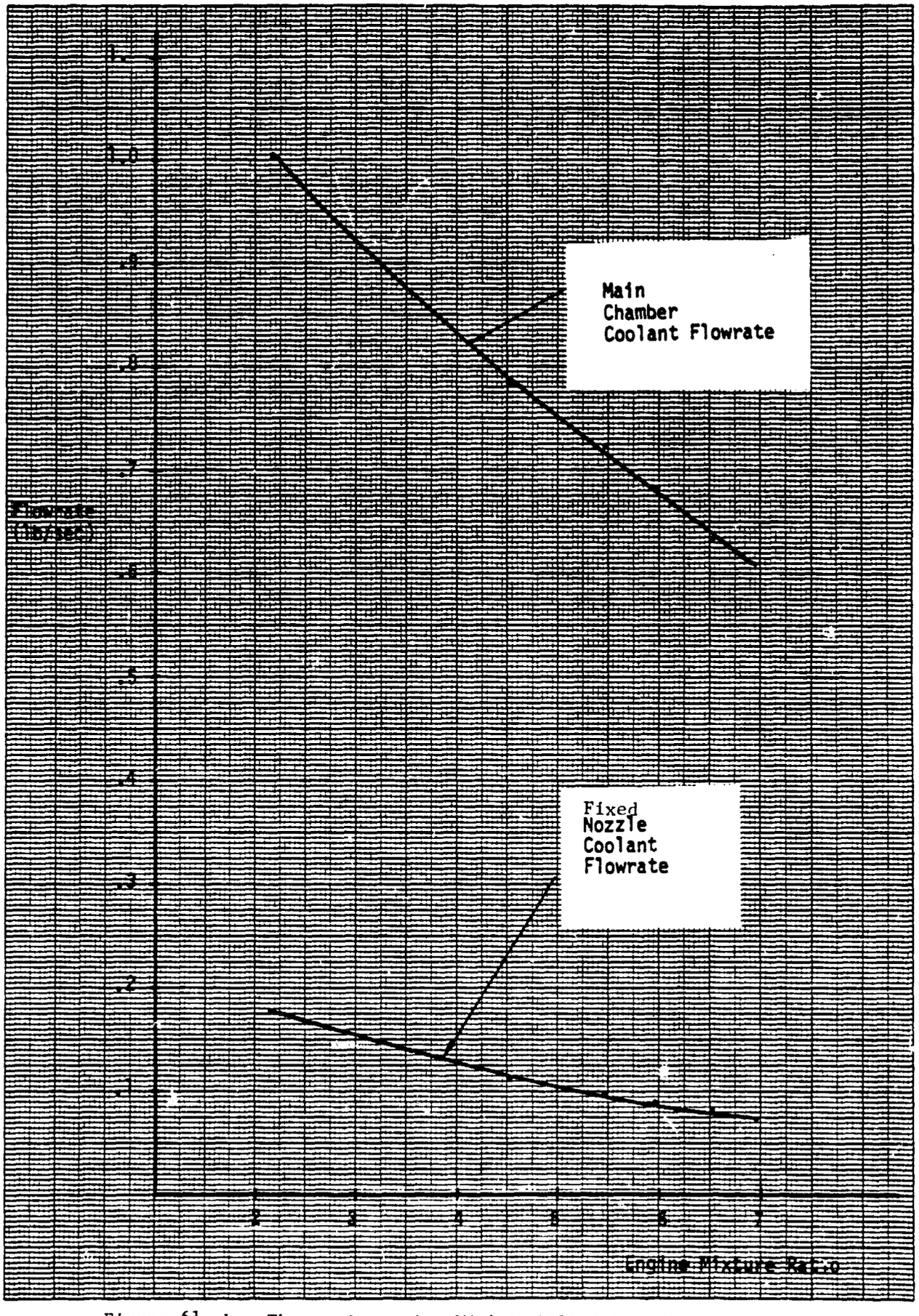

Figure 61. Low Thrust Operation With Modified Fuel Pump
Main Chamber & Nozzle Coolant Flowrates

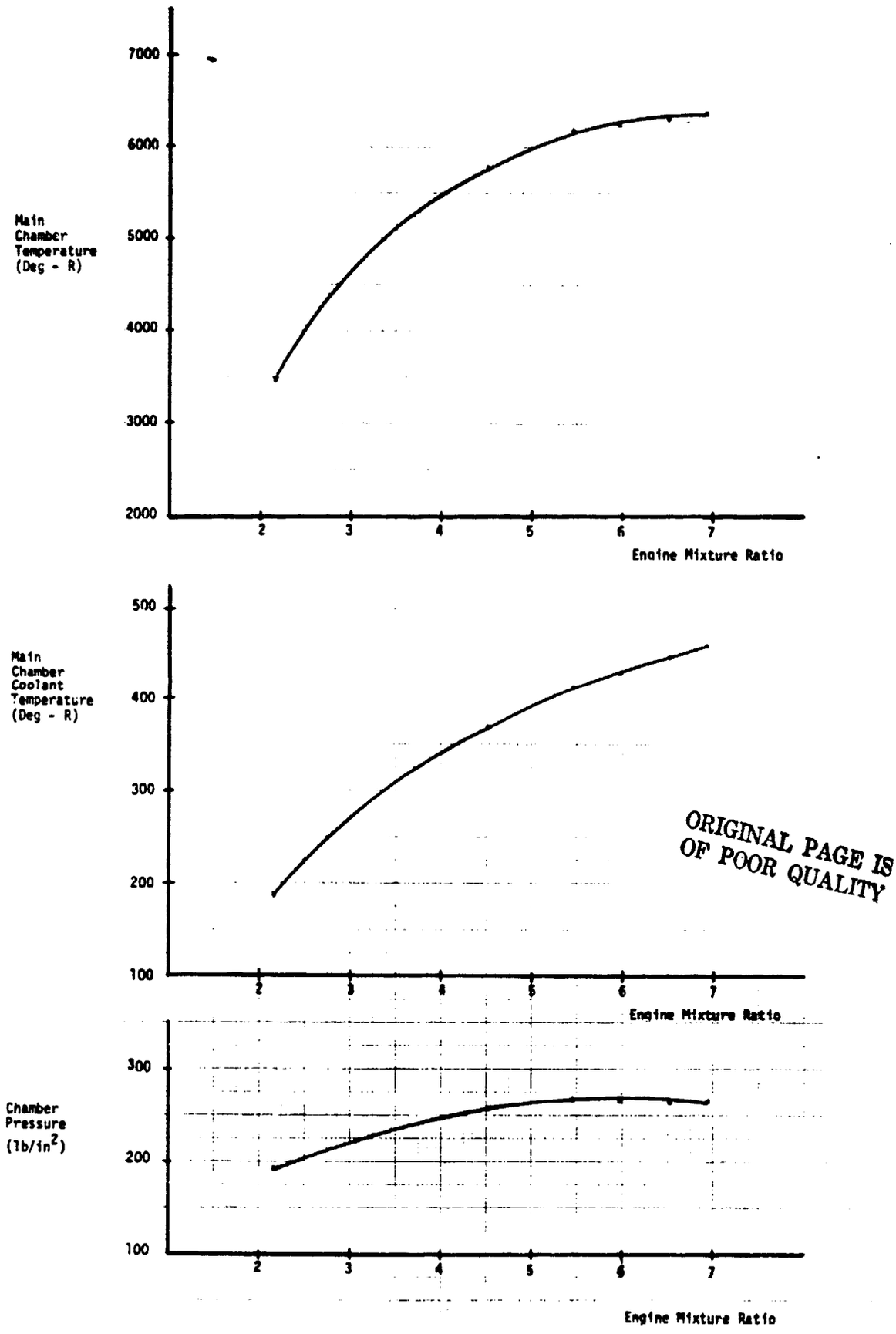

Figure 62. LOW THRUST OPERATION WITH MODIFIED FUEL PUMP
MAIN CHAMBER CONDITIONS

TABLE 22

STEADY STATE PERFORMANCE AT LOW THRUST WITH PUMP RECIRCULATION

	MR = 5.781	MR = 6.032
Thrust (LBF)	1640	1610
Main Chamber Pr. (lb/in^2).....	169.9	166.
Specific Impulse (sec).....	458.3	455.9
Pump		
Main Pump Speed (rpm)		
Fuel.....	23159.	22722.
Oxidizer.....	17808.	17271.
Boost Pump Speed (rpm)		
Fuel.....	13500.	13270.
Oxidizer.....	3420.	2272.
Main Pump Disch. Pr. (psia)		
Fuel.....	277.8	268.5
Oxidizer.....	407.3	386.2
Boost Pump Disch. Pr. (psia)		
Fuel.....	36.57	36.18
Oxidizer.....	70.30	69.11
Main Pump Flowrate (lb/sec)		
Fuel.....	.8845	.8524
Oxidizer.....	3.051	3.029
Preburner		
Gas Temp (^oR).....	621.2	634.6
Preburner Pr (psia).....	203.4	197.8
Turbine		
Main Turbine Flowrate (lb/sec)		
Fuel.....	.3251	.3092
Oxidizer.....	.165	.1569
Boost Turbine Flowrate (lb/sec)....		
Fuel.....	.02937	.02793
Oxidizer.....	.02447	.02327
Valves		
MOV (% Open).....	54.	54.5
Fuel Pump Feedback Valve		
Pos (% - Open).....	7.0	7.0
ΔP Across Valve (psia).....	241.23	232.32
Flowrate thru valve (lb/sec)....	.3568	.3502
Turbine Bypass Valve.....	Closed	Closed
NPSP (ft).....	+1.35	+.93

attainable chamber pressure decreases. With the change in flowrate and propellant density at the main fuel pump, the main pump required NPSH decreases substantially because of the reduced speed, but the available NPSH also decreases since the boost pump discharge pressure decreases substantially from the full thrust values. This indicates that low thrust operation must be carefully considered when the low pressure boost pumps are designed so that sufficient NPSH is supplied for main pump operation.

The results of the Phase II study using fuel pump recirculation to avoid the positive slope region of the fuel H-Q curve indicate that this is a viable method of achieving low thrust operation (1-2K) with a minimum modification of the fuel pump.

INJECTOR PERFORMANCE

An analysis of the OTV Staged Combustion Engine injector operation at a low thrust level (1-2K) was conducted. The results of the analysis show that an optimized injector designed for high thrust operating at low thrust should operate satisfactorily at this level with no modifications. The injector fuel side pressure drop at the low thrust level remains relative high because of the reduced hydrogen density. Consequently, the fuel injection velocity is also high and the resulting injector element mixing and performance should be consistent with the high values demonstrated at the 20K operating level. The oxidizer injection pressure drop at low thrust level operation is substantially reduced. This reduction has little effect on the mixing and performance of the injector elements but could affect the feed system coupled stability of the engine.

Analysis shows that the oxidizer $\Delta P_o/P_c$ ratio at the low thrust level will be approximately .06. Based on SSME and J-2S engine experience, this $\Delta P_o/P_c$ should result in stable engine operation. If, however, hot fire testing shows the engine has feed system coupled instability at the low thrust level, simple injector modification can be incorporated to correct the instability.

There are several alternative approaches which can be used to modify or kit the injector. For an engine which is to be used exclusively at low thrust, the injector would be designed for the low flowrates and the assembly would be manufactured to this specific design. The major assemblies of the injector such as the body, manifold and faceplate would require minimum changes.

The injector elements would be resized with the same number as being used for the 20K thrust level. The oxidizer posts would be sized for the specific low thrust level application and brazed into the injector body. New fuel sleeves may be required to interface with the new oxidizer posts. This approach of a new injector assembly exclusively for low thrust operation offers an efficient injector design which could be kitted for the low thrust mode.

An alternative approach to an injector for low thrust operation is to modify the existing injector by making only an oxidizer post modification. There are several ways to modify the oxidzer post. One method is to use an oxidizer post insert with a smaller orifice flow area to increase the injection pressure drop, Fig.63A. An alternative injector modification is to machine back the oxidizer posts and to braze on a new tip with a reduced diameter integral orifice. This approach is shown in Fig.63B. New fuel sleeve assemblies would be used to interface with the brazed on oxidizer post tips. These changes would result in an injector having proper injection velocities for high combustion efficiency and proper pressure drops for feed system coupled combustion stability.

COMBUSTOR AND NOZZLE COOLING FLOW REQUIREMENTS

Dump-cooled nozzle coolant flow requirements at pumped idle chamber pressure conditions are shown in Fig.64. It is seen that the flowrates available to the nozzle with the mainstage coolant control valve settings are not sufficient to maintain the dump nozzle wall temperatures at the level obtained during mainstage and required for the prescribed engine life. A flowrate of 0.05 lbs/sec was determined for the OTV engine to achieve a slight degree of overcooling. This amount of coolant can be provided to the dump-cooled nozzle by changing the coolant control valve setting when operating at low thrust.

Cooling flow requirements for the combustor are indicated in Fig.65 as a function of mixture ratio at pumped idle conditions. Mainstage coolant values attained with mainstage valve settings result in a high degree of overcooling in the combustor. A flowrate of 0.287 lbs/sec provides adequate cooling at mixture raio of 6:1 for the 166 psia case with fuel pump recirculation and allows redirection of some of the flow to the dump-cooled nozzle, the more critical thrust chamber component at pumped idle mode.

After the dump-cooled nozzle and combustor jacket coolant flow requirements have been determined, the remainder of the available fuel flow is used in

LOX POST INSERT

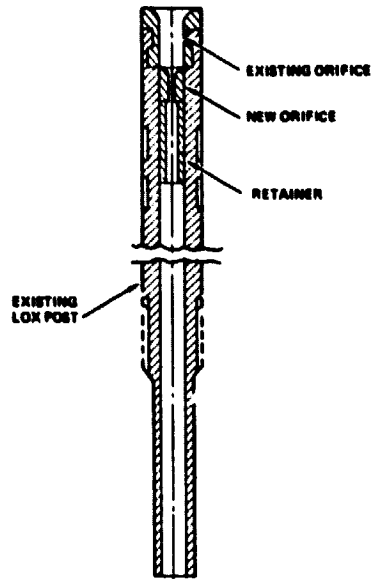

A

BRAZED ON POST TIP

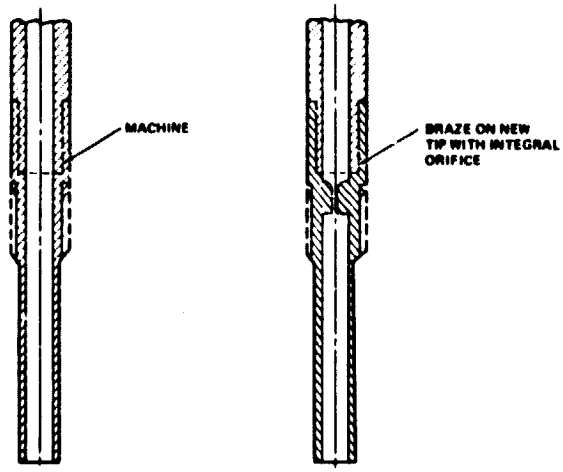

B

Figure 63. Proposed LOX Injector Post Modifications

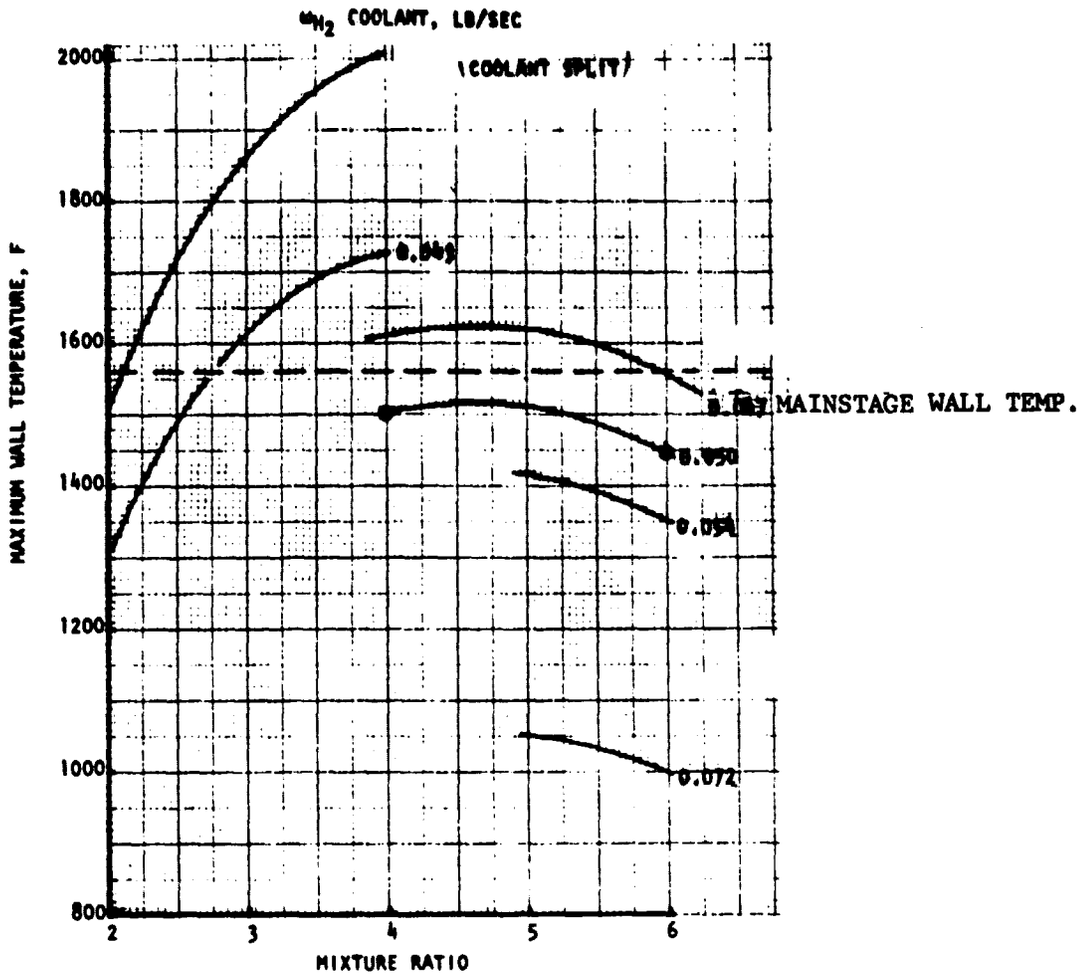

Figure 64. DUMP COOLED NOZZLE FLOW REQUIREMENTS

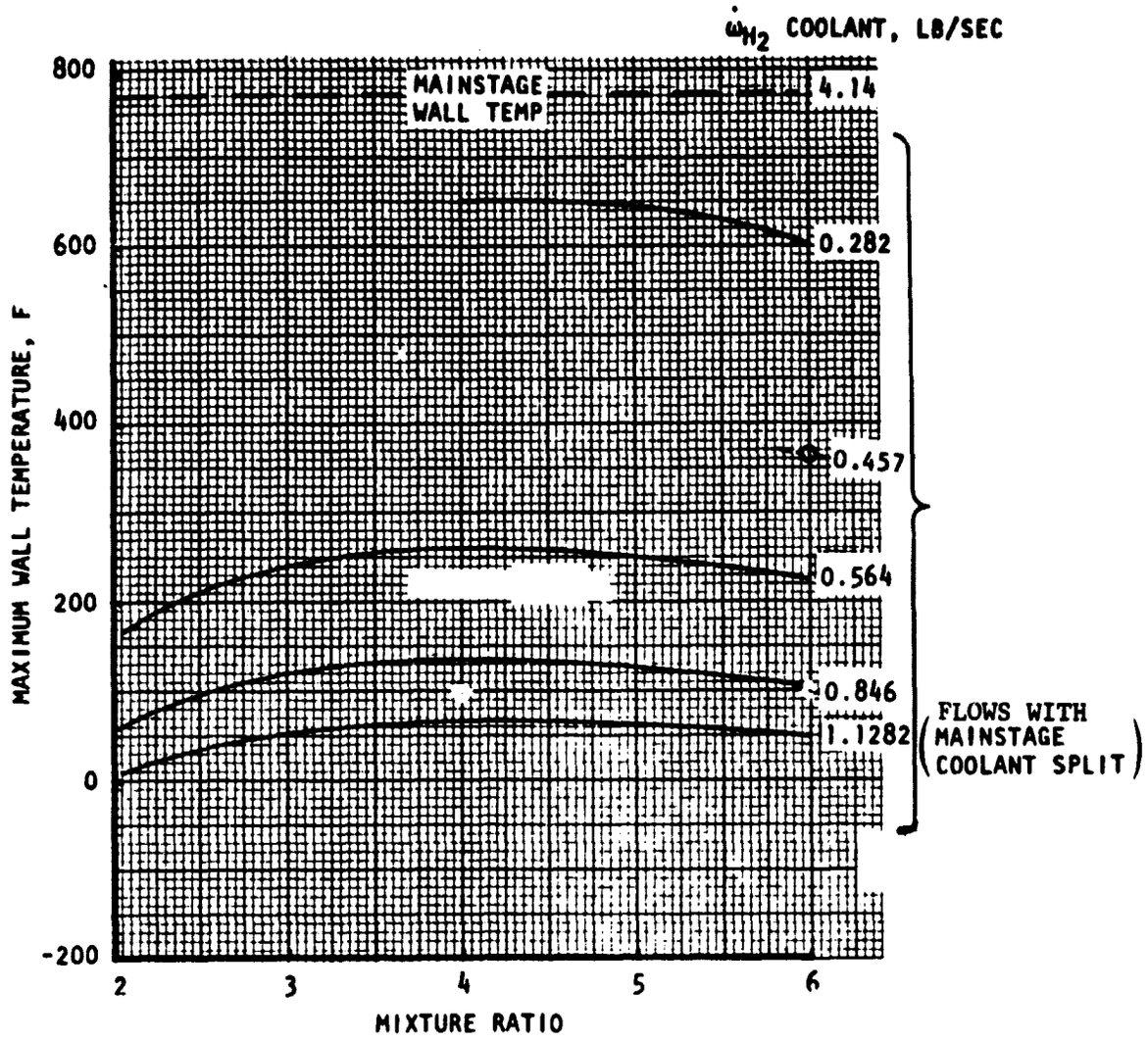

Figure 65. Combustor Cooling Flow Requirements*

(Pc = 200 psia)

the regeneratively-cooled nozzle (Fig.66). The resultant 0.165 lbs/sec is sufficient to provide some degree of overcooling when compared to mainstage wall temperature conditions. The results of the combustor and nozzle cooling analysis indicate that the OTV engine can be adequately cooled during low thrust operation.

ENGINE PERFORMANCE

A detailed power and flow balance point at design mixture ratio of 6:1 is presented in Table 23 for the OTV staged combustion engine concept for both the high and low thrust modes of operation.

Delivered engine performance at design mixture ratio was calculated according to standard JANNAF performance procedures. The performance has as a starting point the theoretical one-dimensional equilibrium performance of the propellants reacted at the conditions existing in the propellant tanks. To this base performance, the effects of propellant heating, pressurization, combustion, friction, divergence, and leakage losses are superimposed. Combustion, kinetic and nozzle divergence losses amount to 4.8 seconds at full-thrust. These losses have been verified through correlation with measured ASE performance. The effects of regenerative heating of the propellants are accounted for in the performance calculations. Pump leakage losses and the improved specific impulse effect of heating and dumping hydrogen in the dump coolant nozzle are included in the calculations.

Based upon the computer model results, the modifications to the OTV staged combustion engine which permit extended operation at low thrust and high mixture ratio are: (1) modification of the main LOX injector, (2) removal of the preburner, and use of fuel pump recirculation. Table 23 summarizes low thrust operation at a high mixture ratio (5.96). High delivered specific impulse (458.5 sec) can be obtained based upon modification of the main injector. A combustion energy release efficiency of .99 is used based upon previous LOX/hydrogen experience kitting of the injector. The reaction kinetics efficiency is .9677 and the boundary layer drag efficiency is .9683 at 1500 pound thrust.

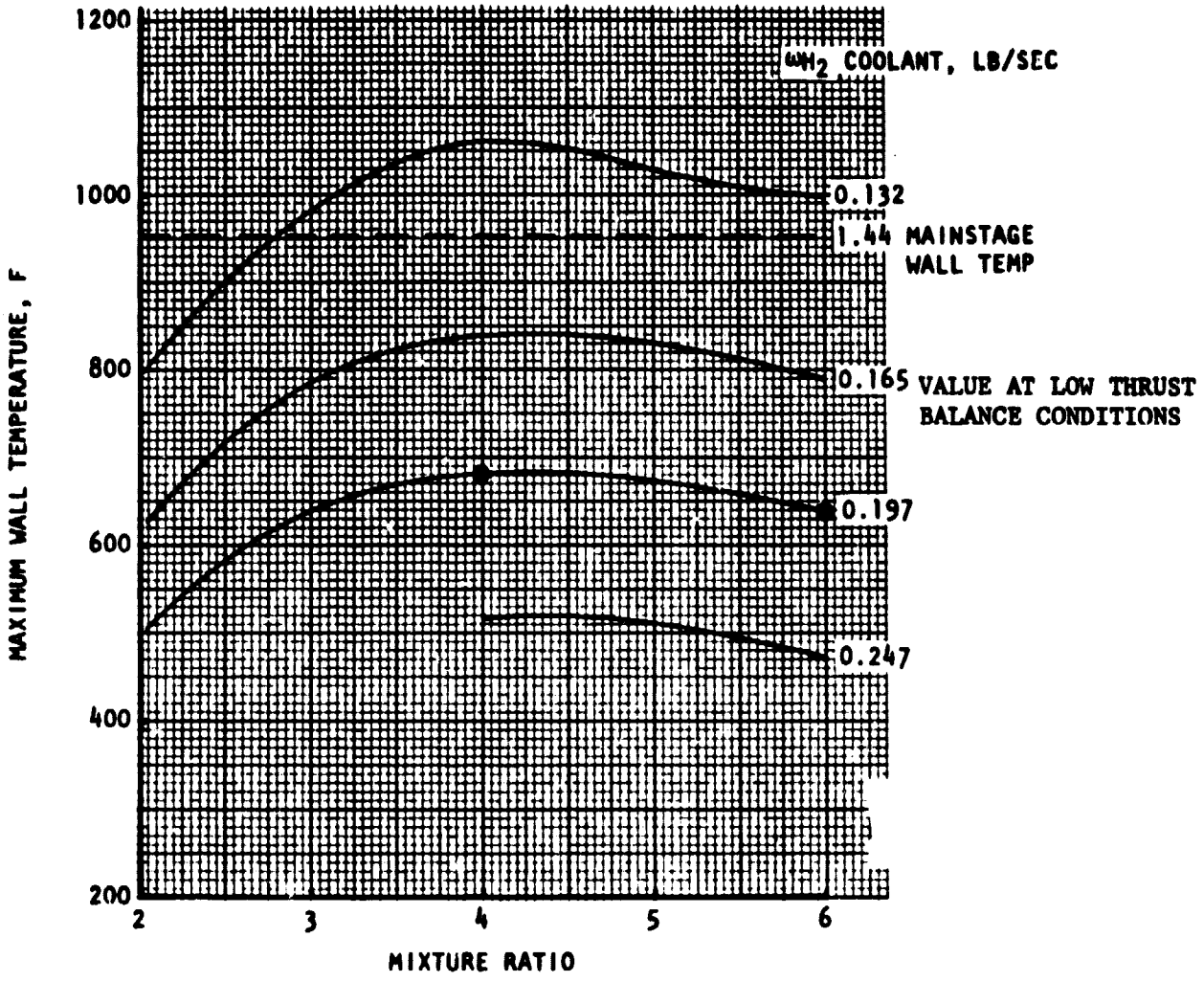

Figure 66. Regeneratively-Cooled Nozzle Flow Requirements (Pc = 200 psia)

TABLE 23. OTV STAGED COMBUSTION ENGINE BALANCE
(HIGH & LOW THRUST MODES) MR = 6

Design Variables	High Thrust Mode	Low Thrust Mode
General		
Thrust, lbF	20,000	1610
Chamber Pressure, PSIA	2000	166
Mixture Ratio, Engine	6.0	6.032
Specific Impulse (Engine), seconds	477.12	455.9
Engine Fuel Flowrate, lb/sec	5.99	0.5022
Engine Oxidizer Flowrate, lb/sec	35.93	3.029
Dump Coolant Fuel Flowrate, lb/sec	0.36	0.05
Preburner		
Preburner Combustion Temperature, R	1860	Not
Preburner Mixture Ratio	0.79	Operating
Total Preburner Flowrate, lb/sec	9.00	
Preburner Combustion Pressure, psia	3306.5	
Turbomachinery		
Low Pressure Oxidizer Pump Speed, rpm	6020	2272
Low Pressure Oxidizer Pump Inlet Pressure, psia	16.3	163
Low Pressure Oxidizer Pump Outlet Pressure, psia	133.4	69.11
Low Pressure Oxidizer Pump Diameter, inches	3.69	3.69
Low Pressure Fuel Pump Speed, rpm	24,681	13,270
Low Pressure Fuel Pump Inlet Pressure, psia	18.82	18.82
Low Pressure Fuel Pump Outlet Pressure, psia	74.3	36.18
Low Pressure Fuel Pump Diameter, inches	3.17	3.17

TABLE 23 (Concluded)

Design Variables	High Thrust Mode	Low Thrust Mode
High Pressure Oxidizer Pump Speed, rpm	70,000	17,271
High Pressure Oxidizer Pump Outlet Pressure, psia	4852	386
High Pressure Oxidizer Pump Diameter, inches	1.71	1.71
High Pressure Fuel Pump Speed, rpm	95,000	22,722
High Pressure Fuel Flowrate, #1 sec	5.99	.8524
High Pressure Fuel Pump Outlet Pressure, psia	4563	268.5
High Pressure Fuel Pump Diameter, inches	3.19	3.19
High Pressure Oxidizer Turbine Diameter, inches	3.32	3.32
High Pressure Oxidizer Turbine Flowrate, lb/sec	2.78	.1569
High Pressure Oxidizer Turbine Admission	0.48	0.48
High Pressure Oxidizer Turbine Tip Speed, ft/sec	1600	394
High Pressure Fuel Turbine Diameter, inches	2.72	2.72
High Pressure Fuel Turbine Flowrate, lb/sec	6.23	.3092
High Pressure Fuel Turbine Admission	1.00	1.00
High Pressure Fuel Turbine Tip Speed, ft/sec	1589.7	380
Cooling Jacket		
Combustor Coolant Flowrate, lb/sec	3.47	.265
Nozzle Coolant Flowrate, lb/sec	1.44	.165

EXPECTED ENGINE LIFE AND RELIABILITY CHANGES

The underlying mission assumptions for engine life and reliability requirements for the low thrust mode of operation are for an unmanned payload delivery type mission. However as a worst case the following assumptions were made:

(a) The engines are used for roundtrip missions between LEO and GEO

(b) The missions are manned

Engine Life

The low thrust adaption of the basic 20K lb thrust staged combustion engine will require stage burn times which are in the order of 12 times longer (for F = 1500 lbs) than those of the basic engine to accomplish the same mission. Low thrust stage burn time t is:

$$t_{L.F.} = t_{H.F.} \frac{F_{H.F.}}{F_{L.F.}} \times \frac{(I_S)_{L.F.}}{(I_S)_{H.F.}}$$

where L.F. = low thrust (1 to 2K lb)
H.F. = high thrust (20K lb)
and F and I_S are thrust and specific impulse

For missions involving a payload transfer from LEO to GEO the burn time requirments are approximately as follows for a low thrust engine, based on data in Tables 40 and C-II, Ref. 2.

Vehicle	Total Mission ΔV (Ref. 1) (ft/sec)	$t_{H.F.}$ (hr)	$t_{L.F.}$ (hr)
APOTV	27,900	0.55	6.7
AMOTV	20,400	0.48	5.9

The low thrust engine burn times are longer then the service free life requirements for the high thrust engine (two hours). This means that

the service free life requirements for the OTV low thrust engine will have to be redefined.

The life duration of the 20K lb thrust engine is limited mainly by the design life of the rotating machinery components, for example by bearing and seal wear. The reduced load and speed levels of the low thrust operation should compensate for the increased firing duration. For example, the rotational speeds of the main oxidizer and fuel pumps are lower by a factor of 4 during low thrust operation than during high thrust operation, the fluid discharge pressures are reduced by a factor of about 20. The combustion chamber has a 200F (70%) lower wall temperature during low thrust operation as compared to high thrust operation.

These lower pressure, thermal load and strain levels result in increased low cycle and high cycle fatigue life and in longer creep limited life of engine components during low thrust operation. Another contributing factor for longer low cycle fatigue life is the much lower ramp rates required for startup and shutdown of the low thrust engine. Lower ramp rates are needed for low thrust engine missions, since the payload requirements call for low accelerations and decelerations. An engine life increase is expected for low thrust operation above the 10 hour life for full thrust operation. The exact magnitude of the life increase would require a more detailed analysis of thrust chamber and pump designs.

Engine Reliability

In a simple model of rocket engine reliability the overall engine reliability is the product of start and mainstage reliabilities, $R_E = R_S \times R_M$. Only mainstage reliability is affected by engine burn time t, $R_M = e^{-\lambda t} \approx 1 - \lambda t$, where λ is the failure rate during mainstage operation,. If the failure rate of the low thrust engine were the same as that of the high thrust engine, the longer burn time of the low thrust engine would result in decreased engine reliability. In order to achieve the same mainstage reliability for low and high thrust operations, the mainstage failure rate at low thrust operation should be less than the failure rate at high thrust operation times the ratio of mainstage firing duration $t_{L.F.}/t_{H.F.}$. This means in general that the driving mainstage failure rates at low thrust operation must be lower by a factor of about 12 in order to achieve equal reliabilities for low thrust and high thrust engine operation. It also means that the failure rates of those components which are little affected by the reduced thrust (such as the boost pumps) must be sufficiently low for both modes of engine operation.

It is expected that the failure rates of components operating at the low thrust design point would be lower than at 20K thrust due to the lower stresses imposed by low speed pump operation, low pressures and low temperatures; many components would be operated at essentially derated conditions. While it is not possible to analytically relate failure rates for operation at low thrust to operation at high thrust the increased margins of safety would imply that a decrease by a factor of 10 or more is achievable. If operation at the low thrust mode requires more start and stop cycle, however, the lower stresses may not be the most significant factor in the probability of a successful start and additional attention during development should be placed on achieving a high start reliability. Full duration engine tests would represent one of the major DDT&E cost items .

DDT&E COSTS

The DDT&E costs for a 20k lb thrust staged combustion engine, modified for low thrust operation, were estimated based on the following groundrules:

1. The low thrust engine development is assumed to be preceeded by the full development of a rated high thrust engine. The low thrust engine development therefore will build on the basis of a rated thrust engine whose operating characteristics have been firmly established by detailed component and engine tests.

2. Engine conversion from rated thrust to low thrust is performed by modifying existing engine components as noted in Table 24.

The ROM cost estimate for DDT&E to convert a 20K lb thrust staged combustion engine to a 1 to 2K lb thrust high performance duration engine is shown in Table 24. Total cost is about $12.75 mission (1980) dollars. The cost itemization uses the same WBS elements as in "Orbit Transfer Vehicle Engine Study, Phase A," July 9, 1979, RI/RD 79-191-2, Vol. IIB, Table 6. The majority of the cost, about 61% is incurred due to engine testing.

ENGINE WEIGHT IMPACT

The conversion of a high thrust staged combustion engine to a low thrust engine will not influence engine weight in any significant amount. Removal of the preburner injector and the oxidizer line and valve will save some 7 to 10 lbs (2% of engine weight), but additiona of a pump recirculation line and control valves will largely compensate for this weight decrease and the resultant low thrust engine weight will be essentially the same as that for high thrust operation (433 lbs).

TABLE 24. DDT&E COST ESTIMATES FOR OTV ENGINE
LOW THRUST MODIFICATIONS

WBS Element	Component Modification	in FY 1980, Millions $
1.1.1.1	Main Fuel Pump	2.25
	Add a recirculation line between pump discharge and pump inlet:	
	Add control valve in fuel pump recirculation line bypass lines:	
	Design, component analysis, control system analysis, component fabrication	
	Pump, HQ Tests	
	60 Turbopump Tests (SSFL)	
1.1.2.1	Main Combustion Chamber Injector	1.05
	Change injection element flow passages:	
	Design, analysis, and fabrication	
	Injector cold flow tests (Lab)	
	30 injector hot fire tests (SSFL)	
1.1.5.2	Control Valves	.45
	To be used for fuel pump recirculation bypass	
	Design, analysis, and fabrication	
1.1.10	Engine Tests	7.80
	300 engine tests at low ramp rates, low thrust, and extended duration (COCA)	
1.1.11	System Engineering & Project Management	1.20
	Total	12.75

IDENTIFICATION OF NEW TECHNOLOGY

New technology required to enable design and construction of a staged combustion engine capable of efficient operation at the low thrust mode has been identified as a part of this task. The required modifications to the basic staged combustion engine are in the fuel pump to allow operation at low thrust and possible modification of the injector to prevent feed system coupled instability. A technology program to modify the MK 48-F liquid hydrogen turbopump is discussed in the following.

A hydrogen turbopump technology program would define the limits of rocket engine turbopump off-design operation, due to throttling, down to low thrust levels and wide variations in mixture ratio. This would permit the operation of centrifugal pumps in regions closer to their design points for the low thrust application

The high performance Rocketdyne developed MK48-F liquid hydrogen turbopump with its newly incorporated axial inlet and inducer would be used as the research turbopump. Pump modification would consist of propellant bypass line to return a portion of the pumped fluid back to the pump inlet line. In this return line, a servo-controlled oxidizer valve would be installed which will control the LH_2 bypass flowrate. In addition, a flow measuring device will be required to measure the bypass flowrate.

The MK48-F turbopump would be driven by ambient hydrogen gas through the turbine, which will supply the required power for any speed desired. The Q/N load curve will be adjusted by the pump discharge servo-throttle valve.

The test series would be conducted as follows: A given speed would be preselected and the discharge throttle valve will be positioned to give a $(Q/N)_R = 1.0$. After speed is attained the discharge throttle valve would be closed, in preselected increments, thus lowering the $(Q/N)_R$. As the peak of the H-Q curve is approached, the pump bypass throttle valve would be opened so that the pump always operates on the negative slope portion of the H-Q curve. As the discharge throttle valve is further closed, the bypass throttle valve is further opened. Two specific areas need defining: (1) The amount of bypass flow and subsequent recirculation that the turbopump can handle until the heating of the bypass fluid causes the pump to stall and, (2) the optimum location upstream of the pump inlet to reinsert the bypass fluid.

Cost to conduct this program is moderate from a hardware standpoint, in that the MK48-F turbopump exists and the bypass throttle valve and control system exist and are operable. Only the bypass line and flow measuring device need be fabricated and installed. A 60 test series would be conducted in APTF, Lima Stand. A month of hardware installation and checkout would be required before the 3 to 4 month test program is conducted. A week should be planned to remove the pump from the facility and disassemble. No special additional facility construction or modification is required. Cost of propellant and facility operation would be the same as for any MK48-F test driven by ambient GH_2. This test program would be most cost effective when combined with the next planned MK48-F test series, since the cost of installation and removal of the hardware would be eliminated.

TASK 10: SAFETY, RELIABILITY AND DEVELOPMENT RISK COMPARISON

Since the OTV is a manrated vehicle, stringent demands for high system reliability and safety are required for the entire OTV, including its propulsion system. The effects of reliability and safety demands on OTV propulsion system selection, on engine design and test philosophy, and on engine cycle were investigated. In addition, a development risk comparison between the staged combustion and advanced expander cycle engines was performed.

The discussion of task study results is structured into four parts. First, the approach to engine manrating, safety, and reliability is reviewed for rocket engines of past manrated space vehicles, from Mercury to Apollo, and of the current Space Shuttle Program. Second, the major manrating, safety and reliability issues for OTV propulsion are addressed. Thirdly, from these issues desirable propulsion system features are derived and a suggested safety and reliability approach for OTV propulsion is presented. Fourth, a development risk methodology is described and results of its application for a cost risk comparison between staged combustor and advanced expander are presented.

ENGINE RELIABILITY CRITERIS FOR PAST AND CURRENT MANRATED SPACE VEHICLES

Mercury, Gemini and Apollo Programs

Early manned space flights used boosters designed for ballistic missiles, and reliability requirements were based on military objectives. The Atlas and Titan I vehicles for the Mercury and Gemini Programs used booster engines with a reliability goal of 0.85 at 90% confidence level, which was successfully demonstrated in 100 tests with some failures allowed. The Saturn booster engines (H-1, F-1, J-2) had an engine reliability goal of 0.99 at 50% confidence level to be demonstrated in 69 predeclared, equivalent full duration tests without failure. This corresponds to a reliability of 0.967 at 90% confidence level. The goal was demonstrated early in the program; however, a large number of development tests was required, over 1200 for the F-1 and J-2, see Fig. 67.

At the time of the first manned Saturn V flight, the F-1 engines had accumulated a total of over 2500 and the J-2 of over 3500 development tests. At the end of the engine programs, the F-1 had demonstrated ∿99.8%, and the J-2 ∿99.7% reliability, both at 50% confidence. These reliabilities were achieved through extensive component and engine test programs, aided by a vigorous quality assurance program. The engines had some component redundancy, such as flight instrumentation and electrical igniters.

A reliability exceeding 0.99 was allocated, but no demonstration required, for the Apollo SPS and LEM engines, see Table 25. High reliability was achieved through redundancy of critical engine components, design verification tests, qual tests and a formal certification program.

The Saturn V boost phase abort safety features were as follows: The Saturn V launch vehicle was held down until all five F-1 engines reached full thrust. If one F-1 engine did not attain full thrust, launch would have been aborted. Safe crew return was possible at all times during the F-1 and J-2 powered Saturn stage flight. Engine out capability with mission continuation was limited to a small part at the end of the first stage boost phase and to some part of the second stage boost phase.

	VEHICLE	ENGINE RELIABILITY GOAL	VERIFICATION
EXPENDABLE ENGINES	• MERCURY ATLAS • GEMINI TITAN I	.85	TEST DEMONSTRATION: 100 TESTS; 90% CONF
	• SATURN BOOSTERS H-1 F-1 J-2	.99	TEST DEMONSTRATION: 69 TESTS, 50% CONF
	• APOLLO SPS LEM DESCENT LEM ASCENT	.9999 .9991 .999982	DESIGN VERIFICATION TESTS QUAL TESTS CERTIFICATION
REUSABLE	• SPACE SHUTTLE SSME OMS RCS	NO NUMERICAL GOAL	DESIGN VERIFICATION SPEC'S LIFE REQUIREMENTS CERTIFICATION

TABLE 25. RELIABILITY CRITERIA FOR MANRATED VEHICLES

Space Shuttle Program

A specific system safety program is being applied to the Space Shuttle Orbiter with the objective of systematically identifying and evaluating potential hazards to the crew, equipment or facilities: Acceptable methods for hazard control are defined; each specification for Space Shuttle propulsion systems requires strict compliance with established hazard evaluation and control methods; hazard analyses are prepared to document compliance with the safety requirements, and concurrence and approval is required at established checkpoints by NASA.

Design verification specifications are prepared for major subsystems and each contractor end item. Each design requirement must be individually verified by a predetermined method, such as test or analysis. NASA agreement of satisfactory verification is also required for each subsystem. The requirements that must be verified prior to major program events are specifically defined. Examples of design verification are engine PSC demonstration and hazard analyses.

The reliability program concentrates on assessing and confirming the engineering design for reliability rather than demonstrating quantitative reliability requirements. Features of the reliability program include:

1. Design review of all components which are capable of causing system failure. These are conducted at pre-planned checkpoints in the layout, detail design and production release sequence. Followup audits assess completion of action items.
2. The failure mode and effect analysis (FMEA) confirms that specified redundancy and fail-safe features have been incorporated. The Critical Items list summarizes design, test and inspection features of items critical to mission success.
3. Failure analysis is conducted on all functional failures to assure that corrective action is taken.
4. Maturity assessment techniques measure progress toward a system capable of reliably performing mission requirements. Both technical and programmatic problem areas are pinpointed.

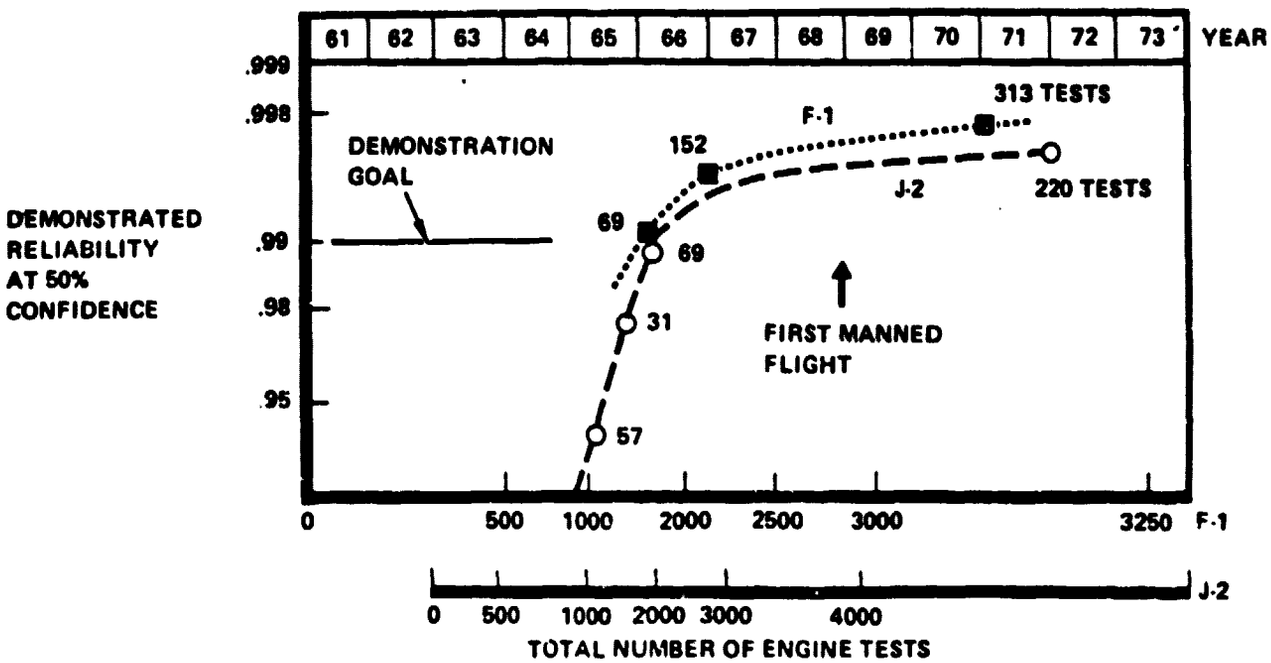

FIGURE 67. DEMONSTRATED F-1 and J-2 RELIABILITIES

The Space Shuttle mission safety features are as follows:
All three SSME engines have to be at full thrust prior to solid rocket ignition. Failure to attain full thrust or loss of component redundancy during this period will cause launch abort. The Space Shuttle Orbiter returns for landing at the launch site or at a contingency landing site in the event an SSME shuts down prior to attaining the desired orbit. The SSME features special design provisions to enhance reliability and safety. These include the following:

1. The engines incorporate a redundant safety limit monitoring system that will shut down the engine if a limit is violated.
2. The electrical control system (controller, instrumentation and interconnections) are redundant. They will fail operational after one failure and are capable of safe engine shutdown after a second failure.
3. The main propellant valve actuators have redundant servo control valves and feature a pneumatic backup for safe closure in the event of hydraulic system failure.
4. The engine controller verifies redundancy and integrity of the operational components prior to launch, during flight and in post-flight turn-around operations.
5. The engine is designed for long-life (55 missions between major overhaul).

Propulsion for maneuvering of the Orbiter while near or in low earth orbit consists of two 6K lb. thrust Orbital Maneuvering Engines (OME), and a Reaction Control System (RCS); all engines are pressure fed with NTO and MMH propellants. The OME's provide propulsion for orbit insertion, orbit transfer, rendezvous, de-orbit and launch abort. Launch abort (either return to launch site, or around-once orbit) can be accomplished with only one OME, or with only four RCS thrusters in the +X direction. The four RCS thrusters can provide a total of 3.5K lb. thrust. One OME and two +X RCS thrusters are packaged with their propellant tanks into one pod. The engines in the two pods are physically separated by one of the three SSME's. All OMS propellant can be fed to

either OME or to the four +X RCS thrusters. Extensive use of redundancy in propellant valves is made, see Fig. 68.

The major safety and reliability requirements that apply to the SSME also apply to the OMS engines. This includes mechanical components of fail-safe design, electrical components which are fail op/fail safe, and redundant propellant valves. All design specifications are verified, and an extensive certification is performed. A reliability goal is not required to be demonstrated.

The reliability and safety approach for past and current engines used on manrated vehicles is summarized in Table 26.

FIGURE 68. SPACE SHUTTLE ORBITAL MANEUVER SUBSYSTEM SCHEMATIC

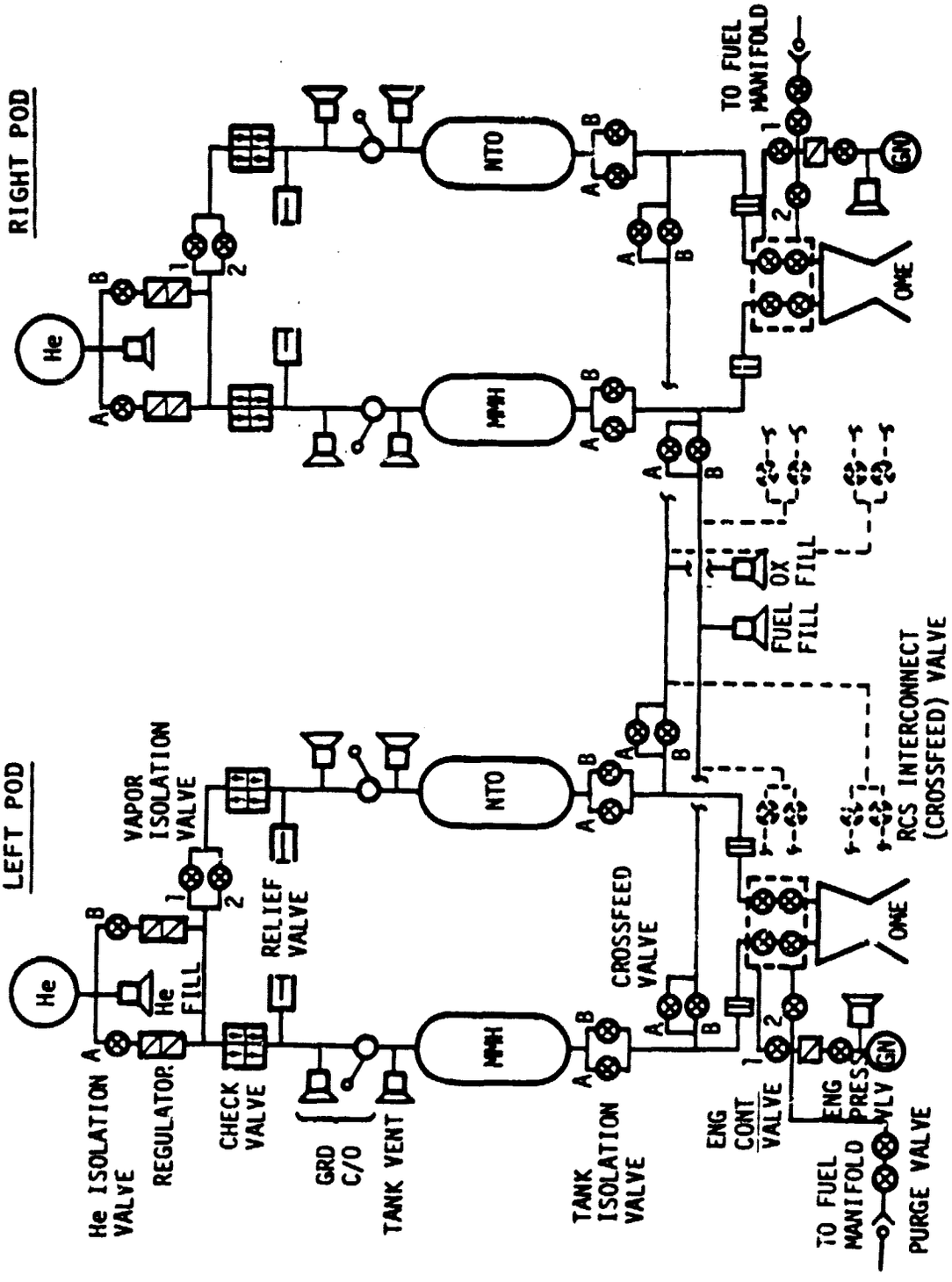

PAST ENGINES - MERCURY, GEMINI, SATURN, APOLLO

- EMPHASIS ON HIGH RELIABILITY; ENGINE SAFETY NOT EXPLICITLY ADDRESSED
- SOME PROGRAM NUMERICAL GOALS FOR RELIABILITY WERE DEMONSTRATED
- FEW REDUNDANT ENGINE COMPONENTS
- LIMITED ENGINE OUT CAPABILITY

CURRENT ENGINES - SPACE SHUTTLE

- EMPHASIS ON SAFETY AS A TOTAL PROGRAM COMMITMENT
- QUALITATIVE TREATMENT OF RELIABILITY
- ENGINE OUT CAPABILITY FOR SAFE RETURN CONSIDERED IMPORTANT
- REDUNDANCY OF SELECTED ENGINE COMPONENTS

TABLE 26. SUMMARY OF RELIABILITY AND SAFETY APPROACH FOR PAST AND CURRENT MANRATED PROGRAM ENGINES.

OTV PROPULSION SYSTEM SAFETY AND RELIABILITY ISSUES

The following points are addressed as major issues for OTV propulsion manrating, safety and reliability:

1. **Do current NASA specifications for the STS and for previous manned space programs adequately cover safety criteria for OTV propulsion, specifically during space flight?**
2. **Which OTV propulsion system configurations are best for mission success and for crew safety from the standpoint of highest success probability?**
3. **How is engine reliability affected by:**
   a. **The number of engine tests**
   b. **Demonstration requirements of reliability goals**
   c. **Engine component redundancy, and**
   d. **Engine cycle?**
4. **What is a viable OTV engine design approach for safety and reliability?**

The study assumed as a groundrule OTV crew safety independently from the existence of a life-boat type vehicle.

Document Review

A number of NASA documents were reviewed to determine the applicability of safety and reliability specifications for OTV engines. This review concluded that several documents contained valuable basic requirements for OTV engine design (e.g., preferred order of design measures), but no specifications were found specifically applicable to OTV engine safety covering the space flight aspects. The reviewed documents are listed in Table 27.

TABLE 27. NASA DOCUMENTS REVIEWED FOR SAFETY AND RELIABILITY

Document No.	Title	Year of Issue	Main Safety & Reliability Requirements
M-D MY 1700.120 (MSFC)	Safety Program Directive No. 1	1969	. Hazard Category Definition and Hazard Analysis Instructions . Defines Preparation of System Safety Plan . Defense In-Depth Through Hazard Reduction Precedence Sequence (Preferred Order of Design Measures)
85M03885 (MSFC)	Guidelines for Performing FMECA's on Space Shuttle	1971	. Instructions for FMEA's . Criticality Category Definition and Criticality Analysis Instructions
NHB 5300.4	Safety, Reliability, Maintainability & Quality Provisions for Space Shuttle	1974	. Similar in scope to M-D MY 1700.120
JSC 11123	STS Payload Safety Guidelines Handbook	1976	. Detailed Design Guidelines for Safety
JSC 07700, Vol. X	Space Shuttle Program: Space Shuttle Flight & Ground System Spec.	1978	. Shuttle Subsystem Redundancy No Less Than Fail-Safe During Entire Mission . Operational Status Verification of Redundant Subsystems . Applies NHB 5300.4
NHB 1700.7	Safety Policy & Requirements for Payloads Using the STS	1979	. Baseline Policy for STS Payloads . Payload Single-failure Tolerant for Critical Hazards . Payload Double-failure Tolerant for Catastrophic Hazards . Three Propellant Valves in Series Required
JSC 13830	Implementation Procedure for STS Payloads System Requirement	1979	. No specific Safety Criteria. Defines Procedures and Instructions

OTV Mission Success and Crew Safety Definition

OTV mission success is defined as successful insertion of a payload into geostationary earth orbit (GEO) and return to low earth orbit (LEO). Using the Reference 2 data, this entails six main engine starts, ΔV requirements of $\sim$28,000 ft/sec for the APOTV, and $\sim$20,000 ft/sec for the AMOTV concept.

OTV crew safety is defined as safe return of the OTV crew to LEO, regardless of the payload disposition. The greatest OTV propulsion demand is for return to LEO from GEO. Using the Reference 2 data, this requires three main engine starts and half the mission ΔV requirements for APOTV (i.e., $\sim$14,000 ft/sec), and one-third of the mission ΔV requirements for the AMOTV (i.e., $\sim$6500 ft/sec).

Best Engine Configurations

Figure 69 shows the reliability improvement achieved by employing two or three engines with engine-out capability. Clusters of two and three engines without engine-out capability are shown as the non-redundant engine curves at the bottom of the graph (1/1, 2/2, 3/3). Engine-out capability curves for two engines with one required, and three engines with one or two required, are shown as the redundant engine curves. The calculations are based on a 5% probability of non-independent failure, that is: 5% of the engine failures can result in damage to an adjacent engine or other propulsion component, causing loss of propulsion capability. This estimate is based on results of engine test firings of past Rocketdyne engine programs.

As shown in Figure 69, for reliabilities greater than 0.95, one redundant engine gives the highest propulsion system success probability. More than two engines would not increase this probability, due to the assumed 5% non-independent failure probability.

FIGURE 69: ENGINE OUT CAPABILITY COMPARISON

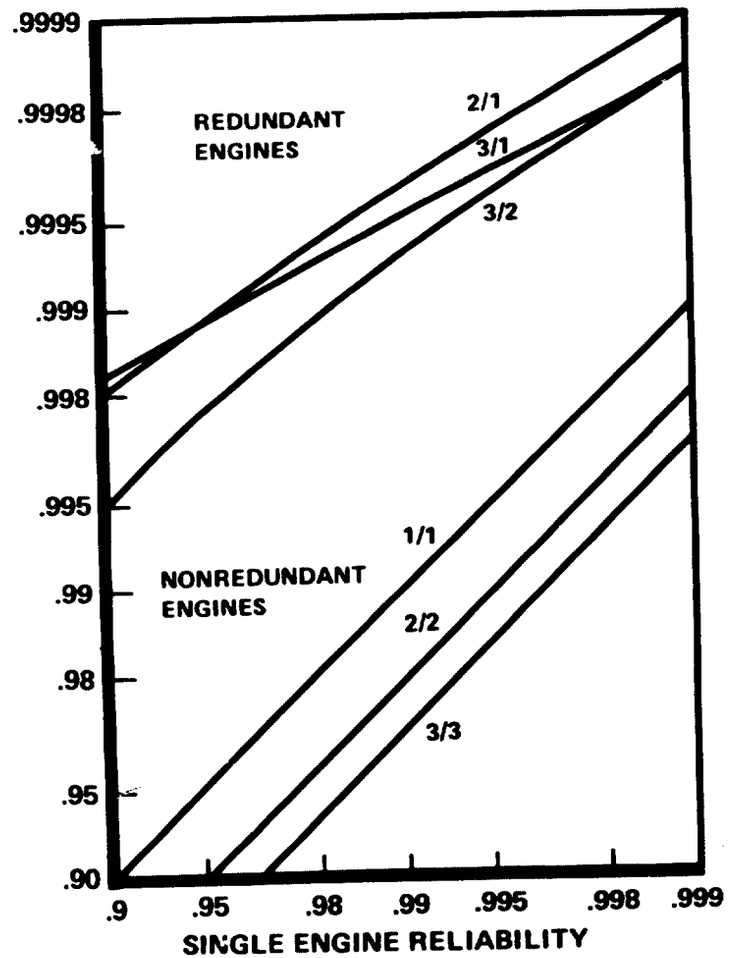

PROPULSION SYSTEM PROBABILITY FOR MISSION SUCCESS OR SAFE RETURN

5% PROBABILITY OF NON-INDEPENDENT FAILURE
SOURCE: H-1, F-1, J-2, SSME HAZARDOUS FAILURES

KEY: 2/1 = TWO ENGINES/ ONE REQUIRED

TWO ENGINES WITH ONLY ONE REQUIRED HAS HIGHEST SAFE RETURN PROBABILITY

Relative failure probability is shown in Fig. 70 for combinations of engine-out capability in clusters of two and three OTV engines. One engine without backup is the comparison standard with a relative failure probability of 1. Addition of a low thrust backup engine for crew safety reduces the failure probability to 0.03. In a cluster of two main engines, both required for the entire mission, but only one for safe crew return, the relative mission failure probability doubles, but crew safety probability is decreased to 0.1. Addition of a low thrust backup engine for crew safety further reduces the relative failure probability to 0.003. The lowest relative failure probability for mission success is realized in a cluster of two main engines with both engines only required for the first burn. Following this, the mission could be completed with only one engine. Three engines, with all three required only for the first burn in the mission, and mission completion by two engines, increases the failure probability, due to the contribution of non-independent engine failure modes affecting more than one engine. The bar chart assumes that the backup engine is not affected by failures of the main engine, and that main engine failures have a 5% chance of non-independency. The reliability of a single main engine was assumed as $\geq$ 0.99, and that of the backup engines as 0.97.

The conclusions from the engine configurations analyzed are as follows:

1. From the standpoint of minimum failure probability, the use of two main engines, either capable of mission completion after the first burn with both engines, is best for mission success. Inherent in this conclusion is the assumed mission groundrule that the mission will not be started with one engine known to be out.
2. For safe crew return, the failure probability can be further reduced if a backup propulsion, for instance, consisting of a low thrust engine, is employed in addition to the two main engines. Either main engine or the backup engine would be able to provide propulsion for safe return from any point in the mission.

The feasibility of using a backup engine for additional crew safety has to be further investigated.

FIGURE 70: ENGINE REDUNDANCY FOR MISSION SUCCESS AND CREW SAFETY

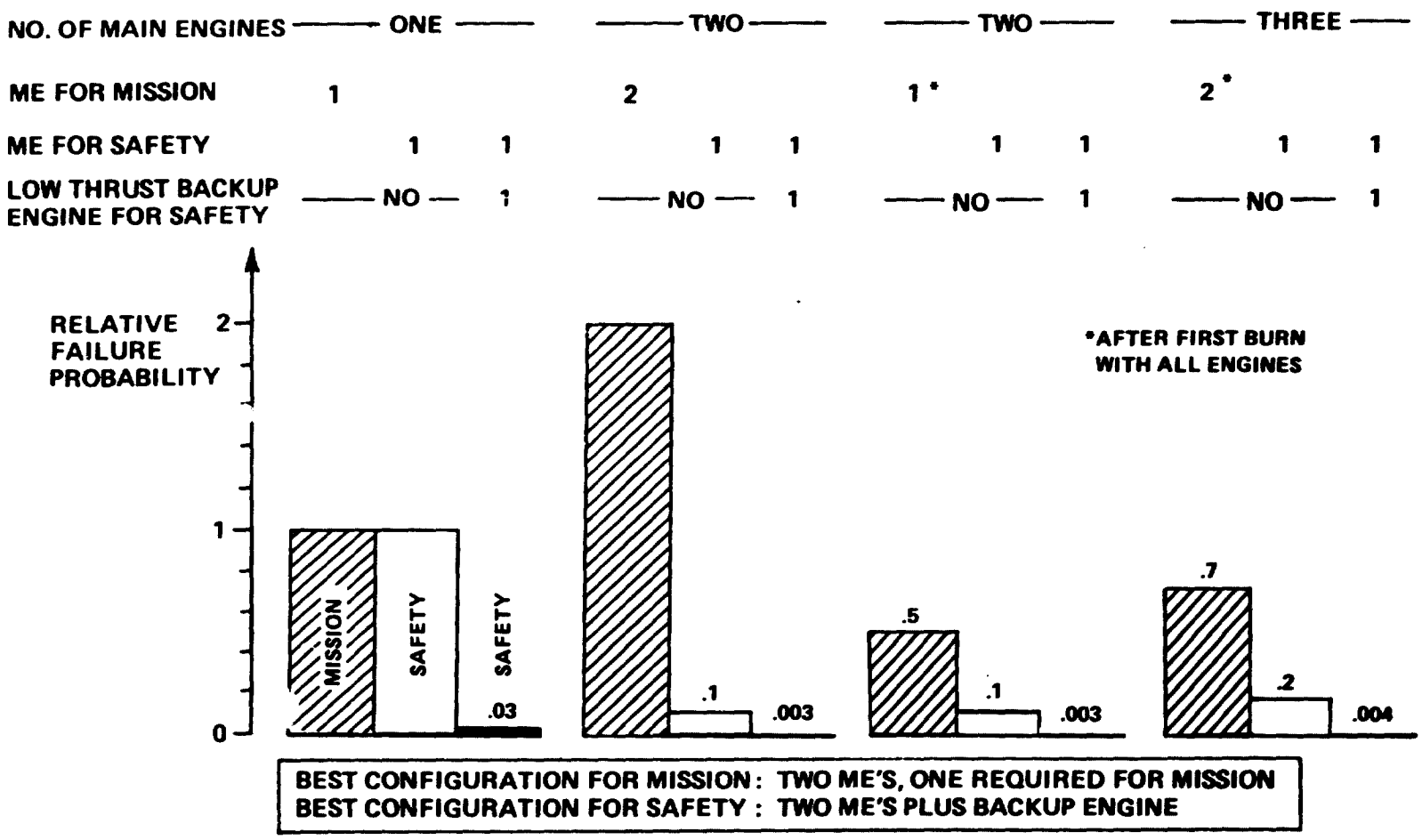

236-295

Rockwell International
Rocketdyne Division

Number of Engine Tests for Reliability Demonstration

If a high engine reliability is required to be demonstrated, a large number of engine tests consisting of successful equivalent mission duty cycles is necessary. The engine mission duty cycle for an OTV going from LEO to GEO and return ($\Delta V \sim 28{,}000$ ft/sec for APOTV) for example, requires six engine starts and a total burn time on the order of 1/2 to 1 hour, depending on thrust and specific impulse. The curves shown in Figure 71 for 50% and 95% confidence levels are obtained from the standard reliability equation:

$$R_E = \left\{1 - \frac{CL}{100}\right\}^{1/N} \text{, where}$$

R_E engine reliability

CL confidence level

N number of successful tests

A successful test is defined as the equivalence of a complete mission duty cycle without engine failure. Since the mission consists of six starts, the duty cycles multiplied by 6 yield the number of required engine starts, also shown in Fig. 71.

The intersection of the 50% curve with the duty cycle axis represents the reliability demonstration goal for the F-1 and J-2 engines (0.990) which required 69 successful tests. For a demonstrated reliability of 0.999, about 700 successful equivalent mission duty cycles are required.

Figure 71 relates the large amount of testing and the associated high cost, if a high numerical reliability demonstration goal by test is required.

FIG. 71: RELIABILITY DEMONSTRATION vs NUMBER OF TESTS

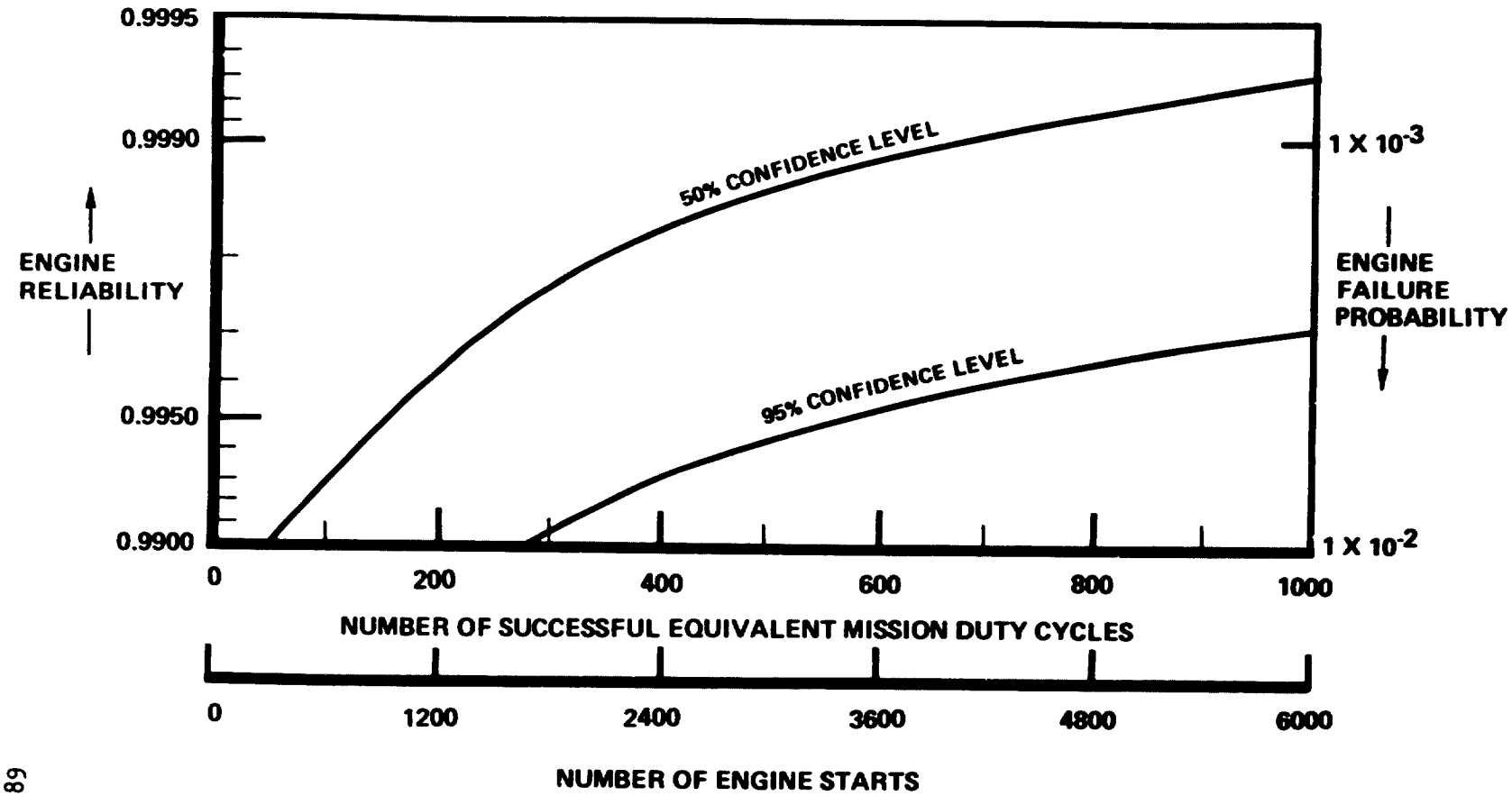

HIGH DEMONSTRATED RELIABILITY REQUIRES LARGE NUMBER OF TESTS

Rockwell International
Rocketdyne Division

236-289

Reliability Demonstration

An assessment of the advantages and disadvantages of numerical reliability demonstration revealed the following:

Advantages: Important advantages are a clear understanding between NASA and the engine contractor of the required engine reliability with a convenient acceptance criterion and a simple measure for program progress and engine manrating. The demonstration goal, if extended to all major OTV subsystems, serves to NASA as an indicator of those subsystems which need additional effort for reliability improvement. Cost-risk analyses and tradeoffs using reliability as a parameter become more credible if the reliabilities are expected to be demonstrated.

Disadvantages: A demonstrated reliability is always based on a reliability allocation which has its origin in a "permissible" crew and vehicle loss. The bases for permissible crew and vehicle losses and for subsystem allocations are arbitrary and difficult to be substantiated. Originally allocated reliability goals which have to be demonstrated may prove to be incorrect by later component testing, and a reallocation may result in program delays and/or cost overruns. Many demonstration tests are required to achieve reliabilities in excess of 99% and may induce a false sense of security since reliability is not a singular measure of safety. A total program commitment to safety, such as presently being pursued in the Space Shuttle program, appears to be a more viable approach.

Effect of Engine Component Redundancy on Engine Reliability

The effect of engine component redundancy on engine reliability can be estimated by first calculating the engine unreliability assuming each component type is not redundant, and then introducing redundancy for those components which can be made redundant. The reliability apportionment for an engine with nonredundant components is based on Rocketdyne component and engine test data. It is impractical to make ducts and lines, the combustion chamber, or the turbopump redundant. Controls, valves, electrical components, flight instrumentation and the controller can employ redundancy. This reduces engine failure probability by one-half, as shown in Table 28. For example, if the engine reliability were assumed as 0.990 without redundant engine components, it would become 0.995 with redundancy.

OTV Engine Design Approach for Safety and Reliability

The objective of the design approach is to protect critical engine functions and critical engine components. This objective can be met with a combination of the following design factors as discussed in more detail below:

- Engine Component Redundancy (i.e. Redundancy within the Engine)
- Fail-safe Features
- Engine Health Monitoring
- Common Mode Failure Protection

Redundancy of Engine Components. Selected components such as start components, controller, flight instrumentation and valve actuation can be made redundant following an evaluation of their function criticality and their individual reliabilities.

The objective of assured engine start and shutdown on command is achieved by redundancy of all critical components required for start and shutdown. These include the controller, igniters, the vehicle power source for ignition and valves or actuators.

TABLE 28: EFFECT OF ENGINE COMPONENT REDUNDANCY

	HYPOTHETICAL ENGINE WITH NO REDUNDANT COMPONENTS		HYPOTHETICAL ENGINE WITH COMPONENT REDUNDANCY	
COMPONENT TYPE	APPORTIONED UNREL.	RELIAB.	DEGREE OF REDUNDANCY	RELIABILITY
SYSTEMS-DUCTS, LINES	9.0	.9991	NONE	.9991
COMBUSTION DEVICES	18.7	.9981	NONE	.9981
TURBOMACHINERY	11.2	.9989	NONE	.9989
CONTROLS - VALVES	18.9	.9981	HALF	.9990
ELECTRICAL & FI	13.3	.9987	FULL	.9999+
CONTROLLER	28.9	.9971	FULL	.9999+
TOTAL	100%	.990		.995

COMPONENT REDUNDANCY RESULTS IN SIGNIFICANT ENGINE RELIABILITY GAIN

In the following, a practical approach for propellant valve redundancy is described. Conflicting objectives exist for main propellant valves: while carried in the Shuttle Orbiter's payload bay, there should be no propellant leakage from the OTV tanks and engines into the bay to preclude premature firing. This objective led NASA to the requirement (NHB 1700.7) that "each propellant delivery system must contain three mechanically independent propellant flow control devices in series that remain closed during all ground and flight phases until the deployed payload has reached a safe distance from the Orbiter".

Once the OTV engines have started, uninterrupted propellant flow to the OTV engines has to be assured for the entire mission. This objective can best me met with only two propellant valves in series but with redundancy for these two valves.

A third objective is to provide positive isolation of propellant from a failed engine to prevent propellant loss through a damaged engine and potential cascading damage to other engines or OTV systems.

All three objectives can be satisfied with three valves in series, of which the tank valve is closed during the OTV residence in the Orbiter payload bay and mechanically locked in the open position following OTV deployment at a safe distance from the Orbiter, see Figure 72. The objective of assured opening and closing of the two remaining valves can best be met with redundant valve actuators and a redundant controller, since those are the components with predominant failures for unplanned propellant flow interruption events.

Fail-Safe Features. An example is engine redline monitoring with automatic engine shutdown if a redline is exceeded, possibly leading to a catastrophic failure and endangering a neighboring engine.

FIGURE 72. **PROPELLENT VALVE REDUNDANCY**

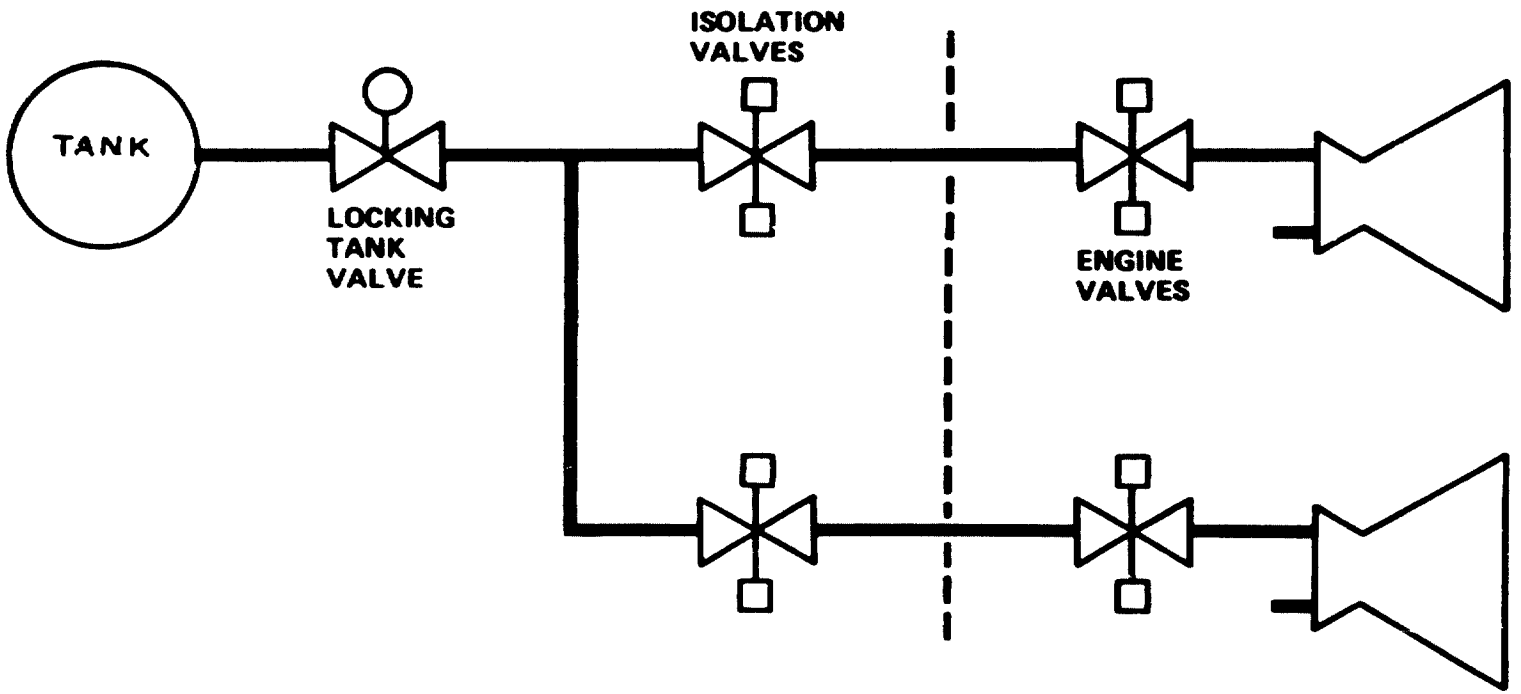

236-294

Rockwell International
Rocketdyne Division

Health Monitoring. Engines for a manrated, reusable vehicle will rely heavily on the capability for engine checkout and health monitoring, with engine status indication available to the vehicle crew. The functions to be performed include the following;

a. Engine ready verification. This will be done as automatic component checkout at preflight and prior to engine ignition.
b. Redline monitoring. Redundant monitoring of all safety-critical parameters for safety confirmation and for fail-safe engine shutdown in case critical parameters exceed redlines.
c. Redundancy management and failure response. When one or more elements of a redundant component fail, switchover to the healthy element has to be performed automatically as part of the failure response.
d. Data reporting for maintenance and reusability. The reusability aspects of the engines require that all component failures are recorded for action by post-flight maintenance operations.

These functions are fulfilled by specific design features, such as a redundant, self-checking controller, specific instrumentation for redlines and engine health monitoring, and redundant sensors for safety-critical functions.

Protection Against Common Mode or Non-Independent Failures. (One failure causing loss of more than one engine.) When more than one engine is used, the probability of common cause, common mode, or non-independent failures has to be reduced. It requires, for example, that fail-safe (i.e., off-) controls are provided to terminate propellant flow to an engine in the event of a catastrophic malfunction. This can be accomplished by valves which close in case the control signal is lost (spring-actuated or pneumatic-reservoir-actuated valves).

Another requirement is the protection of vital controls on the second main engine if the first engine fails. This is accomplished by separating and/or hardening control lines (example: armored electrical harness).

Engine Cycle Effect on Reliability

A comparative reliability analysis was performed for the advanced expander and staged combustor engine configurations. Two approaches were used in the analysis:

1. Qualitative functional comparison
   In this approach selected engineering parameters influencing reliability were established and the "reliability performance" of each component of the two engines was subjectively judged and ranked. The following comparison parameters were chosen:
   - High pressure pump discharge pressure
   - Turbine inlet temperature
   - Combustion chamber pressure
   - Complexity
   - Component redundancy
   - Controllability

The expander reliability ranked slightly higher in this comparison than that of the staged combustor, mainly due to the influence of the first three parameters.

2. Estimated failure rate comparison
   In this approach estimated relative failure rates of components for both configurations were compared. The relative failure rates used for this quantitative comparison were derived from J-2 and SSME component data, modified by appropriate normalization factors between expander and staged combustor engine configurations.

This method also yielded slightly higher reliabilities for the expander. The estimated lower failure rate of the expander can be attributed to lower stresses in the oxidizer system, lower temperatures in the high pressure turbopump, and deletion of preburners.

The analysis resulted in single engine and propulsion system reliabilities, as shown in Table 29. The difference in single engine reliabilities between expander and staged combustor is in the range of 0.06 to 0.12% if a single

engine reference reliability of 0.9950 is assumed. In a propulsion system of two engines, this reliability advantage of the expander decreases to a range of 0.004 to 0.01%.

The conclusions from this reliability comparison were as follows:

- At a given time in development, and at the same funding level, the advanced expander is estimated to be slightly more reliable than the staged combustor.

- The advanced expander reliability advantage is not considered significant enough to reduce the number of engine development tests.

- Both engine configurations can be developed to the same reliability.

TABLE 29: RELIABILITY COMPARISON:
STAGED COMBUSTOR VS. ADVANCED EXPANDER

ENGINE	SINGLE ENGINE RELIABILITY	PROPULSION SYSTEM † RELIABILITY (2 ENGINES)
STAGED COMBUSTOR	0.9950*	0.99950
ADVANCED EXPANDER	0.9956 - 0.9962	0.99954 - 0.99960
Δ RELIAB. OF EXP.	+0.06 TO + 0.12%	+0.004 TO +0.01%

*ASSUMED AS REFERENCE
†WITH 5% NON-INDEPENDENT FAILURE PROBABILITY

SUGGESTED SAFETY AND RELIABILITY APPROACH FOR OTV ENGINES

Based on the task investigation, the following safety and reliability approach for OTV engines is suggested:

Use Current STS Propulsion System Approach for Safety and Reliability

This approach emphasizes design-to safety and reliability, featuring thorough safety and reliability analyses of the design and extensive design verification by test or analysis. Demonstration of numerical reliability goals (as done for H-1, F-1, J-2) is not considered cost effective.

Best Propulsion System Concept With Regard to Mission Success and Crew Safety

Mission Success: Two main engines, with either engine capable of mission completion after the first burn occurred with both engines.

Crew Safety: Two engines with backup propulsion. Either main engine or the backup propulsion are capable of safely returning the OTV and its crew from any point in the mission.

The capability of a backup propulsion for crew safety needs to be investigated and firmly established.

Engine Design Features for Safety and Reliability

The OTV engines should have specific features to enhance safety and reliability. Major features are as follows:

Selected Component Redundancy: Safety critical components should be made redundant. This includes the controller, igniters and critical flight instrumentation.

Fail-Safe Components: Fail-safe features, such as valve closure upon loss of signal, should be incorporated wherever they improve safety and do not degrade mission success.

Protection against Common Mode Failures: Design protection against common mode and non-independent failures should be provided to the greatest possible extent. This includes separation, proper placement, and hardening of vital components.

Engine Checkout and Health Monitoring System: The engine design should include a checkout and health monitoring system which automatically checks for failures, alerts the crew if redlines are exceeded, and shuts down the engine prior to the occurrence of hazardous failures.

Engine Cycle Preference: The advanced expander engine was found to be slightly more reliable than the staged combustion engine at the same development stage. However, this difference is not considered to be significant enough to make an engine cycle selection on the basis of reliability alone.

OTV ENGINE DEVELOPMENT RISK

Definition of Development Risk

Risk, in general, is defined as the product of probability of failure times the consequence of failure. Since the probability of failure is one minus the probability of success, the risk equation is:

$$R = (1 - p_s) \times C_f \quad , \text{ where}$$

R risk

p_s probability of success

C_f consequence of failure

A high risk can therefore either be due to a low probability of success or a large consequence of failure.

There are two kinds of program development risks, a schedule risk and a cost risk. In the schedule risk, the success probability equals the probability to achieve a desired schedule at a given budget. The consequence of failure to achieve the program schedule can be defined as a schedule factor which contains a subjectively or objectively measured decrease in program utility.

The cost risk includes as probability of success the probability to achieve the program objectives at a given schedule, and as consequence a cost factor which measures program cost at the given schedule. The Phase A Extension Work Statement defines this cost risk as development risk; therefore, the cost risk was evaluated for the two engine configurations; i.e., for the advanced expander and the staged combustor. The cost risk was evaluated as a function of attaining slipped and advanced versions of the respective engine DDT&E schedules.

The development risk equation can be expressed as follows:

$CR = (1 - p_s) \times C_f$, where

CR cost risk

p_s probability of achieving DDT&E program objectives, given a schedule

C_f cost factor, change in DDT&E cost for given schedule

Methodology for Determining Development Risk

The development risk was determined for three DDT&E Program schedules:

1. The nominal schedule
2. A schedule advanced by 6 months
3. A schedule slipped by 6 months

The methodology used to obtain quantitative risk results is shown schematically in Fig. 73. The success probabilities and cost changes associated with the three program schedules were determined in two steps for each major OTV engine component by the cognizant component engineers. As a first step, an assessment of potential component problems was performed for each component considering five technology aspects or risk influences. This problem assessment resulted in the definition of specific potential problems, their cures and their potential influence on develpment cost and schedule. Table 30 presents examples of potential development problems for three major WBS elements. Based on this assessment, the component development success probability and required change in effort were estimated for the three program schedules, as the second step. Appendix A contains the survey form which was used to solicit the opinions of the cognizant component engineers on which the component risk assessment was based. The component data were then combined to determine overall program probability of success, cost change, and development risk.

FIGURE 73: METHODOLOGY FOR DEVELOPMENT RISK

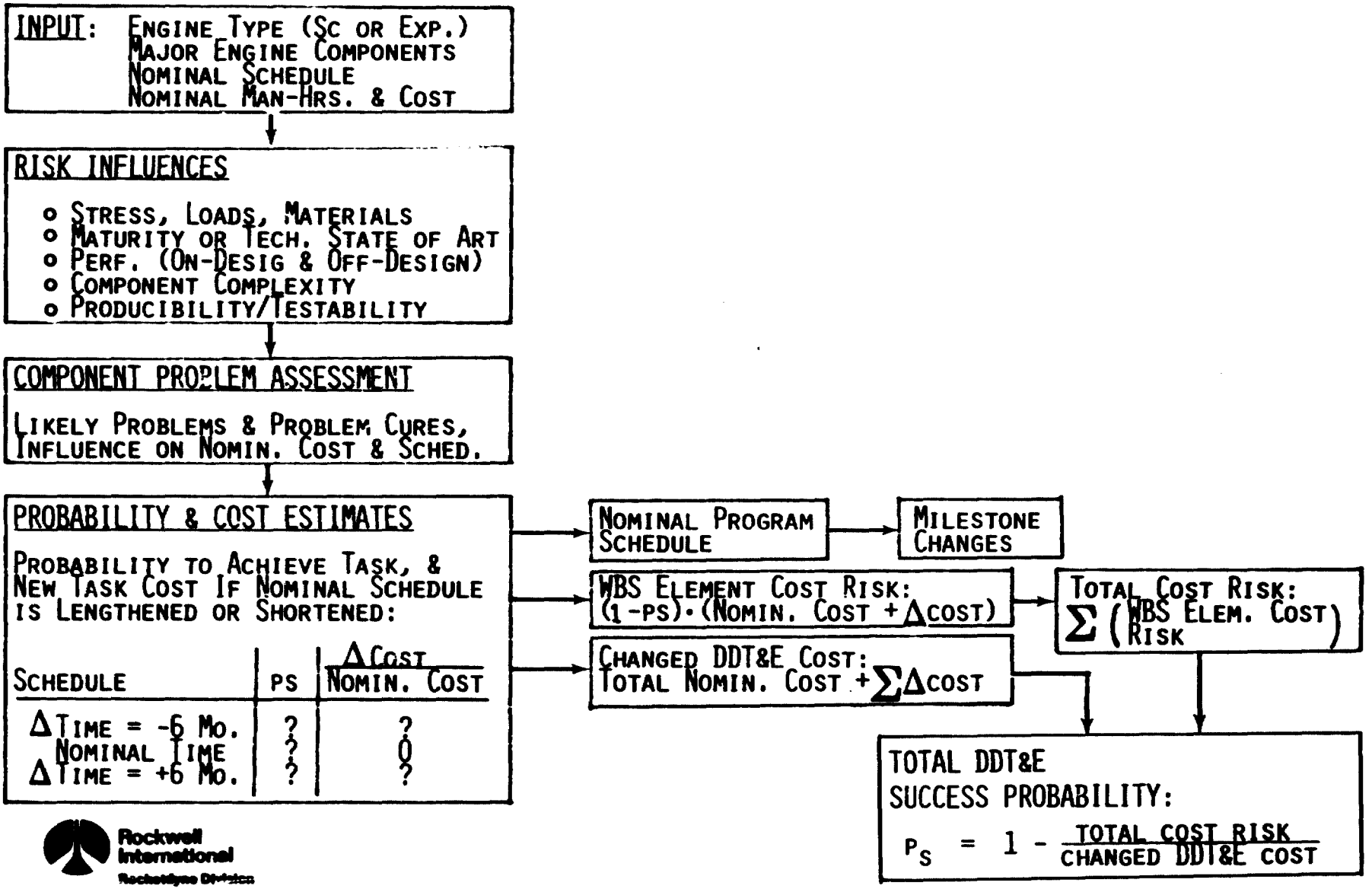

Rockwell International
Rocketdyne Division

TABLE 30: EXAMPLES OF POTENTIAL DEVELOPMENT PROBLEMS

COMPONENT	POTENTIAL PROBLEM	PROBLEM CURE
• HPFTP	COMPONENT LIFE	COMPONENT TESTING, FATIGUE ANALYSIS, BACKUP HARDWARE
	OFF-DESIGN LOW FLOW PERF.	REDESIGN OF CROSSOVER AND RETEST
	MATERIAL PROCUREMENT	ADVANCE MATERIAL PROCUREMENT PLAN
• MAIN THRUST CHAMBER	NARLOY Z PROCUREMENT	ORDER MATERIAL EARLY TO ESTABLISH CENTRIFUGAL CASTING SUPPLIER
• ENGINE TEST	HIGH TEST FREQUENCY	USE SELECTIVE OVER-TIME

Results of Development Risk Assessment

Figure 74 shows the relative DDT&E costs for the 20K staged combustor and for the 10K advanced expander as a function of DDT&E schedule change. Since both engine configurations have practically the same development schedule, the cost-versus-schedule curves are of the same shape. The 20K staged combustor cost at the nominal schedule; i.e., at the schedule presented in Task 6 of Ref. 3, is normalized to one. The 10K advanced expander has an about 5% lower DDT&E cost, as detailed in Vol. II-B.

The costs for both engine configurations do not change significantly when the schedule is shortened by six months, but increase rapidly when the schedule is lengthened.

The development risk, shown in Fig. 75, increases substantially if the schedule is shortened, e.g. more than doubles for a 6-month schedule compression, and decreases if the schedule is lengthened. Fig. 75 also indicates that the development risk of the expander is less than that of the staged combustor at the same schedule.

The reason why the risk increases with a compressed schedule is explained by Fig. 76, which shows the estimated development success probability-versus-schedule changes. For shortened schedules, both staged combustor and expander have significantly decreased success probabilities which account for the higher development risks noted above. Main reasons for the lower success probabilities are that any shortening of the schedule would lead to anticipated difficulties in material procurement, crowding of test schedules, and overloading of development efforts. Fig. 76 also shows that the staged combustor has an about 5% lower success probability compared to the expander at the same development schedule.

The results of the development risk assessment can be summarized as follows:

- The estimated development risk for the 10K-pound thrust advanced expander is less than that for the 20K-pound thrust staged combustor.
- The development risk would be reduced by 1/3 for the staged combustor, and by 1/2 for the expander, if the program schedule would be lengthened by 6 months. The associated program cost increase would amount to about 14%.

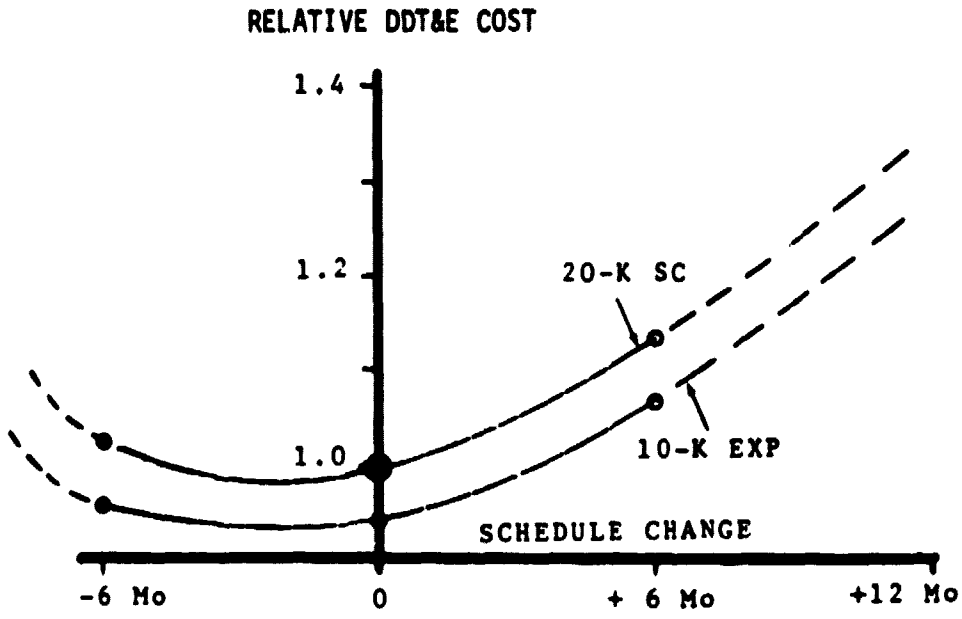

FIGURE 74. RELATIVE DDT&E COST COMPARISON

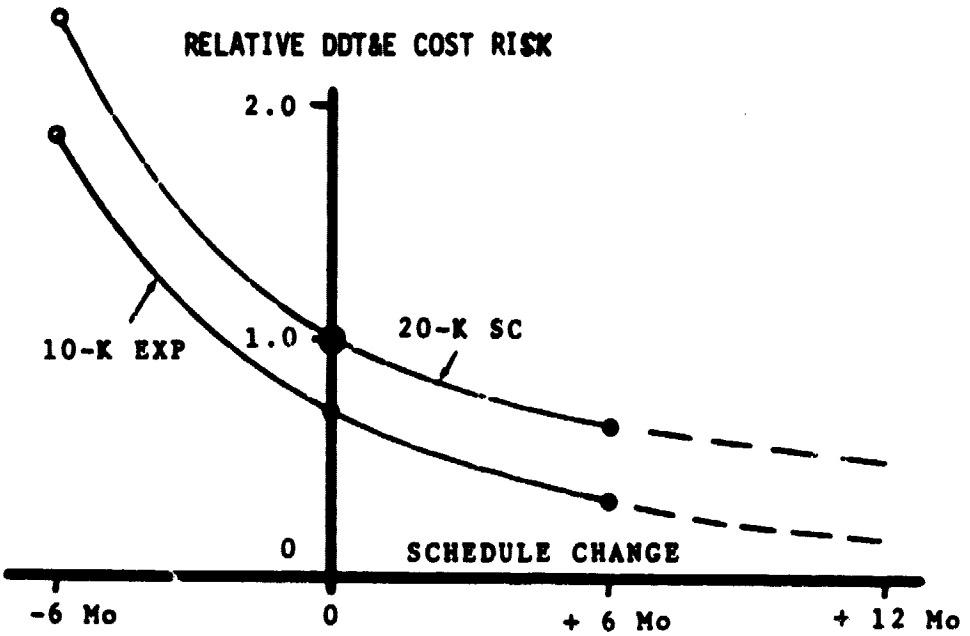

FIGURE 75. RELATIVE DDT&E COST RISK COMPARISON

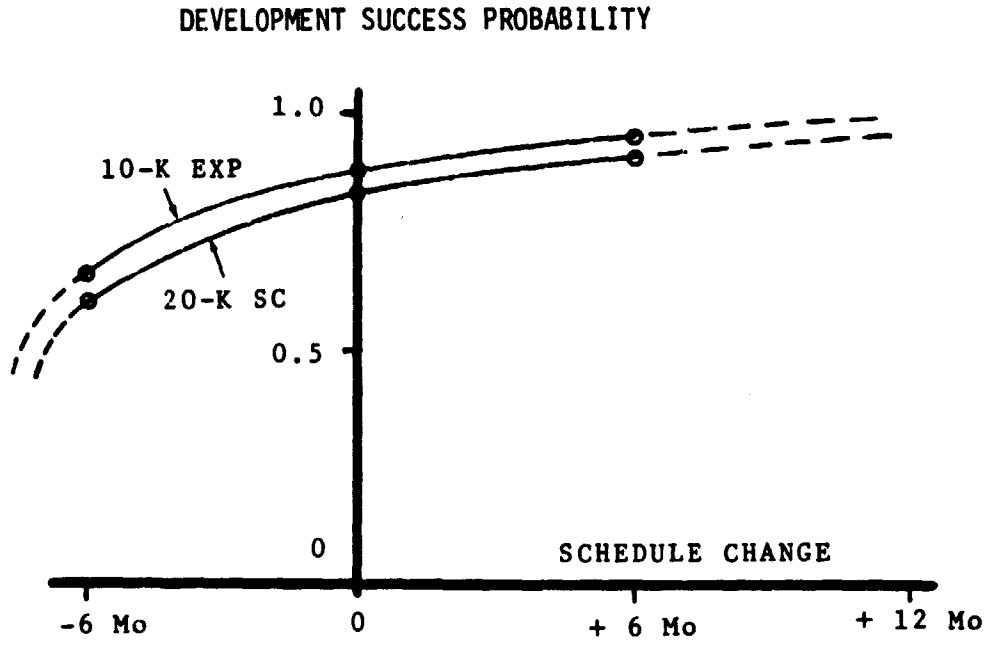

FIGURE 76. DEVELOPMENT SUCCESS PROBABILITY COMPARISON

- Shortening the program schedule would produce practically no change in program costs, but would increase program risk substantially.
- Major risk drivers for both engine configurations were found to be: turbomachinery, controls, and engine testing.

The following qualifications are made to the result of the development risk assessment investigation: though the assessment results are in quantitative form, they are based on informed, but subjective opinions, and should only be used as trend indications and as general guide for judging development risk. The survey form for the cognizant component engineers was problem-finding oriented and the responses are correspondingly conservative. This is exhibited best by the estimated values for success probability at nominal schedule which are less than one. In contrast, the original cost and schedule estimates presented in Tasks 6 and 7 of Reference 3 were success oriented. The lower than 100% development success probability of the Phase A Extension investigation was one of the factors which led to a reevaluation of the development costs for the 20K staged combustor as discussed in Volume II-B.

REFERENCES

1. Orbit-to-Orbit Shuttle Engine Design Study, AFRPL-TR-27, Pratt & Whitney Aircraft, July 1972

2. Orbit Transfer Systems with Emphasis on Shuttle Applications - 1986-1991, NASA Technical Memorandum NASA TM X-73394, April 1977

3. Orbit Transfer Vehicle Study, Phase A, Rocketdyne Report RI/RD 79-191-2, July 1979

APPENDIX A

OTV ENGINE DEVELOPMENT RISK SURVEY FORM

OBJECTIVE

Determine influence of schedule changes on component development cost and on success probability for 20K lb thrust staged combustion engine and for 10K lb thrust advanced expander engine.

PROCEDURE

Determine the influence of development schedule changes on cost and the likelihood of success for each major engine component listed in Table A1 using the following procedure steps, and using the nominal DDT&E schedules, effort and component development costs for the two engine configurations:

1. Determine major potential problems for each component technology aspect shown in the left column of Table A-2.
2. Establish most likely cures or solutions to the potential problems, and enter in Table A-2.
3. Estimate the incremental effects of the potential problems and most likely cures on the nominal component DDT&E schedule and the nominal cost, and enter in Table A-2.
4. Based on the above steps, make the following subjective judgments and enter them in Table A-3.
   a) Success probability (0 to 100%) to keep, lengthen, or shorten the nominal development schedule by the increments given in the left column of Table A-3. When estimating the probability to achieve the development task, consider all DDT&E activities, i.e., design, analysis, development fabrication, materials and processes, and testing.
   b) Required changes of nominal effort associated with the development schedule changes.

TABLE A-1

MAJOR OTV ENGINE COMPONENTS

Low Pressure Oxygen Turbopump

Low Pressure Hydrogen Turbopump

High Pressure Oxygen Turbopump

High Pressure Hydrogen Turbopump

Ignition Systems for Preburner & Main Chamber

Preburner (for staged combustor only)

Thrust Chamber (including upper nozzle, but excluding igniter and gimbal)

Nozzle Assembly (extendible nozzle and extension/retract. mech.)

Gimbal Assembly

Propellant Valves

Control, Pump and Check Valves

Engine Controller

Instrumentation and Electrical

Heat Exchanger

Propellant Ducts & Lines

Engine Testing

TABLE A-2

SURVEY FORM FOR COMPONENT PROBLEM ASSESSMENT

Technology Aspect	Major Potential Problem	Most Likely Cure of Problem	Influence of Problem & Cure on Cost	Influence of Problem & Cure on Schedule
Stress, Loads & Materials				
Maturity or State-of-the-Art				
Performance (On-Design & Off-Design)				
Component Complexity				
Producibility & Testibility				

Example:

Performance	Too low main LOX pump (MLP) efficiency	Redesign & retest MLP impeller to increase	MLP Cost increase ~10%	MLP Schedule slip of ~ 3 months

TABLE A-3

EFFECT OF SCHEDULE CHANGE ON PROBABILITY OF SUCCESS AND COST

Component Development Schedule	Estimated Success Probability for Given Schedule (0 to 100%)	Estimated Required Change in Effort for Given Schedule (% of Man-Months)
Maintain nominal Schedule (Fig. 1 to 4) ($\Delta = 0$)		0
Lengthen schedule by 6 months) ($\Delta = +6$ mo.)		
Shorten schedule by 6 months) ($\Delta = -6$ mo.)		